UNIVERSITY OF NORTH TEXAS
HEALTH SCIENCE CENTER AT FORT WORTH
1970

ABSTRACT

Duncan, Raymond S., N-acylethanolamine signaling in neurons. Doctor of Philosophy (Biomedical Sciences), December, 2008, 356 pp., 1 table, 70 illustrations, bibliography, 576 titles.

Neurodegenerative diseases including Alzheimer's disease are and will continue to be significant health problems as the aging population increases. The maintenance of neuronal calcium homeostasis has been a focus in neurodegenerative disease research for many years. Within the last several years, lipids that activate cannabinoid receptors, and thus called cannabinoids, have gained recognition as neuroprotecants in models of neurodegenerative diseases. A subset of these cannabinoids, the N-acylethanolamines (NAEs), includes the well characterized neuroprotective lipid, arachidonylethanolamine.

Other NAEs, such as palmitoylethanolamine (PEA), are more abundant in neurons and do not activate cannabinoid receptors, suggesting other targets for these lipids exist. Since non-cannabinoid NAEs rapidly accumulate after neuronal injury, it is likely they play a role in cellular responses to injury. Interestingly, some NAEs can alter intracellular Ca^{2+} signaling, but the underlying mechanism of action remains unclear.

I hypothesized that the non-cannabinoid NAEs, such as PEA, protect the hippocampal cell line, HT22, from oxidative stress in part by reducing intracellular calcium release. I determined that HT22 cells and cultured mouse cortical neurons express proteins involved in NAE signaling, thus warranting the use of pharmacological inhibitors of these proteins in subsequent neuroprotection studies.

Using HT22 cells, I determined that PEA exhibits antiproliferative effects and neuroprotects against oxidative stress. In addition, I determined that PEA facilitates the nuclear translocation of putative protective proteins that can be regulated by Ca^{2+} through a mechanism not involving cannabinoid receptor activation. These findings led me to hypothesize that PEA alters release of Ca^{2+} from intracellular stores.

To test this hypothesis, I determined that our cell models express inositol 1,4,5-trisophosphate receptors (IP3Rs) and ryanodine receptors (RyRs) both of which are intracellular Ca^{2+} channels elevated in response to oxidative stress. I determined that treatment of HT22 cells with PEA reduces intracellular Ca^{2+} release elicited by chemical depolarization with KCl. My results suggest that non-cannabinoid NAEs, such as PEA, protect the hippocampal cell line, HT22, from oxidative stress in part by activating putative neuroprotective signaling proteins and by reducing intracellular calcium release.

N-ACYLETHANOLAMINE SIGNALING IN NEURONS

DISSERTATION

Presented to the Graduate Council of the

Graduate School of Biomedical Sciences

University of North Texas Health Science Center at Fort Worth

in Partial Fulfillment of the Requirements

For the Degree of

DOCTOR OF PHILOSOPHY

By

Raymond Scott Duncan, M.A.

Fort Worth, Texas

December 2008

ACKNOWLEDGEMENTS

I would like to extend my deepest gratitude and thanks to Dr. Peter Koulen who has been an exceptional scientist, role model and mentor. Dr. Koulen's guidance and support has helped me learn, develop and grow as a scientist and a person. I would also like to recognize and extend my most sincere thanks to the members of my Graduate Committee: Dr. James Simpkins, Dr. Michael Forster and Dr. Meharvan Singh. They have offered wonderful guidance and advice that have only improved upon my knowledge and work. I also wish to thank my University Member, Dr. Ladislav Dory. I sincerely thank the members of the Koulen lab, both past and present, for their help and support. Specifically, I thank Elaine Gregg, Wanda Medina, JoAnn Yannazzo, Dr. Sung-Yong Hwang, Ji-Yeon Hwang, Dr. Puja Garg, Nataliya Rybalchenko, Dr. Volodymyr Rybalchenko, Dr. Martha Stokely, Dr. Everett Nixon, Mike Grillo, Dr. Hua Xin, Dr. Toyin Mafe, Dr. Angela-Peterson-Ford, Dr. Virginia Pearce, Sandra Longoria, Tiffany Davis, Andrew Payne, Dr. Jens Westhoff, Dr. Christian Madry, Dr. Jiyuan Liu, Dr. Jiexia Quan and Nathalie McClung.

I would like to extend my greatest appreciation and thanks to my wonderful wife, Lauri Duncan, who has always offered me her unyielding support on a daily basis. I could not have conducted or completed this work without it. In addition, I would like to thank my two sons, Ethan and Caden Duncan, for making my life truly more wonderful and giving me the greatest joy and sense of purpose.

TABLE OF CONTENTS

LIST OF TABLES

Chapter 4.1

LIST OF ILLUSTRATIONS

CHAPTER 1

CHAPTER 2

CHAPTER 3.1

CHAPTER 3.2

CHAPTER 3.3

CHAPTER 3.4

CHAPTER 4.1

CHAPTER 4.2

CHAPTER 5

CHAPTER 6

LIST OF ABBREVIATIONS

Aβ – beta amyloid

AD – Alzheimer's disease

AEA – arachidonylethanolamine (anandamide)

AM – acetoxymethyl ester

Ca^{2+} - calcium

CB1 – cannabinoid receptor, type 1

CB2 – cannabinoid receptor, type 2

ERK1/2 – extracellular signal-regulated kinase 1/2

FAAH – fatty acid amide hydrolase

FAD – familial Alzheimer's disease

F/F_0 – fluorescence intensity over initial (baseline) fluorescence intensity

IP3 – inositol 1, 4, 5-trisphosphate

IP3R – inositol 1, 4, 5-trisphosphate receptor

kDa - kilodalton

LEA - lauroylethanolamine

LLEA - linolenoylethanolamine

MAPK – mitogen-activated protein kinase

NAAA – N-acylethanolamine acid amidase

NAE – N-acylethanolamine

NAPE-PLD – N-acylethanolamine-hydrolyzing phospholipase D

NFκB – nuclear factor kappa B

NFATc4 – nuclear factor of activated T-cells c4

NMDA – N-methyl D-aspartic acid

OEA - oleoylethanolamine

p38 – mitogen-activated protein kinase (MAPK) of 38 kilodaltons

PEA - palmitoylethanolamine

PS-1 – presenilin 1

PS-2 – presenilin 2

ROS – reactive oxygen species

RyR – ryanodine receptor

SDS-PAGE – sodium dodecylsulfate polyacrylamide gel electrophoresis

tBHP – tert-butylhydroperoxide

VR1 – vanilloid receptor 1

CHAPTER 1 – INTRODUCTION AND BACKGROUND

Alzheimer's Disease

Alzheimer's disease (AD) is a serious health problem currently affecting 5.2 million people in the US with 5 million of those people over the age of 65 (1). There are predicted to be 454,000 new AD cases per year by the year 2010 and over 7.7 million people in the US will have this disease by the year 2030 (1). There are two different types of AD: familial and sporadic. The most widespread form of AD, sporadic, is characterized by a late onset of symptoms in or after the sixth decade of life and post-mortem observance of amyloid plaques and neurofibrillary tangles in specific brain regions (1). In familial AD, the same pathological hallmarks are present, but the onset of symptoms occurs much earlier in life and there is a strong genetic association with the disease.

Much AD research focus has been placed on understanding the role of amyloid precursor protein (APP) processing and tau hyperphosphorylation which is believed to be a causative mechanism for AD development. Currently, there are drugs available for treating AD including cholinesterase inhibitors and N-methyl-D-aspartate (NMDA) receptor inhibitors, but their efficacy is not great (2, 3). Multiple pathological processes occurring in AD at the cellular level have been described including induction of apoptosis, mitochondrial dysfunction, loss of Ca^{2+} homeostasis and oxidative stress (4 - 7).

Oxidative stress occurs in a wide variety of diseases, most especially in neurodegenerative diseases such as Alzheimer's disease (8). Oxidative stress occurs mainly when mitochondria produce reactive oxygen species (ROS) during oxidative phosphorylation (9). An elevation in ROS may then oxidize lipids, proteins and DNA, thus altering their function (8). Critical

proteins, such as Ca^{2+} pumps and Ca^{2+} channels, are vulnerable to oxidative damage (10 - 13). A rapidly-evolving area in AD research is in neuroprotection against Ca^{2+} toxicity which is a consequence of Aβ exposure in *in vitro* and *in vivo* models of AD (5 - 7). There have been numerous reports of a loss of Ca^{2+} homeostasis in *in vitro* cell culture models and in genetically-modified animals with AD-like pathology (5, 14 - 17).

I hypothesize that maintenance of Ca^{2+} homeostasis under conditions of oxidative stress will lead to neuroprotection. I have characterized the neuroprotective activities of specific lipids, N-acylethanolamines (NAEs), against oxidative stress in a cell culture model system of neurodegeneration. Furthermore, I have characterized the potential role of these lipids on intracellular Ca^{2+} channel activity in HT22 cells and cultured mouse primary cortical neurons. Oxidative stress has a detrimental effect on Ca^{2+} homeostasis and result in altered Ca^{2+} homeostasis can, thereby, lead to further oxidative stress (19 - 21). Data provided in this work is of importance because little is known about the contribution of Ca^{2+} release from intracellular stores on Ca^{2+} toxicity resulting from oxidative stress in neurons. Since dysregulated intracellular Ca^{2+} can lead to increased concentration of reactive oxygen species (ROS) leading to oxidative stress (9). I hypothesize that regulating intracellular Ca^{2+} release through inositol 1, 4, 5-trisphosphate (IP_3) receptors (IP_3Rs) and ryanodine receptors (RyRs) will complement other existing strategies in the treatment of AD. I determined if the saturated non-cannabinioid receptor-activating lipids, N-acylethanolamines (NAEs), are neuroprotective in models of AD and ischemic stroke. In addition, I determined if these NAEs reduce intracellular Ca^{2+} release through IP_3Rs and RyRs possibly representing a novel potential therapeutic strategy for treating neurodegenerative diseases such as AD. The best approach for treating AD, however, will likely

be one that combines treatments regulating Ca^{2+} homeostasis in addition with drugs that maintain neurotransmitter release, antioxidants and anti-inflammatory drugs.

Ischemic stroke

Stroke is the third leading causes of death in the United States with approximately 5.8 million current cases and approximately 780,000 new cases every year (22). Ischemic stroke is caused by a blood flow impediment to specific brain regions resulting in oxygen and glucose deprivation followed by the loss of Ca^{2+} homeostasis (23). Excessive cytosolic Ca^{2+} can lead directly to mitochondrial dysfunction, oxidative stress, and induction of apoptosis, and reperfusion to the affected area results in further oxidative stress (23). The oxidative stress and loss of Ca^{2+} homeostasis observed in ischemic stroke is also similar to that observed in other neurodegenerative diseases such as Alzheimer's disease. These shared cellular pathologies make the pressent study relevent to both diseases. I determined the role of NAEs on IP_3R and RyR activity in HT22 cells and primary cortical neurons. I hypothesize that specific NAEs are neuroprotective against ischemic insults by reducing the activity of the intracellular Ca^{2+} channels IP_3R and RyR. If the ischemia-mediated loss of Ca^{2+} homeostasis and subsequent oxidative stress can be reduced, then a portion of neurons, especially in the penumbra of the ischemic region, may survive ischemic insult, thereby limiting stroke severity. This study is of importance because little is known about the contribution of intracellular Ca^{2+} channels on Ca^{2+} toxicity resulting from anoxia.

Role of Ca^{2+} Homeostasis in Neurodegeneration

Associations between altered Ca^{2+} homeostasis and aging and neurodegenerative diseases such as Alzheimer's disease have been established by a large number of research groups (7, 24). Perhaps the most striking example is that many presenilin mutations leading to familial AD alter Ca^{2+} homeostasis in a variety of cell culture and animal models (7).

The role of IP_3R expression or activity in AD or stroke has been studied for several years, but it is still not clear what role IP_3Rs play in the disease process. Inositol 1, 4, 5-trisphoasphate (IP_3) signaling is altered and IP_3 binding in reduced in brains of AD patients (25 - 28). Cultured neurons exposed to Aβ leads to IP_3R-mediated Ca^{2+} release leading to oxidative stress and cell death (29). Calcium release from IP3Rs is altered in cells expressing mutant PS1 and PS2 proteins and in PS1(M146V) expressing mice (30). Furthermore, cultured cells from PS1/PS2 double knockout mice have elevated IP_3R1 expression (31). Familial Alzheimer's disease (FAD) mutant PS1 expressed in Xenopus oocytes increases endoplasmic reticulum Ca^{2+} stores and IP3R-mediated Ca^{2+} release (32, 33). Similarly, FAD PS2 expression leads to elevated IP_3R-mediated Ca^{2+} release (34).

In *in vivo* models of stroke, IP_3R expression decreases in brain regions such as the hippocampus, but is not clear whether this is a compensatory response to neurodegeneration or whether it contributes to neurodegeneration (35 - 37). In a more recent study, cerebellar hypoxia led to an increase in IP_3R1 and IP_3R2 protein levels and this response could be reversed with antioxidants, suggesting that free radicals may be involved (38). This result suggests that oxidative stress, which occurs both in AD and stroke, results in increased IP_3R expression and may, therefore, result in increased IP_3R-mediated Ca^{2+} release. We determined the role of

oxidative stress on subtype-specific IP_3R and RyR expression levels in HT22 cells and primary cortical neurons.

Evidence for the role of RyR in human disease has been growing over the past several years. Evidence for RyR involvement in neurodegenerative diseases has also been demonstrated. In neurodegenerative disease such as AD, Ca^{2+} dyshomeostasis contributes to neuronal dysfunction (5, 14 - 18). Furthermore, intracellular Ca^{2+} channels, including RyRs, play a role in the progression of the disease by contributing to the overall Ca^{2+} dyshomeostasis in the cell (15 - 18).

RyR expression in brains of AD patients is altered. For example, there is a 40% reduction in cortical ryanodine binding and in tissue from Alzheimer's patients (39). More specifically, there is a 20% reduction in RyR2 expression in these tissues. Aβ peptide treatment of cortical neurons results in an increase in RyR3 expression (18). Furthermore, Aβ treatment of cortical neurons results in RyR-mediated Ca^{2+} release resulting and subsequent cell death (29). It may not be uncommon for different receptor subtypes (i.e., RyR2 versus RyR3) to be regulated differently in response to stimuli including cellular stress. There is also a difference in the technical/methodological approach used for these studies. For example, the reduced RyR2 expression was from the intact cortex from AD brains using ryanodine binding and immunohistochemistry. The increased RyR3 expression and activity is from cultured cortical neurons from mice (or rats) treated with purified Aβ.

Mice expressing mutant PS-1 exhibit increased RyR expression and elevated caffeine-induced Ca^{2+} release (15). Furthermore, treatment with caffeine results invulnerability to Aβ (15). Treatment of cultured neurons from mutant PS-1-knockin and triple AD transgenic (PS-1/PS-2/APP) mice with caffeine increases RyR expression and amplitude of Ca^{2+} release (7). RyR3-

mediated Ca^{2+} release is eleveated in cultured neurons from an AD transgenic model (18). Fibroblasts expressing the PS-2 M239I mutation have reduced intracellular Ca^{2+} release and capacitative Ca^{2+} entry after ER store depletion (40).

The role of RyRs in models of stroke is not completely clear. In the brain, for example, ischemia produced by common carotid artery occlusion results in rapid decrease of ryanodine binding in the gerbil hippocampal CA1 region (41), suggesting that Ca^{2+}-induced Ca^{2+} release (CICR) is altered in the CA1 region during ischemia. In mouse cerebellar granule cells, however, hypoxia results in no detectable change in RyR1 and RyR2 mRNA expression levels (41). The RyR antagonist dantrolene protects liver cells from ischemia, suggesting that RyRs may play a significant role in cellular pathology (42). Furthermore, dantrolene also protects retinal ganglion cells from excitoxic insult (43). These data support the idea that intracellular Ca^{2+} channels such as RyRs may be good pharmacological targets in neurodegenerative diseases.

NAEs, Cannabinoids, and Cannabinoid Receptors

Lipids, aside from being a major constituent of biological membranes, also act as signaling molecules and are ligands at receptors. The well characterized lipids prostaglandin E2 (PGE2) and leukotrienes (LT), for example, bind to G-protein-coupled receptor (GPCR) to exert their algesic and inflammatory actions (44, 45). Other signaling lipids of interest include the more recently characterized N-acylethanolamines (NAEs). The physiological function of only a small number of NAEs have been characterized including arachidonylethanolamine (AEA, anandamide), palmitoylethanolamine (PEA), oleoylethanolamine (OEA), linoleoylethanolamine (LOEA) and linolenoylethanolamine (LNEA) (46 - 49). Only the function of anandamide, however, has been studied extensively.

AEA may be an endogenous ligand for the cannabinoid receptor, although other lipid ligands exist for this receptor (50, 51). Previous studies revealed that cannabinoid receptors were targets of tetrahydrocannabinols (THCs), the active components of marijuana (52). There are two cannabinoid receptors, CB1 and CB2, and anandamide activates both subtypes, albeit at lower affinity than Δ9-THC and 2-arachidonylglycerol (51 - 56). These receptors are seven transmembrane-spanning G-protein-coupled receptors that negatively couple to inhibitory G-proteins ($G_{i/o}$) thereby inhibiting adenylyl cyclase (56 - 59). The cannabinoid receptor-activating (cannabinoid) NAEs are involved in numerous physiological processes including neurotransmission, analgesia, reproduction, feeding, proliferation, inflammation and cytoprotection (60 - 63). Numerous unsaturated NAEs, including AEA, oleoylethanolamine, linoleoylehtanolamine and linolenoylethanolamine bind and activate vanilloid receptor 1 (VR1) cation channels, which are members of the transient receptor potential V (TRPV) channel family (48, 64, 65).

Some NAEs do not bind to or activate cannabinoid receptors or vanilloid receptors, therefore, the molecular target and subsequent function of these NAEs remains to be determined. The presence or absence of these receptors in our cell culture model systems can be used to determine whether pharmacological interventions need to be taken in order to uncover the molecular targets for and function of some non-cannabinoid NAEs.

Downstream Targets of NAEs / NAE Signaling Pathways

Activation of CB1 and CB2 leads to a multitude of intracellular signaling events including the inhibition of adenylyl cyclase activity and subsequent inhibition of cAMP-dependent protein kinase (PKA) activity, activation of the MAP kinase pathway and ERK1/2 phosphorylation, and

increases in focal adhesion kinase (FAK) phosphorylation (66 - 73). Furthermore, cannabinoids inhibit N-, T- and P/Q-type Ca^{2+} currents and VR1-mediated Ca^{2+} influx in multiple cell models through activation of CB1 (74 - 79). Lastly, nuclear transcription factors peroxisome proliferator antigen receptors, PPARα and PPARγ, are activated by some NAEs (80, 81). It is not clear whether non-cannabinoid NAEs, such as PEA, can activate specific kinases and transcription factors or alter Ca^{2+} channel activity in a manner similar to AEA.

Sites of NAE Target Protein Expression

NAE synthesis has been detected in numerous mammalian tissues including epidermis, cardiac tissue and brain tissue with the highest synthetic activity in the microsomal fraction (82 - 90). In the brain, cannabinoid receptors are expressed in numerous brain regions as well as cerebral vasculature (91 - 98). The CB2 receptor (peripheral cannabinoid receptor) has been localized primarily to immune tissues, placenta, uterine smooth muscle and in cerebral vasculature (97 - 99). Recently, the CB2 receptor has been identified in neurons in the brain suggesting that its classification as a peripheral cannabinoid receptor should be re-evaluated (99). The VR1 receptor is predominantly expressed in sensory neurons, brain areas such as the hippocampus, cortex and cerebellum, and in the cerebral vasculature (96, 100, 101). It is not clear whether cultured neurons or cell lines relevant to the study of neurodegenerative diseases coexpress CB1, CB2, VR1 and enzymes involved in NAE synthesis and degradation. This information will determine whether pharmacological interventions need to be taken in order to uncover any potential neuroprotective effects of some non-cannabinoid NAEs in these cell model systems.

NAEs Exhibit Neuroprotective Properties

There is ample evidence demonstrating the neuroprotective effects of NAEs. Indirect evidence for NAE-mediated protection comes from numerous observations that NAE synthesis is upregulated in response to multiple chemical and traumatic insults. For example, some NAEs are produced in rat brain in response to ischemia (102, 103). Furthermore, some NAE species and their precursor molecules, N-acylphosphatidylethanolamines (NAPES), are upregulated in ischemic regions of infarcted canine myocardium (85, 86), suggesting their possible role in cytoprotection. NAE levels are rapidly elevated in response to hemispheric stroke in human patients (104). Cultured rat cortical neurons generate NAPE and NAE species after excitotoxicity mediated by glutamate activation of NMDA receptor (105, 106). Age-related changes in NAEs and expression of targets of NAEs may be altered during age-related neurodegenerative diseases giving way to increased susceptibility. For example, NAEs and NAPEs occur at higher levels in aged rat cortical neuron cultures and aged rats lose the ability to accumulate NAPE levels in the brain in response to ischemia (105, 107).

Direct evidence for NAE-mediated cytoprotection comes from multiple studies. For example, the non-cannabinoid NAE, oleoylethanolamine (OEA), protects rat cardiac mitochondria from peroxide-induced oxidative damage (108). Furthermore, activation of CB1 protects cultured cortical neurons from excitotoxicity and oxidative stress (109 - 111). Intraperitoneal injection of the cannabinoid NAE anadamide into mice and rats reduces the size and severity of AMPA and kainate receptor-induced brain lesions by a mechanism involving activation of CB1 receptor (112). Synthesis of non-cannabinoid NAEs is upregulated in response to injury along with cannabinoid NAEs. Furthermore, non-cannabinoid NAE concentrations are higher than the concentration of cannabinoid NAEs. It stands to reason, therefore, that the non-cannabinoid

NAEs may be involved in cytoprotection, although through a mechanism different from cannabinoids.

Non-Cannabinoid / Vanilloid Receptor Targets of NAEs

Other NAEs that do not bind cannabinoid receptors have been implicated in cytoprotection and as 'entourage' compounds, which are compounds that enhance the activity of other ligands such as anandamide by inhibiting the enzymes that degrade it (65, 113).

Some saturated and monounsaturated NAEs activate the ERK1/2 phosphorylation pathway through a CB1-independent mechanism (114). The NAE oleoylethanolamine (OEA) reduces the formation of iron-induced malondialdehyde (MDA) in rat heart mitochondria, suggesting that it may act as an antioxidant reducing lipid peroxidation (108). Furthermore, some NAEs, including PEA, decrease the mitochondrial inner membrane permeability and may protect cells from ischemic insult (115). Interestingly, the yeast *Saccharomyces cerevisiae*, which does not express cannabinoid or vanilloid receptors, synthesizes various NAE species in response to oxidative stress (116). Plants also synthesize NAEs but do not have cannabinoid or vanilloid receptors (117). These observations further substantiate a non-cannabinoid receptor- and a non-vanilloid receptor-mediated function for some NAEs.

Some NAEs, including palmitoylethanolamine and anandamide, have been shown to stimulate Ca^{2+} release from intracellular stores (115, 118, 119). Palmitoylethanolamine, which does not activate the CB1 receptor, increases Ca^{2+} influx and increases some parameters of sperm motility by an unknown mechanism (120). The NAEs, lauroylethanolamine and oleoylethanolamine, alter the rate of Ca^{2+} flux from sarcoplasmic reticulum vesicles isolated from rabbit skeletal muscle (115). In addition, it was suggested that this alteration of Ca^{2+} release

from intracellular stores in cardiac muscle could lead to increased contractility (115). The mechanism by which NAEs alter intracellular Ca^{2+} concentrations has not been resolved. I will, in part, determine the mechanism by which a small subset of NAEs can alter Ca^{2+} signaling.

NAE Involvement in Ca^{2+} Signaling

In rat cerebellar Purkinje neurons, AEA reduces presynaptic P-type Ca^{2+} currents by a mechanism independent of CB1 or VR1 (121). In addition to other unsaturated lipids, AEA inhibits T-type Ca^{2+} channel currents through a direct interaction depending upon both the hydroxyl group and acyl chain (77). The degree of acyl chain saturation also affects their ability to inhibit currents (77). Treatment of cultured endothelial cells with AEA elicits an increase in intracellular Ca^{2+} through a CB1-dependent mechanism (122).

Lipids can alter the activity of intracellular Ca^{2+} channels. For example, arachidonic acid inhibits IP3R activity and leukotriene B4 activates RyRs (123). There is growing evidence that some of the N-acylethanolamine (NAE) lipids such as arachidonylethanolamine (AEA) and palmitoylethanolamine (PEA) can elicit the release of intracellular Ca^{2+}. In canine kidney cells, AEA leads to intracellular Ca^{2+} release and extracellular Ca^{2+} influx (119). In human osteosarcoma cells, the AEA transport inhibitor inhibitor and VR1 antagonist, AM404, causes release of Ca^{2+} from intracellular stores and Ca^{2+} influx from the extracellular space (124). In cultured hippocampal neurons, the plant cannabinoid, cannabidiol (CBD), leads to Ca^{2+} release from intracellular stores and influx from the extracellular space (125). CB1 and VR1 antagonist treatment resulted in a reduction in these effects (125).

In addition, AEA also leads to Ca^{2+} release via a phospholipase C-linked CB2 receptor (126). In HEK293 cells overexpressing CB1 receptors, treatment with the CB1 agonist, WIN55,212-2

led to an increase in intracellular Ca^{2+} (127). This response was blocked by inhibiting phospholipase, depleting intracellular stores with thapsigargin and inhibition of IP3Rs and RyRs (127). An additional G-protein-coupled receptor (GPCR), GPR55, can be activated by cannabinoids including AEA (128). GPR55 couples to $G\alpha_q$ and $G\alpha_{12}$ and can lead to the release of Ca^{2+} through IP3Rs (128). In addition, GPR55 results in Rho-A-mediated Ca^{2+} transients and subsequent NFAT activation in response to lysophosphatidylinositol (LPI) treatment (129). Furthermore, the NAE oleoylethanolamide (OEA) is believed to be the endogenous ligand for GPR119, a GPCR previously classified as an orphan receptor (130).

AEA treatment of endothelial cells causes the release of Ca^{2+} from caffeine-sensitive stores, suggesting the involvement of RyRs (118). This effect was only slightly reduced by the application of a CB1 antagonist (118). Treatment of cultured hippocampal neurons with CB1 agonists reduces NMDA-mediated Ca^{2+} released from RyRs by reducing PKA phosphorylation of RyR channels (131). This effect is associated with protection against NMDA toxicity (131). Interestingly, in CA1 pyramidal neurons, Ca^{2+}-induced Ca^{2+} release through RyR leads to endocannabinoid release and subsequent depolarization-induced suppression of inhibition (DSI) (132).

Here, I have identified the presence and subcellular localization of proteins involved in NAE signaling in two widely-used cell culture model systems of neurodegeneration. In addition, the alteration of NAE synthesizing and degrading proteins in response to oxidative stress was measured. I also determined that the saturated non-cannabinoid/non-vanilloid NAE PEA is neuroprotective in HT22 cells against oxidiative stress. A 5 – 6 hour exposure to PEA is required to protect HT22 cells which, in turn, correlates with the time required for PEA to alter the immunolocalization of key signaling proteins known to be involved in neuroprotective signaling.

Previous data from our lab indicates that NAEs reduce the open probability of RyRs in a single-channel electrophysiological setup. This preliminary data in addition to the time frame of neuroprotection and changes in signaling proteins is consistent with a role for NAE in Ca^{2+} signaling. To determine what role NAE may have in intracellular Ca^{2+} signaling, the expression and localization of the intracellular Ca^{2+} channels, IP3Rs and RyRs, was characterized in our cell culture models under normal condition and conditions of oxidative stress. In addition, I measured the effect of NAEs on intracellular Ca^{2+} signaling. I was not able to verify that treatment of HT22 cells with PEA for 3 hours or less has an effect on Ca^{2+} signaling. Prolonged treatment of HT22 cells with PEA alters IP_3R2, RyR2 and RyR3 immunoreactivities. Interestingly, data from experiments utilizing a longer PEA pretreatment time suggests that PEA reduces Ca^{2+} transients in response to depolarization. Overall the results of these studies suggest that there is a relationship between the neuroprotective effects of PEA, the ability of PEA to activate neuroprotective kinases and transcription factors, and the ability of PEA to reduce intracellular Ca^{2+} signaling mediated by depolarization. A diagrammatical summary of my results can be found in Fig. 1 below.

REFERENCES

1. www.alz.org
2. Longo FM and Massa SM (2004) Neuroprotective strategies in Alzheimer's disease.NeuroRx. 1(1):117-27.
3. Hull M, Berger M and Heneka M (2006) Disease-modifying therapies in Alzheimer's disease: how far have we come? Drugs. 2006; 66(16):2075-93.

4. Butterfield DA, Howard B, Yatin S, Koppal T, Drake J, Hensley K, Aksenova M, AksenovaM, Subramaniam R, Varadarajan S, Harris-White ME, Pedigo NW and Carney JM (1999) Elevated oxidative stress in models of normal brain aging and Alzheimer's disease. Life Sci. 65(18-19):1883-92.

5. LaFerla FM (2002) Calcium dyshomeostasis and intracellular signalling in Alzheimer's disease. Nat Rev Neurosci. 3(11):862-72.

6. Canevari L, Abramov AY and Duchen MR (2004) Toxicity of amyloid beta peptide: tales of calcium, mitochondria, and oxidative stress. Neurochem Res. 29(3):637-50.

7. Smith IF, Green KN and LaFerla FM (2005) Calcium dysregulation in Alzheimer's disease: recent advances gained from genetically modified animals. Cell Calcium. 2005 Sep-Oct;38(3-4):427-37.

8. Zhu X, Raina AK, Lee HG, Casadesus G, Smith MA and Perry G (2004) Oxidative stress signalling in Alzheimer's disease. Brain Res. 1000(1-2):32-9.

9. Brookes PS, Yoon Y, Robotham JL, Anders MW and Sheu SS (2004) Calcium, ATP, and ROS: a mitochondrial love-hate triangle. Am J Physiol Cell Physiol. 287(4):C817-33.

10. Annunziato L, Pannaccione A, Cataldi , Secondo A, Castaldo P, Di renzo G and Taglialatela M (2002) Modulation of ion channels by reactive oxygen and nitrogen species: a pathophysiological role in brain aging? Neurobiol Aging. 23(5):819-34.

11. Waring P (2005) Redox active calcium ion channels and cell death. Arch Biochem Biophys. 2005 Feb 1;434(1):33-42.

12. Yan Y, Wei CL, Zhang WR, Cheng HP and Liu J (2006) Cross-talk between calcium and reactive oxygen species signaling. Acta Pharmacol Sin. 27(7):821-6.

13. Hool LC and Corry B (2007) Redox control of calcium channels: from mechanisms to therapeutic opportunities. Antioxid Redox Signal. 9(4):409-35.

14. Smith, I. F., Hitt, B., Green, K. N, Oddo, S. & LaFerla, F. M. (2005) Enhanced caffeine-induced Ca2+ release in the 3xTg-AD mouse model of Alzheimer's disease. J Neurochem. 94(6):1711-8.

15. Chan, S. L., Mayne, M., Holden, C. P., Geiger, J. D. & Mattson, M. P. (2000) Presenilin-1 mutations increase levels of ryanodine receptors and calcium release in PC12 cells and cortical neurons. J Biol Chem. 275(24):18195-200.

16. George CH, Higgs GV, Mackrill JJ and Lai FA (2003) Dysregulated ryanodine receptors mediate cellular toxicity: restoration of normal phenotype by FKBP12.6. J Biol Chem. 278(31):28856-64.

17. Stutzmann GE, Smith I, Caccamo A, Oddo S, Laferla FM and Parker I (2006) Enhanced ryanodine receptor recruitment contributes to Ca2+ disruptions in young, adult, and aged Alzheimer's disease mice. J Neurosci. 26(19):5180-9.

18. Supnet, C., Grant, J., Kong, H., Westway, D. & Mayne, M. (2006) Abeta 1-42 increases ryanodine receptor-3 expression and function in TgCRND8 mice. J Biol Chem. Oct 18th, Epub ahead of print.

19. Gunter TE, Yule DI, Gunter KK, Eliseev RA and Salter JD (2004) Calcium and mitochondria. FEBS Lett. 567(1):96-102.

20. Hajnoczky G, Csordas G, Das S, Garcia-Perez C, Saotome M, Sinha Roy S and Yi M (2006) Mitochondrial calcium signalling and cell death: approaches for assessing the role of mitochondrial Ca2+ uptake in apoptosis. Cell Calcium. 40(5-6):553-60.

21. Nicholls DG, Johnson-Cadwell L, Vesce S, Jekabsons M and Yadava N (2007) Bioenergetics of mitochondria in cultured neurons and their role in glutamate excitotoxicity. J Neurosci Res. 85(15):3206-12.

22. Rosamond W et al., American Heat Association Statistics Committee and Stroke Statistics Subcommittee. (2008) Heart disease and stroke statistics--2008 update: a report from the American Heart Association Statistics Committee and Stroke Statistics Subcommittee. Circulation. 117(4):e25-146.

23. White BC, Sullivan JM, DeGracia DJ, O'Neil BJ, Neumar RW, Grossman LI, Rafols JA and Krause GS (2000) Brain ischemia and reperfusion: molecular mechanisms of neuronal injury. J Neurol Sci. 179(S 1-2):1-33.

24. Mattson MP (2007) Calcium and neurodegeneration. Aging Cell. 6(3):337-50.

25. Stokes, CE & Hawthorne, JN (1987) Reduced phosphoinositide concentrations in anterior temporal cortex of Alzheimer-diseased brains. J Neurochem. 48(4):1018-21.

26. Ferrari-DiLeo, G & Flynn, DD (1993) Diminished muscarinic receptor-stimulated [3H]-PIP2 hydrolysis in Alzheimer's disease. Life Sci. 53(25):PL439-44.

27. Cowburn RF, O'Neill C, Bonkale WL, Ohm TG and Fastbom J (2001) Receptor-G-protein signalling in Alzheimer's disease. Biochem Soc Symp. 2001;(67):163-75.

28. Crews, F. T., Kurian, P., & Freund, G. Cholinergic and serotonergic stimulation of phosphoinositide hydrolysis is decreased in Alzheimer's disease. Life Sci. 55(25-26):1993-2002 (1994).

29. Ferreiro, E., Resende, R., Costa, R., Oliveira, C. R. & Pereira, C. M. An endoplasmic-reticulum-specific apoptotic pathway is involved in prion and amyloid-beta peptides neurotoxicity. Neurobiol Dis. 23(3):669-78 (2006).

30. Stutzmann, G. E., Caccamo, A., LaFerla, F. M. & Parker, I. Dysregulated IP3 signaling in cortical neurons of knock-in mice expressing an Alzheimer's-linked mutation in presenilin1 results in exaggerated Ca2+ signals and altered membrane excitability. J Neurosci. 24(2):508-13 (2004).

31. Kasri, N. N., Kocks, S. L., Verbert, L., Hebert, S. S., Callewaert, G., Parys, J. B., Missiaen, L. & De Smedt, H. Up-regulation of inositol 1,4,5-trisphosphate receptor type 1 is responsible for a decreased endoplasmic-reticulum Ca2+ content in presenilin double knock-out cells. Cell Calcium 40(1):41-51 (2006).

32. Leissring, M. A., Paul, B. A., Parker, I., Cotman, C. W., & LaFerla, F. M. Alzheimer's presenilin-1 mutation potentiates inositol 1,4,5-trisphosphate-mediated calcium signaling in Xenopus oocytes. J Neurochem. 72(3):1061-8 (1999).

33. Leissring, M. A., LaFerla, F. M., Callamaras, N. & Parker, I. Subcellular mechanisms of presenilin-mediated enhancement of calcium signaling. Neurobiol Dis. 8(3):469-78 (2001).

34. Leissring, M. A., Parker, I. & LaFerla, F. M. Presenilin-2 mutations modulate amplitude and kinetics of inositol 1, 4,5-trisphosphate-mediated calcium signals. J Biol Chem. 274(46):32535-8 (1999).

35. Jorgensen MB (1993) The role of signal transduction in the delayed necrosis of the hippocampal CA1 pyramidal cells following transient ischemia. Acta Neurol Scand Suppl. 143:1-20.

36. Zhang SX, Zhang JP, Fletcher DL, Zoeller RT and Sun GY (1995) In situ hybridization of mRNA expression for IP3 receptor and IP3-3-kinase in rat brain after transient focal cerebral ischemia. Brain Res Mol Brain Res. 32(2):252-60.

37. Xia J, Simonyi A and Sun GY (1998) Changes in IP3R1 and SERCA2b mRNA levels in the gerbil brain after chronic ethanol administration and transient cerebral ischemia-reperfusion. Brain Res Mol Brain Res. 56(1-2):22-8.

38. Jurkovicova D, Kopacek J, Stefanik P, Kubovcakova L, Zahradnikova A Jr, Zahradnikova A, Pastorekova and Krizanova O (2007) Hypoxia modulates gene expression of IP(3) receptors in rodent cerebellum. Pflugers Arch. 454(3):415-25.

39. Kelliher, M., Fastbom, J., Cowburn, R. F., Bonkale, W., Ohm, T. G., Ravid, R., Sorrentino, V. & O'Neill, C. Alterations in the ryanodine receptor calcium release channel correlate with Alzheimer's disease neurofibrillary and beta-amyloid pathologies. Neuroscience. 92(2):499-513 (1999).

40. Zatti, G., Ghidoni, R., Barbiero, L., Binetti, G., Pozzan, T., Fasolato, C. & Pizzo, P. The presenilin 2 M239I mutation associated with familial Alzheimer's disease reduces Ca2+ release from intracellular stores. Neurobiol Dis. 15(2):269-78 (2004).

41. Nozaki H, Tanaka K, Gomi S, Mihara B, Nogawa S, Nagata E, Kondo T and Fukuucji Y (1999) Role of the ryanodine receptor in ischemic brain damage--localized reduction of ryanodine receptor binding during ischemia in hippocampus CA1. Cell Mol Neurobiol. 19(1):119-31.

42. Lopez-Neblina F, Toledo-Pereyra LH, Toledo AH and Walsh J (2007) Ryanodine receptor antagonism protects the ischemic liver and modulates TNF-alpha and IL-10.J Surg Res. 140(1):121-8.

43. Lei SZ, Zhang D, Abele AE and Lipton SA (1992) Blockade of NMDA receptor-mediated mobilization of intracellular Ca2+ prevents neurotoxicity.Brain Res. 598(1-2):196-202.

44. Hatae N, Sugimoto Y and Ichikawa A (2002) Prostaglandin receptors: advances in the study of EP3 receptor signaling. J Biochem (Tokyo) 131(6):781-784.

45. Toda A, Yokomizo T and Shimizu T (2002) Leukotriene B4 receptors. Prostaglandins Other Lipid Mediat. 68-69:575-585.

46. Jonsson KO, Vandervoorde S, Lambert DM, Tiger G and Fowler CJ (2001) Effects of homologues and analogues of palmitoylethanolamide upon the inactivation of the endocannabinoid anandamide. Br J Pharmacol. 133(8):1263-75.

47. Smart D, Jonsson KO, Vandervoorde S, Lambert DM and Fowler CJ (2002) 'Entourage' effects of N-acyl ethanolamines at human vanilloid receptors. Comparison of effects upon anandamide-induced vanilloid receptor activation and upon anandamide metabolism. Br J Pharmoacol. 136(3):452-8

48. Movahed P, Jonsson BA, Birnir B, Wingstrand JA, Jorgensen TD, Ermund A, Sterner O, Zygmunt PM and Hogestatt ED (2005) Endogenous unsaturated C18 N-acylethanolamines are vanilloid receptor (TRPV1) agonists. J Biol Chem. 280(46):38496-38504.

49. Murillo-Rodriguez E, Desarnaud F and Prospero-Garcia O (2006) Diurnal variation of arachidonoylethanolamine, palmitoylethanolamide and oleoylethanolamide in the brain of the rat. Life Sci. 79(1):30-7.

50. Devane WA, Hanus L, Breuer A, Pertwee RG, Stevenson LA, Griffin G, Gibson D, Mandelbaum A, Etinger A and Mechoulam R (1992) Isolation and structure of a brain constituent that binds to the cannabinoid receptor. Science. 258(5090):1946-1949.

51. Felder CC, Joyce KE, Briley EM, Mansouri J, Mackie K, Blond O, Lai Y, Ma AL and Mitchell (1995) Comparison of the pharmacology and signal transduction of the human cannabinoid CB1 and CB2 receptors.Mol Pharmacol. 1995 Sep;48(3):443-50.

52. Devane WA, Dysarz FA 3rd, Johnson MR, Melvin LS and Howlett AC (1988) Determination and characterization of a cannabinoid receptor in rat brain. Mol Pharmacol. 34(5):605-613.

53. Matsuda LA, Lolait SJ, Brownstein MJ, Young AC and Bonner TI (1990) Structure of a cannabinoid receptor and functional expression of the cloned cDNA. Nature. 346(6284):561-564.

54. Kaminski NE, Abood ME, Kessler FK, Martin BR and Schatz AR (1992) Identification of a functionally relevant cannabinoid receptor on mouse spleen cells that is involved in cannabinoid-mediated immune modulation. Mol Pharmacol. 42(5):736-742.

55. Munro S, Thomas KL and Abu-Shaar M (1993) Molecular characterization of a peripheral receptor for cannabinoids. Nature. 365(6441):61-65.

56. Vogel Z, Barg J, Levy R, Saya D, Heldman E and Mechoulam R (1993) Anandamide, a brain endogenous compound, interacts specifically with cannabinoid receptors and inhibits adenylate cyclase. J Neurochem. 61(1):352-355.

57. Bidaut-Russell M, Devane WA and Howlett AC (1990) Cannabinoid receptors and modulation of cyclic AMP accumulation in the rat brain. J Neurochem. 55(1):21-6.

58. Howlett AC, Bidaut-Russell M, Devane WA, Melvin LS, Johnson MR and Herkenham M (1990) The cannabinoid receptor: biochemical, anatomical and behavioral characterization. Trends Neurosci. 13(10):420-3.

59. Bayewitch M, Avidor-Reiss T, Levy R, Barg J, Mechoulam R and Vogel Z (1995) The peripheral cannabinoid receptor: adenylate cyclase inhibition and G protein coupling. FEBS Lett. 375(1-2):143-147.

60. Fride E (2002) Endocannabinoids in the central nervous system--an overview. Prostaglandins Leukot Essent Fatty Acids. 66(2-3):

61. Parolaro D, Massi P, Rubino T and Monti E (2002) Endocannabinoids in the immune system and cancer. Prostaglandins Leukot Essent Fatty Acids. 66(2-3):319-32.

62. Riegel AC and Lupica CR (2004) Independent presynaptic and postsynaptic mechanisms regulate endocannabinoid signaling at multiple synapses in the ventral tegmental area. J Neurosci. 24(49):11070-8.

63. Eljaschewitsch E, Witting A, Mawrin C, Lee T, Schmidt PM, Wolf S, Hoertnagl H, Raine CS, Schneider-Stock R, Nitsch R and Ullrich O (2006) The endocannabinoid anandamide protects neurons during CNS inflammation by induction of MKP-1 in microglial cells. Neuron. 2006 Jan 5;49(1):67-79.

64. Zygmunt PM, Petersson J, Andersson DA, Chuang H, Sorgard M, Di Marzo V, Julius D and Hogestatt ED (1999) Vanilloid receptors on sensory nerves mediate the vasodilator action of anandamide. Nature. 400(6743):452-457.

65. Smart D, Gunthorpe MJ, Jerman JC, Nasir S, Gray J, Muir AI, Chambers JK, Randall AD and Davis JB (2000) The endogenous lipid anandamide is a full agonist at the human vanilloid receptor (hVR1). Br J Pharmacol. 129(2):227-30.

66. Bouaboula M, Poinot-Chazel C, Bourrie B, Canat X, Calandra B, Rinaldi-Carmona M, Le Fur G and Casellas P (1995) Activation of mitogen-activated protein kinases by

stimulation of the central cannabinoid receptor CB1. Biochem J. 1995 Dec 1;312 (Pt 2):637-41.

67. Wartmann M, Campbell D, Subramaninan A, Burstein SH and Davis RJ (1995) The MAP kinase signal transduction pathway is activated by the endogenous cannabinoid anandamide. FEBS Lett. 359(2-3):133-6.

68. Bouaboula M, Poinot-Chazel C, Marchand J, Canat X, Bourrie B, Rinaldi-Carmona M, Calandra B, Le Fur G and Casellas P (1996) Signaling pathway associated with stimulation of CB2 peripheral cannabinoid receptor. Involvement of both mitogen-activated protein kinase and induction of Krox-24 expression. Eur J Biochem.237(3):704-711.

69. Derkinderen P, Toutant M, Burgaya F, Le Bert M, Siciliano JC, de Franciscis V, Gelman M and Girault JA (1996) Regulation of a neuronal form of focal adhesion kinase by anandamide. Science. 273(5282):1719-22.

70. Skalhegg BS and Tasken K (1997) Specificity in the cAMP/PKA signaling pathway. differential expression, regulation, and subcellular localization of subunits of PKA. Front Biosci. 2:d331-42.

71. Derkinderen P, Toutant M, Kadare G, Ledent C, Parmentier M and Girault JA (2001) Dual role of Fyn in the regulation of FAK+6,7 by cannabinoids in hippocampus. J Biol Chem. 2001 Oct 12;276(41):38289-96.

72. Davis MI, Ronesi J and Lovinger DM (2003) A predominant role for inhibition of the adenylate cyclase/protein kinase A pathway in ERK activation by cannabinoid receptor 1 in N1E-115 neuroblastoma cells. J Biol Chem. 278(49):48973-80.

73. Derkinderen P, Valient E, Toutant M, Corvol JC, Enslen H, Ledent C, Trzaskos J, Caboche J and Girault JA (2003) Regulation of extracellular signal-regulated kinase by cannabinoids in hippocampus. J Neurosci. 23(6):2371-82.

74. Mackie K, Devane WA and Hille B (1993) Anandamide, an endogenous cannabinoid, inhibits calcium currents as a partial agonist in N18 neuroblastoma cells.Mol Pharmacol. 44(3):498-503.

75. Mackie K, Lai Y, Westenbroek R and Mitchell R (1995) Cannabinoids activate an inwardly rectifying potassium conductance and inhibit Q-type calcium currents in AtT20 cells transfected with rat brain cannabinoid receptor. J Neurosci. 15(10):6552-61.

76. Shen M and Thayer SA (1998) The cannabinoid agonist Win55,212-2 inhibits calcium channels by receptor-mediated and direct pathways in cultured rat hippocampal neurons. Brain Res. 1998 Feb 2;783(1):77-84.

77. Chemin J, Monteil A, Perez-Reyes E, Nargeot J and Lory P (2001) Direct inhibition of T-type calcium channels by the endogenous cannabinoid anandamide. EMBO J. 20(24):7033-40.

78. Nogueron MI, Porgilsson B, Schneider WE, Stucky CL and Hillard CJ (2001) Cannabinoid receptor agonists inhibit depolarization-induced calcium influx in cerebellar granule neurons. J Neurochem. 79(2):371-81.

79. Oshita K, Inoue A, Tang HB, Nakata Y, Kawamoto M and Yuge O (2005) CB(1) cannabinoid receptor stimulation modulates transient receptor potential vanilloid receptor 1 activities in calcium influx and substance P Release in cultured rat dorsal root ganglion cells. J Pharmacol Sci. 97(3):377-85.

80. Fu J, Gaetani S, Oveisi F, Lo Verme J, Serrano A, Rodriguez De Fonseca F, Rosengarth A, Luecke H, Di Giancomo B, Tarzia G and Piomelli D (2003) Oleylethanolamide regulates feeding and body weight through activation of the nuclear receptor PPAR-alpha. Nature. 425(6953):90-93.

81. Bouaboula M, Hilairet S, Marchand J, Fajas L, Le Fur G and Casellas P (2005) Anandamide induced PPARgamma transcriptional activation and 3T3-L1 preadipocyte differentiation. Eur J Pharmacol. 517(3):174-81.

82. Colodzin M, Bachur NR, Weissbach H and Udenfriend S (1963) Enzymatic formation of fatty acid amides of ethanolamine by rat liver microsomes. Biochem Biophys Res Commun. 10:165-170.

83. Bachur NR, Masek K, Melmon KL and Udenfriend S (1965) Fatty acid amides of ethanolamine in mammalian tissues. J Biol Chem. 240:1019-1024.

84. Bachur NR and Udenfriend S (1966) Microsomal synthesis of fatty acid amides. J Biol Chem. 241(6):1308-1313.

85. Epps DE, Schmid PC, Natarajan V and Schmid HH (1979) N-Acylethanolamine accumulation in infarcted myocardium. Biochem Biophys Res Commun. 90(2):628-633.

86. Epps DE, Natarajan V, Schmid PC and Schmid HO (1980) Accumulation of N-acylethanolamine glycerophospholipids in infarcted myocardium. Biochim Biophys Acta. 1980 Jun 23;618(3):420-430.

87. Devane WA and Azelrod J (1994) Enzymatic synthesis of anandamide, an endogenous ligand for the cannabinoid receptor, by brain membranes. Proc Natl Acad Sci U S A. 91(14):6698-701.

88. Petersen G and Hansen HS (1999) N-acylphosphatidylethanolamine-hydrolysing phospholipase D lacks the ability to transphosphatidylate. FEBS Lett. 455(1-2):41-4.

89. Tiger G, Stenstrom A and Fowler CJ (2000) Pharmacological properties of rat brain fatty acid amidohydrolase in different subcellular fractions using palmitoylethanolamide as substrate. Biochem Pharmacol. 59(6):647-53.

90. Moesgaard B, Petersen G, Mortensen SA and Hansen HS (2002) Substantial species differences in relation to formation and degradation of N-acyl-ethanolamine phospholipids in heart tissue: an enzyme activity study. Comp Biochem Physiol B Biochem Mol Biol. 131(3):475-82.

91. Herkenham M, Lynn AB, Johnson MR, Melvin LS, de Costa BR and Rice KC Characterization and localization of cannabinoid receptors in rat brain: a quantitative in vitro autoradiographic study. J Neurosci. 11(2):563-83.

92. Herkenham M, Lynn AB, Little MD, Johnson MR, Melvin LS, de Costa BR and Rice KC (1990) Cannabinoid receptor localization in brain. Proc Natl Acad Sci U S A. 87(5):1932-6.

93. Mailleux P, Parmentier M and Vanderhagen JJ (1992) Distribution of cannabinoid receptor messenger RNA in the human brain: an in situ hybridization histochemistry with oligonucleotides.Neurosci Lett. 143(1-2):200-4.

94. Matsuda LA, Bonner TI and Lolait SJ (1993) Localization of cannabinoid receptor mRNA in rat brain. J Comp Neurol. 327(4):535-50.

95. Pettit DA, Harrison MP, Olson JM, Spencer RF and Cabral GA (1998) Immunohistochemical localization of the neural cannabinoid receptor in rat brain. J Neurosci Res. 51(3):391-402.

96. Golech SA, McCarron RM, Chen Y, Bembry J, Lenz F, Mechoulam R, Shohami E and Spatz M (2004) Human brain endothelium: coexpression and function of vanilloid and endocannabinoid receptors. Brain Res Mol Brain Res. 132(1):87-92.

97. Pettit DA, Anders DL, Harrison MP and Cabral GA (1996) Cannabinoid receptor expression in immune cells. Adv Exp Med Biol. 402:119-29.

98. Buckley NE, Hansson S, Harta G and Mezey E (1998) Expression of the CB1 and CB2 receptor messenger RNAs during embryonic development in the rat. Neuroscience. 82(4):1131-49.

99. Gong JP, Onaivi ES, Ishiguro H, Liu QR, Tagliaferro PA, Brusco A and Uhl GR (2006) Cannabinoid CB2 receptors: immunohistochemical localization in rat brain. Brain Res. 1071(1):10-23.

100. Szallasi A, Conte B, Goso C, Blumberg PM and Manzini S (1993) Vanilloid receptors in the urinary bladder: regional distribution, localization on sensory nerves, and species-related differences. Naunyn Schmiedebergs Arch Pharmacol. 347(6):624-9.

101. Toth A, Boczan J, Kedei N, Lizanecz E, Bagi Z, Papp Z, Edes I, Csiba L and Blumberg PM (2005) Expression and distribution of vanilloid receptor 1 (TRPV1) in the adult rat brain. Brain Res Mol Brain Res. 135(1-2):162-8.

102. Natarajan V, Schmid PC and Schmid HH (1986) N-acylethanolamine phospholipid metabolism in normal and ischemic rat brain. Biochim Biophys Acta. 1986 Aug 14;878(1):32-41.

103. Moesgaard B, Jaroszewski JW and Hansen HS (1999) Accumulation of N-acyl-ethanolamine phospholipids in rat brains during post-decapitative ischemia: a 31p NMR study. J Lipid Res. 40(3):515-21.

104. Schabitz WR, Giuffrida A, Berger C, Aschoff A, Schwaninger M, Schwab and Piomelli D (2002) Release of fatty acid amides in a patient with hemispheric stroke: a microdialysis study. Stroke. 33(8):2112-4.

105. Hansen HS, Lauritzen L, Strand AM, Moesgaard B and Frandsen A (1995) Glutamate stimulates the formation of N-acylphosphatidylethanolamine and N-acylethanolamine in cortical neurons in culture. Biochim Biophys Acta. 1258(3):303-8.

106. Hansen HS, Lauritzen L, Strand AM, Vingaard AM, Frandsen A and Schousboe A (1997) Characterization of glutamate-induced formation of N-acylphosphatidylethanolamine and N-acylethanolamine in cultured neocortical neurons. J Neurochem. 69(2):753-61.

107. Moesgaard B, Petersen G, Jaroszewski JW and Hansen HS (2000) Age dependent accumulation of N-acyl-ethanolamine phospholipids in ischemic rat brain. A (31)P NMR and enzyme activity study. J Lipid Res. 41(6):985-90.

108. Parinandi NL and Schmid HH (1988) Effects of long-chain N-acylethanolamines on lipid peroxidation in cardiac mitochondria. FEBS Lett. 237(1-2):49-52.

109. Skaper SD, Buriani A, Dal Toso R, Petrelli L, Romanello S, Facci L and Leon A (1996) The ALIAmide palmitoylethanolamide and cannabinoids, but not anandamide, are protective in a delayed postglutamate paradigm of excitotoxic death in cerebellar granule neurons. Proc Natl Acad Sci U S A. 93(9):3984-9.

110. Marsicano G, Goodenough S, Monory K, Hermann H, Eder M, Cannich A, Azad SC, Cascio MG, Gutierrez SO, van der Stelt M, Lopez-Rodriguez ML, Casanova E, Schutz G, Zieglgansberger W, Di Marzo V, Behl C and Lutz B (2003) CB1 cannabinoid receptors and on-demand defense against excitotoxicity. Science. 302(5642):84-8.

111. Kim SH, Won SJ, Mao XO, Jin K and Greenberg DA (2005) Involvement of protein kinase A in cannabinoid receptor-mediated protection from oxidative neuronal injury. J Pharmacol Exp Ther. 2005 Apr;313(1):88-94.

112. Shouman B, Fontaine RH, Baud O, Schwendimann L, Keller M, Spedding M, Lelievre V and Gressens P (2006) Endocannabinoids potently protect the newborn brain against AMPA-kainate receptor-mediated excitotoxic damage. Br J Pharmacol. 148(4):442-51.

113. De Petrocellis L, Davis JB and Di Marzo V (2001) Palmitoylethanolamide enhances anandamide stimulation of human vanilloid VR1 receptors. FEBS Lett. 506(3):253-6.

114. Berdyshev EV, Schmid PC, Krebsbach RJ, Hillard CJ, Hunag C, Chen N, Dong Z and Schmid HH (2001) Cannabinoid-receptor-independent cell signalling by N-acylethanolamines.Biochem J. 360(Pt 1):67-75.

115. Epps DE, Palmer JW, Schmid HH and Pfeiffer DR (1982) Inhibition of permeability-dependent Ca2+ release from mitochondria by N-acylethanolamines, a class of lipids synthesized in ischemic heart tissue.J Biol Chem. 257(3):1383-1391.

116. Merkel O, Schmid PC, Paltauf F and Schmid HH (2005) Presence and potential signaling function of N-acylethanolamines and their phospholipid precursors in the yeast Saccharomyces cerevisiae. Biochim Biophys Acta. 1734(3):215-9.

117. Chapman KD and Moore TS Jr. (1993) N-acylphosphatidylethanolamine synthesis in plants: occurrence, molecular composition, and phospholipid origin. Arch Biochem Biophys. 301(1):21-33.

118. Mombouli JV, Schaeffer G, Holzmann S, Kostner GM and Graier WF (1999) Anandamide-induced mobilization of cytosolic Ca2+ in endothelial cells. Br J Pharmacol. 126(7):1593-600.

119. Yeh JH, Cheng HH, Hunag CJ, Chung HM, Ghiu HF, Yang YL, Yeh MY, Chen WC, Kao CH, Chou CT and Jan CR (2006) Effect of anandamide on cytosolic Ca(2+) levels and proliferation in canine renal tubular cells. Basic Clin Pharmacol Toxicol. 98(4):416-22.

120. Ambrosini A, Zolese G, Ambrosi S, Bertoli E, Mantero F, Boscaro M and Balercia G (2005) Idiopathic infertility: effect of palmitoylethanolamide (a homologue of anandamide) on hyperactivated sperm cell motility and Ca2+ influx. J Androl. 26(3):429-36.

121. Fisyunov A, Tsinsadze V, Min R, Burnashev N and Lozovaya N (2006) Cannabinoids modulate the P-type high-voltage-activated calcium currents in purkinje neurons. J Neurophysiol. 96(3):1267-77.

122. Fimiani C, Mattocks D, Cavani F, Salzet M, Deutsch D, Pryor S, Bilfinger TV and Stefano GB (1999) Morphine and anandamide stimulate intracellular calcium transients in human arterial endothelial cells: coupling to nitric oxide release. Cell Signal. 1999 Mar;11(3):189-93.

123. Striggow F and Ehrlich BE (1997) Regulation of intracellular calcium release channel function by arachidonic acid and leukotriene B4.Biochem Biophys Res Commun. 237(2):413-8.

124. Chang HT, Huang CC, Cheng HHm Wang JL, Lin KL, Hsu PT, Tsai JY, Liao WC, Lu YC, Huang JK and Jan CR (2008) Mechanisms of AM404-induced [Ca(2+)](i) rise and death in human osteosarcoma cells. Toxicol Lett. 179(1):53-8.

125. Drysdale AJ, Ryan D, Pertwee RG and Platt B (2006) Cannabidiol-induced intracellular Ca2+ elevations in hippocampal cells. Neuropharmacology. 50(5):621-31.

126. Zoratti C, Kipmen-Korgun D, Osibow K, Malli R and Graier WF (2003) Anandamide initiates Ca(2+) signaling via CB2 receptor linked to phospholipase C in calf pulmonary endothelial cells. Br J Pharmacol. 140(8):1351-62.

127. Lauckner JE, Hille B and Mackie K (2005) The cannabinoid agonist WIN55,212-2 increases intracellular calcium via CB1 receptor coupling to Gq/11 G proteins. Proc Natl Acad Sci U S A. 102(52):19144-9.

128. Lauckner JE, Jensen JB, Chen HY, Lu HC, Hille B and Mackie K (2008) GPR55 is a cannabinoid receptor that increases intracellular calcium and inhibits M current. Proc Natl Acad Sci U S A. 105(7):2699-704.

129. Henstridge CM, Balenga NA, Ford LA, Ross RA, Waldhoer M and Irving AJ (2008) The GPR55 ligand L-{alpha}-lysophosphatidylinositol promotes RhoA-dependent Ca2+ signaling and NFAT activation. FASEB J. 2008 Aug 29.

130. Overton HA, Babbs AJ, Doel SM, Fyfe MC, Gardner LS, Griffin G, Jackson HC, Procter MJ, Rasamison CM, Tang-Christensen M, Widdowson PS, Williams GM and Reynet C (2006) Deorphanization of a G protein-coupled receptor for oleoylethanolamide and its use in the discovery of small-molecule hypophagic agents. Cell Metab. 3(3):167-75.

131. Zhuang SY, Bridges D, Grigorenko E, McCloud S, Boon A, Hampson RE and Deadwyler SA (2005) Cannabinoids produce neuroprotection by reducing intracellular calcium release from ryanodine-sensitive stores. Neuropharmacology. 48(8):1086-96.

132. Isokawa M and Alger BE (2006) Ryanodine receptor regulates endogenous cannabinoid mobilization in the hippocampus. J Neurophysiol. 95(5):3001-11.

Fig. 1. A working model of PEA function in neurons. In Chapter2, receptors and metabolic enzymes involved in NAE signaling were identified using immunochemical methods. In addition, exposure of HT22 cells to oxidative stress increases the immunoreactivity of metabolic enzymes involved in NAE signaling. In chapter 3.1, I determined that treatment of HT22 cells with the NAE PEA reduces cellular proliferation possibly by reducing mitochondrial activity. In chapter 3.2, I determined that PEA protects HT22 cells from peroxidative stress. In chapter 3.3, I determined that PEA treatement leads to the nuclear translocation of Akt, pAkt and pERK1/2. In chapter 3.4, I determined that PEA treatment leads to the nuclear translocation of NFκB and NFATc4. In chapter 4.1 we determined that the HT22 cell model system expresses all three IP_3R subtypes with IP_3R2 being expressed predominantly in the nuclear envelope. In chapter 4.2, I determined that, in addition to IP_3Rs, HT22 cells express RyRs and cultured cortical neurons express IP3Rs and RyRs making the study of the effects of NAEs on intracellular Ca^{2+} signaling feasible. In chapter 5, I determined that PEA reduces Ca^{2+} release mediated by chemical depolarization with KCl. Overall the results of these studies suggest that there is a relationship between the neuroprotective effects of PEA, the ability of PEA to activate neuroprotective kinases and transcription factors, and the ability of PEA to reduce intracellular Ca^{2+} signaling mediated by depolarization. Cellular compartments are labeled with italicized blue text. The cellular activities and the proteins affected by PEA are indicated in red text. Red arrows indicate the proposed cellular effects of PEA treatment. The chapter numbers relevant to the information are enclosed in black boxes.

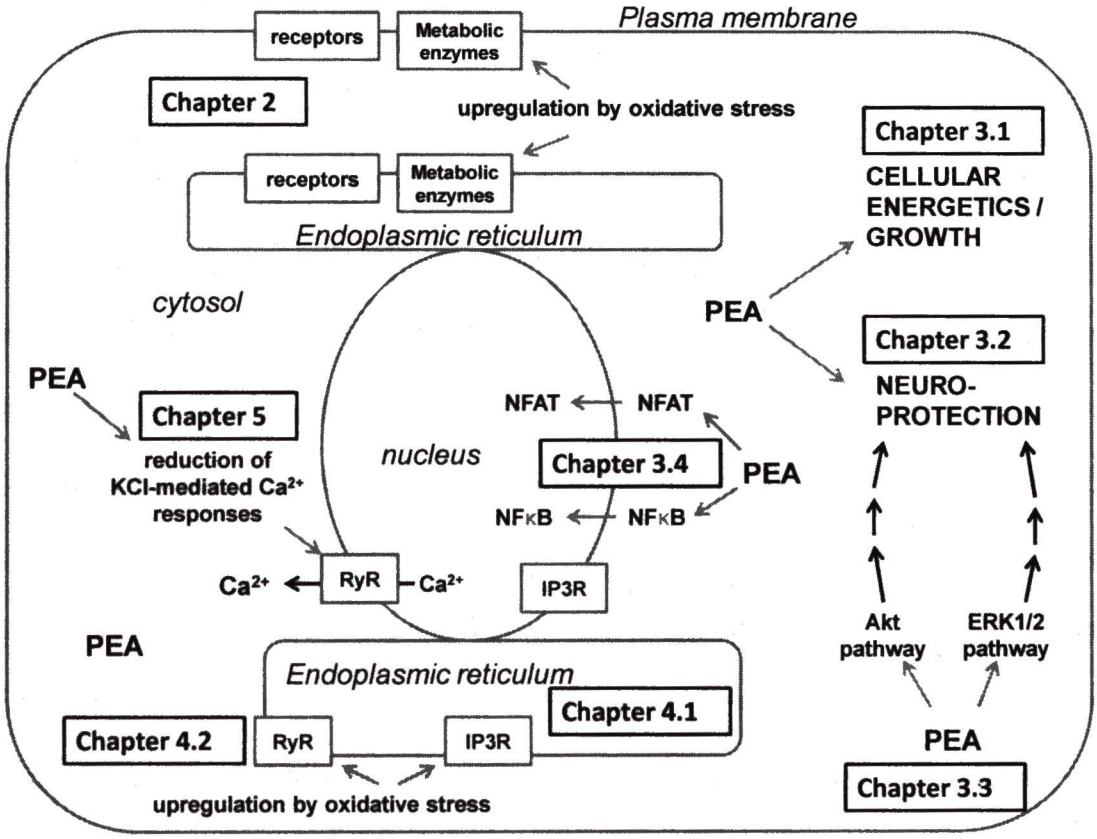
Plasma membrane
receptors
Metabolic enzymes
Chapter 2
upregulation by oxidative stress
receptors
Metabolic enzymes
Endoplasmic reticulum
cytosol
Chapter 3.1
CELLULAR ENERGETICS / GROWTH
PEA
Chapter 3.2
NEURO-PROTECTION
PEA
Chapter 5
reduction of KCl-mediated Ca2+ responses
nucleus
NFAT
NFAT
Chapter 3.4
PEA
NFκB
NFκB
Ca2+
RyR
Ca2+
IP3R
PEA
Akt pathway
ERK1/2 pathway
Endoplasmic reticulum
Chapter 4.1
Chapter 4.2
RyR
IP3R
PEA
Chapter 3.3
upregulation by oxidative stress

CHAPTER 2 – MODELS OF NEURODEGENERATION EXPRESS PROTEINS INVOLVED IN N-ACYLETHANOLAMINE SIGNALING

ABSTRACT

N-acylethanolamines (NAEs) are lipids produced in multiple cell types, including neurons, from a wide variety of organisms. In mammals, NAEs are involved in numerous cellular and physiological processes and their expression is upregulated in response to ischemia and physical trauma suggesting a role in neuroprotection (1-8). Anandamide (AEA), an endocannabinoid NAE, is an agonist at cannabinoid receptors (CB1 and CB2), vanilloid receptor 1 (VR1) and the nuclear transcription factor peroxisome proliferating antigen receptor gamma (PPARγ) (9-16). AEA and related compounds are neuroprotective in models of excitotoxicity, stroke and multiple sclerosis through activation of CB1 (17-22). Although the function of AEA has been well characterized, the function of the more abundant NAEs, such as palmitoylethanolamine (PEA), is unclear. Since all NAEs are synthesized and degraded by many of the same proteins, we hypothesize that other NAEs, such as PEA, are neuroprotective. The identification and co-expresion of NAE signaling proteins in our cell model systems of neurodegeneration will provide a rationale for conducting neuroprotection studies utilizing the less well characterized PEA. I hypothesized that all NAE target proteins are expressed in cortical neurons and HT22 cells, both of which have been used extensively to study neurodegeneration *in vitro* (23, 24). In addition, I hypothesized that oxidative stress would increase the expression of enzymes involved in NAE synthesis and degradation in these model systems. I detected the NAE signaling proteins CB1, CB2, VR1 and the NAE degrading enzyme, fatty acid amide hydroalse (FAAH) in our model systems. In addition, I determined that the less well characterized NAE synthesizing

enzyme N-acylphosphatidylethanolamine-hydrolyzing phospholipase D (NAPE-PLD) and the amidase N-acylethanolamine acid amidase (NAAA) are also expressed in these models. Furthermore, exposure of HT22 cells and cortical neurons to oxidative stress leads to an increase in NAPE-PLD, FAAH and NAAA immunoreactivity. These results lay the groundwork for establishing the role of less well characterized NAEs, such as PEA, and the NAE proteins NAPE-PLD and NAAA in commonly-used in vitro models of neurodegeneration and neuroprotection. In addition, this work identifies the molecular targets of NAEs for pharmacological interventions to be utilized in future neurodegeneration studies.

INTRODUCTION

N-acylethanolamines (NAEs) are bioactive lipids predominantly synthesized from membrane N-acylphosphatidylethanolamine (NAPE) precursors through the enzymatic action of N-acylphosphatidylethanolamine-hydrolyzing phospholipase D (NAPE-PLD) (25, 26). Degradation of NAEs occurs predominantly through the action of two amidase enzymes, fatty acid amide hydrolase (FAAH) and N-acylethanolamine acid amidase (NAAA) (27 - 29). The physiological function of only a small number of NAEs have been characterized including arachidonylethanolamine (AEA, anandamide) and, to a lesser extent, palmitoylethanolamine (PEA), oleoylethanolamine (OEA), linoleoylethanolamine (LOEA) and linolenoylethanolamine (LNEA) (9, 16, 30, 31).

AEA, an endocannabinoid, is involved in numerous physiological processes including neurotransmission, analgesia, reproduction, feeding, proliferation, inflammation and cytoprotection (32 – 36). AEA is an endogenous ligand for the cannabinoid receptor, the target

of tetrahydrocannabinols (THCs), the active components of marijuana (9, 37). There are currently two known cannabinoid receptors, CB1 and CB2, and anandamide activates both subtypes (9 – 11, 38 - 40). These receptors are seven transmembrane-spanning G-protein-coupled receptors that negatively couple to inhibitory G-proteins ($G_{i/o}$) thereby inhibiting adenylyl cyclase (10, 41 – 43). In the brain, cannabinoid receptors are expressed in numerous brain regions as well as cerebral vasculature (44 – 49). Recently, the CB2 receptor has been identifies in neurons in the brain suggesting that its classification as a peripheral cannabinoid receptor should be reevaluated (50).

Activation of CB1 and CB2 leads to a multitude of intracellular signaling events including the inhibition of adenylyl cyclase activity and subsequent inhibition of cAMP-dependent protein kinase (PKA) activity and activation of Akt/PKB, MAP kinase/ERK1/2 phosphorylation, and focal adhesion kinase (FAK) phosphorylation (51 – 59). Furthermore, cannabinoids inhibit N-, T- and P/Q-type Ca^{2+} currents and VR1-mediated Ca^{2+} influx in multiple cell models through activation of CB1 (60 – 65).

Numerous unsaturated NAEs, including AEA, OEA, LOEA and LNEA bind and activate vanilloid receptor 1 (VR1) cation channels, which are members of the transient receptor potential V (TRPV) channel family (12, 13, 16). The VR1 receptor is expressed in brain areas such as the hippocampus, cortex and cerebellum, and in the cerebral vasculature (66).

The saturated NAEs such as PEA do not activate CB1 (67). PEA is thought to be a CB2 agonist but it exhibits lower affinity and potency than other endogenous lipids making it an unlikely agonist for CB2 receptors (67, 68). PEA is thought to be mediate an 'entourage' effect by competing with AEA for FAAH and thus rendering AEA less prone to degradation (30, 31). The function of other non-cannabinoid NAEs, however, is poorly understood (17, 30, 67, 69).

Furthermore, it is not clear what the molecular target or targets for some NAEs are and which signaling pathways may be affected by the actions of non-cannabinoid NAEs. We hypothesize that non-cannabinoid NAEs are neuroprotective and the characterization of NAE target proteins, therefore, is critical in determining the possible mechanism of action in neuroprotection.

There is ample evidence demonstrating the neuroprotective effects of NAEs. Indirect evidence for NAE-mediated protection comes from numerous observations that NAPE and NAE synthesis is upregulated in response to multiple chemical and traumatic environmental insults, suggesting their possible role in cytoprotection (1-8). Direct evidence for NAE-mediated cytoprotection comes from multiple studies (17-22, 70). Little has been published on the molecular targets for and function of some NAEs in neurons, especially the saturated NAE PEA and monounsaturated OEA. Characterizing the presence and localization of known NAE signaling proteins in neurons will more effectively allow the study of the function of a wide variety of NAEs. Furthermore, carrying out this characterization in commonly-used *in vitro* models of neurodegeneration will help determine potential roles of some NAEs in neuroprotection or neurodegeneration. In the present study, I determined that cultured cortical neurons and HT22 cells express CB1, CB2, VR1, NAPE-PLD, FAAH and NAAA. In addition, I determined that oxidative stress leads to an increase in NAPE-PLD, FAAH and NAAA immunoreactivity. These results identify the molecular targets for pharmacological interventions in future neuroprotection studies using NAEs in these model systems.

MATERIALS AND METHODS

Antibodies

Rabbit anti CB1, CB2 and VR1 were purchased from EMD/Calbiochem (San Diego, CA) or Chemicon (Temecula, CA). Rabbit anti-NAPE-PLD and NAAA antibodies were purchased from EzBiolab (Westfield, IN). The NAPE-PLD and NAAA affinity purified antibodies were compared to the preimmune and precipitated sera to determine specificity.

Cell Culture

HT22 cells were grown and maintained at a moderate confluency (<60%) in Dulbecco's Modified Eagle's (DME) medium with 4.5g/mol glucose, 2mM glutamine, 1mM sodium pyruvate (Hyclone, Logan, UT) containing 10% heat-inactivated bovine growth serum (BGS) (Hyclone). Mouse primary cortical neurons were obtained from postnatal day 2 (P2) C57B/L6 mice. After removal of the scalp and skull cap, an approximately $1mm^3$ piece of frontal cortex was removed from each hemisphere and digested in 0.25% trypsin at 37°C for 20 min. The tissue was then briefly triturated with a fire-polished glass pipet or a disposable plastic pipet tip and centrifuged at 1,000 x g for 5 minutes. After removal of the trypsin, the resulting pellet was resuspended in complete media and triturated followed by centrifugation at 500 x g for 5 minutes. The pellet was triturated and centrifuged once more. The pellet was resusended in complete medium and passed through a 40μm cell strainer and the resulting cell suspension was plated onto a substrate appropriate for the given technique. Primary cortical neurons were maintained in Neurobasal A media with 2% donor horse serum (DHS), 2% B27 supplement and

penicillin-streptomycin-fungizone antibiotic for 10 – 14 days depending on suitable development of neurites.

Immunoblotting

Western blotting was conducted as described elsewhere (71). In brief, HT22 cell pellets were lysed in ice-cold cell lysis buffer (50mM Tris-HCl (pH 7.4), 150mM NaCl, 1mM EGTA, 1mM Na_3VO_4, 1mM NaF, 2% NP-40) with added protease inhibitor cocktail (Roche Diagnostics, Mannheim, Germany). Electrophoresis samples were denatured and run with prestained broad range molecular weight markers (BioRad, Hercules, CA) in either 4-15% gradient SDS polyacrylamide gels (BioRad, Hercules, CA) or freshly made 8% SDS-PAGE gels. Proteins were transferred from the gel to a PVDF membrane (Pall Life Sciences, Ann Arbor, MI), incubated in milk solution (5% powdered milk, 1% BSA, 0.005% tween-20 in phosphate-buffered saline; pH 7.4) and incubated overnight in primary antibody diluted in milk at 4° C. After washing three times in PBS, the membrane was incubated in milk solution containing horseradish peroxidase-labeled goat anti-rabbit or anti-mouse secondary antibody for 1 hour at room temperature in the dark. After washing, the membrane was developed using a chemiluminescent reagent kit (Super Signal West Dura, Pierce Biotechnology, Rockford, IL) followed by visualization using a UVP Epichemi 3 darkroom (UVP, Inc/, Upland, CA) with a mounted Hamamatsu C8484-51-03G camera (Hammamatsu, Japan) and LabWorks 4.5.0 software version 4.5.0 (UVP, Inc., Upland, CA).

Immunocytochemistry and immunofluorescence

Immunocytochemistry and immunofluorescence was conducted as described elsewhere (71). In brief, HT22 cells were grown for 24 - 48 hours to a density of <30% on poly-L-lysine-coated glass coverslips. Fixation of cells was carried out using 4% paraformaldehyde for 15 minutes followed by washing with PBS. After blocking with preincubation solution (10% normal goat serum, 1% BSA, 0.05% tween-20 in PBS) for 1 hour, primary antibodies diluted in incubation buffer (3% normal goat serum, 1% BSA, 0.05% tween-20 in PBS) were added to cells. Primary antibody incubation was carried out at 4°C overnight. After washing with PBS, fluorescent Alexa488- or Alexa594-labeled goat anti-rabbit or goat anti-mouse IgG secondary antibody (Invitrogen) diluted in incubation solution (1:1000) was applied to cells for 1 hour at room temperature. Coverslips were washed in PBS three times and mounted onto glass slides with ProLong anti-fade reagent with DAPI (Invitrogen) and stored at 4°C overnight. Image acquisition was conducted with an Olympus IX70 fluorescence microscope (Olymus, Japan) using 20X magnification. Images were saved into a 24-bit TIFF format.

Generation of Sublethal Oxidative Stress

HT22 cells on coverlips were treated with tert-butylhydroperoxide (tBHP) (Acros Organics, Geel, Belgium) at a concentration range of 2 - 10μM overnight (16 – 20 hours) prior to fixation with 4% PFA and subsequent immunocytochemistry. We have previously determined that tBHP concentrations at or below 10μM have no significant effect on HT22 cell viability.

Microfluorimetric Analysis of Images

Microfluorimetric analysis was conducted on TIFF images using Simple PCI (version 6.0) software (Compix). First, regions of interest within the soma of cells were selected followed by measurement of fluorescence intensity (greylevel). Data was exported into Microsoft Excel and graphed.

Densitometry

Densitometry of immunoblots was carried out using Lab Works version 4.0 software. First, a preset rectangular region was placed over each band consistent with the protein molecular weight followed by intensity measurement. The same was done for actin-labeled bands. Resulting numerical data were exported and graphed in Microsoft Excel as intensity of protein of interest over actin intensity.

Groups and Statistics

For all microfluorimetry experiments, five (5) microscope fields per treatment group were analyzed for NAPE-PLD, FAAH and NAAA. For NAPE-PLD, the number of cells analyzed for untreated, 2μM, 6μM, 10μM and 15μM tBHP groups was 98, 87, 95, 90 and 97 cells, respectively. For FAAH, the number of cells analyzed for untreated, 2μM, 6μM, 10μM and 15μM tBHP groups was 65, 98, 82, 111 and 104 cells, respectively. For NAAA, the number of cells analyzed for untreated, 2μM, 6μM, 10μM and 15μM tBHP groups was 101, 94, 68, 86 and 116 cells, respectively.

An F-test was conducted in Excel between each treatment group and the untreated control group to determine which type of T-test should be used for group comparisons. The mean fluorescence intensity from each treatment group was separately compared to the mean

fluorescence intensity of the untreated control group using a two-sample T-test with either equal or unequal variances.

RESULTS

Immunofluorescent detection of NAE signaling proteins in HT22 cells and primary cortical neurons

Both cannabinoid receptors, CB1 and CB2, are expressed in HT22 cells and mouse primary cortical neurons as demonstrated by indirect immunofluorescence and Western blot analysis (Figs. 1 and 2). Indirect immunofluorescence was used to determine the overall subcellular distribution of the CB1 and CB2 in both cell model systems.

In HT22 cells and cortical primary neurons, CB1 is predominantly expressed in the plasma membrane and in intracellular compartments such as the endoplasmic reticulum (ER) and the nuclear region (Fig. 1). In primary cortical neurons, CB1 is expressed in the soma and in neurites (Fig. 1). Western blot analysis reveals that in cortical tissue, an intense CB1 band appears at approximately 70 – 75 kDa and at 180 kDa (Fig. 1). The HT22 lysate lane reveals a very faint band at approximately 180 kDa (Fig. 1). Mouse CB1 has 473 amino acids and a calculated molecular weight of 53 kDa and an apparent MW of approximately 60 kDa with faint bands at approximately 23, 72 and 180 kDa (72). In addition, there is also a report of an apparent MW for CB1 of 45 – 50 kDa (73).

In both models systems CB2 exhibits a predominant intracellular localization with little or no labeling in the nuclear region (Fig. 2). Interestingly, CB2 immunoreactivity in HT22 cells is strongest intracellular regions or patches on two opposite sides (poles) of the cell (Fig. 2). There

has been some controversy about whether the so-called 'peripheral' cannabinoid receptor, CB2, is present in neurons. These results demonstrate the clear presence of CB2 immunoreactivity in neurons as well as in non-neuronal cells from the cortex. These findings support data from others demonstrating the presence of CB2 immunoreactivity in neurons (50). Western blot analysis reveals that both model systems exhibit a CB2 band at approximately 45 kDa and a faint band at approximately 50 kDa (Fig. 2). The HT22 cell lysate lane exhibits prominent CB2 bands at 30 kDa and 90 kDa (Fig. 2). Mouse CB2 has 347 amino acids and a calculated molecular weight of 38 kDa (NCBI). Apparent molecular weights of approximately 45 and 63 kDa are reported for CB2 (Calbiochem).

In addition, HT22 cells and mouse primary cortical neurons express VR1 as demonstrated by Western blot analysis (Fig. 3). Immunofluorescence was used to determine the overall subcellular distribution of the VR1 in both cell model systems. In both cell models, VR1 is predominantly expressed intracellularly with some plasma membrane expression (Fig. 3). Western blot analysis reveals that both models express VR1-immunoreactive bands (Fig. 3). The cortical lysate lane exhibits a faint band at approximately 95 KDa and stronger bands at 60 and 80 kDa (Fig. 3). The HT22 lysate lane exhibits predominant bands at approximately 150 kDa and doublet bands at 80 and 84 kDa (Fig. 3). The pattern of observed bands between the cortical lysate and HT22 lysate lanes is different, but each has bands at molecular weights observed by others (74). VR1 has 839 amino acids with a calculated molecular weight of 94.8 kDa (NCBI). Others have reported an apparent molecular weight for VR1 at approximately 100 kDa (Chemicon), 200 kDa and a doublet at 84/80 kDa (74).

NAPE-PLD, FAAH and NAAA are expressed in both cell culture model systems as determined by Western blot and immunofluorescence analysis. FAAH expression in both cell

models is predominantly intracellular as determined by immunofluorescence (Fig. 4). Western blot analysis reveals FAAH immunoreactive bands at 50 kDa with faint bands at 65 and 120 kDa in the HT22 lysate lane and bands at approximately 40, 55 and 120 kDa in the cortical tissue lane. FAAH has 579 amino acids with a calculated molecular weight of 63 kDa (NCBI). Others have reported a 60 – 65 kDa single band in COS cells overexpressing FAAH (27).

NAPE-PLD immunoreactivity in HT22 and primary cortical neurons is extremely weak suggesting either very weak expression levels or that the antibody is not suitable for use in immunocytochemistry (Fig. 5). HT22 cells and cultured cortical neurons exhibit very weak NAPE-PLD immunoreactivity as determined by indirect immunofluorescence. Cultured cortical neurons exhibit slightly better labeling than HT22 cells. NAPE-PLD immunoreactivity is faint in both cortical tissue and HT22 cell lysates. Both models exhibit a faint band at approximately 70 kDa. In addition, the HT22 cell lysate exhibits a more priominent band at 60 – 65 kDa. Mouse NAPE-PLD has 396 amino acids with a calculated molecular weight of 45.6 kDa (NCBI). The most prominent band shown above is at ~55 – 60 kDa with several other faint bands above and below.

NAAA expression in HT22 cells and primary cortical neurons is predominanatly intracellular (Fig. 6). HT22 cells and cultured cortical neurons exhibit weak NAAA immunoreactivity as determined by indirect immunofluorescence. Cultured cortical neurons exhibit more robust labeling that HT22 cells. NAAA immunoreactivity appears to be present predominantly in the ER/cytosolic compartment (Fig. 6). Western blot analysis reveals that cortical tissue and HT22 cell lysates exhibit positive immunoreactivity for NAAA (Fig. 6). In both model systems, a prominent band appears at approximately 25 and 40 kDa (fig. 6). Furthermore, a faint band is observed at 80 – 90 kDa in the HT22 lysate lane. Mouse NAAA has 362 amino acids with a

calculated molecular weight of 39.9 kDa (NCBI). The above blot indicates a prominent band at 39 – 45 kDa consistent with the calculated molecular weight.

Oxidative and Anoxic Insult Alters the Expression of Proteins Involved in NAE Synthesis and Degradation

Overnight exposure of HT22 cells to sublethal tBHP led to an increase in NAPE-PLD immunoreactivity (Fig. 7). Concentrations of tBHP between 2 and 10μM resulted in a similar increase in immunoreactivity whereas a 15μM tBHP exposure led to a further increase in immunoreactivity (Fig. 7). As a result, we conclude that, in HT22 cells, oxidative stress increases NAPE-PLD expression.

Overnight exposure of HT22 cells to sublethal tBHP led to a significant increase in FAAH immunoreactivity as tBHP concentrations approached toxic levels only (10 to 15μM) (Fig. 8). Overnight exposure of cultured primary cortical neurons to sublethal tBHP had no effect on FAAH immunoreactivity (Fig. 8). As a result, we conclude that, in HT22 cells, oxidative stress increases FAAH expression. In cultured primary cortical neurons, however, oxidative stress has no effect on FAAH expression.

Exposure of HT22 cells to sublethal tBHP leads to an increase in NAAA immunreactivity at tBHP concentrations approaching lethality (10 - 15μM) (Fig. 9). Western blot analysis on lysates from HT22 cells exposed to sublethal tBHP reveals that NAAA immunoreactivity is significantly increased in response to oxidative exposure. The top panel shows NAAA while the actin loading control in shown in the panel below.

DISCUSSION

Here, I report that two commonly-used cell model systems of neurodegeneration, HT22 cells and cultured mouse primary cortical neurons, express several proteins involved in NAE signaling. Specifically, I detected CB1, CB2, VR1, FAAH, NAAA and NAPE-PLD in these cell models using immunochemical methods. This data suggests that CB2 is expressed in HT22 cells and primary cortical neurons and, therefore, should be considered a receptor in the CNS. This study supports the findings from others that neurons express CB2, a receptor previously thought to be present only in non-neuronal tissue (50). In addition, I measured changes in NAAA immunoreactivity in response to oxidative stress further supporting the important role that the NAE signaling system plays in neurodegenerative diseases.

My data provides relevant information about both cannabinoid and non-cannabinoid proteins in two cell model systems of neurodegeneration. Experimental studies relevant to neurodegenerative diseases utilize the HT22 cells model system and mouse cortical neurons (23, 24). Since cannabinoids have gained a lot of attention as neuroprotectants in the last several years, determination of the protein targets for cannabinoids is important. Furthermore, there is interest in the function of non-cannabinoid NAEs as they relate to neuroprotection. Characterization of the relevant proteins involved in NAE signaling will determine what pharmacological interventions, if any, must be included in experimental studies seeking to elucidate the function of non-cannabinoid NAEs and to rule out the so-called entourage effects of some NAEs.

I used immunocytochemistry and indirect immunofluorescence to detect NAE signaling proteins. As always with immunocytochemistry, it is difficult to determine the specificity of

antibodies without use of a blocking peptide, which were not utilized in these studies. Antibodies used in this study, except for NAAA and NAPE-PLD, have been characterized and used by others (27, 72 - 74). To verify that the immunofluorescently-labeled proteins were indeed NAE proteins, I conducted Western blots on cell lysates using the same antibodies when possible. In most cases, a band either corresponding to the calculated molecular weight of the protein of interest or bands previously observed by and described by others appeared (27, 72 - 74). Since I used cortical tissue and not enriched neurons from culture for my Western blots, I can not definitively rule out the contribution of non-neuronal cells (glia) to the immunoreactivity.

Since a wide variety of NAEs are produced in response to toxic stimuli and the well-characterized NAE AEA exhibits neuroprotective properties, the NAE species that do not activate cannabinoid and vanilloid receptors also likely play a role in the neuroprotective process, albeit through a different mechanism of action (1 – 8, 17 – 22). This study underscores the need to include cannabinoid and vanilloid receptor antagonists when determining any potential non-cannabinoid/non-vanilloid effects of NAEs or similar compounds in these cell culture model systems. Furthermore, a pharmacological approach will determine if the mechanism of action for NAEs, such as PEA or OEA, act through the proposed AEA-enhancing entourage effect. It is not clear that this observed entourage effect is physiologically-relevant.

REFERENCES

1. Natarajan V, Schmid PC and Schmid HH (1986) N-acylethanolamine phospholipid metabolism in normal and ischemic rat brain. Biochim Biophys Acta. 1986 Aug 14;878(1):32-41.

2. Hansen HS, Lauritzen L, Strand AM, Moesgaard B and Frandsen A (1995) Glutamate stimulates the formation of N-acylphosphatidylethanolamine and N-acylethanolamine in cortical neurons in culture. Biochim Biophys Acta. 1258(3):303-8.

3. Hansen HS, Lauritzen L, Strand AM, Vingaard AM, Frandsen A and Schousboe A (1997) Characterization of glutamate-induced formation of N-acylphosphatidylethanolamine and N-acylethanolamine in cultured neocortical neurons. J Neurochem. 69(2):753-61.

4. Moesgaard B, Jaroszewski JW and Hansen HS (1999) Accumulation of N-acyl-ethanolamine phospholipids in rat brains during post-decapitative ischemia: a 31p NMR study. J Lipid Res. 40(3):515-21.

5. Moesgaard B, Petersen G, Jaroszewski JW and Hansen HS (2000) Age dependent accumulation of N-acyl-ethanolamine phospholipids in ischemic rat brain. A (31)P NMR and enzyme activity study. J Lipid Res. 41(6):985-90.

6. Hansen HH, Ikonomidou C, Bittigau P, Hansen SH and Hansen HS (2001) Accumulation of the anandamide precursor and other N-acylethanolamine phospholipids in infant rat models of in vivo necrotic and apoptotic neuronal death. J Neurochem. 76(1):39-46.

7. Schabitz WR, Giuffrida A, Berger C, Aschoff A, Schwaninger M, Schwab and Piomelli D (2002) Release of fatty acid amides in a patient with hemispheric stroke: a microdialysis study. Stroke. 33(8):2112-4.

8. Berger C, Schmid PC, Schabitz WR, Wolf M, Schwab S and Schmid HH (2004) Massive accumulation of N-acylethanolamines after stroke. Cell signalling in acute cerebral ischemia? J Neurochem. 88(5):1159-67.

9. Devane WA, Hanus L, Breuer A, Pertwee RG, Stevenson LA, Griffin G, Gibson D, Mandelbaum A, Etinger A and Mechoulam R (1992) Isolation and structure of a brain constituent that binds to the cannabinoid receptor. Science. 258(5090):1946-1949.

10. Vogel Z, Barg J, Levy R, Saya D, Heldman E and Mechoulam R (1993) Anandamide, a brain endogenous compound, interacts specifically with cannabinoid receptors and inhibits adenylate cyclase. J Neurochem. 61(1):352-355.

11. Felder CC, Joyce KE, Briley EM, Mansouri J, Mackie K, Blond O, Lai Y, Ma AL and Mitchell (1995) Comparison of the pharmacology and signal transduction of the human cannabinoid CB1 and CB2 receptors. Mol Pharmacol. 48(3):443-50.

12. Zygmunt PM, Petersson J, Andersson DA, Chuang H, Sorgard M, Di Marzo V, Julius D and Hogestatt ED (1999) Vanilloid receptors on sensory nerves mediate the vasodilator action of anandamide. Nature. 400(6743):452-457.

13. Smart D, Gunthorpe MJ, Jerman JC, Nasir S, Gray J, Muir AI, Chambers JK, Randall AD and Davis JB (2000) The endogenous lipid anandamide is a full agonist at the human vanilloid receptor (hVR1). Br J Pharmacol. 129(2):227-30.

14. Fu J, Gaetani S, Oveisi F, Lo Verme J, Serrano A, Rodriguez De Fonseca F, Rosengarth A, Luecke H, Di Giancomo B, Tarzia G and Piomelli D (2003) Oleylethanolamide regulates feeding and body weight through activation of the nuclear receptor PPAR-alpha. Nature. 425(6953):90-93.

15. Bouaboula M, Hilairet S, Marchand J, Fajas L, Le Fur G and Casellas P (2005) Anandamide induced PPARgamma transcriptional activation and 3T3-L1 preadipocyte differentiation. Eur J Pharmacol. 517(3):174-81.

16. Movahed P, Jonsson BA, Birnir B, Wingstrand JA, Jorgensen TD, Ermund A, Sterner O, Zygmunt PM and Hogestatt ED (2005) Endogenous unsaturated C18 N-acylethanolamines are vanilloid receptor (TRPV1) agonists. J Biol Chem. 280(46):38496-38504.

17. Skaper SD, Buriani A, Dal Toso R, Petrelli L, Romanello S, Facci L and Leon A (1996) The ALIAmide palmitoylethanolamide and cannabinoids, but not anandamide, are protective in a delayed postglutamate paradigm of excitotoxic death in cerebellar granule neurons. Proc Natl Acad Sci U S A. 93(9):3984-9.

18. Hansen HS, Moesgaard B, Petersen G and Hansen HH (2002) Putative neuroprotective actions of N-acyl-ethanolamines.Pharmacol Ther. 95(2):119-26.

19. Marsicano G, Goodenough S, Monory K, Hermann H, Eder M, Cannich A, Azad SC, Cascio MG, Gutierrez SO, van der Stelt M, Lopez-Rodriguez ML, Casanova E, Schutz G, Zieglgansberger W, Di Marzo V, Behl C and Lutz B (2003) CB1 cannabinoid receptors and on-demand defense against excitotoxicity. Science. 302(5642):84-8.

20. Kim SH, Won SJ, Mao XO, Jin K and Greenberg DA (2005) Involvement of protein kinase A in cannabinoid receptor-mediated protection from oxidative neuronal injury. J Pharmacol Exp Ther. 2005 Apr;313(1):88-94.

21. Van der Stelt M and DiMarzo V (2005) Cannabinoid receptors and their role in neuroprotection. Neuromolecular Med. 2005;7(1-2):37-50.

22. Shouman B, Fontaine RH, Baud O, Schwendimann L, Keller M, Spedding M, Lelievre V and Gressens P (2006) Endocannabinoids potently protect the newborn brain against AMPA-kainate receptor-mediated excitotoxic damage. Br J Pharmacol. 148(4):442-51.

23. Green PS, Gridley KE and Simpkins JW (1998) Nuclear estrogen receptor-independent neuroprotection by estratrienes: a novel interaction with glutathione. Neuroscience. 84(1):7-10.

24. Sagara Y and Schubert D (1998) The activation of metabotropic glutamate receptors protects nerve cells from oxidative stress. J Neurosci. 18(17):6662-71.

25. Di Marzo V, De Petrocellis L, Sepe N and Buono A (1996) Biosynthesis of anandamide and related acylethanolamides in mouse J774 macrophages and N18 neuroblastoma cells. Biochem J. 316 (Pt 3):977-84.

26. Petersen G and Hansen HS (1999) N-acylphosphatidylethanolamine-hydrolysing phospholipase D lacks the ability to transphosphatidylate. FEBS Lett. 455(1-2):41-4.

27. Giang DK, Cravatt BF (1997) Molecular characterization of human and mouse fatty acid amide hydrolases. Proc Natl Acad Sci U S A. 94(6):2238-42.

28. Ueda N, Puffenbarger RA, Yamamoto S and Deutsch D (2000) The fatty acid amide hydrolase (FAAH). Chem Phys Lipids. 108(1-2):107-21.

29. Ueda N, Tsuboi K and Lambert DM (2005) A second N-acylethanolamine hydrolase in mammalian tissues. Neuropharmacology. 48(8):1079-85.

30. Jonsson KO, Vandervoorde S, Lambert DM, Tiger G and Fowler CJ (2001) Effects of homologues and analogues of palmitoylethanolamide upon the inactivation of the endocannabinoid anandamide. Br J Pharmacol. 133(8):1263-75.

31. Smart D, Jonsson KO, Vandervoorde S, Lambert DM and Fowler CJ (2002) 'Entourage' effects of N-acyl ethanolamines at human vanilloid receptors. Comparison of effects upon anandamide-induced vanilloid receptor activation and upon anandamide metabolism. Br J Pharmoacol. 136(3):452-8

32. Mazzari S, Canella R, Petrelli L, Marcolongo G and Leon A (1996) N-(2-hydroxyethyl)hexadecanamide is orally active in reducing edema formation and inflammatory hyperalgesia by down-modulating mast cell activation. Eur J Pharmacol. 300(3):227-236.

33. Fride E (2002) Endocannabinoids in the central nervous system--an overview. Prostaglandins Leukot Essent Fatty Acids. 66(2-3):221-33.

34. Parolaro D, Massi P, Rubino T and Monti E (2002) Endocannabinoids in the immune system and cancer. Prostaglandins Leukot Essent Fatty Acids. 66(2-3):319-32.

35. Riegel AC and Lupica CR (2004) Independent presynaptic and postsynaptic mechanisms regulate endocannabinoid signaling at multiple synapses in the ventral tegmental area. J Neurosci. 24(49):11070-8.

36. Eljaschewitsch E, Witting A, Mawrin C, Lee T, Schmidt PM, Wolf S, Hoertnagl H, Raine CS, Schneider-Stock R, Nitsch R and Ullrich O (2006) The endocannabinoid anandamide protects neurons during CNS inflammation by induction of MKP-1 in microglial cells. Neuron. 2006 Jan 5;49(1):67-79.

37. Devane WA, Dysarz FA 3rd, Johnson MR, Melvin LS and Howlett AC (1988) Determination and characterization of a cannabinoid receptor in rat brain. Mol Pharmacol. 34(5):605-613.

38. Matsuda LA, Lolait SJ, Brownstein MJ, Young AC and Bonner TI (1990) Structure of a cannabinoid receptor and functional expression of the cloned cDNA. Nature. 346(6284):561-564.

39. Kaminski NE, Abood ME, Kessler FK, Martin BR and Schatz AR (1992) Identification of a functionally relevant cannabinoid receptor on mouse spleen cells that is involved in cannabinoid-mediated immune modulation. Mol Pharmacol. 42(5):736-742.

40. Munro S, Thomas KL and Abu-Shaar M (1993) Molecular characterization of a peripheral receptor for cannabinoids. Nature. 365(6441):61-65.

41. Howlett AC, Bidaut-Russell M, Devane WA, Melvin LS, Johnson MR and Herkenham M (1990) The cannabinoid receptor: biochemical, anatomical and behavioral characterization. Trends Neurosci. 13(10):420-3.

42. Bidaut-Russell M, Devane WA and Howlett AC (1990) Cannabinoid receptors and modulation of cyclic AMP accumulation in the rat brain. J Neurochem. 55(1):21-6.

43. Bayewitch M, Avidor-Reiss T, Levy R, Barg J, Mechoulam R and Vogel Z (1995) The peripheral cannabinoid receptor: adenylate cyclase inhibition and G protein coupling. FEBS Lett. 375(1-2):143-147.

44. Herkenham M, Lynn AB, Little MD, Johnson MR, Melvin LS, de Costa BR and Rice KC (1990) Cannabinoid receptor localization in brain. Proc Natl Acad Sci U S A. 87(5):1932-6.

45. Herkenham M, Lynn AB, Johnson MR, Melvin LS, de Costa BR and Rice KC (1991) Characterization and localization of cannabinoid receptors in rat brain: a quantitative in vitro autoradiographic study. J Neurosci. 11(2):563-83.

46. Mailleux P, Parmentier M and Vanderhagen JJ (1992) Distribution of cannabinoid receptor messenger RNA in the human brain: an in situ hybridization histochemistry with oligonucleotides.Neurosci Lett. 143(1-2):200-4.

47. Matsuda LA, Bonner TI and Lolait SJ (1993) Localization of cannabinoid receptor mRNA in rat brain. J Comp Neurol. 327(4):535-50.

48. Buckley NE, Hansson S, Harta G and Mezey E (1998) Expression of the CB1 and CB2 receptor messenger RNAs during embryonic development in the rat. Neuroscience. 82(4):1131-49.

49. Pettit DA, Harrison MP, Olson JM, Spencer RF and Cabral GA (1998) Immunohistochemical localization of the neural cannabinoid receptor in rat brain. J Neurosci Res. 51(3):391-402.

50. Gong JP, Onaivi ES, Ishiguro H, Liu QR, Tagliaferro PA, Brusco A and Uhl GR (2006) Cannabinoid CB2 receptors: immunohistochemical localization in rat brain. Brain Res. 1071(1):10-23.

51. Bouaboula M, Poinot-Chazel C, Bourrie B, Canat X, Calandra B, Rinaldi-Carmona M, Le Fur G and Casellas P (1995) Activation of mitogen-activated protein kinases by stimulation of the central cannabinoid receptor CB1. Biochem J. 1995 Dec 1;312 (Pt 2):637-41.

52. Wartmann M, Campbell D, Subramaninan A, Burstein SH and Davis RJ (1995) The MAP kinase signal transduction pathway is activated by the endogenous cannabinoid anandamide. FEBS Lett. 359(2-3):133-6.

53. Bouaboula M, Poinot-Chazel C, Marchand J, Canat X, Bourrie B, Rinaldi-Carmona M, Calandra B, Le Fur G and Casellas P (1996) Signaling pathway associated with stimulation of CB2 peripheral cannabinoid receptor. Involvement of both mitogen-activated protein kinase and induction of Krox-24 expression. Eur J Biochem.237(3):704-711.

54. Derkinderen P, Toutant M, Burgaya F, Le Bert M, Siciliano JC, de Franciscis V, Gelman M and Girault JA (1996) Regulation of a neuronal form of focal adhesion kinase by anandamide. Science. 273(5282):1719-22.

55. Skalhegg BS and Tasken K (1997) Specificity in the cAMP/PKA signaling pathway. differential expression, regulation, and subcellular localization of subunits of PKA. Front Biosci. 2:d331-42.

56. Gomez del Pulgar T, Velasco G and Guzman M (2000) The CB1 cannabinoid receptor is coupled to the activation of protein kinase B/Akt. Biochem J. 347(Pt 2):369-73.

57. Derkinderen P, Toutant M, Kadare G, Ledent C, Parmentier M and Girault JA (2001) Dual role of Fyn in the regulation of FAK+6,7 by cannabinoids in hippocampus. J Biol Chem. 2001 Oct 12;276(41):38289-96.

58. Davis MI, Ronesi J and Lovinger DM (2003) A predominant role for inhibition of the adenylate cyclase/protein kinase A pathway in ERK activation by cannabinoid receptor 1 in N1E-115 neuroblastoma cells. J Biol Chem. 278(49):48973-80.

59. Derkinderen P, Valient E, Toutant M, Corvol JC, Enslen H, Ledent C, Trzaskos J, Caboche J and Girault JA (2003) Regulation of extracellular signal-regulated kinase by cannabinoids in hippocampus. J Neurosci. 23(6):2371-82.

60. Mackie K, Devane WA and Hille B (1993) Anandamide, an endogenous cannabinoid, inhibits calcium currents as a partial agonist in N18 neuroblastoma cells.Mol Pharmacol. 44(3):498-503.

61. Mackie K, Lai Y, Westenbroek R and Mitchell R (1995) Cannabinoids activate an inwardly rectifying potassium conductance and inhibit Q-type calcium currents in AtT20 cells transfected with rat brain cannabinoid receptor. J Neurosci. 15(10):6552-61.

62. Shen M and Thayer SA (1998) The cannabinoid agonist Win55,212-2 inhibits calcium channels by receptor-mediated and direct pathways in cultured rat hippocampal neurons. Brain Res. 1998 Feb 2;783(1):77-84.

63. Chemin J, Monteil A, Perez-Reyes E, Nargeot J and Lory P (2001) Direct inhibition of T-type calcium channels by the endogenous cannabinoid anandamide. EMBO J. 20(24):7033-40.

64. Nogueron MI, Porgilsson B, Schneider WE, Stucky CL and Hillard CJ (2001) Cannabinoid receptor agonists inhibit depolarization-induced calcium influx in cerebellar granule neurons. J Neurochem. 79(2):371-81.

65. Oshita K, Inoue A, Tang HB, Nakata Y, Kawamoto M and Yuge O (2005) CB(1) cannabinoid receptor stimulation modulates transient receptor potential vanilloid receptor 1 activities in calcium influx and substance P Release in cultured rat dorsal root ganglion cells. J Pharmacol Sci. 97(3):377-85.

66. Toth A, Boczan J, Kedei N, Lizanecz E, Bagi Z, Papp Z, Edes I, Csiba L and Blumberg PM (2005) Expression and distribution of vanilloid receptor 1 (TRPV1) in the adult rat brain. Brain Res Mol Brain Res. 135(1-2):162-8.

67. Lambert DM and Di Marzo V (1999) The palmitoylethanolamide and oleamide enigmas : are these two fatty acid amides cannabimimetic? Curr. Med. Chem. 6 (8):757-773.

68. Sugiura T, Kondo S, Kishimoto S, Miyashita T, Nakane S, Kodaka T, Suhara Y, Takayama H and Waku L (2000) Evidence that 2-arachidonoylglycerol but not N-palmitoylethanolamine or anandamide is the physiological ligand for the cannabinoid CB2 receptor. Comparison of the agonistic activities of various cannabinoid receptor ligands in HL-60 cells. J Biol Chem. 275(1):605-12.

69. Berdyshev EV, Schmid PC, Krebsbach RJ, Hillard CJ, Hunag C, Chen N, Dong Z and Schmid HH (2001) Cannabinoid-receptor-independent cell signalling by N-acylethanolamines.Biochem J. 360(Pt 1):67-75.

70. Parinandi NL and Schmid HH (1988) Effects of long-chain N-acylethanolamines on lipid peroxidation in cardiac mitochondria. FEBS Lett. 237(1-2):49-52.

71. Duncan RS, Hwang SY and Koulen P (2007) Differential inositol 1,4,5-trisphosphate receptor signaling in a neuronal cell line. Int J Biochem Cell Biol. 39(10):1852-62.

72. Gerard CM, Mollereau C, Vassart G and Parmentier M (1991) Molecular cloning of a human cannabinoid receptor which is also expressed in testis. Biochem J. 279 (Pt 1):129-34.

73. Shire D, Carillon C, Kaghad M, Calandra B, Rinaldi-Carmona M, Le Fur G, Caput D and Ferrara P (1995) An amino-terminal variant of the central cannabinoid receptor resulting from alternative splicing. J Biol Chem. 270(8):3726-31.

74. Rosenbaum T, Awaya M and Gordon SE (2002) Subunit modification and association in VR1 ion channels. BMC Neurosci. 2002 Mar 22;3:4.

FIGURES

Fig. 1 - Expression of CB1 in HT22 Cells and Mouse Cortical Neurons. Using indirect immunofluorescence, both HT22 cells and cultured mouse cortical neurons exhibit CB1 immunoreactivity (IR) in both the ER/cytosolic and nuclear compartments (scalebar is 25μm). Immunolabeling of CB1 in cortical neurons reveals prominent labeling of neurites. Western blot analysis reveals that in cortical tissue, an intense band appears at approximately 70 – 75 kDa and at 180 kDa. The HT22 lysate lane reveals a very faint band at approximately 180 kDa. Mouse CB1 has 473 amino acids and a calculated molecular weight of approximately 53 kDa (72). The expected molecular weight is indicated by the red arrow. The protein bands are reported to exhibit apparent molecular weights of approximately 60 kDa with faint bands at approximately 23, 72 and 180 kDa (Calbiochem). A report of an apparent molecular weight of 45 – 50 kDa also exist (73).

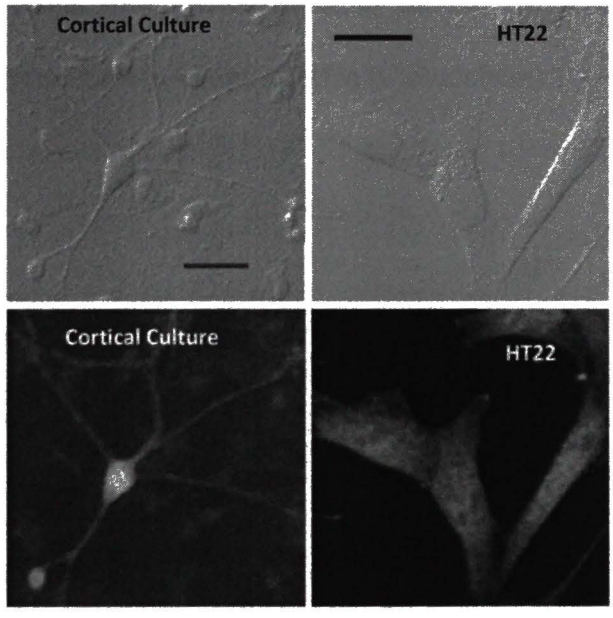

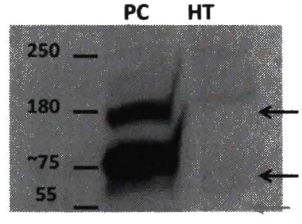

Green: CB1

Yellow:
CB1 + NeuN

Blue: DAPI

Fig. 2 - Expression of CB2 in HT22 Cells and Mouse Cortical Neurons. HT22 cells and culture mouse primary cortical neurons exhibit CB2 immunoreactivity predominantly in the ER/cytosolic compartment and not in the nuclear compartment (scalebar is 25μm). Western blot analysis reveals that both model systems exhibit a band at approximately 45 kDa and a faint band at approximately 50 kDa. The HT22 cell lysate lane exhibits prominent bands at 30 kDa and 90 kDa. Mouse CB2 has 347 amino acids and a calculated molecular weight of 38 kDa (NCBI). The expected molecular weight is indicated by the red arrow. CB2 also exhibits apparent molecular weights of approximately 45 and 63 kDa (Calbiochem).

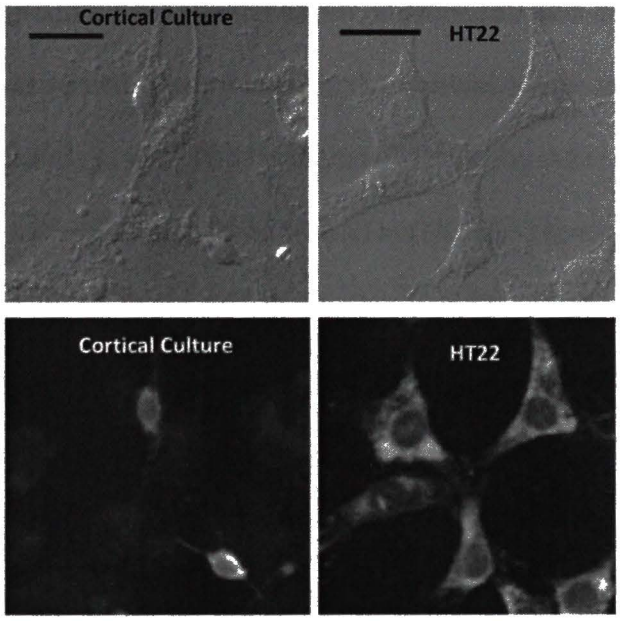

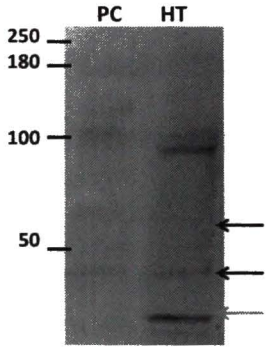

Green: CB2

Yellow/Orange: CB2 + NeuN

Blue: DAPI

Fig. 3 - Expression of VR1 in HT22 Cells and Mouse Cortical Neurons. HT22 cells and cortical neurons exhibit VR1 immunoreactivity predominantly in the ER/cytosolic compartment (scalebar is 10μm for primary neurons and 25μm for HT22 cells). Western blot analysis reveals that both models express VR1-immunoreactive bands. The cortical lysate lane exhibits a faint band at approximately 95 kDa and stronger bands at 60 and 80 kDa. The HT22 lysate lane exhibits a predominant band at approximately 150 kDa and doublet bands at 80 and 84 kDa. The pattern of observed bands between the cortical lysate and HT22 lysate lanes are different, but each have bands at molecular weights observed by others (74). VR1 has 839 amino acids with a calculated molecular weight of 94.8 kDa (NCBI). The expected molecular weight is indicated by the red arrow. An apparent molecular weight of approximately 100 kDa has been reported (Calbiochem), but the band in the image is approximately 90 - 95 kDa. A report from Rosenbaum et al. 2002 indicates apparent molecular weights of 200 kDa and 84/80 kDa (doublet) (74).

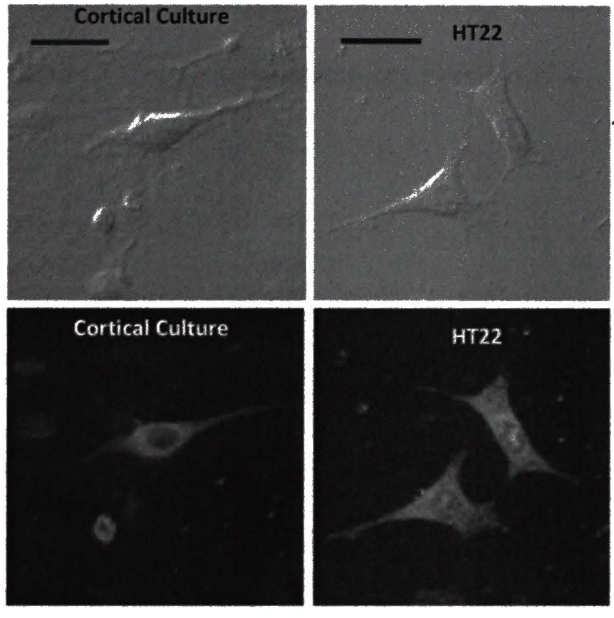

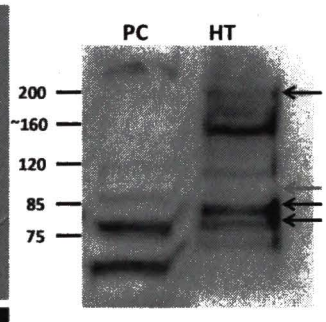

Green: VR1

Yellow/Orange: VR1 + NeuN

Blue: DAPI

Fig. 4 - Expression of FAAH in HT22 Cells and Mouse Cortical Neurons. HT22 cells and cortical neurons exhibit FAAH immunoreactivity predominantly in the ER/cytosolic compartment as determined by immunofluorescence (scalebar is 25μm). Western blot analysis reveals FAAH immunoreactive bands at 50 kDa with faint bands at 65 and 120 kDa in the HT22 lysate lane and bands at approximately 40, 55 and 120 kDa in the cortical tissue lane. FAAH has 579 amino acids with a calculated molecular weight of 63 kDa (NCBI). The expected molecular weight is indicated by the red arrow. A report from Giang et al. 1997 indicates a 60 – 65 kDa single band in COS cells overexpressing FAAH (27).

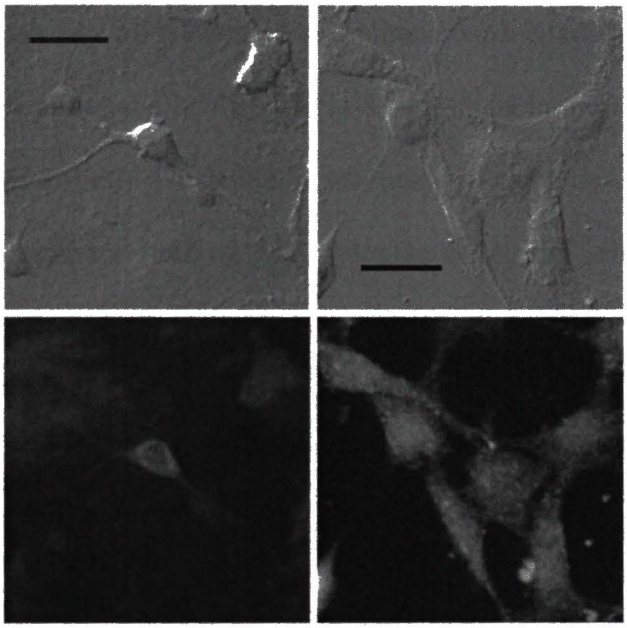

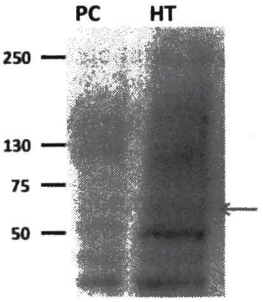

Green: FAAH

Yellow/Orange: FAAH + NeuN

Blue: DAPI

Fig. 5 - Expression of NAAA in HT22 Cells and Mouse Cortical Neurons. HT22 cells and cultured cortical neurons exhibit weak NAAA immunoreactivity as determined by indirect immunofluorescence (scalebar is 25μm). Cultured cortical neurons exhibit more robust labeling that HT22 cells. NAAA immunoreactivity appears to be present predominantly in the ER/cytosolic compartment. Western blot analysis reveals that cortical tissue (1) and HT22 cell lysates (10,000 x g pellet, 2 and 10,000 x g supernatant, 3) exhibit positive immunoreactivity for NAAA. In both model systems, a prominent band appears at approximately 25 and 40 kDa. Furthermore, a faint band is observed at 80 – 90 kDa in the HT22 lysate lane. Mouse NAAA has 362 amino acids with a calculated molecular weight of 39.9 kDa (NCBI). The above blot indicates a prominent band at 39 – 45 kDa consistent with the calculated molecular weight (arrow).

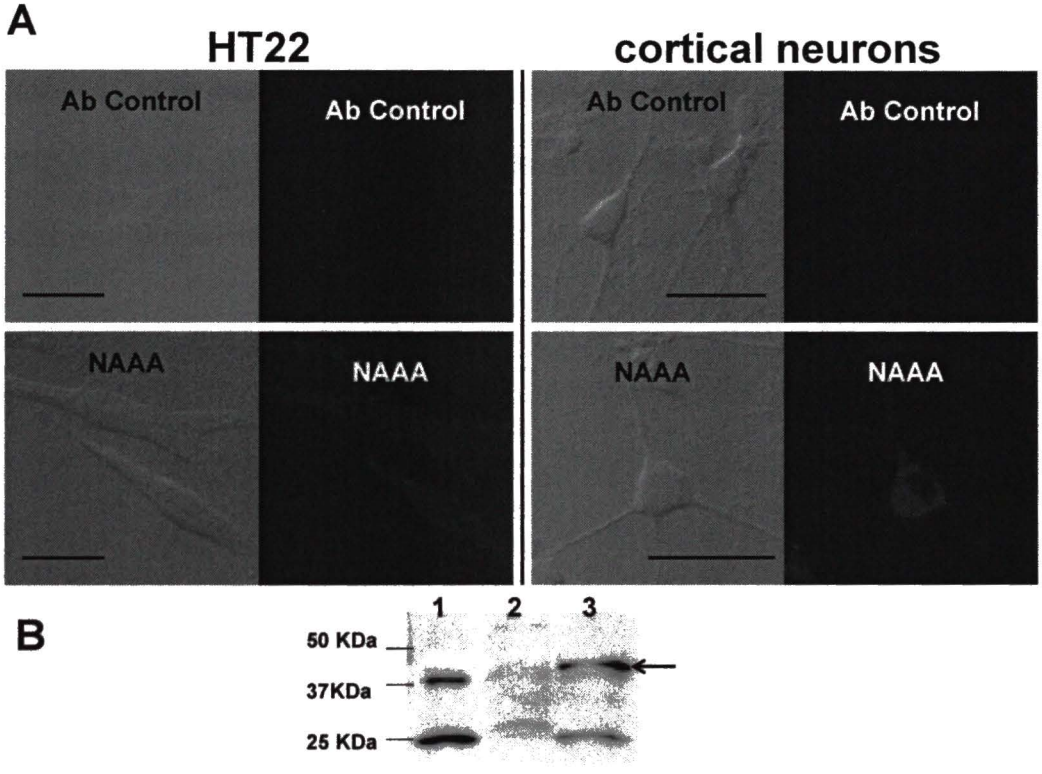
A
HT22
cortical neurons
Ab Control
Ab Control
Ab Control
Ab Control
NAAA
NAAA
NAAA
NAAA
B
1
2
3
50 KDa
37KDa
25 KDa

Fig. 6 - Expression of NAPE-PLD in HT22 Cells and Mouse Cortical Neurons. HT22 cells and cultured cortical neurons exhibit very weak NAPE-PLD immunoreactivity as determined by indirect immunofluorescence (scalebar is 25μm). Cultured cortical neurons exhibit slightly better labeling than HT22 cells. NAPE-PLD immunoreactivity is faint in both cortical tissue (1) and HT22 cell lysates (10,000 x g pellet, 2 and 10,000 x g supernatant, 3). Both models exhibit a faint band at approximately 70 kDa. In addition, the HT22 cell lysate exhibits a more prominent band at 60 – 65 kDa. Mouse NAPE-PLD has 396 amino acids with a calculated molecular weight of 45.6 kDa (NCBI) (arrow). The most prominent band shown above is at approximately 55 – 60 kDa with several other faint bands above and below.

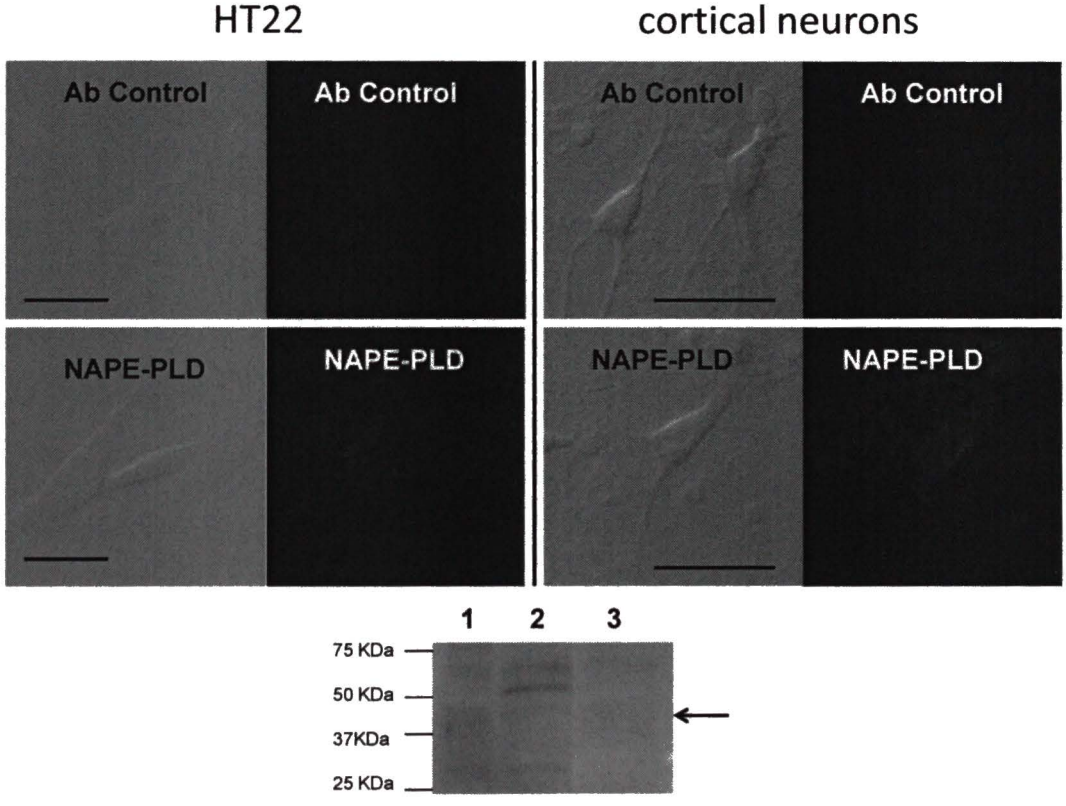
HT22
cortical neurons
Ab Control
Ab Control
Ab Control
Ab Control
NAPE-PLD
NAPE-PLD
NAPE-PLD
NAPE-PLD
1
2
3
75 KDa
50 KDa
37KDa
25 KDa

Fig. 7 - Exposure of HT22 Cells to Oxidative Stress Increases NAPE-PLD Immunoreactivity. Exposure of HT22 cells to overnight sublethal tBHP leads to an increase in NAPE-PLD immunreactivity as detmined by microfluorimetry. Five (5) microscope fields per treatment group were analyzed for NAPE-PLD. The number of cells analyzed for untreated, 2μM, 6μM, 10μM and 15μM tBHP groups was 98, 87, 95, 90 and 97 cells, respectively; * = $\leq$ 0.05, *** = $\leq$ 0.001.

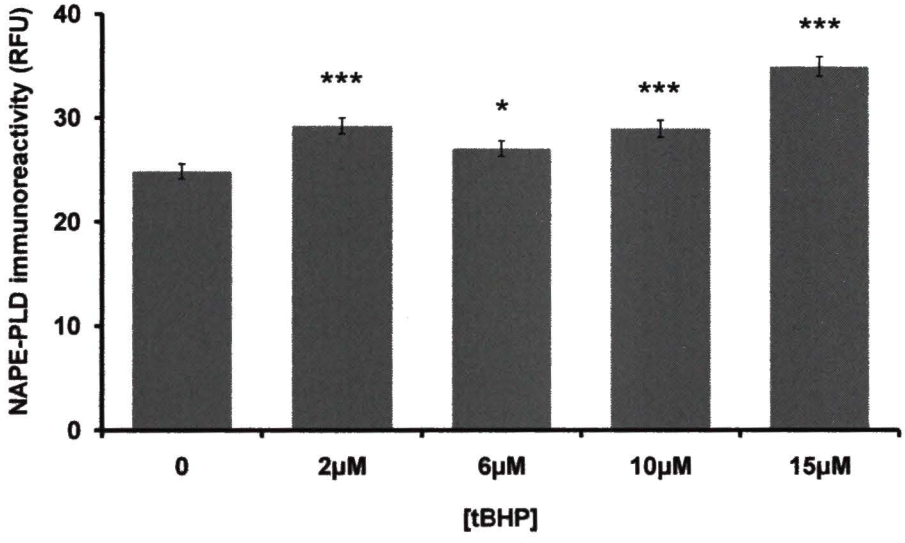
NAPE-PLD immunoreactivity (RFU)
40
30
20
10
0
***
*
***
***
0
2μM
6μM
10μM
15μM
[tBHP]

Fig. 8 - Exposure of HT22 Cells to Oxidative Stress Increases FAAH Immunoreactivity. Exposure of HT22 cells to overnight sublethal tBHP leads to an increase in FAAH immunreactivity as determined by microfluorimetry. Five (5) microscope fields per treatment group were analyzed for FAAH. The number of cells analyzed for untreated, 2μM, 6μM, 10μM and 15μM tBHP groups was 65, 98, 82, 111 and 104 cells, respectively; *** = ≤ 0.001.

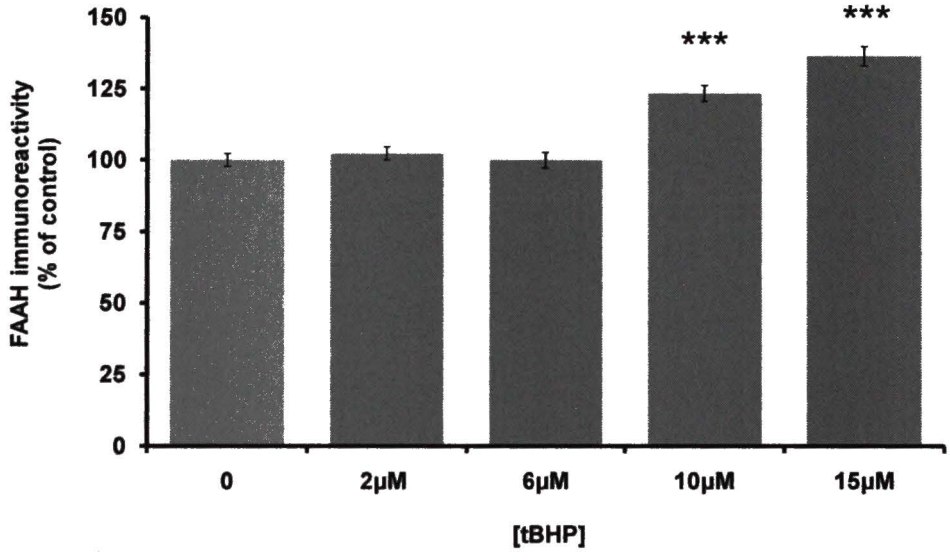
150
125
100
75
50
25
0
FAAH immunoreactivity
(% of control)
***
***
0
2μM
6μM
10μM
15μM
[tBHP]

Fig. 9 - Exposure of HT22 Cells to Oxidative Stress Increases NAAA Immunoreactivity. (A), Exposure of HT22 cells to overnight sublethal tBHP leads to an increase in NAAA immunreactivity as detmined by microfluorimetry. (B), Western blot analysis on lysates from HT22 cells exposed to sublethal tBHP reveals that NAAA immunoreactivity is significantly increased in response to oxidative exposure. The top panel shows NAAA while the actin loading control in shown in the panel below. Five (5) microscope fields per treatment group were analyzed for NAAA. The number of cells analyzed for untreated, 2μM, 6μM, 10μM and 15μM tBHP groups was 101, 94, 68, 86 and 116 cells, respectively; ** = ≤ 0.01, *** = ≤ 0.001.

A

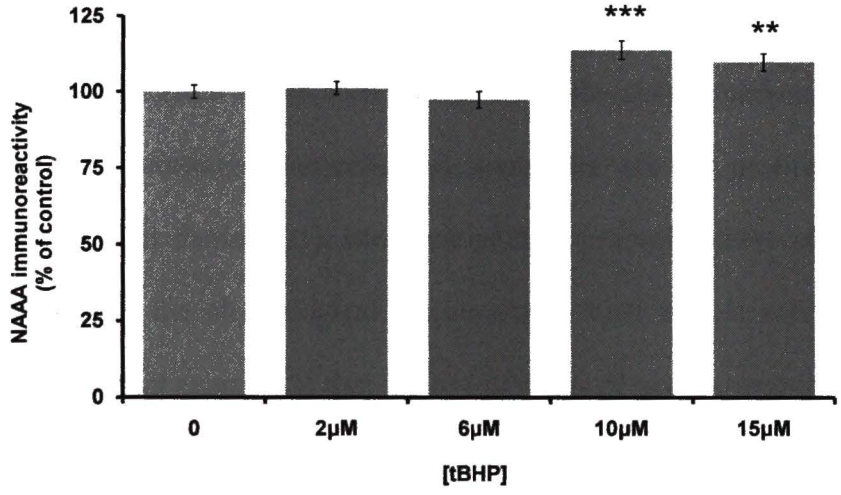
125
100
75
50
25
0
NAAA immunoreactivity
(% of control)
***
**
0
2μM
6μM
10μM
15μM
[tBHP]

B

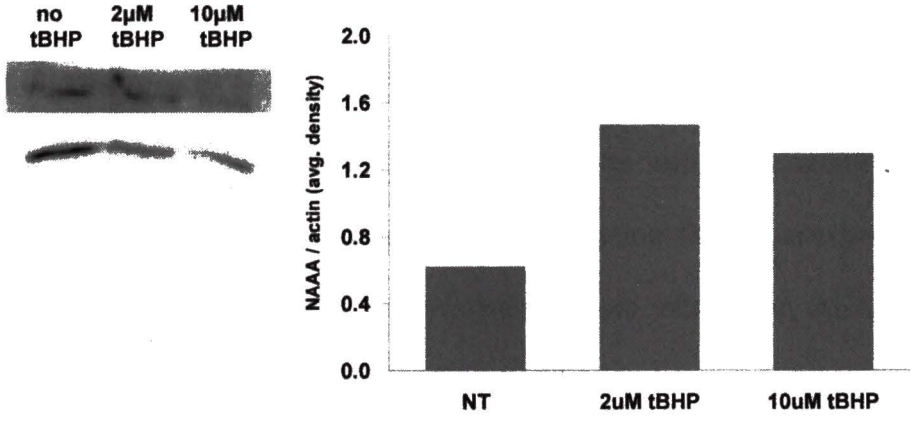
no
tBHP
2μM
tBHP
10μM
tBHP
2.0
1.6
1.2
0.8
0.4
0.0
NAAA / actin (avg. density)
NT
2uM tBHP
10uM tBHP

CHAPTER 3.1 – ANTIPROLIFERATIVE AND APOPTOTIC EFFECTS OF NAEs IN HT22 CELLS AND PRIMARY CORTICAL NEURONS

ABSTRACT

Cellular proliferation is a process involved in normal growth and development of an organism as well as in pathophysiological states such as cancer. In the central nervous system, neurons, with the exception of neuroprogentior cells and stem cells, are not proliferative and do not regenerate themselves after damage (1). Proliferative and antiproliferative effects of drugs are important in determining the physiological consequences such as cell survival in models of disease. One such important example is that the use of drugs of neuroprotection studies utilizing proliferative cell lines of neuronal origin. The effective chemical insults often used in neuroprotection studies, such as peroxides, depend upon cellular density. It stands to reason that if a compound exhibits antiprolerative effects, cells may become more vulnerable to the toxic effects of the insult. Over the last several years, the multiple functions of cannabinoids and the function of proteins that they interact with have become much clearer and have received a great deal of attention. The putative endogenous cannabinoid (endocannabinoid) anandamide (AEA) is a partial agonist at cannabinoid receptors (CB1 and CB2) as well as an agonist at the transient receptor potential V1 (TRPV1) channel and the transcription factor peroxisome proliferator-activated receptor γ (PPARγ) (2 - 7). N-acylethanolamines, other than AEA, are much less understood. For example, the saturated NAE palmitoylethanolamine (PEA) contentiously is thought to be a ligand of the type 2 cannabinoid receptor (CB2) (8, 9). In addition, the AEA-enhancing entourage effects of PEA make its function more challenging to study (10, 11). Many other NAE species exist and most do not have appreciable affinity for CB1, CB2 or VR1. The

neuroprotective effects of NAEs in models of epilepsy, ischemia and neuroinflammation make them significant to study (12 – 17). In order to determine any putative effects of the less well characterized NAEs, such as PEA and SEA, it is first necessary to determine if these NAEs themselves have antiproliferative or toxic effects. I hypothesized that PEA decreases HT22 cell proliferation. In this study, I determined that PEA reduces HT22 cell proliferation and has no significant effect on HT22 viability. These studies lay the groundwork for better understanding the potential neuroprotective effects that non-cannabinoid NAEs have in neurodegenerative diseases.

INTRODUCTION

The N-acylethanolamines (NAEs) are lipids involved in signal transduction in a wide variety of cells (2 – 11). The best characterized and most studied NAE is arachidonylethanolamine (AEA) or anandamide. AEA was shown to be one of the endogenous ligands for the cannabinoid receptor, the target of the psychoactive constituent of marijuana, tetrahydrocannibinols (THCs) (2, 18).

Interestingly, AEA levels in a variety of tissues including the brain are relatively low compared to other NAE species such as PEA (19, 20). NAE precursor synthesis is differentially affected by apotosis and necrosis (21). For example, NMDA-induced excitotoxicty results in increased levels of all NAPE species (22). Work in macrophages has shown that the NAE palmitoylethanolamine (PEA) has CB2 receptor-independent effects (23) and others propose that PEA does not activate CB2 (24, 25).

AEA stimulates the proliferation of hemopoetic cells (26, 27) and it also affects mast cells and macrophages (28). Cannabinoids have exhibited some antiproliferative effects in cancer cells and

are variable and depend greatly upon cell type. Their influence on proliferation also differs between the endogenous, plant and synthetic cannbinoids. AEA inhibits proliferation of the breast cancer cell lines MCF-7 and EFM-19 by a CB1-mediated mechanism (29). AEA antiproliferation through CB1 led to the reduced expression of the prolactin receptor, which is involved in proliferation of these cancer cell lines (29) and this outcome is dependent upon inhibition of PKA and activation of the MAPK pathway (30). In addition, AEA inhibits proliferation of human breast cancer cells by inhibiting Cdk2, thus inducing cell cycle arrest (31). AEA also inhibits cell adhesion and migration of human breast cancer cells through a possible mechanism involving CB1 receptor modulation of focal adhesion kinase (FAK) (32). The proliferation of the C6 glioma cell line is inhibited by AEA and 2-AG (33).

The effect of PEA on cell proliferation is different from that observed for AEA. There my knowledge is no evidence of PEA directly reducing cellular proliferation except through probable AEA-enhancing entourage effects. For example, exposure of human breast cancer cells to PEA (up to 10μM) enhances the antiproliferative effects of VR1 agonists (34). PEA, itself, has no effect on proliferation but acts to affect proliferation through entourage effects (34). Another study showed that prolonged PEA treatment resulted in reduced FAAH expression resulting in AEA-induced human breast cancer cell proliferation (35). PEA, unlike AEA, had no effect on C6 glioma cell proliferation (36).

Here, I provide evidence that PEA reduces the proliferation of the murine hippocampal cell line, HT22. This analysis is significant because HT22 cells are a widely-used for neuroprotection studies. Furthermore, cell density may be a critical factor in cellular vulnerability to toxic agents used in models of neurodegenerative diseases such as oxidative stress. Previous observations show that cell density renders HT22 cells more sensitive to tert-butylhydroperoxide (tBHP)

toxicity. The data presented here suggest that reduced cellular proliferation may need to be taken into account when determining potential neuroprotective effects of PEA in a proliferative cell line such as HT22.

MATERIALS AND METHODS

Chemicals

Palmitoylethanolamine (PEA) was purchased from Alexis Biochemicals (Switzerland). Linolenoylethanolamine was purchased from Sigma (St. Louis, MO). Lauroylethanolamine (LEA) was provided by Kent Chapman at the University of North Texas, Denton, TX. JWH-015, AM-1242 and AM-630 was purchased from Alexis Biochemicals. Calcein-acetoxymethyl ester (AM) was purchased from Alexis Biochemicals or EMD/Calbiochem. 5-(and-6)-carboxy-2',7'-dichlorodihydrofluorescien diacetate (CH_2DCFDA) was purchased from (Invitrogen/Molecular Probes).

Cell culture

HT22 were cultured as described previously (Duncan et al. 2007). In brief, HT22 cells were grown in DMEM with high glucose and 1mM sodium pyruvate (Mediatech), 2mM Glutamax (Invitrogen), 5% bovine growth serum (BGS) (Hyclone) and peniciilin-streptomycin (Mediatech). Cultures were kept at a confluency of less than 70% during the culturing process. Cells were removed from flasks during routine culturing by using either 0.25% trypsin in EBSS without Ca^{2+} and with EGTA (Hyclone) or cell lifting buffer (Hank's balanced salt solution without Ca^{2+} or Mg^{2+} (Hyclone) with 1mM EGTA).

Assessment of cellular proliferation

The fluorimetric calcein-AM and colorimetric MTT assays were conducted in 96 well plates in order to assess cell proliferation in a high-throughput format. All 96 well plate assays for HT22 cell proliferation were conducted using a cell density of 2,000 – 5,000 cells/well. Calcein-AM fluorescence was measured using a fluorimetric plate reader (Perkin-Elmer Victor^3) with filters accommodating 485nm excitation and 530nm emmission light. The MTT assay was measured at an absorbance wavelength of 560nm using the same plate reader.

Cell counts were carried out using a hemocytometer by counting at least three separate 1mm^2 fields and averaging the counts. HT22 cells were grown in 25cm^2 flasks and treated with either 0.67% EtOH or 100μM PEA for 16 -24 hours. After this preincubation time, cells were split into 96 well plates at a density of 4,000 cells/well and incubated for 6 hours. After the brief incubation, cells from both groups (EtOH or PEA pretreated groups) were treated with 100μM PEA overnight. A calcein-AM and MTT assay was conducted to determine if there were differences between the two groups. Alternatively, after incubation overnight in 100μM PEA, cells were trypsinized and counted using a hemocytometer. These cells were then plated into black-walled 96 well plates at 20,000 cells/ml and, 5 – 6 hours later, treated again with either 0.67% EtOH or 100μM PEA overnight.

Assessment of oxidative stress

HT22 cells were plated in 96 well plates at 20,000 cells/ml and grown overnight. The cells were then loaded with 10μM CH_2DCFDA for 45 minutes, washed and then treated for 5 hours with PEA or palmitate (PA) at 10, 50 and 100μM concentrations. The cells were then rinsed and CH_2DCFDA fluorescence was read in a fluorimetric plate reader (Perkin-Elmer Victor^3) with filters accommodating 485nm excitation and 530nm emmission light. CH_2DCFDA fluorescence

was measured after 5 hours to determine if PEA (or PA) alone has an effect on the oxidative status in HT22 cells. As a control, 50 and 100μM tBHP for 5 hours was included in the same plate as a control for oxidative stress in the assay. Furthermore, a separate plate of HT22 cells was insulted (for 5 hours) with tBHP concentrations from 5μM to 200μM to verify the dose-dependent increase in CH_2DCFDA fluorescence elicited by tBHP.

Statistics

An F-test was conducted in Excel between each treatment group and the untreated control group to determine which type of T-test should be used for group comparisons. The mean fluorescence intensity from each treatment group was separately compared to the mean fluorescence intensity of the untreated control group using a two-sample T-test with either equal or unequal variances. A P-value of less than or equal to 0.05 was considered significant.

RESULTS

Assessment of HT22 Proliferation after PEA Exposure

Treatment of HT22 cells overnight (16 – 20 hours) with PEA (from 20 to 120μM) leads to a slight reduction in calcein-AM fluorescence, which only reaches statistical significance at 20μM and 120μM concentrations (Fig. 1A). As a result, it can be concluded that reduction in fluorescence mediated by PEA does not exhibit a dose-dependent effect. Overnight treatment of HT22 cells with other NAEs such as linolenoylethanolamine (LLEA) at concentrations from 5 – 50μM lead to a slight reduction in calcein-AM fluorescence (Fig. 1B). PEA treatment of HT22 cells leads to a dramatic decrease in MTT reduction indicating that PEA is either toxic or it alters mitochondrial activity (Fig. 3A). Microscopic observation of PEA treated cells prior to or during

MTT loading provides no evidence for a toxic effect of PEA as cells exhibit normal morphology (data not shown).

Work from others suggests that PEA is an endogenous ligand at CB2 receptors (2, 3). To rule out any effects of PEA at $G_{i/o}$-coupled CB2 receptors, we conducted calcein-AM and MTT assays on HT22 cells treated with the CB2 receptor agonists JWH-015 and AM1241. Treatment of HT22 cells with JWH-015 or AM1241 was not able to mimic the effects of PEA on calcein-AM fluorescence or MTT absorbance (Fig. 2 and 3, respectively). Interestingly, JWH-015 within a concentration range from 0.1 to 10μM has no significant effect on MTT absorbance (Fig. 3B). In fact, AM1241 at 0.1 to 1μM had no effect on MTT absorbance, but at 10μM, it dramatically and significantly increased MTT absorbance, suggesting that PEA effects on MTT reduction by mitochondria are the opposite for that observed for AM1241 (Fig. 3B). PEA is considered a weak partial agonist at CB2, whereas JWH-015 and AM1241 are considered potent selective agonists at CB2. It stands to reason that, if the anitproliferative effects of PEA were mediated through activation of CB2, then JWH-015 and AM1242 treatment would be expected to yield similar results and likely even greater effects than measured for PEA.

In addition, HT22 cells were treated with PEA in the presence or absence of the potent and selective CB2 antagonist AM630. Treatment of cells with AM630 was not able to block or reverse the PEA-mediated reduction in calcein-AM fluorescence (data not shown). In fact, AM-630 treatment alone results in a trend toward an increase in calcein-AM fluorescence which is the opposite effect measured for PEA (data not shown). Treatment with AM-630 has no significant effect on MTT reduction in HT22 cells and it does not block PEAs ability to significantly decrease MTT reduction.

Cells pretreated overnight with 100μM PEA exhibit no significant change in cell number as determined by hemocytometer counts compared to the vehicle controls (101,250 cells/ml for vehicle versus 130,000 for 100μM PEA pretreated) (Fig. 4A). The calcein-AM results for the same cells replated at the same density and retreated overnight with PEA reveal that the PEA-treated cells were much more 'sensitive' to a second exposure of PEA than vehicle treated cells (Fig. 4B). These results suggest that the putative antiproliferative effects of PEA may take several hours to appear thus affecting the calcein-AM assay on the second day more that the cell counts on the first.

Subsequent hemocytomoeter counts demonstrated that there was a trend toward a decrease in cell number for the PEA-pretreated cells (~25% decrease) compared to the vehicle-treated cells, but this decrease was not statistically significant (Fig. 5). Calcein-AM results suggest that, for the vehicle-treated group, PEA treatment results in a slight decrease in cell number compared to the vehicle-treated group, but the decrease failed to reach statistical significance (Fig. 5). For the PEA-treated group, however, PEA-retreatment resulted in a significant decrease (~17% decrease) in calcein-AM fluorescence compare to the vehicle-treated control group (Fig 5). These provide evidence for an antiproliferative effect for PEA that takes several hours to take effect. Furthermore, these results do not support the view that PEA treatment 'removes' a PEA-sensitive subpopulation of HT22 cells thereby resulting in PEA-resistant cells.

In addition, exposure of HT22 cells to 50 and 100μM PEA for 72 hours results in a dramatic and significant decrease in cell number as determined by hemocytomoeter counts (Fig. 6). The EtOH vehicle-treated cells went from 100,000 cells/ml to over 1,350,000 cells/ml in 72 hours. The PEA-treated cells went from 100,000 cells/ml to no more than 290,000 cells/ml within the same period of time (Fig. 6). Overall, these results suggest that, after several hours of PEA

exposure, cell division begins to slow and after another day of exposure, cell division slows very significantly or ceases.

Assessment of HT22 Cell Death after PEA Exposure

To rule out possible apoptotic effects of NAEs on HT22 cells, cell viability assays were conducted on cells treated overnight with NEAs. Overnight incubation of HT22 cells with 10μM and 100μM LEA or 10μM and 100μM PEA did NOT cause any statistically-significant increase in HT22 apoptosis (TUNEL-labeling) (Fig. 7). Likewise, the number of attached cells (as determined by the number of DAPI-stained nuclei among the different treatment conditions) showed no significant difference (Fig. 7). There is no difference between vehicle and 100μM PEA-treated cells. Therefore, it is unlikely that these concentrations of NAEs cause appreciable apoptosis. The cell count data (quantitation of DAPI-labeled nuclei) rule out any significant cell loss. Furthermore, treatment of HT22 cells with PEA does not lead to elevated extracellular glucose-6 phosphate dehydrogenase activity, a marker for necrotic cell death (data not shown).

We determined whether treatment of HT22 cells with PEA results in oxidative stress, which is one indicator of cellular degeneration. HT22 cells loaded with the redox-sensitive fluorescent indicator dye, CH_2DCFA, and treated with 10 - 100μM PEA reveal that CH_2DCFDA fluorescence is slightly increased (+3.6%) by 100μM PEA (but not by 10 or 50μM PEA) (Fig. 8). This PEA-mediated increase in CH_2DCFDA fluorescence, however, is only a very small fraction of the increase elicited by toxic concentrations of tBHP (+3.6% versus +273%) (Fig. 8). In another experiment, oxidative insult of HT22 cells with 20μM tBHP for 5 hours results in a dramatic and significant increase in CH_2DCFDA fluorescence (204% increase) (data not shown).

This suggests that PEA (up to 100μM) likely does not cause significant oxidative stress and toxicity.

Work from others has revealed a strong connection between mitochondrial activity and cellular proliferation (38 - 40). Because PEA at high concentrations (100μM) reduces cell proliferation, calcein-AM fluorescence and MTT absorbance, but doesn't cause appreciable cell death, we thought that PEA may alter mitochondrial activity. To determine PEAs effects on HT22 mitochondrial membrane potential, cells were loaded with the dye MitoTracker Red. HT22 cells were treated with 100μM PEA for 5 hours and then loaded with MitoTracker Red for 45 minutes. Microscopic observation and subsequent microfluorimetric analysis revealed that PEA-treated cells exhibited reduced MitoTracker Red fluorescence compared to vehicle controls (Fig. 9).

DICSUSSION

Here I provide evidence that PEA exhibits antiproliferative effects in the hippocampal cell line HT22. Since neither a known antiproliferative compound nor a mitogen was used in any of the antiproliferation experiments with PEA, it is currently unclear whether PEA is a mild or potent antiproliferative compound. Nonetheless, these results indicate that caution must be taken when assessing any potential neuroprotective effects elicited by PEA in proliferative cell line population. Since PEA reduces cellular proliferation, a population of cells pretreated with it may be more vulnerable to oxidative stress or other insults. I have observed a relative decrease in HT22 cell viability at a low cell density when exposed to tBHP compared to when cells are at a higher cell density. As a result, any neuroprotective effect elicited by PEA may be

underestimated due to the antiproliferative effects on the overall population. It also stands to reason that a measureable protective effect by PEA in HT22 cells may be masked by antiproliferation. Since primary neurons are terminally differentiated, antiproliferative effects of PEA would not likely have an effect on cell population vulnerability to oxidant exposure. My findings also suggest that PEA may be an attractive compound to study for diseases where cellular proliferation plays a role in overall pathology, such as cancer.

In order to determine if the observed antiproliferative effects of PEA were due to activation of CB2, I treated HT22 cells with the CB2 agonists, JWH-015 and AM-1241 (Fig. 3). Treatement with these agonists did not mimic the antiproliferative effects of PEA, suggesting that CB2 activation is not involved in PEAs effect. In fact, the CB2 agonist JWH-015 had no effect on HT22 proliferation while AM-1241 increased cell proliferation. I did not, however, include a CB2 antagonist such as AM-630 with the CB2 agonists to verify that the effects of JWH-015 and AM-1241 were indeed due to CB2 activation and not activation of a yet undetermined receptor.

I utilized a PEA pretreatment followed by a retreatment paradigm to assess whether PEA is toxic or if it exhibits antiproliferative effects. If an overnight (16 – 20 hour) PEA exposure caused significant cell death, then presumably the cell number would be significantly lower and the cell morphology would be altered. This was not the case as determined by microscopic observations and cell counts. If, however, PEA was simply antiproliferative, then the initial overnight PEA treatment would result in a slow or gradual reduction in cellular proliferation which would further be reduced by a second exposure to PEA. Any antiproliferative effects of PEA should become more prominent after a longer time of exposure. My microscopic observations, cell counts and plate reader assays (calcein-AM and MTT assays) support an antiproliferative effect of PEA but do not support a toxic effect of PEA.

Cannabinoids have exhibited some pro-apoptotic effects in cancer cells. Cannabinoid-induced ceramide accumulation results in apoptosis of glioma cells (41). Treatment of prostate cancer cell lines with (AEA) results in reduced EGF receptor expression and EGF-mediated cell growth followed by cell death through a mechanism partially dependent upon ceramide production (42). The apoptotic effects of cannabinoids are also thought to occur through the activation of vanilloid receptor 1 (VR1) (43). Interestingly, activation of CB1 receptor can protect cells against cell death mediated by VR1 activation (43). In a cervical carcinoma cell line and glioma cell lines, AEA treatment results in apoptosis of cells expressing VR1 and activation of CB1 or CB2 protects these cells from cell death (44, 45). Since PEA does not directly activate VR1, it would not likely have the same effect as AEA.

In a neuroblastoma and lymphoma cell line, AEA treatment results in an increase in intracellular Ca^{2+} concentration, uncoupling of the mitochondrial electron transport chain, and release of cytochrome c resulting in apoptosis (43). Congeners of AEA, such as linoleoylethanolamide, oleoylethanolamide, and palmitoylethanolamide did not lead to apoptosis. My results provide preliminary evidence that PEA treatment of HT22 cells results in a decrease in markers of mitochondrial activity in addition to reducing cellular proliferation in the hippocampal cell line HT22.

REFERENCES

1. Gage FH, Ray J and Fisher LJ (1995) Isolation, characterization, and use of stem cells from the CNS. Annu Rev Neurosci. 18:159-92.

2. Devane WA, Hanus L, Breuer A, Pertwee RG, Stevenson LA, Griffin G, Gibson D, Mandelbaum A, Etinger A and Mechoulam R (1992) Isolation and structure of a brain constituent that binds to the cannabinoid receptor. Science. 258(5090):1946-1949.

3. Vogel Z, Barg J, Levy R, Saya D, Heldman E and Mechoulam R (1993) Anandamide, a brain endogenous compound, interacts specifically with cannabinoid receptors and inhibits adenylate cyclase. J Neurochem. 61(1):352-355.

4. Zygmunt PM, Petersson J, Andersson DA, Chuang H, Sorgard M, Di Marzo V, Julius D and Hogestatt ED (1999) Vanilloid receptors on sensory nerves mediate the vasodilator action of anandamide. Nature. 400(6743):452-457.

5. Smart D, Gunthorpe MJ, Jerman JC, Nasir S, Gray J, Muir AI, Chambers JK, Randall AD and Davis JB (2000) The endogenous lipid anandamide is a full agonist at the human vanilloid receptor (hVR1). Br J Pharmacol. 129(2):227-30.

6. Fu J, Gaetani S, Oveisi F, Lo Verme J, Serrano A, Rodriguez De Fonseca F, Rosengarth A, Luecke H, Di Giancomo B, Tarzia G and Piomelli D (2003) Oleylethanolamide regulates feeding and body weight through activation of the nuclear receptor PPAR-alpha. Nature. 425(6953):90-93.

7. Bouaboula M, Hilairet S, Marchand J, Fajas L, Le Fur G and Casellas P (2005) Anandamide induced PPARgamma transcriptional activation and 3T3-L1 preadipocyte differentiation. Eur J Pharmacol. 517(3):174-81.

8. Lambert DM and Di Marzo V (1999) The palmitoylethanolamide and oleamide enigmas : are these two fatty acid amides cannabimimetic? Curr. Med. Chem. 6 (8):757-773.

9. Sugiura T, Kondo S, Kishimoto S, Miyashita T, Nakane S, Kodaka T, Suhara Y, Takayama H and Waku L (2000) Evidence that 2-arachidonoylglycerol but not N-

palmitoylethanolamine or anandamide is the physiological ligand for the cannabinoid CB2 receptor. Comparison of the agonistic activities of various cannabinoid receptor ligands in HL-60 cells. J Biol Chem. 275(1):605-12.

10. Jonsson KO, Vandervoorde S, Lambert DM, Tiger G and Fowler CJ (2001) Effects of homologues and analogues of palmitoylethanolamide upon the inactivation of the endocannabinoid anandamide. Br J Pharmacol. 133(8):1263-75.
11. Smart D, Jonsson KO, Vandervoorde S, Lambert DM and Fowler CJ (2002) 'Entourage' effects of N-acyl ethanolamines at human vanilloid receptors. Comparison of effects upon anandamide-induced vanilloid receptor activation and upon anandamide metabolism. Br J Pharmoacol. 136(3):452-8
12. Skaper SD, Buriani A, Dal Toso R, Petrelli L, Romanello S, Facci L and Leon A (1996) The ALIAmide palmitoylethanolamide and cannabinoids, but not anandamide, are protective in a delayed postglutamate paradigm of excitotoxic death in cerebellar granule neurons. Proc Natl Acad Sci U S A. 93(9):3984-9.
13. Hansen HS, Moesgaard B, Petersen G and Hansen HH (2002) Putative neuroprotective actions of N-acyl-ethanolamines.Pharmacol Ther. 95(2):119-26.
14. Marsicano G, Goodenough S, Monory K, Hermann H, Eder M, Cannich A, Azad SC, Cascio MG, Gutierrez SO, van der Stelt M, Lopez-Rodriguez ML, Casanova E, Schutz G, Zieglgansberger W, Di Marzo V, Behl C and Lutz B (2003) CB1 cannabinoid receptors and on-demand defense against excitotoxicity. Science. 302(5642):84-8.
15. Kim SH, Won SJ, Mao XO, Jin K and Greenberg DA (2005) Involvement of protein kinase A in cannabinoid receptor-mediated protection from oxidative neuronal injury. J Pharmacol Exp Ther. 2005 Apr;313(1):88-94.

16. Van der Stelt M and DiMarzo V (2005) Cannabinoid receptors and their role in neuroprotection. Neuromolecular Med. 2005;7(1-2):37-50.

17. Shouman B, Fontaine RH, Baud O, Schwendimann L, Keller M, Spedding M, Lelievre V and Gressens P (2006) Endocannabinoids potently protect the newborn brain against AMPA-kainate receptor-mediated excitotoxic damage. Br J Pharmacol. 148(4):442-51.

18. Devane WA, Dysarz FA 3rd, Johnson MR, Melvin LS and Howlett AC (1988) Determination and characterization of a cannabinoid receptor in rat brain. Mol Pharmacol. 34(5):605-613.

19. Schmid PC, Kuwae T, Krebsbach RJ and Schmid HH (1997) Anandamide and other N-acylethanolamines in mouse peritoneal macrophages. Chem Phys Lipids. 87(2):103-10.

20. Kuwae T, Shiota Y, Schmid PC, Krebsbach R and Schmid HH (1999) Biosynthesis and turnover of anandamide and other N-acylethanolamines in peritoneal macrophages. FEBS Lett. 459(1):123-7.

21. Hansen HH, Ikonomidou C, Bittigau P, Hansen SH and Hansen HS (2001) Accumulation of the anandamide precursor and other N-acylethanolamine phospholipids in infant rat models of in vivo necrotic and apoptotic neuronal death. J Neurochem. 76(1):39-46.

22. Hansen HS, Lauritzen L, Strand AM, Vinggaard AM, Frandsen A and Schousboe A (1997) Characterization of glutamate-induced formation of N-acylphosphatidylethanolamine and N-acylethanolamine in cultured neocortical neurons. J Neurochem. 69(2):753-61.

23. Ross RA, Brockie HC and Pertwee RG (2000) Inhibition of nitric oxide production in RAW264.7 macrophages by cannabinoids and palmitoylethanolamide. Eur J Pharmacol. 401(2):121-30.

24. Lambert DM and Di Marzo V (1999) The palmitoylethanolamide and oleamide enigmas : are these two fatty acid amides cannabimimetic? Curr. Med. Chem. 6 (8):757-773.

25. Sugiura T, Kondo S, Kishimoto S, Miyashita T, Nakane S, Kodaka T, Suhara Y, Takayama H and Waku L (2000) Evidence that 2-arachidonoylglycerol but not N-palmitoylethanolamine or anandamide is the physiological ligand for the cannabinoid CB2 receptor. Comparison of the agonistic activities of various cannabinoid receptor ligands in HL-60 cells. J Biol Chem. 275(1):605-12.

26. Derocq JM, Bouaboula M, Marchand J, Rinaldi-Carmona M, Segui M and Casellas P (1998) The endogenous cannabinoid anandamide is a lipid messenger activating cell growth via a cannabinoid receptor-independent pathway in hematopoietic cell lines. FEBS Lett. 425(3):419-25.

27. Valk P, Verbakel S, Vankan Y, Hol S, Mancham S, Ploemacher R, Mayen A, Lowenberg B and Delwel R (1997) Anandamide, a natural ligand for the peripheral cannabinoid receptor is a novel synergistic growth factor for hematopoietic cells. Blood. 90(4):1448-57.

28. Facci L, Dal Toso R, Romanello S, Buriani A, Skaper SD and Leon A (1995) Mast cells express a peripheral cannabinoid receptor with differential sensitivity to anandamide and palmitoylethanolamide. Proc Natl Acad Sci U S A. 92(8):3376-80.

29. De Petrocellis L, Melck D, Palmisano A, Bisogno T, Laezza C, Bifulco M and Di marzo V (1998) The endogenous cannabinoid anandamide inhibits human breast cancer cell proliferation. Proc Natl Acad Sci U S A. 1998 Jul 7;95(14):8375-80.

30. Melck D, Rueda D, Galve-Roperh I, De Petrocellis L, Guzman M and Di Marzo V (1999) Involvement of the cAMP/protein kinase A pathway and of mitogen-activated protein

kinase in the anti-proliferative effects of anandamide in human breast cancer cells. FEBS Lett. 1999 Dec 17;463(3):235-40.

31. Laezza C, Pisanti S, Crescenzi E and Bifulco M (2006) Anandamide inhibits Cdk2 and activates Chk1 leading to cell cycle arrest in human breast cancer cells. FEBS Lett. 580(26):6076-82.

32. Grimaldi C, Pisanti S, Laezza C, Malfitano AM, Santoro A, Vitale M, Caruso MG, Notarnicola M, Iacuzzo I, Portella G, Di Marzo V and Bifulco M (2006) Anandamide inhibits adhesion and migration of breast cancer cells. Exp Cell Res. 312(4):363-73.

33. Fowler CJ, Jonsson K, Andersson A, Juntunen T, Vandervoorde S, Lambert DM, Jerman JC and Smart D (2003) Inhibition of C6 glioma cell proliferation by anandamide, 1-arachidonoylglycerol, and by a water soluble phosphate ester of anandamide: variability in response and involvement of arachidonic acid. Biochem Pharmacol. 66(5):757-67.

34. De Petrocellis L, Bisogno T, Ligresti A, Bifulco M, Melck D and Di Marzo V (2002) Effect on cancer cell proliferation of palmitoylethanolamide, a fatty acid amide interacting with both the cannabinoid and vanilloid signalling systems. Fundam Clin Pharmacol. 16(4):297-302.

35. Di Marzo V, Melck D, Orlando P, Bisogno T, Zagoory O, Bifulco M, Vogel Z and De Petrocellis L (2001) Palmitoylethanolamide inhibits the expression of fatty acid amide hydrolase and enhances the anti-proliferative effect of anandamide in human breast cancer cells. Biochem J. 358(Pt 1):249-55.

36. Jacobsson SO, Wallin T and Fowler CJ (2001) Inhibition of rat C6 glioma cell proliferation by endogenous and synthetic cannabinoids. Relative involvement of cannabinoid and vanilloid receptors. J Pharmacol Exp Ther. 299(3):951-9.

37. Duncan RS, Hwang SY and Koulen P (2007) Differential inositol 1,4,5-trisphosphate receptor signaling in a neuronal cell line. Int J Biochem Cell Biol. 39(10):1852-62.

38. Preston TJ, Abadi A, Wilson L and Singh G (2001) Mitochondrial contributions to cancer cell physiology: potential for drug development. Adv Drug Deliv Rev. 49(1-2):45-61.

39. Galli S, Labato MI, Bal de Kier Joffe E, Carreras MC and Poderoso JJ (2003) Decreased mitochondrial nitric oxide synthase activity and hydrogen peroxide relate persistent tumoral proliferation to embryonic behavior. Cancer Res. 63(19):6370

40. Carreras MC, Converso DP, Lorenti AS, Barbich M, Levisman DM, Jaitovich A, Antico Arciuch VG, Galli S and Poderoso JJ (2004) Mitochondrial nitric oxide synthase drives redox signals for proliferation and quiescence in rat liver development. Hepatology. 40(1):157-66.

41. Galve-Roperh I, Sanchez C, Cortes ML, Gomez del Pulgar T, Izquierdo M and Guzman M (2000) Anti-tumoral action of cannabinoids: involvement of sustained ceramide accumulation and extracellular signal-regulated kinase activation. Nat Med. 6(3):313-9.

42. Mimeault M, Pommery N, Wattez N, Bailly C and Henichart JP (2003) Anti-proliferative and apoptotic effects of anandamide in human prostatic cancer cell lines: implication of epidermal growth factor receptor down-regulation and ceramide production. Prostate. 56(1):1-12.

43. Maccarrone M, Lorenzon T, Bari M, Melino G and Finazzi-Agro A (2000) Anandamide induces apoptosis in human cells via vanilloid receptors. Evidence for a protective role of cannabinoid receptors. J Biol Chem. 275(41):31938-45.

44. Contassot E, Tenan M, Schnuriger V, Pelte MF and Dietrich PY (2004) Arachidonyl ethanolamide induces apoptosis of uterine cervix cancer cells via aberrantly expressed vanilloid receptor-1. Gynecol Oncol. 93(1):182-8.

45. Contassot E, Wilmotte R, Tenan M, Belkouch MC, Schnuriger V, de Tribolet N, Burkhardt K and Dietrich PY (2004) Arachidonylethanolamide induces apoptosis of human glioma cells through vanilloid receptor-1.J Neuropathol Exp Neurol. 63(9):956-63.

FIGURES

Fig. 1 – NAE treatment of HT22 cells leads to reduced calcein-AM fluorescence.

(a), Treatment of HT22 cells overnight (16 – 20 hours) with PEA (from 20 to 120μM) leads to a slight reduction in calcein-AM fluorescence, but only reaches statistical significance at 20μM and 120μM concentrations. (b), Treatment of HT22 cells overnight (16 – 20 hours) with LLEA (from 5 to 50μM) leads to a slight reduction in calcein-AM fluorescence. For (a) and (b), *n* equals five (5) plates totaling 36 wells per condition. P-values ≤ 0.05 and ≤ 0.01 are indicated by * and **, respectively.

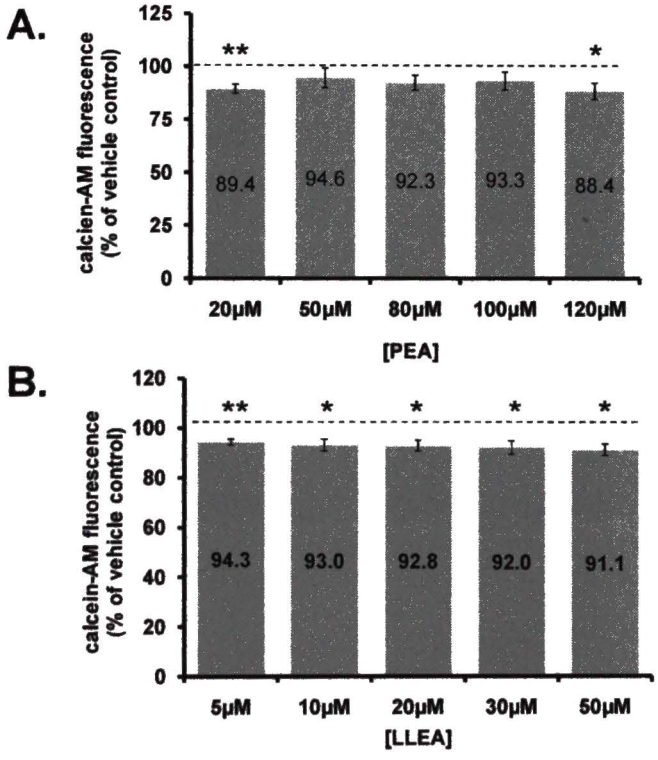
A.
calcien-AM fluorescence
(% of vehicle control)
125
100
75
50
25
0
**
*
89.4
94.6
92.3
93.3
88.4
20μM
50μM
80μM
100μM
120μM
[PEA]
B.
calcein-AM fluorescence
(% of vehicle control)
120
100
80
60
40
20
0
**
*
*
*
*
94.3
93.0
92.8
92.0
91.1
5μM
10μM
20μM
30μM
50μM
[LLEA]

Fig. 2 – Effects of PEA on calcein-AM fluorescence are independent of CB2. Overnight treatment of HT22 cells with 100μM PEA results in a decrease in calcein-AM fluorescence. Treatment of cells with JWH-015 and AM1241, selective and potent agonists of the CB2 receptor, do not exhibit a similar effect on calcein-AM fluroescence. For this study, *n* equals three (3) experiments totaling 12 wells per condition. A P-value of ≤ 0.05 is indicated by *.

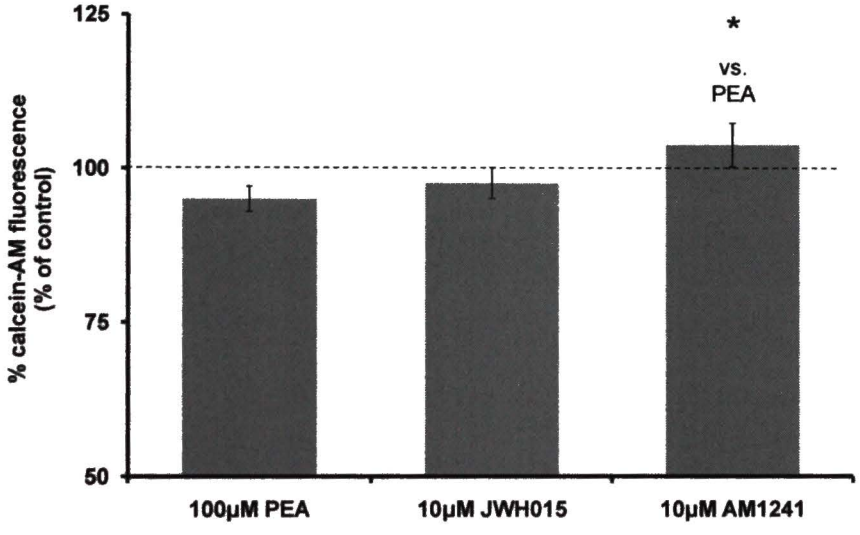
125
100
75
50
% calcein-AM fluorescence
(% of control)
*
vs.
PEA
100μM PEA
10μM JWH015
10μM AM1241

Fig. 3 – Effects of PEA on MTT reduction are independent of CB2 . Overnight treatment of HT22 cells with 100μM PEA results in a dramatic decrease in MTT reduction (A). Treatment of cells with JWH-015 and AM1241, selective and potent agonists of the CB2 receptor, have the opposite effect on MTT reduction (B). For this study, *n* equals three (3) experiments totaling 12 wells per condition. A P-value of ≤ 0.001 is indicated by ***.

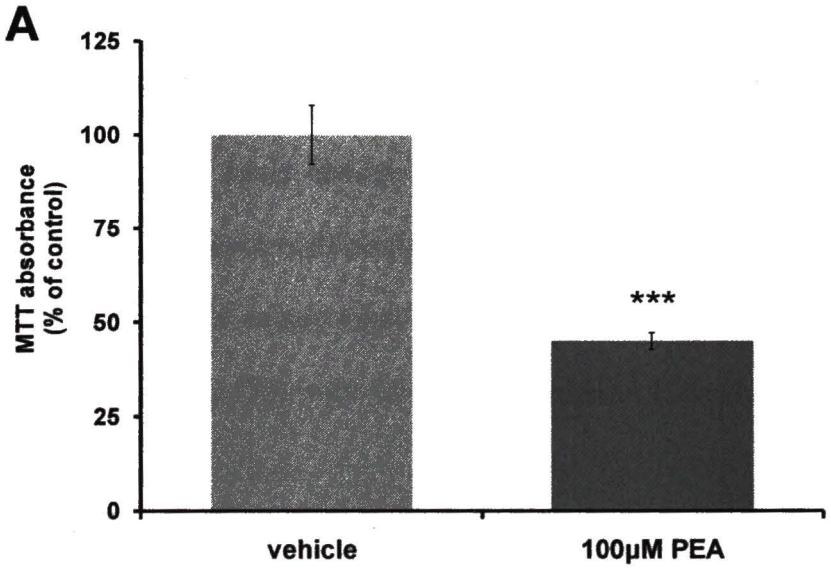
A
125
100
75
50
25
0
MTT absorbance
(% of control)
***
vehicle
100μM PEA

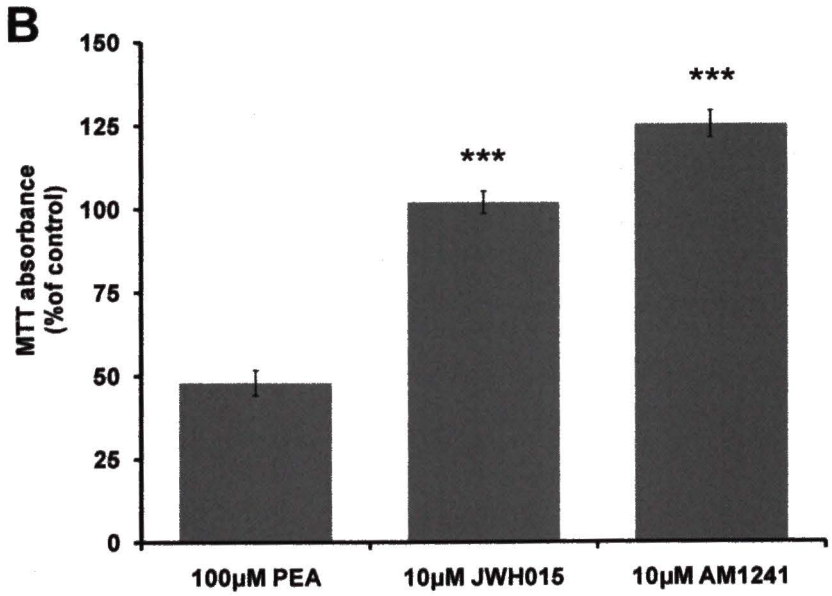
B
150
125
100
75
50
25
0
MTT absorbance
(%of control)
***
***
100μM PEA
10μM JWH015
10μM AM1241

Fig. 4 – PEA exposure affects calcein-AM fluorescence more than cell number. Overnight (16 – 20 hour) exposure of HT22 cells to 100μM PEA has no significant effect on cell number as determined by hemocytomoeter counts, although there is a trend toward an increase (top graph). After plating at the same density the next day followed by retreatment with 100μM PEA, calcein-AM fluorescence (cell proliferation) significantly decreased (bottom graph). For the cell counts (top graph), *n* equals eight (8) wells per condition. For the calcein-AM data (bottom graph), *n* equals thirty (30) wells for each condition. A P-value of ≤ 0.001 is indicated by ***.

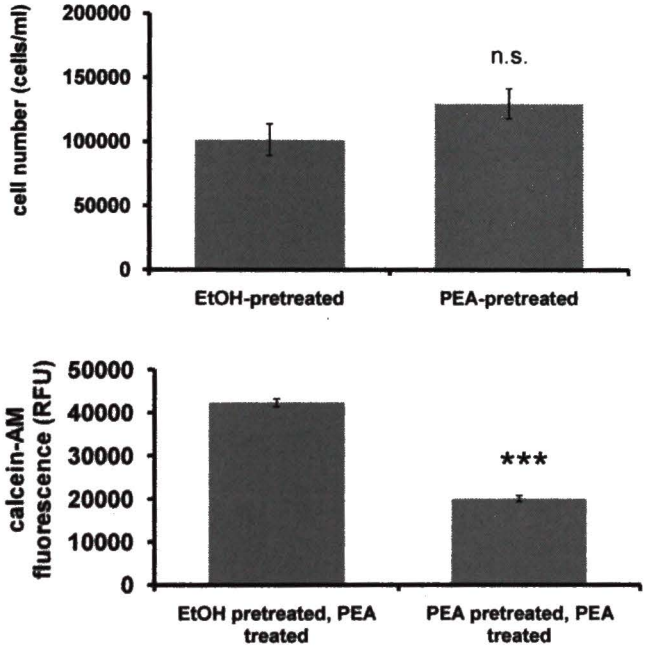
cell number (cells/ml)
200000
150000
100000
50000
0
n.s.
EtOH-pretreated
PEA-pretreated
calcein-AM fluorescence (RFU)
50000
40000
30000
20000
10000
0
***
EtOH pretreated, PEA treated
PEA pretreated, PEA treated

Fig. 5 – Antiproliferative effects of PEA are greater over longer periods of exposure time. HT22 cells were treated overnight (16 – 20 hours) with 100μM PEA (or EtOH vehicle). Cells from these treatment groups were then plated into a 96 well plate and each population was treated with either 100M PEA or EtOH vehicle. After another overnight incubation in PEA (or EtOH), a calcein-AM assay was conducted. For the hemocytometer cell counts (top graph), *n* equals five (5) wells per condition. For the calcein-AM data (bottom graph), *n* equals twenty-four (24) wells for EtOH pretreated/EtOH treated and PEA pretreated/ EtOH treated conditions while n equals thirty (30) wells for the EtOH pretreated/PEA treated and PEA pretreated/PEA treated conditions. A P-value of ≤ 0.001 is indicated by ***.

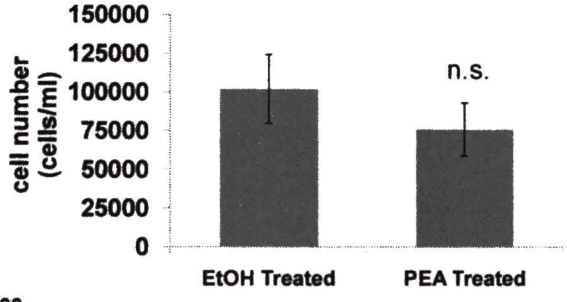
150000
125000
100000
75000
50000
25000
0
cell number (cells/ml)
n.s.
EtOH Treated
PEA Treated

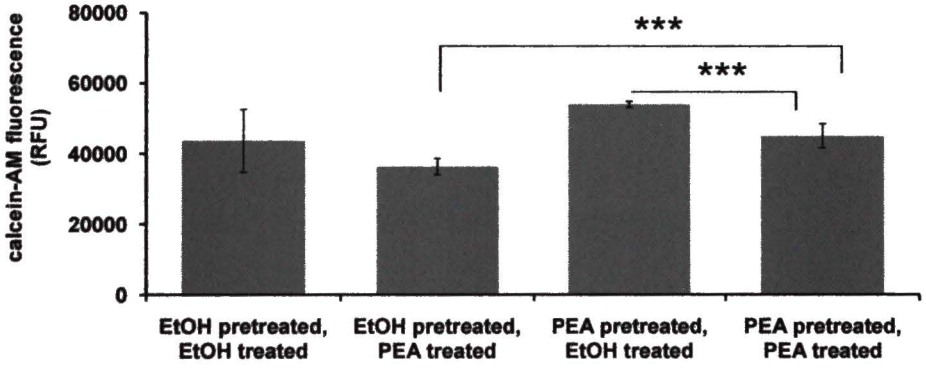
80000
60000
40000
20000
0
calcein-AM fluorescence (RFU)
***
***
EtOH pretreated, EtOH treated
EtOH pretreated, PEA treated
PEA pretreated, EtOH treated
PEA pretreated, PEA treated

Fig. 6 – Chronic PEA treatment leads to profound inhibition of cell growth. A chronic (72 hour) exposure of HT22 cells to 50 and 100μM PEA results in a dramatic and significant decrease (>80% decrease) in cell number compared to EtOH vehicle controls as determined by hemocytometer counts. For this study, *n* equals three (3) wells for the vehicle and five (5) wells for the PEA condition. A P-value of < 0.01 and ≤ 0.001 is indicated by ** and ***, respectively.

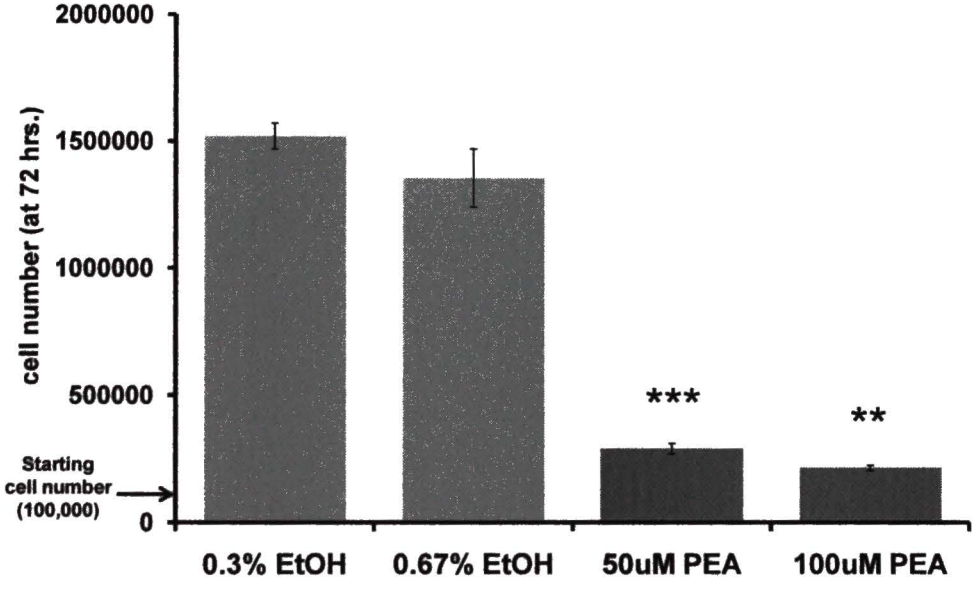
2000000
1500000
1000000
500000
0
cell number (at 72 hrs.)
Starting cell number (100,000)
***
**
0.3% EtOH
0.67% EtOH
50uM PEA
100uM PEA

Fig. 7 – PEA does not cause apoptosis in HT22 cells. Microscopic counts of fixed HT22 cells previously exposed overnight (16 – 20 hours) to LEA or PEA reveal no significant cell loss (top graph). Furthermore, TUNEL labeling of the same NAE-treated samples reveals no significant increase in apototic cells compared to vehicle controls (bottom graph). For this study, *n* equals four (4) microscope fields (at 20X magnification) for each condition.

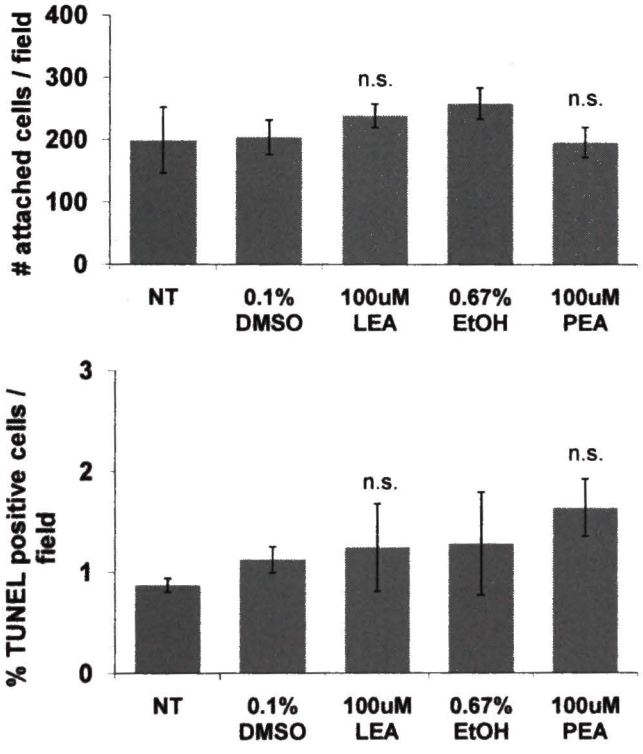
attached cells / field
400
300
200
100
0
n.s.
n.s.
NT
0.1% DMSO
100uM LEA
0.67% EtOH
100uM PEA
% TUNEL positive cells / field
3
2
1
0
n.s.
n.s.
NT
0.1% DMSO
100uM LEA
0.67% EtOH
100uM PEA

Fig. 8 – High concentrations of PEA cause does not cause oxidative stress. Treatment of CH_2DCFDA-loaded HT22 cells with 100μM PEA (but not 10 or 50μM PEA) for 5 hours results in a very slight but significant increase (+3.6%) in CH_2DCFDA fluorescence. Compared to the increase in fluorescence elicited by tBHP (+273%), however, the PEA-mediated effect was very small and likely would not lead to oxidative stress and cell death. For this study, *n* equals five (5) wells for each condition. A P-value of < 0.01 and ≤ 0.001 is indicated by ** and ***, respectively.

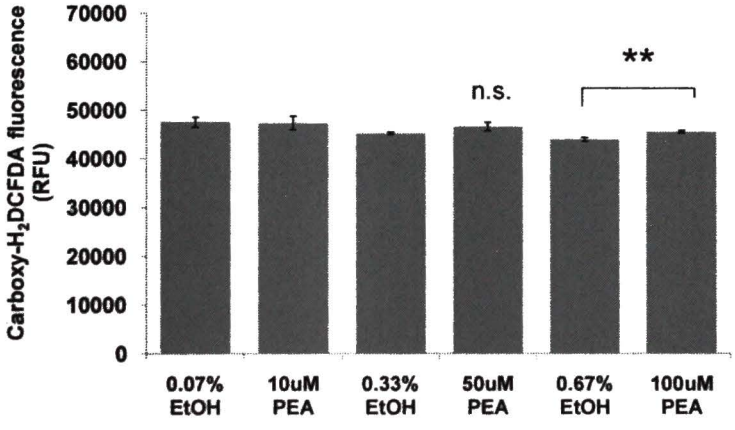
Carboxy-H2DCFDA fluorescence (RFU)
70000
60000
50000
40000
30000
20000
10000
0
n.s.
**
0.07% EtOH
10uM PEA
0.33% EtOH
50uM PEA
0.67% EtOH
100uM PEA

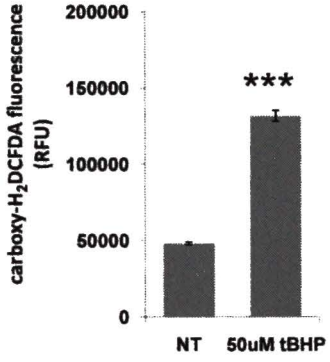
carboxy-H2DCFDA fluorescence (RFU)
200000
150000
100000
50000
0
***
NT
50uM tBHP

Fig. 9 – PEA treatment causes a reduction in mitochondrial membrane potential in HT22 cells. Treatment of HT22 cells for 5 hours with 100μM PEA results in a reduction in the fluorescence of the mitochondrial activity-sensitive dye MitoTracker Red fluorescence, suggesting that PEA alters mitochondrial activity. For this study, *n* equals three (3) coverslips for each condition with three (3) microscope fields (at 20X magnificantion) per coverslip. The number of cells analyzed were 229 cells and 193 cells for EtOH and PEA, respectively. A P-value of ≤ 0.001 is indicated by ***.

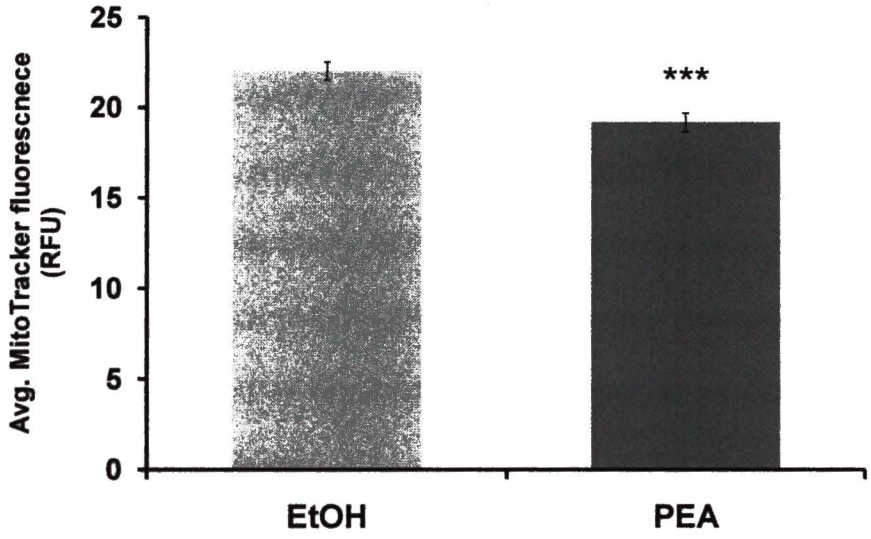
Avg. MitoTracker fluorescnece (RFU)
25
20
15
10
5
0
***
EtOH
PEA

CHAPTER 3.2 – NEUROPROTECTION OF HT22 CELLS BY NAEs

ABSTRACT

N-acylethanolamines (NAEs) are lipids upregulated in response to tissue injury are involved in cytoprotection (1 – 11). Arachidonylethanolamine (AEA) is a well characterized NAE that is an endogenous ligand at cannabinoid and vanilloid receptors, but it exists in small quantities relative to other NAE species (11 – 17). The abundant quantity of other NAE species, such as palmitoylethanolamine (PEA), together with the uncertainty of their function has prompted me to examine their neuroprotective poperties. I hypothesized that PEA protects HT22 cells from oxidative stress. I determined that PEA protects HT22 cells from oxidative stress and that a PEA preincubation time of 5 – 6 hours is required to offer protection. These results establish a role for PEA as a neuroprotectant against oxidative stress, which occurs in a variety of neurodegenerative diseases such as Alzheimer's disease.

INTRODUCTION

Cannabinoids exhibit neuroprotective properties against a wide variety of pathological insults including excitotoxicity, oxidative stress and hypoxia (2 – 4, 6 - 11). Cannbinoids activate CB1 and CB2 leading to downregulation of PKA and activation of the ERK MAPK pathway, which has been shown to be a neuroprotective signaling pathway (12, 14, 18 - 23). Furthermore, the activation of Akt by cannabinoids further supports their role as neuroprotectants (24, 25).

Win 55212 and CP 55940 activation of CB1 rdecreases NMDA-mediated hippocampal neuron cell death (26). NMDA-induced intracellular Ca^{2+} increases were also reversed by Win

55212 and by ryanodine, suggesting that RyR is a target for CB1 signaling. Activation of CB1 results in a reduction in PKA-mediated RyR phosphorylation and reduced RyR activity and subsequent Ca^{2+} toxicity (26). By utilizing a CB1 knockout mouse model, it was shown that CB1 offers protection of cortical neurons against kainite-induced excitotoxicity (10). PEA, but not AEA, reduces glutamate toxicity in cerebellar granule cells and this effect was antagonized with AEA (2).

$CB1^{-/-}$ mice exhibit increased neuronal death caused by $FeCl_2$ insult (27). The CB1 agonist Win 55212 reduces $FeCl_2$-induced neuronal death by a CB1-dependent mechanism involving inhibition of PKA but not activation of PI3K (27). PEA can partially protect cells from peroxidative stress induced by tert-butylhydroperoxide (tBHP) (28). Oxyhomologation of the amide bond of PEA results in increased protection against oxidative stress and intracellular Ca^{2+} overload (28).

In addition to protecting against general excitotoxicity, hypoxia and oxidative stress, cannabinoids protect neurons in specific models of Alzheimer's disease (29). For example, in AD brains, CB1 receptor expression is reduced (30) and CB2 and FAAH is upregulated in glia associated with neuritic plaques (31). Aβ treatment of C6 glioma cells results in a decrease in both CB1 and AEA levels and increase CB2 levels (32). Administration of AEA protects differentiated human cell line from Aβ peptide toxicity (33). Treatment of these cells with a CB1 agonist and CB2 antagonist reduced reactive gliosis induced by Aβ insult, suggesting that CB2 may be a potential target for the treatment of AD (32). CB1 expression is reduced in human AD brain (34). Both CB1 and CB2 nitration is increased and senile plaques express CB1 and CB2. Furthermore, synthetic cannabinoid administration to rats prevents microglial activation, loss of neurons and cognitive impairment (34).

Interestingly, AEA levels in various tissues including the brain are relatively low compared to other NAE species such as PEA (16, 17). NAE precursor synthesis is differentially affected by apotosis and necrosis (35). For example, NMDA-induced excitotoxicty results in increased levels of all NAPE species (1).

Some saturated and monounsaturated NAEs have been shown to activate ERK1/2 phosphorylation pathway through a CB1-independent mechanism (36). The NAE oleoylethanolamine (OEA) reduces the formation of iron-induced malondialdehyde (MDA) in rat heart mitochondria, suggesting that it may act as an antioxidant reducing lipid peroxidation (37). Furthermore, some NAEs, including PEA, decrease the mitochondrial inner membrane permeability and may protect cells from ischemic insult (38). Interestingly, the yeast *Saccharomyces cerevisiae*, which does not express cannabinoid or vanilloid receptors, synthesizes various NAE species in response to oxidative stress (39). This result further substantiates a non-cannabinoid receptor- and a non-vailloid receptor-mediated function for some NAEs.

MATERIALS AND METHODS

Chemicals

Palmitoylethanolamine (PEA), URB-597, JWH-015, AM-1242 and AM-630 was purchased from Alexis Biochemicals (Switzerland). Linolenoylethanolamine was purchased from Sigma (St. Louis, MO). Lauroylethanolamine (LEA) was provided by Kent Chapman at the University of North Texas, Denton, TX. N,N-bis(2-hydroxyethyl)-hexadecanamide (palmitoyldiethanolamine, PDEA) and hexadecanoic acid adamantan-1-ylamide (palmitoyladamantanamide, PAA) were purchased from Avanti polar lipids. Calcein-

acetoxymethyl ester (AM) was purchased from Alexis Biochemicals or EMD/Calbiochem. 5-(and-6)-carboxy-2',7'-dichlorodihydrofluorescien diacetate (CH_2DCFDA) was purchased from (Invitrogen/Molecular Probes). Tert-butylhydroperoxide (tBHP was purchased from Acros Organics (Belgium). N-cyclohexanecorbonylpentadecylamine (N-CHCPDA) was purchased from Cayman Chemical.

Cell culture

HT22 were cultured as described previously (40). In brief, HT22 cells were grown in DMEM with high glucose and 1mmM sodium pyruvate (Mediatech), 2mM Glutamax (Invitrogen), 5% bovine growth serum (BGS) (Hyclone) and peniciilin-streptomycin (Mediatech). Cultures were kept at a confluency of less than 70% during the culturing process. Mouse primary cortical neurons were obtained from postnatal day 2 (P2) mice after anesthesia on ice. Animals were decapitated and the scalp and skull was removed without disturbing the integrity of the brain. A 1 – 1.5mm^2 piece of cortex was removed from each hemisphere of the brain with fine-tipped #5/45 forceps and placed into 0.25% trypsin in HBSS with EGTA and without Ca^{2+}. Tissue was incubated in trypsin at 37° C for 20 minutes followed by addition of 1 volume of complete media and subsequent trituration several times with a fire-polsihed glass pipet or a 1ml capacity micropipette tip. Tissue was centrifuged at 1,000 x g for 5 minutes to pellet the viscous tissue. Media was removed and the pellet was resuspended in 2 ml of complete media followed by trituration. Cells were centrifuged again at 400 x g for 5 minutes. The supernatant was removed and the pellet was resuspended in 2ml of complete media followed by trituration. The resulting cell suspension was passed through a 40μm cell strainer and quantitated using a hemocytometer. Cell density was adjusted to 1 X 10^6 – 2 X 10^6 cells/ml depending upon the application. All

neurons were plated on either poly-D-lysine/laminin-coated 12mm coverslips (BioCoat™ BD Biosciences) or poly-L-lysine-coated 12mm coverslips depending upon the application. Mixed neuronal cultures were maintained at 37°C / 5% CO_2 environment for 7 – 14 days. Before using coverslips, neurons were inspected visually under a microscope to determine their development of neurites and overall healthy appearance. Only cultures with the majority of neurons bearing neurites were used in experiments.

Assessment of cell viability

Oxidative stress was induced by exposing cells to tert-butylhydroperoxide (tBHP). The fluorimetric calcein-AM and VYBRANT cytotoxicity assay (Invitrogen) and the colorimetric MTT assays (Invitrogen) were conducted in 96 well plates in order to assess cell viability in a high-throughput format. All 96 well plate assays for HT22 cell proliferation were conducted using a cell density of 2,000 cells/well unless noted otherwise. For the calcein-AM assay, media was removed from plates followed by replacement with Hank's balanced salt solution (HBSS) with 2mM $CaCl_2$ and calcein-AM dye at a final concentration of 4μM for 20 minutes to load cells. Calcein-AM fluorescence was measured using a fluorimetric plate reader (Perkin-Elmer Victor^3) with filters accommodating 485nm excitation and 530nm emission light. The VYBRANT cytotoxicity assays were conducted according to the manufacturer's instructions with a substrate reaction time of 5 – 6 hours at 37°C and read at 530nm excitation and 560nm emission. The MTT assay was measured at an absorbance wavelength of 560nm using the same plate reader. All raw data was analyzed, normalized and graphed in Microsoft Excel. Alternatively, HT22 cells were treated with 0.1, 1, 10 or 100μM PEA for ~1 hour followed by exposure to highly toxic concentrations of tBHP (30μM) for a relatively short duration (11 – 12

hours versus 16 – 20 hours). VYBRANT cytotoxicity and calcein-AM assays were then conducted.

The fluorimetric terminal deoxynucleotidyl transferase (TdT)-mediated-dUTP nick-end labeling (TUNEL) assay (Promega, Madison, WI) was used to measure apoptosis according to the manufacturer's protocol. For neuroprotection assay using TUNEL, HT22 cells (at ~50% confluency on coverlips) were treated with either LEA or PEA (10 and 100μM) for two (2) hours followed by a 15μM tBHP insult overnight. A TUNEL assay was conducted according to the manufacturer's protocol. Coverslips were counterstained with ProLong Anti-Fade reagent with DAPI. Images were acquired at 20X using the Olympus IX-70 fluorescence microscope.

Measurement of cellular oxidative stress

HT22 cells in 96 well plates were loaded with 10μM CH_2DCFDA for 45 min. The media was removed and replaced with media containing 100μM PEA (or vehicle) followed by incubation in PEA for 1 hour. tBHP (100μM) was added to the wells followed by incubation for up to 4 hours. Readings were taken at 3 hours (in the complete DMEM medium) and later at 4 hours in added HBSS.

Statistics

An F-test was conducted in Excel between each treatment group and the untreated control group to determine which type of T-test should be used for group comparisons. The mean fluorescence intensity from each treatment group was separately compared to the mean fluorescence intensity of the untreated control group using a two-sample T-test with either equal or unequal variances. A P-value of less than or equal to 0.05 was considered significant.

RESULTS

Oxidative insult in HT22 cells

From initial fluorimetric viability assays, we determined which oxidant would be suitable for use in neuroprotection assays. We concluded glutamate was not suitable due to the fact that many of our cell stocks were HT22 cells were glutamate-resistant. This result is consistent with previous reports of glutamate resistance in the HT22 cell line (Sagara et al. 1998). Exposure of HT22 cells to 2,2'-dithiodipyridine (DTDP) leads to cell detachment prior to change in cell morphology (data not shown) making it a poor choice for use in assays. Hydrogen peroxide (H_2O_2) did not kill HT22 cells as effectively as tBHP and it is less stable making it undesirable for use in our assays. We conclude that tBHP is the best choice as an oxidant due to its stability relative to H_2O_2 and its lipid peroxidizing properties. In order to determine effective tBHP concentrations for experiments, HT22 cells were exposed to 2, 4, 6, 10 or 15μM tBHP overnight (16 – 20 hours) followed by a calcein-AM assay and MTT assay. Concentrations of tBHP below and up to 10μM resulted in no measureable decrease in calcein-AM fluorescence, while 15μM tBHP led to an approximate 10% decrease in calcein-AM fluorescence. Concentrations of tBHP at or below 10μM did not decrease MTT reduction. Exposure of cells to 15μM tBHP resulted in a significant decrease in MTT reduction, suggesting that tBHP becomes significantly toxic at this concentration. The potency of tBHP is variable which we attribute to possible phenotypic variation of HT22 cells over increasing passage numbers and degradation of tBHP stocks over time. To address this, we used HT22 passage numbers of 35 or under and we acquired new stocks of tBHP once diminished potency became apparent.

Fluorimetric assessment of oxidative stress HT22 cells

HT22 cells loaded with 10μM 5-(and-6)-carboxy-2',7'-dichlorodihydrofluorescien diacetate (CH_2DCFDA) were exposed to tBHP concentrations between 1 and 200μM for up to 6 hours. The cells were read in the plate reader at 485nm/530nm to detect changes in CH_2DCFDA fluorescence. Another plate from the same cell stock at the same density was allowed to grow overnight (16 – 20 hours) before a calcein-AM was conducted. Cells treated with tBHP concentrations up to 10μM did not exhibit a decrease in calcein-AM fluorescence (Fig. 1). At 15μM tBHP, however, there was a substantial and statistically significant decrease in calcein-AM fluorescence, suggesting that this concentration is toxic. tBHP concentrations from 15 – 200 exhibited a precipitous drop in calcein-AM fluorescence. The LC_{50} for tBHP in most experiments lies within the 15 and 25μM range (Fig. 1).

Cells treated with tBHP concentrations up to 5μM did not exhibit an increase in DCFDA fluorescence, but at 10μM tBHP, there was a slight but significant increase in DCFDA fluorescence (Fig. 1). tBHP concentrations from 15 – 200 exhibited a precipitous increase in DCFDA fluorescence (Fig. 1). The approximate EC_{50} for tBHP in this experiment (with 0μM tBHP as a minimal fluorescence reading and 100μM as a maximal fluorescence reading) was 25 - 30μM. As expected, there is an inverse relationship between calcein-AM and CH_2DCFDA fluorescence in response to tBHP. At concentrations of 15μM tBHP and higher, oxidative stress (CH_2DCFDA fluorescence) increases and cell viability (calcein-AM fluorescence) decreases significantly.

Effect of Acute and Short-Term PEA Treatment on HT22 cell viability

HT22 cells in 96 well plates were treated with 100μM PEA, 20μM tBHP or PEA and tBHP at the same time (co-treatment paradigm) followed by overnight (16 – 20 hour) incubation. A calcein-AM and MTT assay was conducted to assess cell viability. Not surprisingly, treatment of HT22 cells with 100μM PEA leads to a reduction in calcein-AM fluorescence (10 – 15 % reduction) confirming its antiproliferative properties. Application of 20μM tBHP resulted in mild to moderate reduction in calcein-AM fluroescence (~30 – 40%) and addition of PEA together with tBHP (co-treatment paradigm) resulted in a very slight trend toward protection, but this effect was not significant (data not shown). Treatment of HT22 cells with 100μM PEA results in a dramatic and significant reduction in MTT absorbance compared to vehicle controls. Previous cell viability experiments rule out potentially toxic effects on PEA on HT22 cells. Therefore, we interpret that the decrease in MTT reduction may be due to an effect of PEA on mitochondrial activity. The addition of PEA with tBHP resulted in a further decrease in MTT absorbance compared to vehicle with tBHP (data not shown). These results suggest that PEA does not protect HT22 cells against tBHP when applied together with tBHP.

Pretreatment of HT22 cells with 100μM PEA 1 hour prior to tBHP exposure led to a trend toward an increase in calcein-AM and decrease in VYBRANT fluorescence (Fig. 2). This suggests that 100μM PEA is produces a trend toward protection against highly-toxic levels of tBHP (30μM). The 10μM PEA treatment followed by tBHP exposure led to a non-significant trend toward protection against tBHP as measured by the calcein-AM assay and G6PD cytotoxicity assay (data not shown).

HT22 cells were treated with PEA (10 and 100μM) for 1 hour prior to an overnight 30μM tBHP exposure. Treatment with both 10 and 100μM PEA resulted in a slight but significant

reduction in calcein-AM fluorescence and but only 100μM PEA led to a reduction in MTT absorbance. In the presence of tBHP, however, 100μM PEA resulted in a trend toward protection using the calcein-AM and G6PD cytotoxicity assays, but it failed to reach statistical significance (Fig. 2).

A 5 – 6 hour PEA treatment protects HT22 from oxidative stress

HT22 cells were treated with PEA (10 and 100μM) for 5 - 6 hours prior to overnight tBHP exposure. A 6 hour 100μM PEA pretreatment significantly protected HT22 cells from tBHP exposure as indicated by an increase in calcein-AM fluorescence (Fig. 3). In addition, VYBRANT cytoxicity assay results indicate that PEA exhibit neuroprotective properties as well. (Fig. 3) PEA pretreatment had no effect on the changes in MTT absorbance resulting from tBHP exposure.

Effect of Prolonged PEA Treatment on HT22 Cells Exposed to Oxidative Stress

Pretreatment of HT22 cells with 100μM PEA overnight (16 hours) prior to a 6 hour 20μM tBHP insult led to a trend toward an increase in calcein-AM fluorescence and significant decrease in VYBRANT fluorescence, suggesting protection against tBHP-mediated necrotic cell death (Fig. 4). Similar results were seen with a 40μM LLNEA pretreatment (data not shown).

In a similar experiment, overnight PEA pretreatment prior to tBHP exposure resulted in a trend toward a trend toward decrease calcein-AM fluorescence (Fig. 5; p=0.090) and a significant decrease in MTT absorbance (data not shown). These results suggest that an overnight (12hr.) PEA pretreatment does not protect HT22 cells against tBHP, but the tBHP

toxicity was significantly less than observed in previous experiments. I conclude, therefore, that PEAs ability to neuroprotect is greater under high tBHP toxicity.

DISCUSSION

From these studies, I conclude that PEA (at 100μM) protects HT22 cells from peroxidative stress but only if cells are pretreated with PEA for 5 – 6 hours prior to tBHP exposure. Shorter PEA pretreatment times led to a trend toward protection in some cases. Interestingly, PEA pretreatment of HT22 cells for several hours did not protect cells from tBHP insult. This study identifies PEA as a neuroprotectant that is endogenous to cells. In addition, previous studies indicate that PEA pretreatment (10μM and 50μM) for 5 hours prior to exposure to a brief anoxic insult led to a slight but significant decrease in CH_2DCFDA fluorescence (approximately 9.3% decrease) (data not published). This suggests that PEA may decrease cellular oxidative stress in cells.

Short pretreatment of cells with PEA offers no protection. I interpret this as a possible requirement for cells to accumulate exogenously-applied PEA before protective effects can be observed. Alternatively, PEA treatment may initiate protective signaling pathways within the cells that require a minimum amount of time to exert their effects thereby rendering the cell more resistant to oxidative stress. Treatment of cells with PEA for several hours does not protect cells. It is possible that this prolonged PEA treatment results in reduced proliferative capacity of cells thus rendering them more sensitive to oxidative stress. My previous study identified antiproliferative effects of PEA which supports this hypothesis. Alternatively, exposure of cells to prolonged PEA may result in significant degradation into palmitic acid at a time when the

initial stages of oxidative stress begin. It is possible that this renders the cells sensitive to oxidative stress. It is also possible that prolonged exposure to PEA may lead to a downregulation in target proteins involved in the neuroprotective effect thus rendering cells sensitive to oxidative stress. From a representative TUNEL assay, pretreatment of HT22 cells 50μM PEA prior to an 8 hour exposure to 20μM tBHP led to an increase in the number of attached cells and a trend toward a decrease in the number of TUNEL-positive cells. This suggests that prolonged PEA exposure may delay apoptosis.

In the majority of calcein-AM experiments with a 1 – 2 hour PEA pretreatment paradigm, the percent change in calcein-AM fluorescence of the 100μM PEA-treated/tBHP-exposed cells versus PEA-treated cells alone was slightly (~10%) but significantly higher than that of vehicle-treated/tBHP-exposed cells versus vehicle alone. In other words, 100μM PEA, although reducing calcein-AM fluorescence, offers slight neuroprotection against tBHP. It is important to note that PEA exhibits antiproliferative properties in HT22 cells. As a result, the population of cells surviving tBHP exposure may exhibit reduced proliferative capacity potentially leading to further reduction in calcein-AM fluorescence. In other words, protective effects of PEA may be masked by its antiprolifertive effects. It stands to reason, therefore, that protective effects of PEA may be underestimated.

Alternative strategies to PEA treatment have been implemented to test for neuroprotective effects of NAEs. For example, treatment of HT22 cells with the NAAA inhibitor, N-cyclohexanecarbonylpentadecylamine (N-CHCPDA), was expected to exhibit some neuroprotective effects or to enhance PEAs neuroprotective effects. Interestingly, treatment of HT22 cells with 10μM N-CHCPDA led to an increase (~50% increase) in VYBRANT fluorescence (released G6PD), suggesting that N-CHCPDA at this concentration is inherently

toxic to HT22 cells. This is interesting because the reported IC50 for this inhibitor is only ~4 - 5μM (41). PEA (100μM) addition alone has no effect on VYBRANT fluorescence suggesting that the cell death elicited by N-CHCPDA is likely not due to elevation of endogenous PEA. This suggests that caution should be taken when using N-CHCPDA to elicit increases in endogenous NAEs.

Furthermore, treatment of HT22 cells with 10μM palmitic acid (PA), a degradation product of PEA, exhibited significant inherent toxicity. This result excludes the possibility that effects observed for PEA are due to PA.

In addition, treatment of HT22 cells with the PEA analog palmitoyldiethanolamine (PDEA) at 10μM had no effect on clacein-AM fluorescence but it significantly increased VYBRANT fluorescence, suggesting some toxicity. Treatment with 100μM PDEA, however, exhibited a dramatic and significant decreased in calcein-AM fluorescence and an increase in VYBRANT fluorescence, suggesting that PDEA is very toxic at this concentration.

From our studies with PEA, it is apparent that PEAs ability to protect HT22 cells from oxidative stress increases as the severity of the tBHP insult increases. For example, when HT22 cells are pretreated with 100μM PEA for 6 hours followed by overnight exposure to low (sublethal) tBHP concentrations (0 - 10μM tBHP), calcein-AM fluorescence and MTT was reduced compared to vehicle controls. When PEA-pretreated HT22 cells are exposed to high (lethal) tBHP concentrations (20 - 40μM tBHP) there is an increase in calcein-AM fluorescence compared to the vehicle controls. PEA had no effect on decreased MTT reduction resulting from toxic tBHP concentrations. Furhtermore, pretreatment of cells with 10μM PEA did not have the same effect as 100μM concentrations. This kill curve experimental approach determined that

PEA is antiproliferative to HT22 cells under normal and sublethal conditions, but protective under conditions of toxicity.

When cell viability in the calcein-AM assay was plotted against tBHP concentration as a line graph, 10μM PEA treatment exhibited a downward line with poor fit ($r^2 = 0.415$). Similar results for 10μM PEA were seen with the MTT assay. When cell viability was plotted against tBHP concentration as a line graph, 100μM PEA treatment exhibited an upward line with a very good fit ($r^2 = 0.820$). Similar results for 100μM PEA were seen with the MTT assay with an r^2 value of 0.785. This analysis suggests that, in the calcein-AM and MTT assays, 100μM PEA (but not 10μM PEA) leads to increased protection of HT22 cells compared to vehicle as the concentration of tBHP rises.

REFERENCES

1. Hansen HS, Lauritzen L, Strand AM, Moesgaard B and Frandsen A (1995) Glutamate stimulates the formation of N-acylphosphatidylethanolamine and N-acylethanolamine in cortical neurons in culture. Biochim Biophys Acta. 1258(3):303-8.
2. Skaper SD, Buriani A, Dal Toso R, Petrelli L, Romanello S, Facci L and Leon A (1996) The ALIAmide palmitoylethanolamide and cannabinoids, but not anandamide, are protective in a delayed postglutamate paradigm of excitotoxic death in cerebellar granule neurons. Proc Natl Acad Sci U S A. 93(9):3984-9.
3. Hampson AJ, Gimaldi M, Axelrod J and Wink D (1998) Cannabidiol and (-) Delta9-tetrahydrocannabinol are neuroprotective antioxidants. Proc Natl Acad Sci U S A. 95(14):8268-73.

4. Shen M and Thayer SA (1998) Cannabinoid receptor agonists protect cultured rat hippocampal neurons from excitotoxicity. Mol Pharmacol. 54(3):459-62.

5. Moesgaard B, Jaroszewski JW and Hansen HS (1999) Accumulation of N-acyl-ethanolamine phospholipids in rat brains during post-decapitative ischemia: a 31p NMR study. J Lipid Res. 40(3):515-21.

6. Nagayama T, Sinor AD, Simon RP, Chen J, Graham SH, Jin K and Greenberg DA (1999) Cannabinoids and neuroprotection in global and focal cerebral ischemia and in neuronal cultures. J Neurosci. 19(8):2987-95.

7. Chen Y and Buck J (2000) Cannabinoids protect cells from oxidative cell death: a receptor-independent mechanism. J. Pharmacol. Exp. Ther. 293(3): 807-12.

8. Hampson AJ and Grimaldi M (2001) Cannabinoid receptor activation and elevated cyclic AMP reduce glutamate neurotoxicity. Eur J Neurosci. 13(8):1529.

9. van der Stelt M, Velhuis WB, Maccarrone M, Nar PR, Nicolay K, Veldink GA, DiMarzo V and Vliegenthart JF (2002) Acute neuronal injury, excitotoxicity, and the endocannabinoid system. Mol Neurobiol. 2002 Oct-Dec;26(2-3):317-46.

10. Marsicano G, Goodenough S, Monory K, Hermann H, Eder M, Cannich A, Azad SC, Cascio MG, Gutierrez SO, van der Stelt M, Lopez-Rodriguez ML, Casanova E, Schutz G, Zieglgansberger W, Di Marzo V, Behl C and Lutz B (2003) CB1 cannabinoid receptors and on-demand defense against excitotoxicity. Science. 302(5642):84-8.

11. Shouman B, Fontaine RH, Baud O, Schwendimann L, Keller M, Spedding M, Lelievre V and Gressens P (2006) Endocannabinoids potently protect the newborn brain against AMPA-kainate receptor-mediated excitotoxic damage. Br J Pharmacol. 148(4):442-51.

12. Bidaut-Russell M, Devane WA and Howlett AC (1990) Cannabinoid receptors and modulation of cyclic AMP accumulation in the rat brain. J Neurochem. 55(1):21-6.

13. Devane WA, Hanus L, Breuer A, Pertwee RG, Stevenson LA, Griffin G, Gibson D, Mandelbaum A, Etinger A and Mechoulam R (1992) Isolation and structure of a brain constituent that binds to the cannabinoid receptor. Science. 258(5090):1946-1949.

14. Vogel Z, Barg J, Levy R, Saya D, Heldman E and Mechoulam R (1993) Anandamide, a brain endogenous compound, interacts specifically with cannabinoid receptors and inhibits adenylate cyclase. J Neurochem. 61(1):352-355.

15. Smart D, Gunthorpe MJ, Jerman JC, Nasir S, Gray J, Muir AI, Chambers JK, Randall AD and Davis JB (2000) The endogenous lipid anandamide is a full agonist at the human vanilloid receptor (hVR1). Br J Pharmacol. 129(2):227-30.

16. Schmid PC, Kuwae T, Krebsbach RJ and Schmid HH (1997) Anandamide and other N-acylethanolamines in mouse peritoneal macrophages. Chem Phys Lipids. 87(2):103-10.

17. Kuwae T, Shiota Y, Schmid PC, Krebsbach R and Schmid HH (1999) Biosynthesis and turnover of anandamide and other N-acylethanolamines in peritoneal macrophages. FEBS Lett. 459(1):123-7.

18. Bouaboula M, Poinot-Chazel C, Bourrie B, Canat X, Calandra B, Rinaldi-Carmona M, Le Fur G and Casellas P (1995) Activation of mitogen-activated protein kinases by stimulation of the central cannabinoid receptor CB1. Biochem J. 1995 Dec 1;312 (Pt 2):637-41.

19. Wartmann M, Campbell D, Subramaninan A, Burstein SH and Davis RJ (1995) The MAP kinase signal transduction pathway is activated by the endogenous cannabinoid anandamide. FEBS Lett. 359(2-3):133-6.

20. Bouaboula M, Poinot-Chazel C, Marchand J, Canat X, Bourrie B, Rinaldi-Carmona M, Calandra B, Le Fur G and Casellas P (1996) Signaling pathway associated with stimulation of CB2 peripheral cannabinoid receptor. Involvement of both mitogen-activated protein kinase and induction of Krox-24 expression. Eur J Biochem.237(3):704-711.

21. Nilsen J, Chen S and Brinton RD (2002) Dual action of estrogen on glutamate-induced calcium signaling: mechanisms requiring interaction between estrogen receptors and src/mitogen activated protein kinase pathway. Brain Res. 930(1-2):216-34.

22. Luo Y and DeFranco DB (2006) Opposing roles for ERK1/2 in neuronal oxidative toxicity: distinct mechanisms of ERK1/2 action at early versus late phases of oxidative stress. J Biol Chem. 281(24):16436-42.

23. Singh M (2006) Progesterone-induced neuroprotection. Endocrine. 29(2):271-4.

24. Gomez del Pulgar T, Velasco G and Guzman M (2000) The CB1 cannabinoid receptor is coupled to the activation of protein kinase B/Akt. Biochem J. 347(Pt 2):369-73.

25. Brunet A, Datta SR and Greenberg ME (2001) Transcription-dependent and -independent control of neuronal survival by the PI3K-Akt signaling pathway. Curr Opin Neurobiol. 11(3):297-305.

26. Zhuang SY, Bridges D, Grigorenko E, McCloud S, Boon A, Hampson RE and Deadwyler SA (2005) Cannabinoids produce neuroprotection by reducing intracellular calcium release from ryanodine-sensitive stores. Neuropharmacology.48(8):1086-96.

27. Kim SH, Won SJ, Mao XO, Jin K and Greenberg DA (2005) Involvement of protein kinase A in cannabinoid receptor-mediated protection from oxidative neuronal injury. J Pharmacol Exp Ther. 2005 Apr;313(1):88-94.

28. Lombardi G, Miglio G, Varsaldi F, Minassi A and Appendino G (2007) Oxyhomologation of the amide bond potentiates neuroprotective effects of the endolipid N-palmitoylethanolamine. J Pharmacol Exp Ther. 320(2):599-606.

29. Sarne Y and Mechoulam R (2005) Cannabinoids: between neuroprotection and neurotoxicity. Curr Drug Targets CNS Neurol Disord. 4(6):677-84.

30. Westlake TM, Howlett AC, Bonner TI, Matsuda LA and Herkenham M (1994) Cannabinoid receptor binding and messenger RNA expression in human brain: an in vitro receptor autoradiography and in situ hybridization histochemistry study of normal aged and Alzheimer's brains. Neuroscience. 63(3):637-52.

31. Benito C, Nunez E, Tolon RM, Carrier EJ, Rabano A, Hillard CJ and Romero J (2003) Cannabinoid CB2 receptors and fatty acid amide hydrolase are selectively overexpressed in neuritic plaque-associated glia in Alzheimer's disease brains. J Neurosci. 23(35):11136-41.

32. Esposito G, Iuvone T, Savani C, Scuderi C, De Filipis D, Papa M, Di Marzo V and Steardo L (2007) Opposing control of cannabinoid receptor stimulation on amyloid-beta-induced reactive gliosis: in vitro and in vivo evidence. J Pharmacol Exp Ther. 322(3):1144-52.

33. Milton NG (2002) Anandamide and noladin ether prevent neurotoxicity of the human amyloid-beta peptide. Neurosci Lett. 332(2):127-30.

34. Ramirez BG, Blazquez C, Gomez del Pulgar T, Guzman M and de Ceballos ML (2005) Prevention of Alzheimer's disease pathology by cannabinoids: neuroprotection mediated by blockade of microglial activation.J Neurosci. 25(8):1904-13.

35. Hansen HH, Ikonomidou C, Bittigau P, Hansen SH and Hansen HS (2001) Accumulation of the anandamide precursor and other N-acylethanolamine phospholipids in infant rat models of in vivo necrotic and apoptotic neuronal death. J Neurochem. 76(1):39-46.

36. Berdyshev EV, Schmid PC, Krebsbach RJ, Hillard CJ, Hunag C, Chen N, Dong Z and Schmid HH (2001) Cannabinoid-receptor-independent cell signalling by N-acylethanolamines.Biochem J. 360(Pt 1):67-75.

37. Parinandi NL and Schmid HH (1988) Effects of long-chain N-acylethanolamines on lipid peroxidation in cardiac mitochondria. FEBS Lett. 237(1-2):49-52.

38. Epps DE, Palmer JW, Schmid HH and Pfeiffer DR (1982) Inhibition of permeability-dependent Ca2+ release from mitochondria by N-acylethanolamines, a class of lipids synthesized in ischemic heart tissue.J Biol Chem. 257(3):1383-1391.

39. Merkel O, Schmid PC, Paltauf F and Schmid HH (2005) Presence and potential signaling function of N-acylethanolamines and their phospholipid precursors in the yeast Saccharomyces cerevisiae. Biochim Biophys Acta. 1734(3):215-9.

40. Duncan RS, Hwang SY and Koulen P (2007) Differential inositol 1,4,5-trisphosphate receptor signaling in a neuronal cell line. Int J Biochem Cell Biol. 39(10):1852-62.

41. Tsuboi K, Hillingham C, Vandervoorde S, Lambert DM and Ueda N (2004) N-cyclohexanecarbonylpentadecylamine: a selective inhibitor of the acid amidase hydrolysing N-acylethanolamines, as a tool to distinguish acid amidase from fatty acid amide hydrolase. Biochem J. 379(Pt 1):99-106.

FIGURES

Fig. 1 – Characterization of tBHP toxicity in HT22 cells. HT22 cells were treated for 6 hour or overnight with various tBHP concentrations (1 - 100μM) prior to conducting a CH_2DCFDA assay to assess oxidative stress or calcein-AM assay to assess cell viability. Oxidative stress begins at 10μM tBHP exposure while loss of cell viability begins at 15μM tBHP exposure. For this study, *n* equals six (6) wells per condition. A P-value of ≤ 0.05, ≤ 0.01 and ≤ 0.001 is indicated by *, ** and ***, respectively.

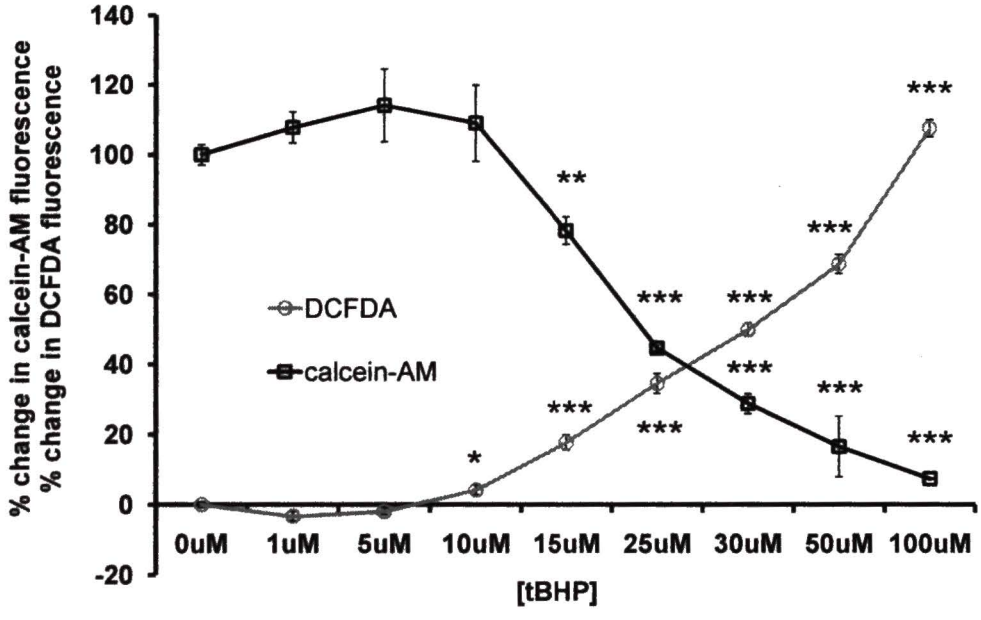
% change in calcein-AM fluorescence
% change in DCFDA fluorescence
140
120
100
80
60
40
20
0
-20
DCFDA
calcein-AM
*
**
***
0uM
1uM
5uM
10uM
15uM
25uM
30uM
50uM
100uM
[tBHP]

Fig. 2 – A one (1) hour PEA pretreatment does not protect HT22 cells from tBHP exposure. HT22 cells were pretreated with 100μM PEA for 1 hour prior to an overnight tBHP exposure. PEA pretreatment led to a trend toward neuroprotection. For this study, *n* equals six (6) wells per condition. A P-value of ≤ 0.01 is indicated by **.

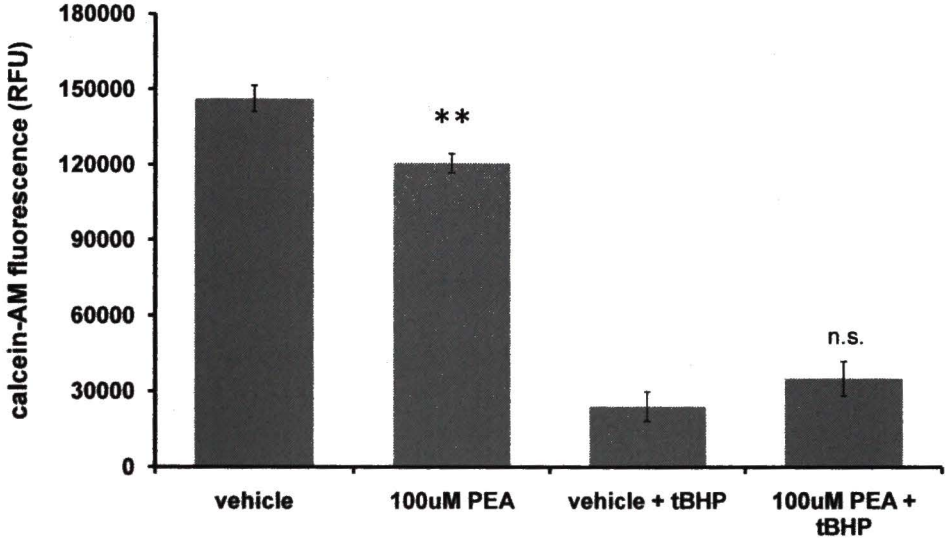
calcein-AM fluorescence (RFU)
180000
150000
120000
90000
60000
30000
0
**
n.s.
vehicle
100uM PEA
vehicle + tBHP
100uM PEA + tBHP

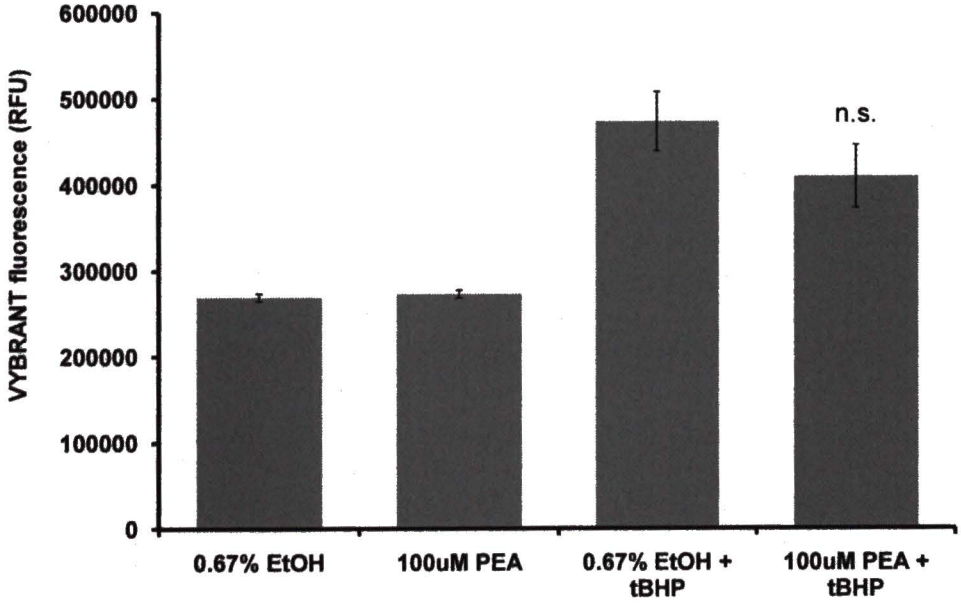
VYBRANT fluorescence (RFU)
600000
500000
400000
300000
200000
100000
0
n.s.
0.67% EtOH
100uM PEA
0.67% EtOH + tBHP
100uM PEA + tBHP

Fig. 3 – A five - six (5 - 6) hour PEA pretreatment protects HT22 cells from tBHP exposure. HT22 cells were pretreated with 100μM PEA for 5 - 6 hours prior to an overnight tBHP exposure. PEA pretreatment led to a significant neuroprotection against oxidative stress. For this study, *n* equals five (5) wells per condition. A P-value of ≤ 0.05 and ≤ 0.01 is indicated by * and **, respectively.

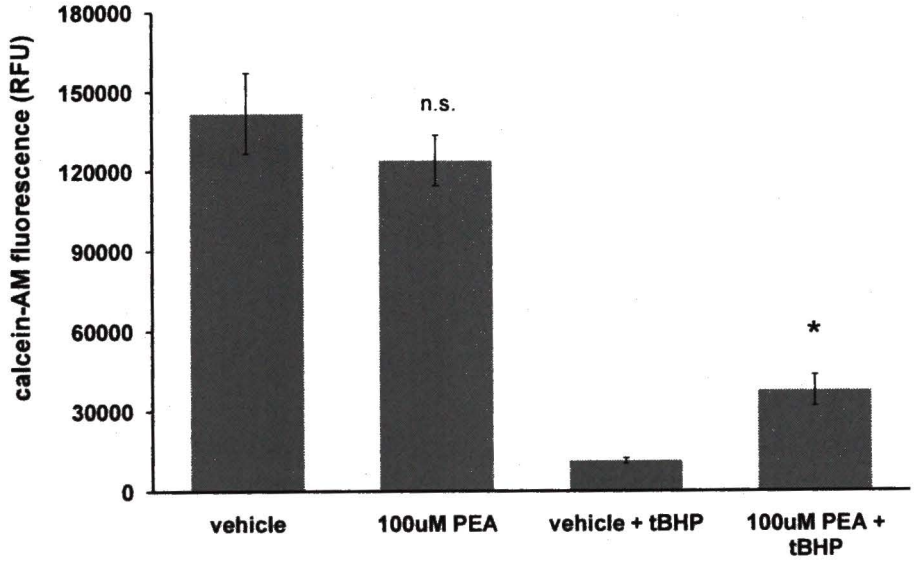
calcein-AM fluorescence (RFU)
180000
150000
120000
90000
60000
30000
0
n.s.
*
vehicle
100uM PEA
vehicle + tBHP
100uM PEA + tBHP

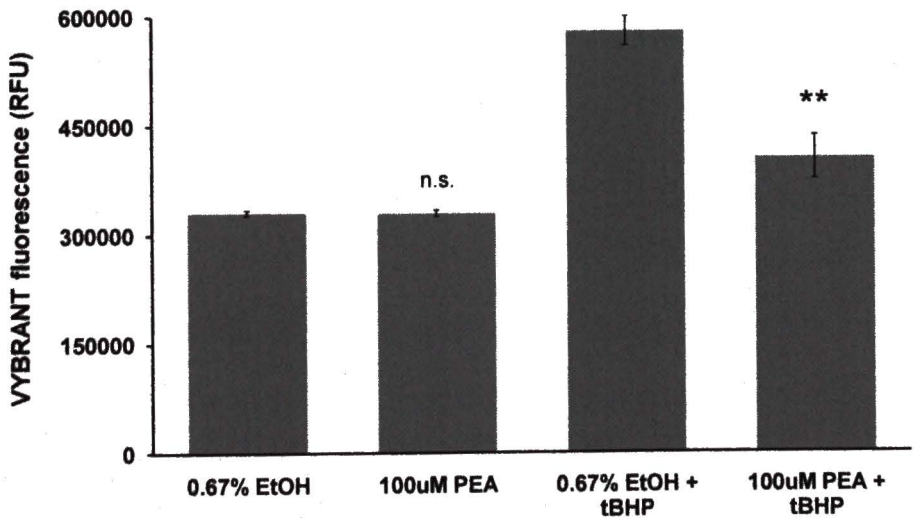
VYBRANT fluorescence (RFU)
600000
450000
300000
150000
0
n.s.
**
0.67% EtOH
100uM PEA
0.67% EtOH + tBHP
100uM PEA + tBHP

Fig. 4 – A prolonged (overnight) PEA pretreatment exhibits a protective trend against oxidative stress in HT22 cells. HT22 cells were pretreated with 100μM PEA overnight (16 hours) to an eight (8) hour tBHP exposure. PEA pretreatment led to a trend toward an increase in calcein-AM fluorescence and a significant decrease in VYBRANT fluorescence suggesting neuroprotection against necrosis. For this study, *n* equals three (3) wells per condition. A P-value of ≤ 0.001 is indicated by ***.

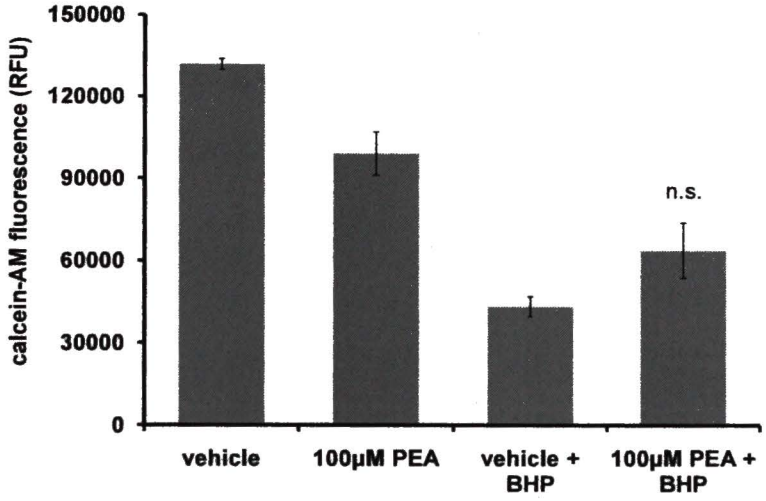
150000
120000
90000
60000
30000
0
calcein-AM fluorescence (RFU)
n.s.
vehicle
100μM PEA
vehicle + BHP
100μM PEA + BHP

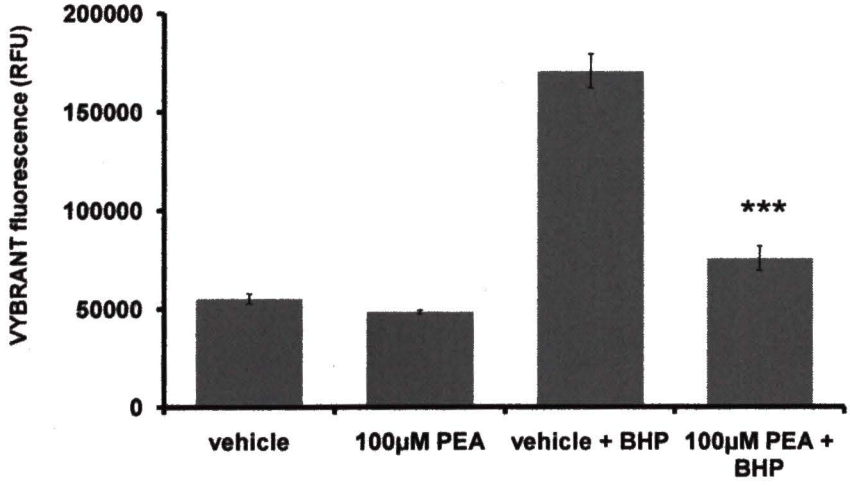
200000
150000
100000
50000
0
VYBRANT fluorescence (RFU)
***
vehicle
100μM PEA
vehicle + BHP
100μM PEA + BHP

Fig. 5 - A prolonged (overnight) PEA pretreatment fails to protect against mildly-toxic oxidative stress in HT22 cells. HT22 cells were pretreated with 100μM PEA overnight (12 hours) to an overnight tBHP exposure. PEA pretreatment led to a reduction in calcein-AM fluorescence suggesting a failure to protect against a mild degree of oxidative stress. For this study, *n* equals five (5) wells per condition.

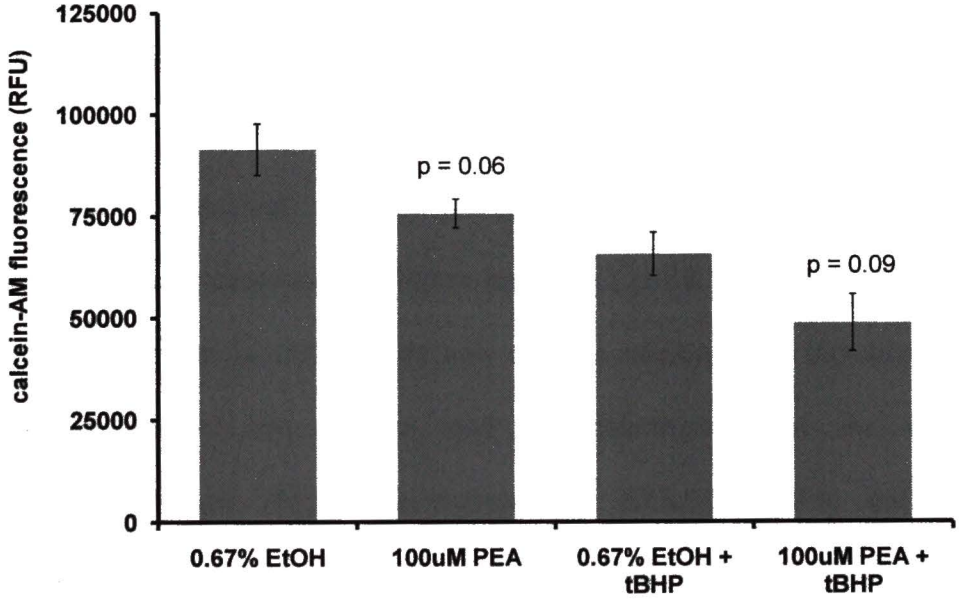
125000
100000
75000
50000
25000
0
calcein-AM fluorescence (RFU)
p = 0.06
p = 0.09
0.67% EtOH
100uM PEA
0.67% EtOH + tBHP
100uM PEA + tBHP

CHAPTER 3.3 – NAEs ALTER THE ACTIVITY OF KINASES INVOLVED IN NEUROPROTECTIVE SIGNALING

ABSTRACT

Cells respond to their environment in a variety of ways including activation of intracellular signal transduction cascades. Neurons can respond to toxic stimuli, in part, by activating key proteins such as protein kinases to facilitate an adaptive response thereby increasing the probability of survival. Two well characterized families of protein kinases involved in neuroprotective signaling are the mitogen-activated protein kinases (MAPKs) such as extracellular signal-transducing receptor kinase 1/2 (ERK1/2) and Akt (1 – 5). I hypothesized that PEA treatment of HT22 cells and cortical neurons can increase pAkt and pERK1/2 immunreactivity. In the present study, I determined that the lipid neuroprotectant palmitoylethanolamine (PEA) can activate the ERK1/2 MAPK and Akt proteins using microfluorimetric measurements. Here, I reveal that PEA can increase ERK1/2 and Akt phosphorylation and nuclear translocation of Akt and pAkt which suggests that the neuroprotective effects of PEA may be mediated, in part, by activation of these kinases. Furthermore, I provide evidence that this effect of PEA is not mediated through the activation of cannabinoid receptor type 2 (CB2).

INTRODUCTION

Some protein kinases, including mitogen-activated proteins kinases (MAPKs) and protein kinase B (Akt) have been shown to initiate neuroprotective responses (1 – 5). In the murine hippocampal cell line, HT22, short-term activation of ERK1/2 is involved in a cellular adaptive

response to glutamate toxicity (4). In PC12 cells, H_2O_2 treatment leads to the rapid phosphorylation of ERK1/2 and p38 (6). In hypoxic hippocampal neurons, the anesthetic isoflurane increases release of Ca^{2+} from IP_3R stores and increases the phosphorylation of the ERK1/2 MAPK and Akt proteins leading to neuroprotection (7). Progesterone can increase the recruitment and subsequent activation of PKA, MAPK and the PI-3K/Akt pathways leading to neuroprotection (5).

Akt is a member of the AGC kinase family of kinases and its activity is involved in a variety of cellular functions including proliferation, growth, metabolism and survival. It is implicated in neuroprotection and is involved in a variety of cancers (1, 2). In neurons, Akt activation results in in neuroprotection by inhibiting pro-apoptotic proteins including Bad, FOXO, GSK3α/β and caspase-9 (2). Akt activation can inhibit FOXO- and p53-mediated transcription of death genes such as FasL and Bax (8). Akt can phosphorylate Raf proteins to subsequently inhibit the ERK1/2 and p38 MAPK pathways (2).

Cannabinoids activate CB1 and CB2 cannabinoid receptors, both of which are coupled to the inhibitory G-protein $G_{i/o}$ ultimately leading to a reduction of cAMP and subsequent downregulation of PKA activity (9 – 11). For example, the endogenous cannabinoid (endocannabinoid), arachidonylethanolamine (AEA), can activate the ERK1/2, p38 and JNK MAPKs in addition to Akt (12 - 19).

Cannabinoids exhibit neuroprotective properties against a wide variety of pathological insuts including excitotoxicity, oxidative stress and hypoxia (20 - 29). Cannabinoid activation CB1 and CB2 leading to downregulation of PKA and activation of the ERK MAPK pathway, which has been shown to be a neuroprotective signaling pathway (3 – 5, 12 - 14). Furthermore, the activation of Akt further supports a role for cannabinoids as neuroprotectants (15, 19). In

addition to protecting against general excitotoxicity, hypoxia and oxidative stress, cannabinoids protect neurons in specific models of Alzheimer's disease, Parkinson's disease and other neurodegenerative diseases (30). For example, in AD brains, CB1 receptor expression is reduced and FAAH is upregulated (31, 32).

The AEA transport inhibitor AM404 and fatty acid amide hydrolase (FAAH) inhibitor AM374 lead to elevated AEA levels and they both increase MAPK activation in hippocampal slice cultures as well as reducing markers of neuronal degeneration (33). This result was also measured *in vivo* and was blocked with a CB1 antagonist. AM374 injected into rats led to increased AEA levels and activated the ERK MAPK pathway (34). Injection of AM374 also reduced the neuronal damage induced by kainite injection in addition to improving behavioral deficits. In mice, CB1 is involved in the regulation of ERK1/2, Akt and calcineurin activity in the amygdala during extinction of the conditioned fear response (35).

Studies in immune cell reveals that the NAE palmitoylethanolamine (PEA) has CB2 receptor-independent effects (36). Several NAEs including AEA, linolenoylethanolamine, oleoylethanolamine, oleoylethanolamine and palmitoylethanolamine (PEA), lead to increase ERK phosphorylation and AP-1 activity in mouse JB6 epidermal cells (37). The CB1 agonist Win 55212, however, could not stimulate ERK phosphorylation or AP-1 activation suggesting a CB1-independent function of NAEs in cell signaling and gene transcription (37).

I previously showed that the non-cannabinoid NAE, PEA, protects HT22 cells from peroxidative stress. Here I determined whether PEA treatment of HT22 cells alters ERK1/2 MAPK and Akt phosphorylation and nuclear translocation within a time frame consistent with neuroprotection. Furthermore, I provide evidence that these effects of PEA are not mediated by activation of CB2.

MATERIALS AND METHODS

Cell culture

HT22 were cultured as described previously (38). In brief, HT22 cells were grown in DMEM with high glucose and 1mmM sodium pyruvate (Mediatech), 2mM Glutamax (Invitrogen), 5% bovine growth serum (BGS) (Hyclone) and peniciilin-streptomycin (Mediatech). Cultures were kept at a confluency of less than 70% during the culturing process.

Mouse primary cortical neurons were obtained from postnatal day 2 (P2) mice after anesthesia on ice. Animals were decapitated and the scalp and skull was removed without disturbing the integrity of the brain. A 1 – 1.5mm^2 piece of cortex was removed from each hemisphere of the brain with fine-tipped #5/45 forceps and placed into 0.25% trypsin in HBSS with EGTA and without Ca^{2+}. Tissue was incubated in trypsin at 37° C for 20 minutes followed by addition of 1 volume of complete media and subsequent trituration several times with a fire-polsihed glass pipet or a 1ml capacity micropipette tip. Tissue was centrifuged at 1,000 x g for 5 minutes to pellet the viscous tissue. Media was removed and the pellet was resuspended in 2 ml of complete media followed by trituration. Cells were centrifuged again at 400 x g for 5 minutes. The supernatant was removed and the pellet was resuspended in 2ml of complete media followed by trituration. The resulting cell suspension was passed through a 40μm cell strainer and quantitated using a hemocytometer. Cell density was adjusted to 1 X 10^6 – 2 X 10^6 cells/ml depending upon the application. All neurons were plated on either poly-D-lysine/laminin-coated 12mm coverslips (BioCoat™ BD Biosciences) or poly-L-lysine-coated 12mm coverslips depending upon the application. Mixed neuronal cultures were maintained at 37°C / 5% CO_2 environment for 7 – 14 days. Before using coverslips, neurons were inspected visually under a microscope to determine

their development of neurites and overall healthy appearance. Only cultures with the majority of neurons bearing neurites were used in experiments.

E18 rat PC neurons were ordered from Genlantis Corporation and plated at ~4,000 – 8,000 cells/coverslip on 12mm poly-L-lysine-coated coverslips. Neurons were maintained for 8 days in vitro before PEA and LEA treatments.

Immunocytochemistry after PEA treatment

HT22 cells were plated on poly-L-lysine-coated 12mm coverslips at 40,000 cells/ml and maintained for 24 hours. The media was removed and replaced with media containing 100μM PEA or LEA (or EtOH vehicle) for various s time points (2 - 6 hours). After the PEA or LEA exposure, the cells were rinsed and fixed with 4% PFA followed by immunocytochemistry (ICC) using polyclonal sera rasied against Akt, phosphor-Akt, ERK1/2, phosphor-ERK1/2, p38 or monoclonal rabbit anti-phospho-p38 antibody. After completion of ICC and mounting, images were acquired using an Olympus IX70 fluorescence microscope. TIFF images were analyzed in Simple PCI by selecting three (3) background ROIs followed by nuclear then cytosolic ROIs for each cell. The nuclear and cytosolic data was separated in Excel and graphed.

Statistics

An F-test was conducted in Excel between each treatment group and the untreated control group to determine which type of T-test should be used for group comparisons. The mean fluorescence intensity from each treatment group was separately compared to the mean fluorescence intensity of the untreated control group using a two-sample T-test with either equal or unequal variances. A P-value of less than or equal to 0.05 was considered significant.

RESULTS

NAE treatment increases Akt/PKB and phospho-Akt/PKB kinase immunoreactivity

Exposure of HT22 cells to PEA, but not LEA, for four (4) and six (6) hours resulted in a significant increase in nuclear pAkt immunoreactivity (Fig. 1). When nuclear versus cytosolic pAkt immunreactivity was calculated as a ratio, four (4) and six (6) hour PEA exposure and six (6) hour LEA exposure resulted in an increased value (Fig. 2).

In addition, treatment of cultured postnatal day 2 (P2) mouse cortical neurons with LEA and PEA resulted in an increase in nuclear Akt immunoreactivity (Fig. 3). PEA treatment, but not LEA treatment, resulted in an increase in cytosolic Akt immunoreactivity (Fig. 3). The nuclear / cytosolic Akt ratio was significantly increased in both LEA- and PEA-treated cells (Fig. 3). Treatment of cortical neurons with LEA resulted in a significant decrease in nuclear pAkt but no change in cytosolic pAkt (Fig. 4). Treatment with PEA, however, resulted in a significant increase in both nuclear and cytosolic pAkt immunoreactivity (Fig. 4). The nuclear / cytosolic pAkt IR ratio was significantly reduced for LEA-treated and dramatically and significantly increased for PEA-treated cells (Fig. 4). Like for HT22 cells, this suggest that these effects are specific for PEA.

Similarly, in rat embryonic day 18 (E18) cortical neurons, nuclear pAkt immunoreactivity was slightly increased by 2 hour PEA treatment and significantly increased after 4 hour PEA treatment compared to vehicle controls (data not shown). Furthermore, LEA exposure for 2 and 4 hours resulted in a slight increase in nuclear pAkt levels compared to controls (data not shown).

To determine whether or not PEAs effects on Akt phosphorylation and nuclear translocation required activation of CB2, HT22 cells were treated with the CB2 agonists, JWH-015 and

AM1241, for 6 hours prior to Akt and pAkt immunolabeling. Treatment of HT22 cells with 10μM JWH-015 had no effect on nuclear or cytosolic Akt immunreactivity but it led to a decrease in cytosolic pAkt immunreactivity (Fig. 5). Treatment of cells with 10μM AM1241 led to a significant increase in nuclear Akt immunreactivity, but it had no effect on pAkt immunoreactivity (Fig. 5). Additional studies with JWH-105 failed to mimic the effects of PEA on Akt and pAkt immunoreactivity in HT22 cells. This suggests that PEAs ability to increase nuclear Akt and pAkt is through a CB2-independent mechanism.

Alternatively, the CB2 antagonist, AM630 was utilized to rule out CB2 activation in PEAs effects on Akt and pAkt. A 6 hour treatment of cells with AM630 led to a significant increase in nuclear Akt compared to PEA-treated cells. Furthermore, AM630 treatment resulted in a dramatic and significant decrease in cytosolic Akt similar to that observed with PEA. Interestingly, combined treatment with PEA and AM630 led to an increase in nuclear Akt immunoreactivity, but cytoslic Akt immunoreactivity was not changed. A 6 hour treatment of cells with AM630 led to a significant increase in nuclear Akt and a decrease in cytoslic Akt immunreactivity similar to that observed for PEA-treated cells, indicating that PEAs effects were not mediated through CB2 receptor activation. Interestingly, combined treatment with PEA and AM630 had no effect on nuclear Akt immunoreactivity, but it decreased cytoslic Akt immunoreactivity. These results suggest that alterations in Akt and pAkt compartmentalization are affected differently by PEA and AM630. These results do not provide evidence that CB2 activation is responsible for the observed changes in Akt and pAkt immunoreactivities in HT22 cells.

Effect of NAE treatment on ERK1/2 and phospho-ERK1/2immunoreactivity

Exposure of HT22 cells to 30 minute or 60 minute PEA or LEA had no effect on ERK1/2 immunoreactivity. Exposure of cells to PEA for 30 minutes, but not 60 minutes, however, led to a significant increase in nuclear and cytosolic phospho-ERK1/2 (pERK) immunoreactivity (Fig. 7). Exposure of HT22 cells to LEA for 60 minutes led to an increase in nuclear and cytosolic pERK immunoreactivity (Fig. 7). Treatment of HT22 cells with the CB2 agonist, JWH-015, for 60 minutes had no effect on ERK1/2 or pERK1/2 immunoreactivity, suggested that LEAs effects observed at 60 minutes were not attributable to CB2 activation (Fig. 8).

Effect of NAE treatment on p38 and phospho-p38 MAPKimmunoreactivity

Exposure of HT22 cells to PEA for 30 minutes had no effect on nuclear phospho-p38 immunoreactivity, but there was a trend toward a decrease in phospho-p38 immunoreactivity (Fig. 9). Exposure of cells to PEA for 60 minutes, however, resulted in a dramatic and significant decrease in both nuclear and cytosolic phospho-p38 immunoreactivity (Fig. 9). Exposure of HT22 cells to LEA for 30 minutes led to a significant increase in nuclear phospho-p38 immunoreactivity. Exposure of cells to PEA for 60 minutes, however, resulted in a dramatic and significant increase in cytosolic phospho-p38 immunoreactivity (Fig. 9). These results suggest that LEA affects phopho-p38 localization differently than that of PEA.

DISCUSSION

Here, I provided evidence that PEA treatment, and to lesser extent LEA treatment, can facilitate the nuclear translocation of Akt and pAkt in a neuronal cell line and in cultured cortical neurons. Furthermore, I determined that PEA and LEA can lead to a rapid and transient increase

in nuclear and cytosolic pERK1/2, but not ERK1/2. In addition, I determined that PEA exposure leads to a significant reduction in nuclear and cytoslic phopsho-p38 immunoreactivity in HT22 cells. I previously determined that PEA pretreatment for five (5) to six (6) hours protects HT22 cells from oxidative stress. Together, these data suggest that PEA and LEA activate kinases known to be involved in neuroprotective signaling, thus providing a possible mechanism by which NAEs neuroprotect.

Numerous studies have revealed that the cannabinoid NAE, AEA, is neuroprotective through activation of CB1 (20 - 29). Since the saturated NAEs, PEA and LEA, do not bind CB1 and they exhibit poor affinity for CB2, I hypothesized that these NAEs exhibit neuroprotective properties by a mechanism independent of CB2 (39, 40). To rule out CB2-mediated effects in PEA neuroprotective signaling, I measured the effect of CB2 agonists on Akt/pAkt and ERK/pERK immunoreactivity. The CB2 agonist, JWH-015 had no effect on nuclear Akt or pAkt immunoreactivity in HT22 cells. The CB2 agonist AM1241, however, increased nuclear Akt immunoreactivity, but it had no effect on pAkt immunoreactivity. Together, these data suggest that PEAs effect on Akt and pAkt were not mediated through CB2 activation. Further evidence for this comes from the observation that treatment of cells with the CB2 antagonist, AM630, mimics instead of inhibits the effects of PEA on cytosolic Akt immunoreactivity and nuclear and cytosolic pAkt immunoreactivity in HT2 cells.

There are several reports of AEA activating the ERK1/2 MAPK pathway through activation of CB1 (12 - 15). Here, I determined that the non-cannabinoid PEA can increase nuclear pERK1/2 translocation and this effect can not be mimicked by the CB2 agonist JWH-015. Also, the p38 MAPK pathway is altered by PEA. PEA treatment of HT22 cells leads to a rapid reduction in nuclear and cytosolic phospo-p38 immunoreactivity.

Overall, my data suggests that PEA activates the neuroprotective Akt and ERK1/2 MAPK signaling pathways by a CB2-independent mechanism. These effects are within the timeframe required to cause neuroprotection in HT22 cells. Interestingly, PEA-mediated elevation of pERK1/2 immunoreactivity occurs much earlier that measured elevation of Akt and pAkt nuclear translocation. This suggests that the ERK1/2 MAPK pathway is activated before the Akt signaling pathway.

Previous studies indicate that activation of Akt can result in phosphorylation of inositol 1, 4, 5-trisphosphate receptors (IP3Rs) and lead to enhanced Ca^{2+} release (41, 42). Interestingly, intracellular Ca^{2+} can activate a wide variety of signaling pathways including those mediated by Ras, which include the PI3-K/Akt and MAPK pathways (43). These data, in part, are consistent with a possible effect of PEA on Ca^{2+} signaling in neurons.

REFERENCES

1. Fayard E, Tintignac LA, Baudry A and Hemmings BA (2005) Protein kinase B/Akt at a glance.
   J Cell Sci. 118(Pt 24):5675-8
2. Manning BD and Cantley LC (2007) AKT/PKB signaling: navigating downstream. Cell. 129(7):1261-74.
3. Nilsen J, Chen S and Brinton RD (2002) Dual action of estrogen on glutamate-induced calcium signaling: mechanisms requiring interaction between estrogen receptors and src/mitogen activated protein kinase pathway. Brain Res. 930(1-2):216-34.

4. Luo Y and DeFranco DB (2006) Opposing roles for ERK1/2 in neuronal oxidative toxicity: distinct mechanisms of ERK1/2 action at early versus late phases of oxidative stress. J Biol Chem. 281(24):16436-42.

5. Singh M (2006) Progesterone-induced neuroprotection. Endocrine. 29(2):271-4.

6. Zhang L and Jope RS (1999) Oxidative stress differentially modulates phosphorylation of ERK, p38 and CREB induced by NGF or EGF in PC12 cells. Neurobiol Aging. 20(3):271-8.

7. Gray JJ, Bickler PE, Fahlman CS, Zhan X and Schuyler JA (2005) Isoflurane neuroprotection in hypoxic hippocampal slice cultures involves increases in intracellular Ca2+ and mitogen-activated protein kinases. Anesthesiology. 102(3):606-15.

8. Brunet A, Datta SR and Greenberg ME (2001) Transcription-dependent and -independent control of neuronal survival by the PI3K-Akt signaling pathway. Curr Opin Neurobiol. 11(3):297-305.

9. Bidaut-Russell M, Devane WA and Howlett AC (1990) Cannabinoid receptors and modulation of cyclic AMP accumulation in the rat brain. J Neurochem. 55(1):21-6.

10. Vogel Z, Barg J, Levy R, Saya D, Heldman E and Mechoulam R (1993) Anandamide, a brain endogenous compound, interacts specifically with cannabinoid receptors and inhibits adenylate cyclase. J Neurochem. 61(1):352-355.

11. Bayewitch M, Avidor-Reiss T, Levy R, Barg J, Mechoulam R and Vogel Z (1995) The peripheral cannabinoid receptor: adenylate cyclase inhibition and G protein coupling. FEBS Lett. 375(1-2):143-147.

12. Bouaboula M, Poinot-Chazel C, Bourrie B, Canat X, Calandra B, Rinaldi-Carmona M, Le Fur G and Casellas P (1995) Activation of mitogen-activated protein kinases by stimulation of the central cannabinoid receptor CB1. Biochem J. 1995 Dec 1;312 (Pt 2):637-41.

13. Wartmann M, Campbell D, Subramaninan A, Burstein SH and Davis RJ (1995) The MAP kinase signal transduction pathway is activated by the endogenous cannabinoid anandamide. FEBS Lett. 359(2-3):133-6.

14. Bouaboula M, Poinot-Chazel C, Marchand J, Canat X, Bourrie B, Rinaldi-Carmona M, Calandra B, Le Fur G and Casellas P (1996) Signaling pathway associated with stimulation of CB2 peripheral cannabinoid receptor. Involvement of both mitogen-activated protein kinase and induction of Krox-24 expression. Eur J Biochem.237(3):704-711.

15. Gomez del Pulgar T, Velasco G and Guzman M (2000) The CB1 cannabinoid receptor is coupled to the activation of protein kinase B/Akt. Biochem J. 347(Pt 2):369-73.

16. Rueda D, Galve-Roperh I, Haro A and Guzman M (2000) The CB(1) cannabinoid receptor is coupled to the activation of c-Jun N-terminal kinase. Mol Pharmacol. 58(4):814-20

17. Derkinderen P, Ledent C, Parmentier M and Girault JA (2001) Cannabinoids activate p38 mitogen-activated protein kinases through CB1 receptors in hippocampus. J Neurochem. 77(3):957-60.

18. Derkinderen P, Valient E, Toutant M, Corvol JC, Enslen H, Ledent C, Trzaskos J, Caboche J and Girault JA (2003) Regulation of extracellular signal-regulated kinase by cannabinoids in hippocampus. J Neurosci. 23(6):2371-82.

19. Sanchez MG, Ruiz-Llorente L, Sanchez AM and Diaz-Laviada I (2003) Activation of phosphoinositide 3-kinase/PKB pathway by CB(1) and CB(2) cannabinoid receptors expressed in prostate PC-3 cells. Involvement in Raf-1 stimulation and NGF induction. Cell Signal. 15(9):851-9.

20. Skaper SD, Buriani A, Dal Toso R, Petrelli L, Romanello S, Facci L and Leon A (1996) The ALIAmide palmitoylethanolamide and cannabinoids, but not anandamide, are protective in

a delayed postglutamate paradigm of excitotoxic death in cerebellar granule neurons. Proc Natl Acad Sci U S A. 93(9):3984-9.

21. Hampson AJ, Gimaldi M, Axelrod J and Wink D (1998) Cannabidiol and (-)Delta9-tetrahydrocannabinol are neuroprotective antioxidants. Proc Natl Acad Sci U S A. 95(14):8268-73.

22. Shen M and Thayer SA (1998) Cannabinoid receptor agonists protect cultured rat hippocampal neurons from excitotoxicity. Mol Pharmacol. 54(3):459-62.

23. Moesgaard B, Jaroszewski JW and Hansen HS (1999) Accumulation of N-acyl-ethanolamine phospholipids in rat brains during post-decapitative ischemia: a 31p NMR study. J Lipid Res. 40(3):515-21.

24. Nagayama T, Sinor AD, Simon RP, Chen J, Graham SH, Jin K and Greenberg DA (1999) Cannabinoids and neuroprotection in global and focal cerebral ischemia and in neuronal cultures. J Neurosci. 19(8):2987-95.

25. Chen Y and Buck J (2000) Cannabinoids protect cells from oxidative cell death: a receptor-independent mechanism. J. Pharmacol. Exp. Ther. 293(3): 807-12.

26. Hampson AJ and Grimaldi M (2001) Cannabinoid receptor activation and elevated cyclic AMP reduce glutamate neurotoxicity. Eur J Neurosci. 13(8):1529.

27. van der Stelt M, Velhuis WB, Maccarrone M, Nar PR, Nicolay K, Veldink GA, DiMarzo V and Vliegenthart JF (2002) Acute neuronal injury, excitotoxicity, and the endocannabinoid system. Mol Neurobiol. 2002 Oct-Dec;26(2-3):317-46.

28. Marsicano G, Goodenough S, Monory K, Hermann H, Eder M, Cannich A, Azad SC, Cascio MG, Gutierrez SO, van der Stelt M, Lopez-Rodriguez ML, Casanova E, Schutz G,

Zieglgansberger W, Di Marzo V, Behl C and Lutz B (2003) CB1 cannabinoid receptors and on-demand defense against excitotoxicity. Science. 302(5642):84-8.

29. Shouman B, Fontaine RH, Baud O, Schwendimann L, Keller M, Spedding M, Lelievre V and Gressens P (2006) Endocannabinoids potently protect the newborn brain against AMPA-kainate receptor-mediated excitotoxic damage. Br J Pharmacol. 148(4):442-51.
30. Sarne Y and Mechoulam R (2005) Cannabinoids: between neuroprotection and neurotoxicity. Curr Drug Targets CNS Neurol Disord. 4(6):677-84.
31. Westlake TM, Howlett AC, Bonner TI, Matsuda LA and Herkenham M (1994) Cannabinoid receptor binding and messenger RNA expression in human brain: an in vitro receptor autoradiography and in situ hybridization histochemistry study of normal aged and Alzheimer's brains. Neuroscience. 63(3):637-52.
32. Benito C, Nunez E, Tolon RM, Carrier EJ, Rabano A, Hillard CJ and Romero J (2003) Cannabinoid CB2 receptors and fatty acid amide hydrolase are selectively overexpressed in neuritic plaque-associated glia in Alzheimer's disease brains. J Neurosci. 23(35):11136-41.
33. Karanian DA, Brown QB, Makriyannis A, Kosten TA and Bahr BA (2005) Dual modulation of endocannabinoid transport and fatty acid amide hydrolase protects against excitotoxicity. J Neurosci. 25(34):7813-20.
34. Karanian DA, Karim SL, Wood JT, Williams JS, Lin S, Makriyannis A and Bahr BA (2007) Endocannabinoid enhancement protects against kainic acid-induced seizures and associated brain damage. J Pharmacol Exp Ther. 322(3):1059-66.
35. Cannich A, Wotjak CT, Kamprath K, Hermann H, Lutz B and Marsicano G (2004) CB1 cannabinoid receptors modulate kinase and phosphatase activity during extinction of conditioned fear in mice. Learn Mem. 11(5):625-32.

36. Ross RA, Brockie HC and Pertwee RG (2000) Inhibition of nitric oxide production in RAW264.7 macrophages by cannabinoids and palmitoylethanolamide. Eur J Pharmacol. 401(2):121-30.

37. Berdyshev EV, Schmid PC, Krebsbach RJ, Hillard CJ, Hunag C, Chen N, Dong Z and Schmid HH (2001) Cannabinoid-receptor-independent cell signalling by N-acylethanolamines.Biochem J. 360(Pt 1):67-75.

38. Duncan RS, Hwang SY and Koulen P (2007) Differential inositol 1,4,5-trisphosphate receptor signaling in a neuronal cell line. Int J Biochem Cell Biol. 39(10):1852-62.

39. Lambert DM and Di Marzo V (1999) The palmitoylethanolamide and oleamide enigmas : are these two fatty acid amides cannabimimetic? Curr. Med. Chem. 6 (8):757-773.

40. Sugiura T, Kondo S, Kishimoto S, Miyashita T, Nakane S, Kodaka T, Suhara Y, Takayama H and Waku L (2000) Evidence that 2-arachidonoylglycerol but not N-palmitoylethanolamine or anandamide is the physiological ligand for the cannabinoid CB2 receptor. Comparison of the agonistic activities of various cannabinoid receptor ligands in HL-60 cells. J Biol Chem. 275(1):605-12.

41. Koulen P, Madry C, Duncan RS, Hwang JY, Nixon E, McClung N, Gregg EV and Singh M (2008) Progesterone potentiates IP(3)-mediated calcium signaling through Akt/PKB. Cell Physiol Biochem. 21(1-3):161-72.

42. Hwang JY, Duncan RS, Madry C, Singh M and Koulen P, Effects of progesterone on calcium signaling in hippocampal neurons, Cell Calcium, in press.

43. Rosen LB, Ginty DD, Weber MJ and Greenberg ME (1994) Membrane depolarization and calcium influx stimulate MEK and MAP kinase via activation of Ras. Neuron. 12(6):1207-21

FIGURES

Fig. 1 – PEA treatment of HT22 cells leads to an increase in nuclear pAkt immunoreactivity. A four (4) and six (6) hour treatment led to a significant increase in nuclear pAkt immunoreactivity in HT22 cells. The structurally similar NAE, LEA, had no significant effect on nuclear pAkt immunoreactivity. For the four (4) hour treatment groups, *n* equals 78, 70 and 85 cells for vehicle, LEA and PEA treatments, respectively. For the six (6) hour treatment groups, *n* equals 64, 71 and 71 cells for vehicle, LEA and PEA treatments, respectively. A P-value of ≤ 0.01 is indicated by **.

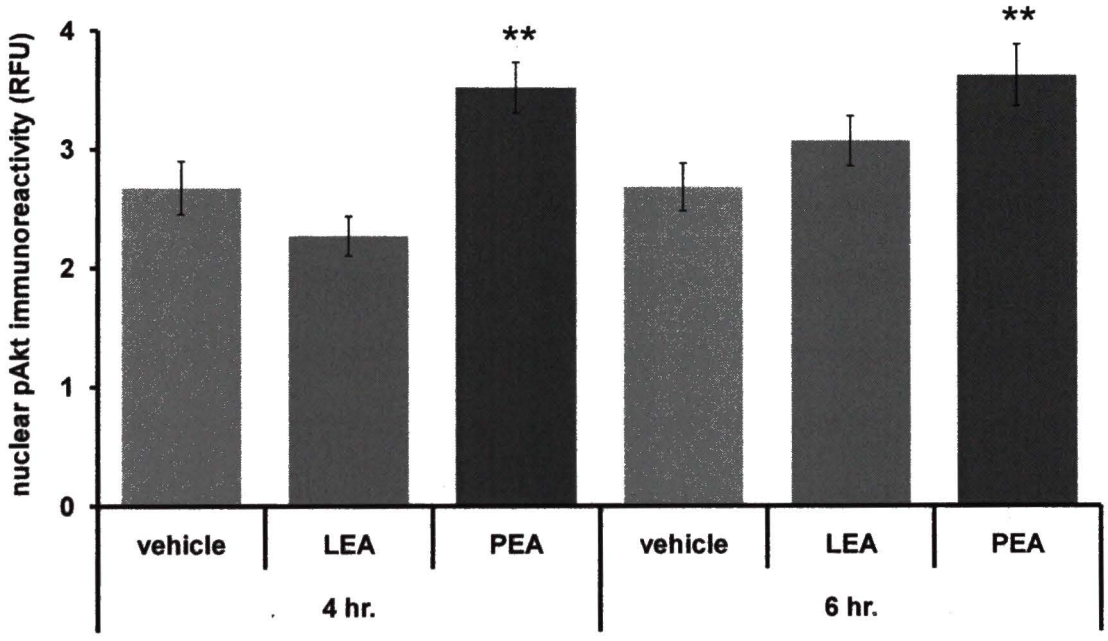
nuclear pAkt immunoreactivity (RFU)
4
3
2
1
0
**
**
vehicle
LEA
PEA
vehicle
LEA
PEA
4 hr.
6 hr.

Fig. 2 – PEA and LEA treatment of HT22 cells leads to a significant increase in the nuclear / cytosolic pAkt ratio. After a four (4) hour PEA exposure, nuclear / cytoslic pAkt ratio is increased in HT22 cells. It requires a six (6) hour LEA exposure to have a similar effect. For the two (2) hour treatment groups, *n* equals 54, 67 and 51 cells for vehicle, LEA and PEA treatments, respectively. For the four (4) hour treatment groups, *n* equals 78, 70 and 85 cells for vehicle, LEA and PEA treatments, respectively. For the six (6) hour treatment groups, *n* equals 64, 71 and 71 cells for vehicle, LEA and PEA treatments, respectively. A P-value of ≤ 0.05 and ≤ 0.001 is indicated by * and ***, respectively.

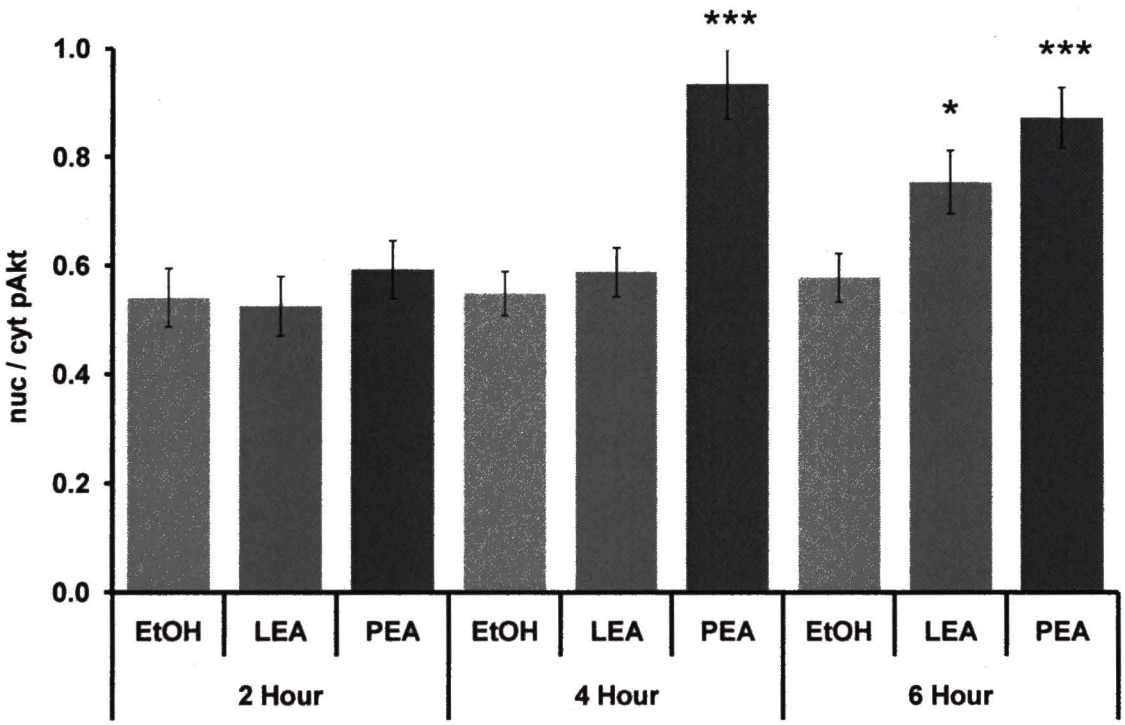
***
***
*
1.0
0.8
0.6
0.4
0.2
0.0
nuc / cyt pAkt
EtOH
LEA
PEA
EtOH
LEA
PEA
EtOH
LEA
PEA
2 Hour
4 Hour
6 Hour

Fig. 3 – PEA treatment of cultured primary cortical neurons leads to an increase in nuclear and cytosolic Akt immunoreactivity. A six (6) hour PEA treatment led to a significant increase in both nuclear and cytosolic Akt immunoreactivity in cultured cortical neurons. LEA treatment increased nuclear Akt immunoreactivity but had no effect on cytosolic immunoreactivity. Furthermore, both NAEs increase the nuclear / cytosolic Akt ratio in neurons. For this study, *n* equals 48, 34 and 48 cells for vehicle, LEA and PEA treatments, respectively. A P-value of ≤ 0.05 and ≤ 0.001 is indicated by * and ***, respectively.

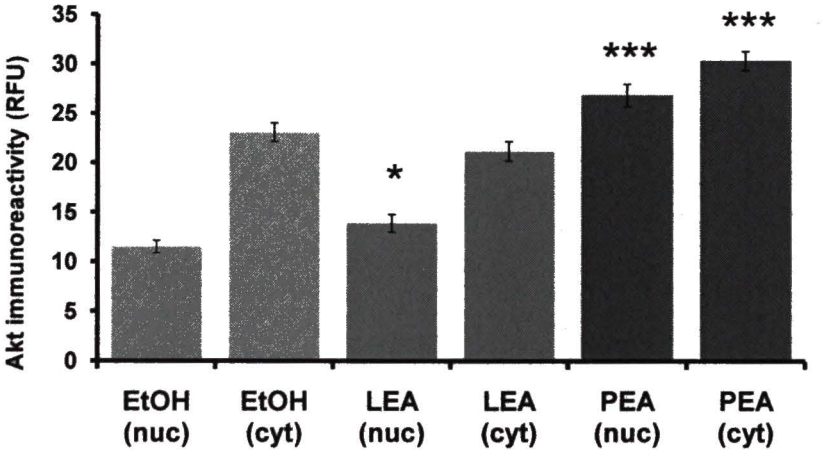
Akt immunoreactivity (RFU)
35
30
25
20
15
10
5
0
*
***
***
EtOH (nuc)
EtOH (cyt)
LEA (nuc)
LEA (cyt)
PEA (nuc)
PEA (cyt)

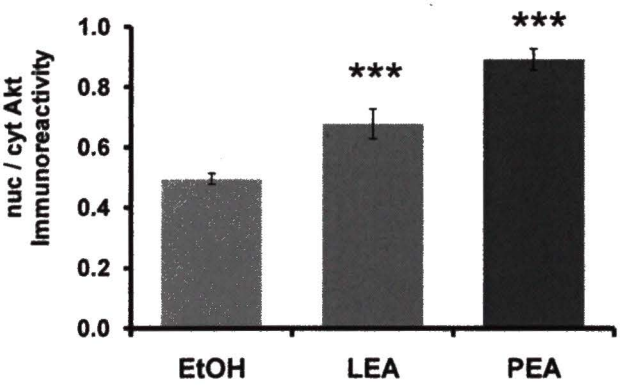
nuc / cyt Akt Immunoreactivity
1.0
0.8
0.6
0.4
0.2
0.0
***
***
EtOH
LEA
PEA

Fig. 4 – PEA treatment of cultured primary cortical neurons leads to an increase in nuclear and cytosolic pAkt immunoreactivity. A six (6) hour PEA treatment led to a significant increase in both nuclear and cytosolic pAkt immunoreactivity in cultured cortical neurons. LEA treatment, however, decreased nuclear pAkt immunoreactivity but had no effect on cytosolic immunoreactivity. Furthermore, PEA increased while LEA decreased the nuclear / cytosolic pAkt ratio in neurons. For this study, *n* equals 39, 46 and 69 cells for vehicle, LEA and PEA treatments, respectively. A P-value of ≤ 0.05 and ≤ 0.001 is indicated by * and ***, respectively.

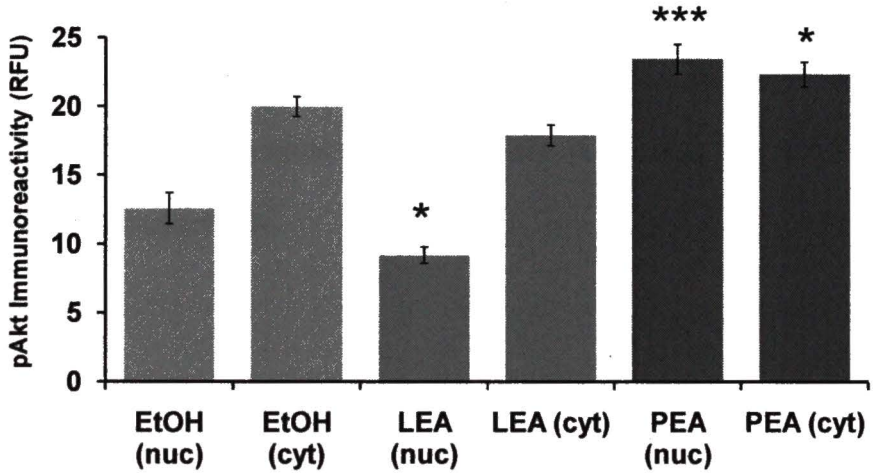
pAkt Immunoreactivity (RFU)
25
20
15
10
5
0
***
*
*
EtOH (nuc)
EtOH (cyt)
LEA (nuc)
LEA (cyt)
PEA (nuc)
PEA (cyt)

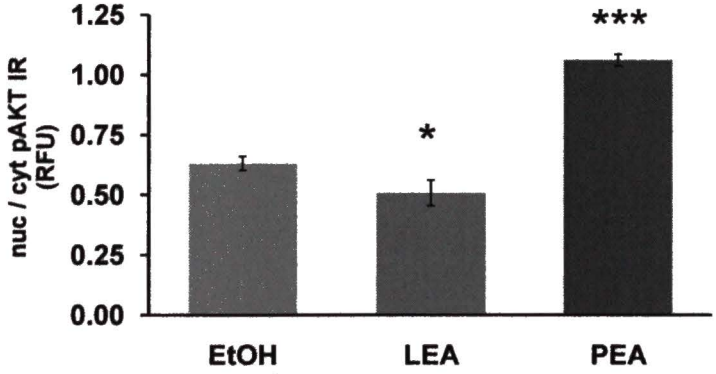
nuc / cyt pAKT IR (RFU)
1.25
1.00
0.75
0.50
0.25
0.00
***
*
EtOH
LEA
PEA

Fig. 5 – The CB2 agonist AM1241, but not JWH-015, increases nuclear Akt immunoreactivity. Treatment of HT22 cells with the CB2 agonist JWH-015 had no effect on nuclear Akt immunoreactivity. Treatment with AM1241, however, led to an increase in nuclear Akt immunoreactivity. Treatment of HT22 cells with the CB2 agonists JWH-015 and AM1241 had no effect on nuclear or cytosolic pAkt immunoreactivity. In fact, JWH-015 led to a reduction in pAkt immunoreactivity. For the Akt study, *n* equals 61, 56 and 59 cells for vehicle, JWH-015 and AM-1241 treatments, respectively. For the pAkt study, *n* equals 80, 91 and 64 cells for vehicle, JWH-015 and AM-1241 treatments, respectively. A P-value of ≤ 0.01 and ≤ 0.001 is indicated by ** and ***, respectively.

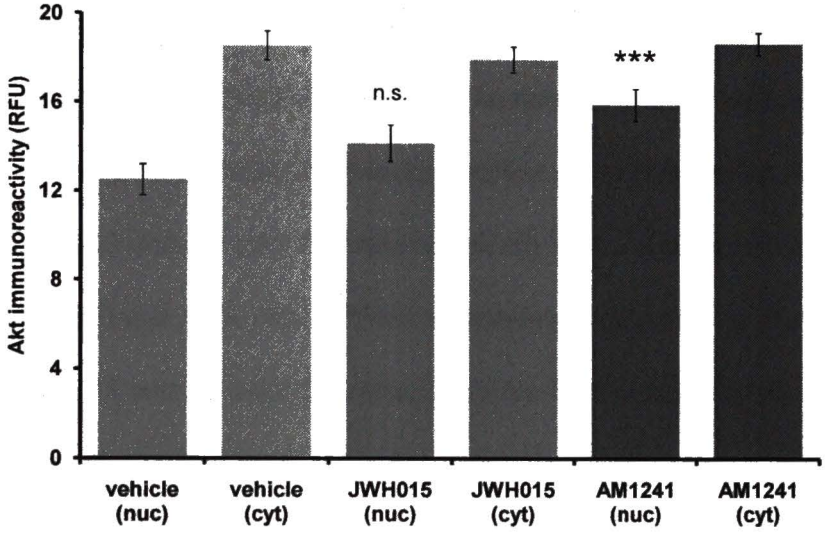
Akt immunoreactivity (RFU)
20
16
12
8
4
0
n.s.
***
vehicle (nuc)
vehicle (cyt)
JWH015 (nuc)
JWH015 (cyt)
AM1241 (nuc)
AM1241 (cyt)

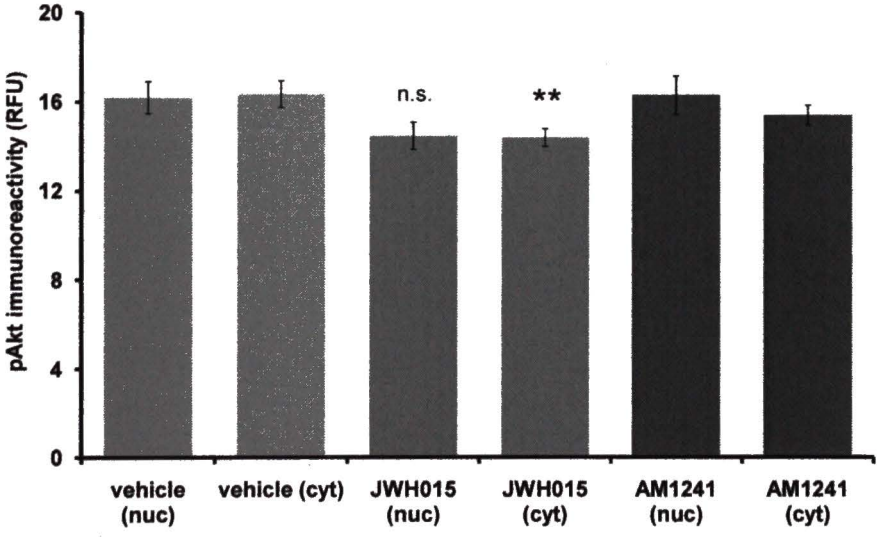
pAkt immunoreactivity (RFU)
20
16
12
8
4
0
n.s.
**
vehicle (nuc)
vehicle (cyt)
JWH015 (nuc)
JWH015 (cyt)
AM1241 (nuc)
AM1241 (cyt)

Fig. 6 – The CB2 antagonist, AM630, alters Akt and pAkt immunoreactivity in HT22 cells. Treatment of HT22 cells with AM630 leads to an increase in nuclear and a decrease in cytosolic Akt and pAkt immunoreactivity in a more pronounced manner than PEA. Cotreatment of cells with both PEA and MA630 results in an increase in nuclear Akt with no effect on cytosolic Akt and a decrease in cytosolic pAkt with no effect on nuclear pAkt. For the Akt study, *n* equals 50, 66, 52, 53, 62 and 65 cells for vehicle (PEA), PEA, vehicle (AM-630), AM-630, vehicle (PEA and AM-630) and PEA and AM-630 treatments, respectively. For the pAkt study, *n* equals 56, 75, 94, 78, 75 and 89 cells for vehicle (PEA), PEA, vehicle (AM-630), AM-630, vehicle (PEA and AM-630) and PEA and AM-630 treatments, respectively. A P-value of ≤ 0.05, < 0.01 and ≤ 0.001 is indicated by *, ** and ***, respectively.

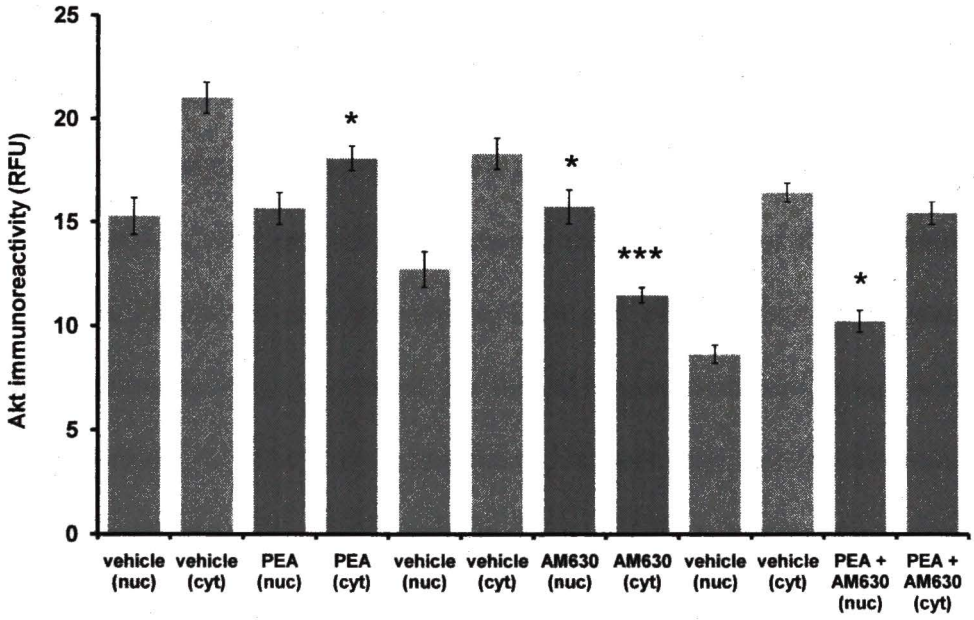
Akt immunoreactivity (RFU)
25
20
15
10
5
0
*
*
***
*
vehicle (nuc)
vehicle (cyt)
PEA (nuc)
PEA (cyt)
vehicle (nuc)
vehicle (cyt)
AM630 (nuc)
AM630 (cyt)
vehicle (nuc)
vehicle (cyt)
PEA + AM630 (nuc)
PEA + AM630 (cyt)

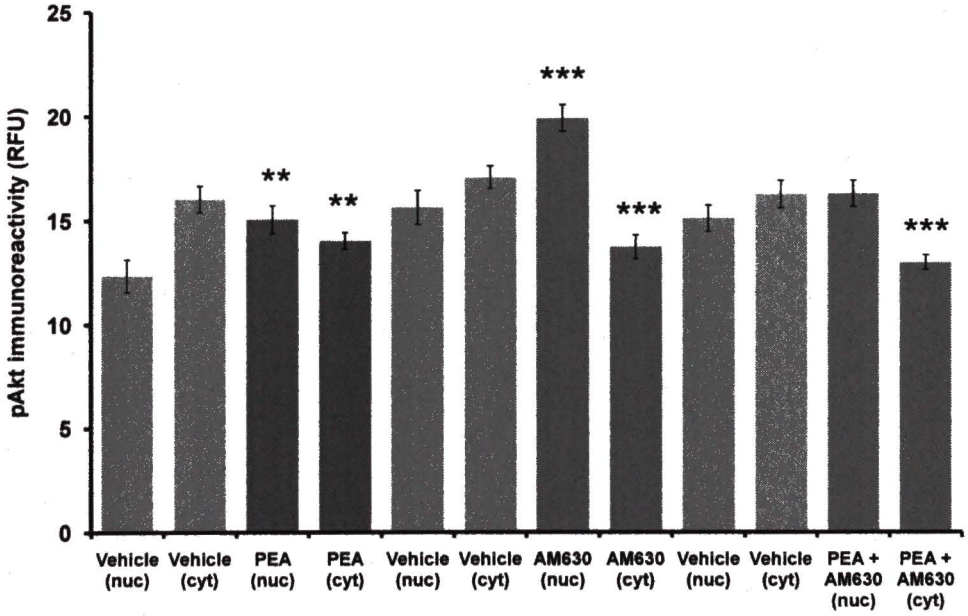
pAkt immunoreactivity (RFU)
25
20
15
10
5
0
**
**
***
***
***
Vehicle (nuc)
Vehicle (cyt)
PEA (nuc)
PEA (cyt)
Vehicle (nuc)
Vehicle (cyt)
AM630 (nuc)
AM630 (cyt)
Vehicle (nuc)
Vehicle (cyt)
PEA + AM630 (nuc)
PEA + AM630 (cyt)

Fig. 7 – PEA and LEA increase nuclear and cytosolic pERK1/2 immunoreactivity in HT22 cells. A brief, 30 minute PEA treatment of HT22 cells results in a transient increase in nuclear and cytosolic pERK/12 (but not ERK1/2) immunoreactivity. Treatment of cells with LEA for 60 min. (but not 30 min.) leads to an increase in nuclear and cytosolic ERK1/2 immunoreactivity. In the ERK1/2 immunofluorescence experiment, for the 30 minute treatment group, *n* equals 24, 33 and 34 cells for vehicle, LEA and PEA treatments, respectively. For the 60 minute treatment group, *n* equals 26, 25 and 32 cells for vehicle, LEA and PEA treatments, respectively. In the pERK1/2 immunofluorescence experiment, for the 30 minute treatment group, *n* equals 46, 35 and 81 cells for vehicle, LEA and PEA treatments, respectively. For the 60 minute treatment group, *n* equals 41, 63 and 57 cells for vehicle, LEA and PEA treatments, respectively. A P-value of ≤ 0.001 is indicated by ***.

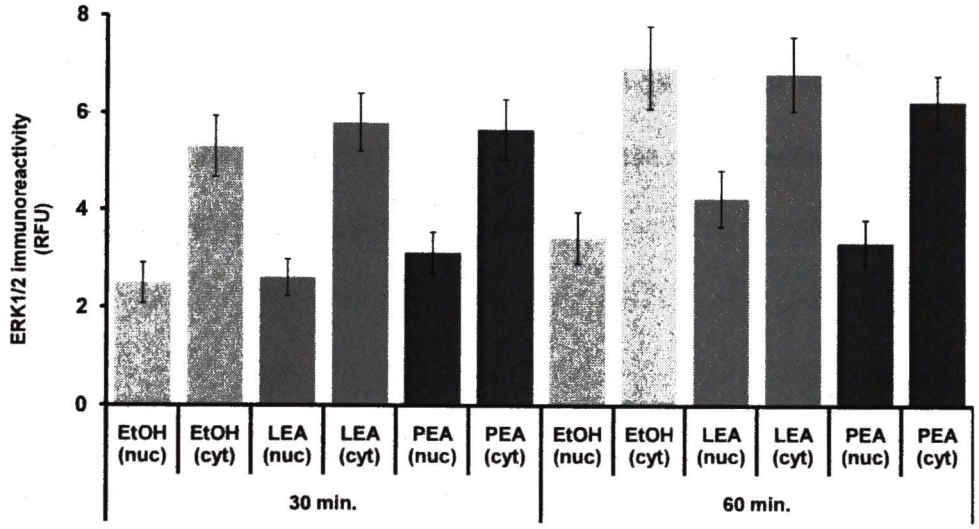
ERK1/2 immunoreactivity (RFU)
8
6
4
2
0
EtOH (nuc)
EtOH (cyt)
LEA (nuc)
LEA (cyt)
PEA (nuc)
PEA (cyt)
EtOH (nuc)
EtOH (cyt)
LEA (nuc)
LEA (cyt)
PEA (nuc)
PEA (cyt)
30 min.
60 min.

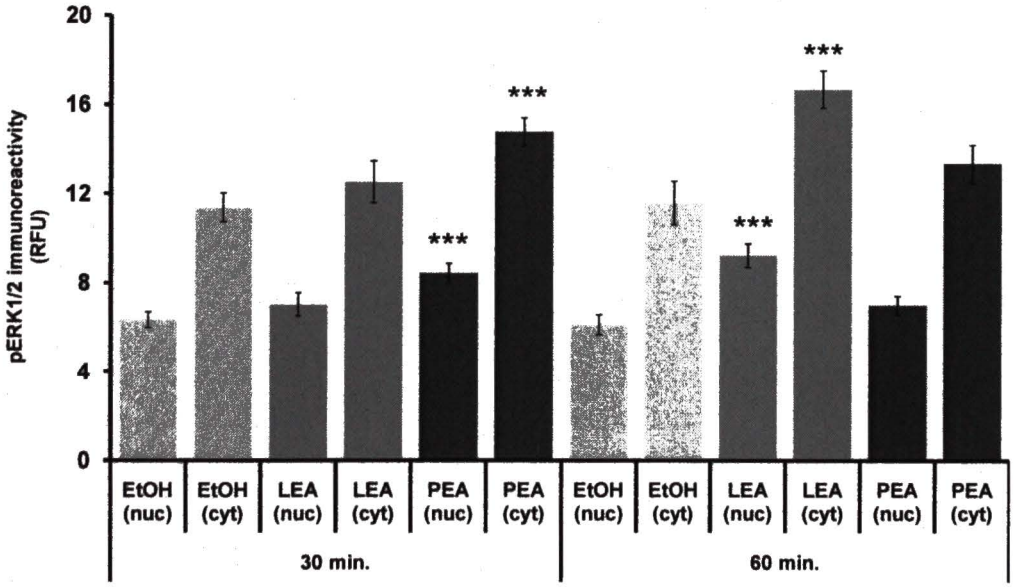
pERK1/2 immunoreactivity (RFU)
20
16
12
8
4
0
***
***
***
***
EtOH (nuc)
EtOH (cyt)
LEA (nuc)
LEA (cyt)
PEA (nuc)
PEA (cyt)
EtOH (nuc)
EtOH (cyt)
LEA (nuc)
LEA (cyt)
PEA (nuc)
PEA (cyt)
30 min.
60 min.

Fig. 8 – Treatment of HT22 cells with JWH-15 for 60 minutes has no effect on ERK/12 or pERK1/2 immunoreactivity. Treatment of HT22 cells with the CB2 agonist JWH-015 fails to significantly increase ERK1/2 or pERK1/2 immunoreactivity. In the ERK1/2 immunofluorescence experiment, *n* equals 54 and 59 cells for vehicle and JWH-015 treatments, respectively. In the pERK1/2 immunofluorescence experiment, *n* equals 34 and 40 cells for vehicle and JWH-015 treatments, respectively.

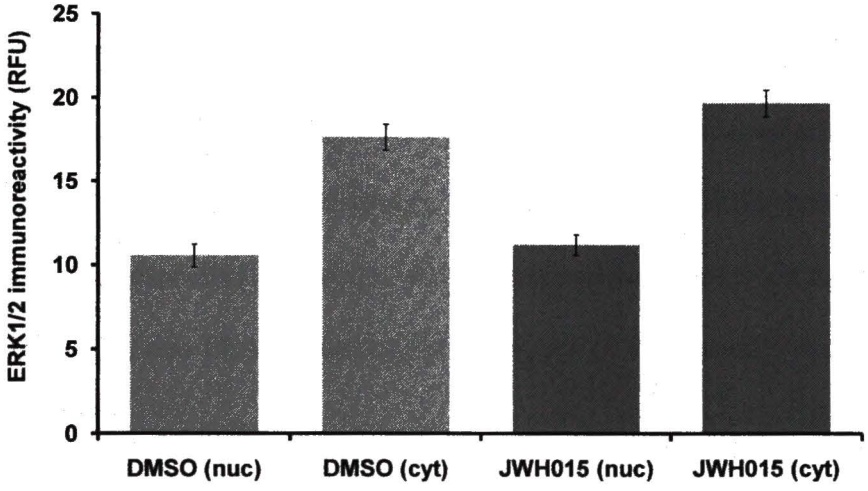
ERK1/2 immunoreactivity (RFU)
25
20
15
10
5
0
DMSO (nuc)
DMSO (cyt)
JWH015 (nuc)
JWH015 (cyt)

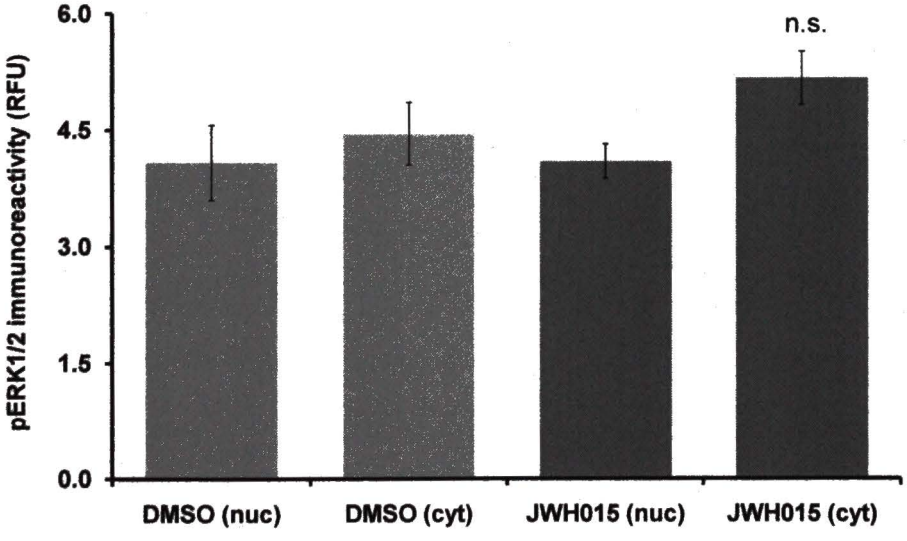
pERK1/2 immunoreactivity (RFU)
6.0
4.5
3.0
1.5
0.0
n.s.
DMSO (nuc)
DMSO (cyt)
JWH015 (nuc)
JWH015 (cyt)

Fig. 9 – NAEs alter phospho-p38 MAPK immunoreactivity in HT22 cells. Treatment of HT22 cells with PEA for 30 min. had no effect on phospho-p38 immunoreactivity. A 60 minute exposure, however, resulted in a dramatic and significant decrease in both nuclear and cytosolic phospho-p38 immunoreactivity. Interestingly, LEA treatment led to an increase in nuclear phospho-p38 at 30 minute and an increase in cytosolic phospho-p38 at 60 minutes. In this study, for the 30 minute treatment group, *n* equals 42, 32 and 35 cells for vehicle, LEA and PEA treatments, respectively. For the 60 minute treatment group, *n* equals 50, 29 and 41 cells for vehicle, LEA and PEA treatments, respectively. A P-value of ≤ 0.05 and ≤ 0.001 is indicated by * and ***.

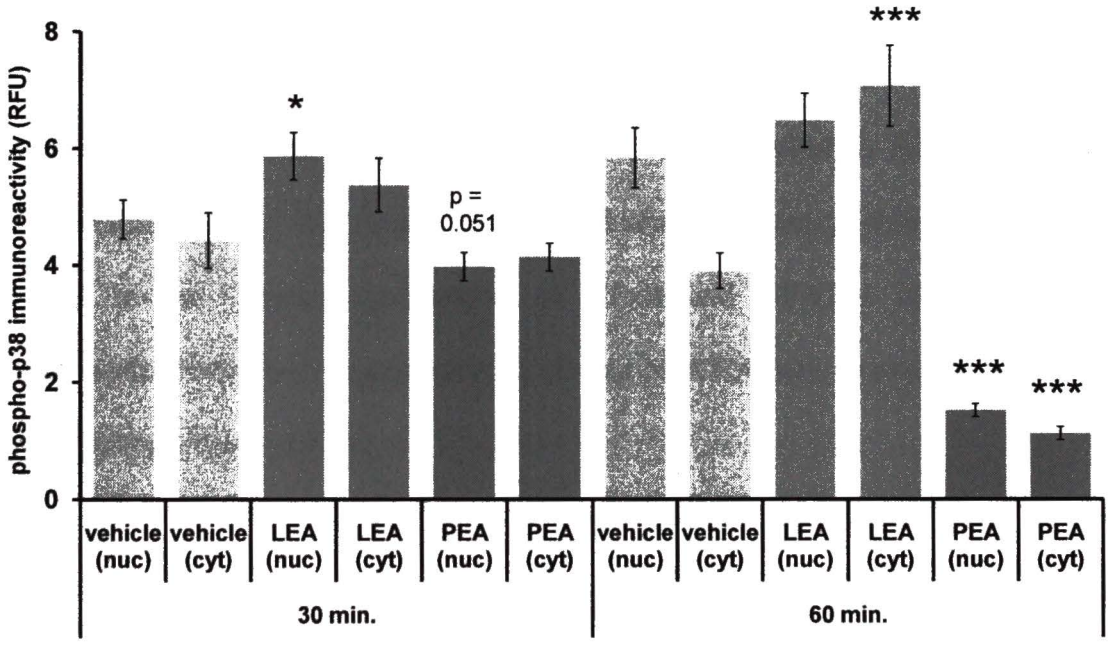
phospho-p38 immunoreactivity (RFU)
8
6
4
2
0
*
p =
0.051
***
***
***
vehicle (nuc)
vehicle (cyt)
LEA (nuc)
LEA (cyt)
PEA (nuc)
PEA (cyt)
vehicle (nuc)
vehicle (cyt)
LEA (nuc)
LEA (cyt)
PEA (nuc)
PEA (cyt)
30 min.
60 min.

CHAPTER 3.4 – EFFECTS OF NAEs ON THE ACTIVITY OF TRANSCRIPTION FACTORS INVOLVED IN NEUROPROTECTIVE SIGNALING

ABSTRACT

The activation of specific transcription factors and the subsequent alteration in gene expression may facilitate an adaptive response to a stressful environment thereby decreasing cell death. Two examples of transcription factors involved in neuronal signaling are nuclear factor kappa B (NFκB) and nuclear factor of activated T-cells 3 (NFATc4) (1 – 5). I hypothesized that PEA increases the nuclear translocation of NFκB and NFATc4 in HT22 cells and primary cortical neurons. Here, I determined that the lipid neuroprotectant palmitoylethanolamine (PEA) can lead to the nuclear translocation of NFκB and NFATc4 using microfluorimetric measurements. These data suggests that NFκB and NFATc4 may, in part, mediate the observed neuroprotective effects of PEA.

INTRODUCTION

The NFκB is a ubiquitous transcription factor composed of heterodimers of RelA (p65), RelB, RelC, p50 and p52 (3). IKK activation activation of NFκB occurs through liberating the transactivation domain of the RelA/p65 subunit (6). In addition, a variety of kinases, including PKAc, PKCζ, Akt, CKII and GSK3β, can directly phosphorylate the RelA (p65) subunit of NFκB leading to the subsequent activation NFκB (7).

Activated NFκB can regulate the expression of a variety of genes in neurons including those involved in apoptosis and neuroprotection (3). Whether NFκB activation in neurons leads to

neuroprotection of enhances neurodegeneration is currently not clear. Glutamate can activate NFκB in cerebellar cultures (8) and NFκB activation can lead to the transcription of genes that inhibit apoptosis and protect neurons against oxidative stress (1, 8, 9).

More than 200 physiological stimuli have been shown to activate NFκB (10) and it can, in turn, activate the transcription of a very large number of genes. NFκB activity has been studied most extensively in the field of immunology as NFκB is a major regulator of the immune response and in viral gene expression. NFκB is kept in an inactive state through an interaction with IκB. IκB, in turn, is inactivated through phosphrylation by IκB kinase (IKK), casein kinase II (CSII) or c-Src (4). A variety of other kinases, including PKAc, PKCζ, Akt, CKII and GSK3β, can phosphorylate the RelA (p65) subunit of NFκB leading to the subsequent activation NFκB (4).

In neurons, NFκB activation plays a role in neuroprotection and neurodegeneration depending upon which NFκB protein subunits form heterodimers (11). In HT22 cells, exposure to glutamate resulted in the activation of NFκB (RelA/p65) followed by delayed cell death (11). Its not clear, however, what effect activated NFκB (RelA/p65) has on cells HT22 cells exposed directly to oxidants such as tert-butylhydroperoxide (tBHP).

The NFAT family of transcription factors is made up of several members and each becomes activated by dephosphorylation of the calcium sensor / translocation domain by the phosphatase calcineurin (5). This dephosphorylation exposes the nuclear localization sequence leading to protein import into the nucleus. NFATc4 is also believed to be involved in neurite outgrowth through neurotrophins such as BDNF and NGF (5). Calcium release from intracellular stores by IP_3Rs may activate NFAT and, interestingly, NFATc4 can regulate IP_3R1 gene expression by binding specific sites in the IP_3R1 promoter (2, 12). In skeletal muscle cells and C2C12 cells,

depolarization results in RyR-mediated NFAT activation and long lasting, low frequency stimulation increases this activation (13).

Immune cells function is modulated by cannabinoid activation of CB1 and CB2 (14). Anandamide (AEA) stimulates the proliferation of hemopoetic cells (15, 16) and it also affects mast cells and macrophages (17). Cannabinoids activate CB1 and CB2 cannabinoid receptors, both of which are coupled to the inhibitory G-protein $G_{i/o}$ ultimately leading to a reduction of cAMP and subsequent downregulation of PKA activity. Activation of PKA in immune cells results can lead to activation of NFAT, CREB and NFκB resulting in increased immune function (18, 19).

Cannabinoids exhibit neuroprotective properties against a wide variety of pathological insults including excitotoxicity, oxidative stress and hypoxia (20 - 29). Activation of the protein kinase Akt further supports a role for cannabinoids as neuroprotectants. In mice, CB1 is involved in the regulation of Akt and calcineurin activity in the amygdala during extinction of the conditioned fear response (30), suggesting that cannabinoids may activate NFκB and NFAT through activation of Akt and calcineurin, respectively.

Several non-cannabinoid NAEs including linolenoylethanolamine (LNEA), oleoylethanolamine (OEA), stearoylethanolamine (SEA) and palmitoylethanolamine (PEA) lead to increase ERK phosphorylation and AP-1 activity in mouse JB6 epidermal cells (31). The CB1 agonist, Win 55212, could not stimulate ERK phosphorylation or AP-1 activation suggesting a CB1-independent function of NAEs in cell signaling and gene transcription (31). Furthermore, studies using immune cells has shown that PEA has CB2 receptor-independent effects (32). Since non-cannabinoid NAEs have also been shown to activate neuroprotective signaling

pathways, I hypothesized that the non-cannabinoid NAE, PEA, can lead to the nuclear translocation of NFκB and NFATc4.

MATERIALS AND METHODS

Cell culture

HT22 were cultured as described previously (33). In brief, HT22 cells were grown in DMEM with high glucose and 1mmM sodium pyruvate (Mediatech), 2mM Glutamax (Invitrogen), 5% bovine growth serum (BGS) (Hyclone) and penicilin-streptomycin (Mediatech). Cultures were kept at a confluency of less than 70% during the culturing process. Mouse primary cortical neurons were obtained from postnatal day 2 (P2) mice after anesthesia on ice. Animals were decapitated and the scalp and skull was removed without disturbing the integrity of the brain. A 1 – 1.5mm^2 piece of cortex was removed from each hemisphere of the brain with fine-tipped #5/45 forceps and placed into 0.25% trypsin in HBSS with EGTA and without Ca^{2+}. Tissue was incubated in trypsin at 37° C for 20 minutes followed by addition of 1 volume of complete media and subsequent trituration several times with a fire-polsihed glass pipet or a 1ml capacity micropipette tip. Tissue was centrifuged at 1,000 x g for 5 minutes to pellet the viscous tissue. Media was removed and the pellet was resuspended in 2 ml of complete media followed by trituration. Cells were centrifuged again at 400 x g for 5 minutes. The supernatant was removed and the pellet was resuspended in 2ml of complete media followed by trituration. The resulting cell suspension was passed through a 40μm cell strainer and quantitated using a hemocytometer. Cell density was adjusted to 1 X 10^6 – 2 X 10^6 cells/ml depending upon the application. All neurons were plated on either poly-D-lysine/laminin-coated 12mm coverslips (BioCoat™ BD Biosciences) or poly-L-lysine-coated 12mm coverslips depending upon the application. Mixed

neuronal cultures were maintained at 37°C / 5% CO_2 environment for 7 – 14 days. Before using coverslips, neurons were inspected visually under a microscope to determine their development of neurites and overall healthy appearance. Only cultures with the majority of neurons bearing neurites were used in experiments.

Immunocytochemistry after PEA treatment

Primary cortical neurons at 10 – 14 d.i.v. were treated with 100μM PEA (or EtOH vehicle) for 2 or 4 hours after which they were fixed with 4% paraformaldehyde and subjected to immunocytochemisty as described elsewhere using rabbit anti-NFκB (Santa Cruz Biotechnology), anti-NFATc4 (Santa Cruz Biotechnology) and mouse anti-NF, 70KDa (Chemicon) (33). Images were acquired with the Olympus IX-70 fluorescence microscope and intensity analysis was done using Simple PCI 6.0 by defining cytosolic and nuclear regions of interest. Alternatively, rat E18 cortical neurons from Genlantis Corporation were plated on poly-L-lysine-coated 12mm coverslips and maintained in culture for 7 days before treatments and subsequent immunocytochemistry.

Statistics

An F-test was conducted in Excel between each treatment group and the untreated control group to determine which type of T-test should be used for group comparisons. The mean fluorescence intensity from each treatment group was separately compared to the mean fluorescence intensity of the untreated control group using a two-sample T-test with either equal or unequal variances. A P-value of less than or equal to 0.05 was considered significant.

RESULTS

Effect of NAE treatment on NFκB (RelA/p65) immunoreactivity

Exposure of HT22 cells to PEA for 2 hours resulted in a significant increase in nuclear NFκB (p65) (Fig. 1) and a significant decrease in cytosolic NFκB (p65) (data not shown). Interestingly, exposure of HT22 cells to 4 hour PEA did not significantly alter NFκB immunoreactivity or localization compared to vehicle controls. There was, however, a trend toward an increase in NFκB in the nucleus ($p = 0.076$).

In mouse primary cortical neurons, a two (2) and four (4) hour PEA treatment resulted in an increase in nuclear NFκB (RelA/p65) immunoreactivity compared to vehicle controls (Fig. 2). The nuclear translocation of NFκB was greater for the 4 hour PEA-treated group compared to the 2 hour PEA-treated group (Fig. 2). The amount of cytosolic NFκB in the PEA-treated group exhibited a non-significant trend ($p = 0.175$) toward an increase only at the 4 hour PEA treatment time point (data not shown). Interestingly, exposure of rat E18 cortical neurons to PEA had no effect on NFkB immunoreactivity (data not shown).

Effect of NAE treatment on NFATc4 immunoreactivity

Exposure of HT22 cells to PEA for four (4) hours (but not for two (2) hours) leads to a significant increase in nuclear NFATc4 immunoreactivity (Fig. 3). In addition, exposure of cultured mouse primary cortical neurons with PEA for two (2) and four (4) hours resulted in a significant increase in nuclear NFATc4 immunoreactivity (Fig. 4). The amount of cytosolic NFATc4 in the PEA-treated group exhibited a significant decrease only at the 4 hour PEA treatment time point. Exposure of rat E18 cortical neurons to 100μM PEA for 4 hours resulted in

a significant increase in nuclear NFATc4 immunoreactivity (data not shown). Treatment of HT22 cells with the CB2 agonist, JWH-015, was not able to increase NFATc4 immunoreactivity (Fig. 5), suggesting that PEAs effects on NFATc4 are not mediated by CB2.

DISCUSSION

Here, I provided evidence that PEA treatment can facilitate the nuclear translocation of NFκB (RelA/p65) and NFATc4 in a neuronal cell line and in cultured cortical neurons. I previously determined that PEA pretreatment for five (5) to six (6) hours protects HT22 cells from oxidative stress. Together, these data suggest that PEA can activate transcription factors known to be involved in neuroprotective signaling, thus providing a possible mechanism by which NAEs neuroprotect.

Numerous studies have revealed that the cannabinoid NAE, AEA, is neuroprotective through activation of CB1 (20 - 29). Since the saturated NAEs, PEA and LEA, do not bind CB1 and they exhibit poor affinity for CB2, I hypothesized that these NAEs exhibit neuroprotective properties by a mechanism independent of CB2. To rule out any potential role of CB2 activation on the alteration of NFκB and NFATc4 immunoreactivity, I measured the effect of a CB2 agonist on nuclear NFATc4 immunoreactivity. The CB2 agonist, JWH-015 had no effect on nuclear NFATc4 immunoreactivity in HT22 cells, suggesting that PEAs effect on NFATc4 were not mediated through CB2 activation. This result is similar to our observation that CB2 agonists do not mimic the effects of PEA on Akt/pAkt and ERK/pERK immunreactivities in HT22 cells.

Overall, my data suggests that PEA activates NFκB and NFATc4 signaling pathways by a CB2-independent mechanism. These effects are within the timeframe required to cause PEA-mediated neuroroptection in HT22 cells. Activation of CB1 leads to the regulation of Akt and

calcineurin activity in the amygdala (30). This suggests that cannabinoids may activate down stream componenets of Akt and calcineurin such as NFκB and NFAT, respectively. Previously, I determined that PEA can induce Akt and pAkt nuclear translocation. This result is consistent with the hypothesis that PEA-mediated effects on Akt may be, in turn, be involved in NFκB nuclear tranlocation.

Previous studies indicate that activation of Akt can result in phosphorylation of inositol 1, 4, 5-trisphosphate receptors (IP3Rs) and lead to enhanced Ca^{2+} release (34, 35). Interestingly, intracellular Ca^{2+} can activate calcineurin and, subsequently NFAT (12, 13). These data, in part, are consistent with a possible effect of PEA on Ca^{2+} signaling in neurons as evidenced by NFAT nuclear translocation.

REFERENCES

1. Wang CY, Mayo MW, Komeluk RG, Goeddel DV and Baldwin AS Jr. (1998) NF-kappaB antiapoptosis: induction of TRAF1 and TRAF2 and c-IAP1 and c-IAP2 to suppress caspase-8 activation. Science. 281(5383):1680-3.
2. Groth and Mermelstein (2003) Brain-derived neurotrophic factor activation of NFAT (nuclear factor of activated T-cells)-dependent transcription: a role for the transcription factor NFATc4 in neurotrophin-mediated gene expression. J Neurosci. 23(22):8125-34.
3. Massa PT, Aleyasin H, Park DS, Mao X and Barger SW (2006) NFkappaB in neurons? The uncertainty principle in neurobiology. J Neurochem. 97(3):607-18.
4. Tergaonkar V (2006) NFkappaB pathway: a good signaling paradigm and therapeutic target. Int J Biochem Cell Biol. 2006;38(10):1647-53

5. Nguyen T and Di Giovanni S (2008) NFAT signaling in neural development and axon growth. Int J Dev Neurosci. 26(2):141-5.

6. Madrid LV, Mayo MW, Reuther JY, and Baldwin AS Jr. (2001) Akt stimulates the transactivation potential of the RelA/p65 Subunit of NF-kappa B through utilization of the Ikappa B kinase and activation of the mitogen-activated protein kinase p38. J Biol Chem. 276(22):18934-40.

7. Perkins ND (2006) Post-translational modifications regulating the activity and function of the nuclear factor kappa B pathway. Oncogene. 25(51):6717-30.

8. Guerrini L, Blassi F and Denis-Donini S (1995) Synaptic activation of NF-kappa B by glutamate in cerebellar granule neurons in vitro. Proc Natl Acad Sci U S A. 92(20):9077-81.

9. Mattson MP, Goodman Y, Luo H, Fu W and Furukawa K (1997) Activation of NF-kappaB protects hippocampal neurons against oxidative stress-induced apoptosis: evidence for induction of manganese superoxide dismutase and suppression of peroxynitrite production and protein tyrosine nitration. J Neurosci Res. 49(6):681-97

10. Pahl HL (1999) Activators and target genes of Rel/NF-kappaB transcription factors. Oncogene. 18(49):6853-66.

11. Ishige K, Tanaka M, Arakawa M, Saito H and Ito Y (2005) Distinct nuclear factor-kappaB/Rel proteins have opposing modulatory effects in glutamate-induced cell death in HT22 cells. Neurochem Int. 47(8):545-55. Epub 2005 Sep 22.

12. Graef IA, Mermelstein PG, Stankunas K, Neilson JR, Deisseroth, Tsien RW and Crabtree GR (1999) L-type calcium channels and GSK-3 regulate the activity of NF-ATc4 in hippocampal neurons. Nature. 401(6754):703-8.

13. Valdes JA, Gaggero E, Hidalgo J, Leal N, Jaimovich E and Carrasco MA (2008) NFAT activation by membrane potential follows a calcium pathway distinct from other activity-related transcription factors in skeletal muscle cells. Am J Physiol Cell Physiol. 294(3):C715-25.

14. Parolaro D, Massi P, Rubino T and Monti E (2002) Endocannabinoids in the immune system and cancer. Prostaglandins Leukot Essent Fatty Acids. 66(2-3):319-32.

15. Derocq JM, Bouaboula M, Marchand J, Rinaldi-Carmona M, Segui M and Casellas P (1998) The endogenous cannabinoid anandamide is a lipid messenger activating cell growth via a cannabinoid receptor-independent pathway in hematopoietic cell lines. FEBS Lett. 425(3):419-25.

16. Valk P, Verbakel S, Vankan Y, Hol S, Mancham S, Ploemacher R, Mayen A, Lowenberg B and Delwel R (1997) Anandamide, a natural ligand for the peripheral cannabinoid receptor is a novel synergistic growth factor for hematopoietic cells. Blood. 90(4):1448-57.

17. Facci L, Dal Toso R, Romanello S, Buriani A, Skaper SD and Leon A (1995) Mast cells express a peripheral cannabinoid receptor with differential sensitivity to anandamide and palmitoylethanolamide. Proc Natl Acad Sci U S A. 92(8):3376-80.

18. Jeon YJ, Yang KH, Pulaski JT and Kaminski NE (1996) Attenuation of inducible nitric oxide synthase gene expression by delta 9-tetrahydrocannabinol is mediated through the inhibition of nuclear factor- kappa B/Rel activation. Mol Pharmacol. 50(2):334-41.

19. Yea SS, Yang KH and Kaminski NE (2000) Role of nuclear factor of activated T-cells and activator protein-1 in the inhibition of interleukin-2 gene transcription by cannabinol in EL4 T-cells. J Pharmacol Exp Ther. 292(2):597-605.

20. Skaper SD, Buriani A, Dal Toso R, Petrelli L, Romanello S, Facci L and Leon A (1996) The ALIAmide palmitoylethanolamide and cannabinoids, but not anandamide, are protective in a delayed postglutamate paradigm of excitotoxic death in cerebellar granule neurons. Proc Natl Acad Sci U S A. 93(9):3984-9.

21. Hampson AJ, Gimaldi M, Axelrod J and Wink D (1998) Cannabidiol and (-)Delta9-tetrahydrocannabinol are neuroprotective antioxidants. Proc Natl Acad Sci U S A. 95(14):8268-73.

22. Shen M and Thayer SA (1998) Cannabinoid receptor agonists protect cultured rat hippocampal neurons from excitotoxicity. Mol Pharmacol. 54(3):459-62.

23. Moesgaard B, Jaroszewski JW and Hansen HS (1999) Accumulation of N-acyl-ethanolamine phospholipids in rat brains during post-decapitative ischemia: a 31p NMR study. J Lipid Res. 40(3):515-21.

24. Nagayama T, Sinor AD, Simon RP, Chen J, Graham SH, Jin K and Greenberg DA (1999) Cannabinoids and neuroprotection in global and focal cerebral ischemia and in neuronal cultures. J Neurosci. 19(8):2987-95.

25. Chen Y and Buck J (2000) Cannabinoids protect cells from oxidative cell death: a receptor-independent mechanism. J. Pharmacol. Exp. Ther. 293(3): 807-12.

26. Hampson AJ and Grimaldi M (2001) Cannabinoid receptor activation and elevated cyclic AMP reduce glutamate neurotoxicity. Eur J Neurosci. 13(8):1529.

27. van der Stelt M, Velhuis WB, Maccarrone M, Nar PR, Nicolay K, Veldink GA, DiMarzo V and Vliegenthart JF (2002) Acute neuronal injury, excitotoxicity, and the endocannabinoid system. Mol Neurobiol. 2002 Oct-Dec;26(2-3):317-46.

28. Marsicano G, Goodenough S, Monory K, Hermann H, Eder M, Cannich A, Azad SC, Cascio MG, Gutierrez SO, van der Stelt M, Lopez-Rodriguez ML, Casanova E, Schutz G, Zieglgansberger W, Di Marzo V, Behl C and Lutz B (2003) CB1 cannabinoid receptors and on-demand defense against excitotoxicity. Science. 302(5642):84-8.

29. Shouman B, Fontaine RH, Baud O, Schwendimann L, Keller M, Spedding M, Lelievre V and Gressens P (2006) Endocannabinoids potently protect the newborn brain against AMPA-kainate receptor-mediated excitotoxic damage. Br J Pharmacol. 148(4):442-51.

30. Cannich A, Wotjak CT, Kamprath K, Hermann H, Lutz B and Marsicano G (2004) CB1 cannabinoid receptors modulate kinase and phosphatase activity during extinction of conditioned fear in mice. Learn Mem. 11(5):625-32.

31. Berdyshev EV, Schmid PC, Krebsbach RJ, Hillard CJ, Hunag C, Chen N, Dong Z and Schmid HH (2001) Cannabinoid-receptor-independent cell signalling by N-acylethanolamines.Biochem J. 360(Pt 1):67-75.

32. Ross RA, Brockie HC and Pertwee RG (2000) Inhibition of nitric oxide production in RAW264.7 macrophages by cannabinoids and palmitoylethanolamide. Eur J Pharmacol. 401(2):121-30.

33. Duncan RS, Hwang SY and Koulen P (2007) Differential inositol 1,4,5-trisphosphate receptor signaling in a neuronal cell line. Int J Biochem Cell Biol. 39(10):1852-62.

34. Koulen P, Madry C, Duncan RS, Hwang JY, Nixon E, McClung N, Gregg EV and Singh M (2008) Progesterone potentiates IP(3)-mediated calcium signaling through Akt/PKB. Cell Physiol Biochem. 21(1-3):161-72.

35. Hwang JY, Duncan RS, Madry C, Singh M and Koulen P, Effects of progesterone on calcium signaling in hippocampal neurons, Cell Calcium, in press.

FIGURES

Fig. 1 – PEA treatment of HT22 cells leads to an increase in nuclear NFκB immunoreactivity. A two (2) and four (4) hour treatment led to a significant increase in nuclear NFκB immunoreactivity in HT22 cells. For the two (2) hour treatment groups, *n* equals 42 and 48 cells for vehicle and PEA treatments, respectively. For the four (4) hour treatment groups, *n* equals 70 and 87 cells for vehicle and PEA treatments, respectively. A P-value of ≤ 0.05 is indicated by *.

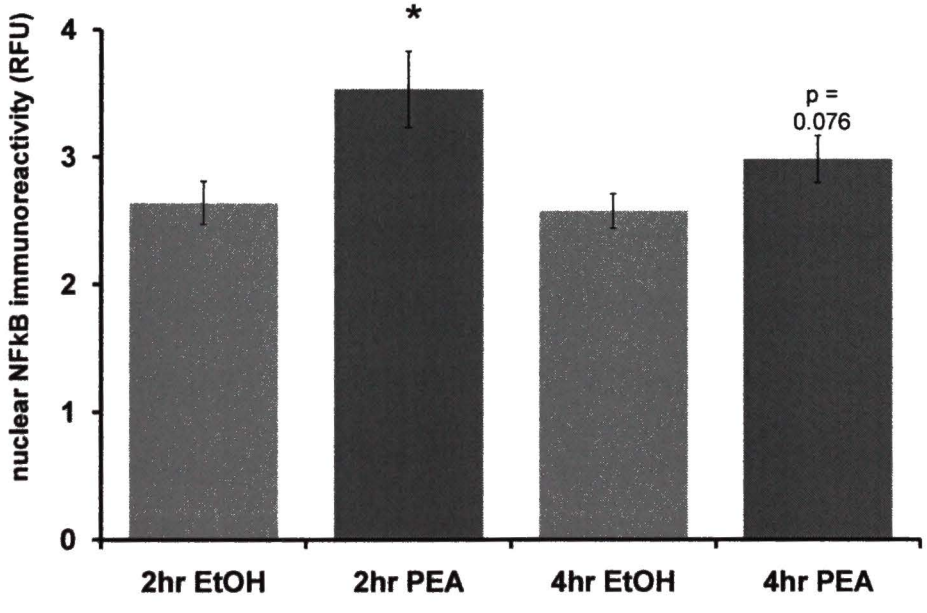
nuclear NFkB immunoreactivity (RFU)
4
3
2
1
0
*
p =
0.076
2hr EtOH
2hr PEA
4hr EtOH
4hr PEA

Fig. 2 – PEA treatment of mouse primary cortical neurons leads to an increase in nuclear NFκB immunreactivity. A two (2) and four (4) hour treatment led to a significant increase in nuclear NFκB immunoreactivity in cortical neurons. For the two (2) hour treatment groups, *n* equals 37 and 56 cells for vehicle and PEA treatments, respectively. For the four (4) hour treatment groups, *n* equals 74 and 42 cells for vehicle and PEA treatments, respectively. A P-value of ≤ 0.001 is indicated by ***.

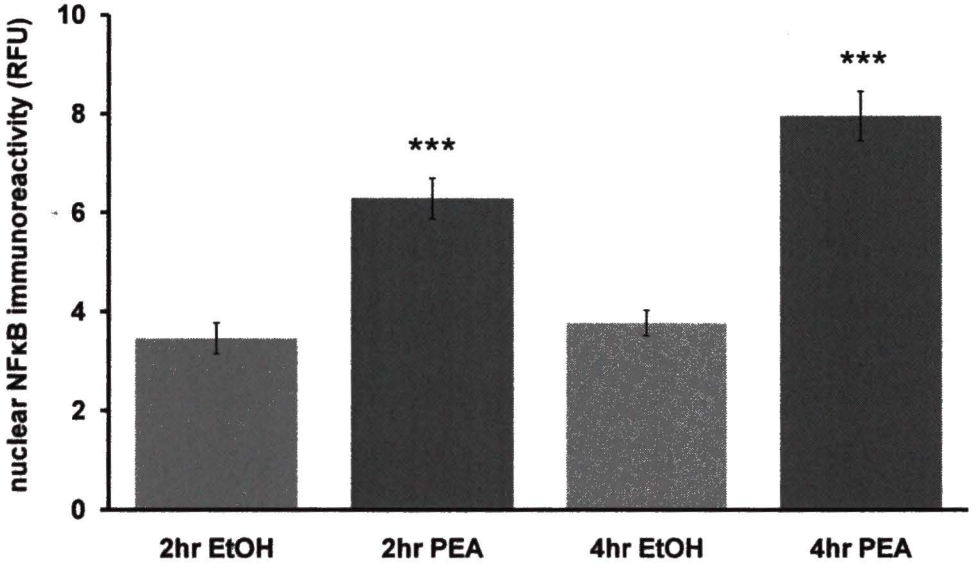
nuclear NFκB immunoreactivity (RFU)
10
8
6
4
2
0
***
***
2hr EtOH
2hr PEA
4hr EtOH
4hr PEA

Fig. 3 – PEA treatment of HT22 cells leads to an increase in nuclear NFATc4 immunreactivity. A four (4) hour treatment led to a significant increase in nuclear NFATc4 immunreactivity in HT22 cells. For the two (2) hour treatment groups, *n* equals 31 and 34 cells for vehicle and PEA treatments, respectively. For the four (4) hour treatment groups, *n* equals 35 and 27 cells for vehicle and PEA treatments, respectively. A P-value of ≤ 0.01 is indicated by **.

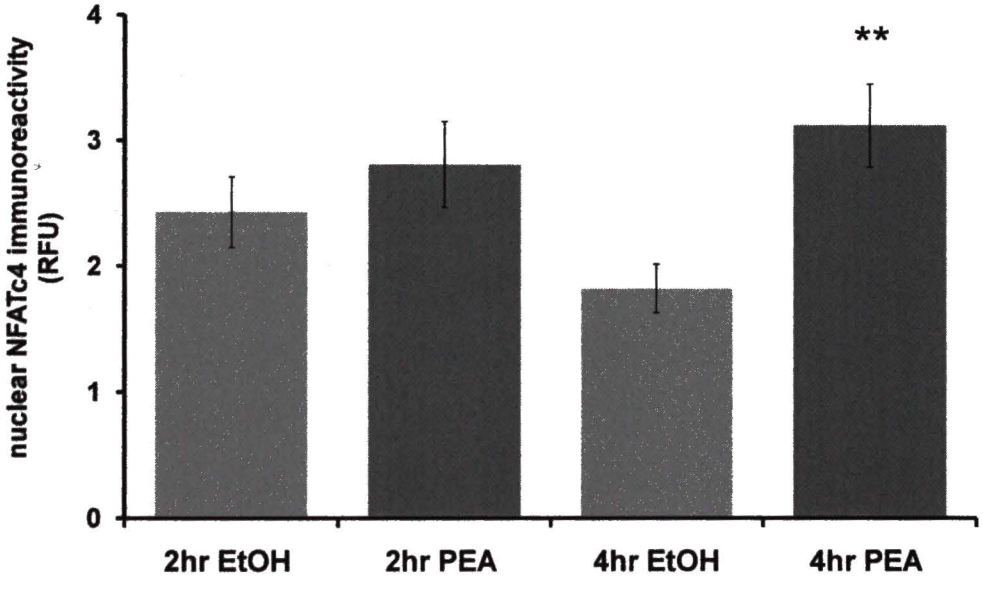
nuclear NFATc4 immunoreactivity (RFU)
4
3
2
1
0
**
2hr EtOH
2hr PEA
4hr EtOH
4hr PEA

Fig. 4 – PEA treatment of mouse cortical neurons leads to an increase in nuclear NFATc4 immunreactivity. A two (2) and four (4) hour PEA treatment led to a significant increase in nuclear NFATc4 immunreactivity in cortical neurons. For the two (2) hour treatment groups, *n* equals 36 and 56 cells for vehicle and PEA treatments, respectively. For the four (4) hour treatment groups, *n* equals 72 and 53 cells for vehicle and PEA treatments, respectively. A P-value of ≤ 0.001 is indicated by ***.

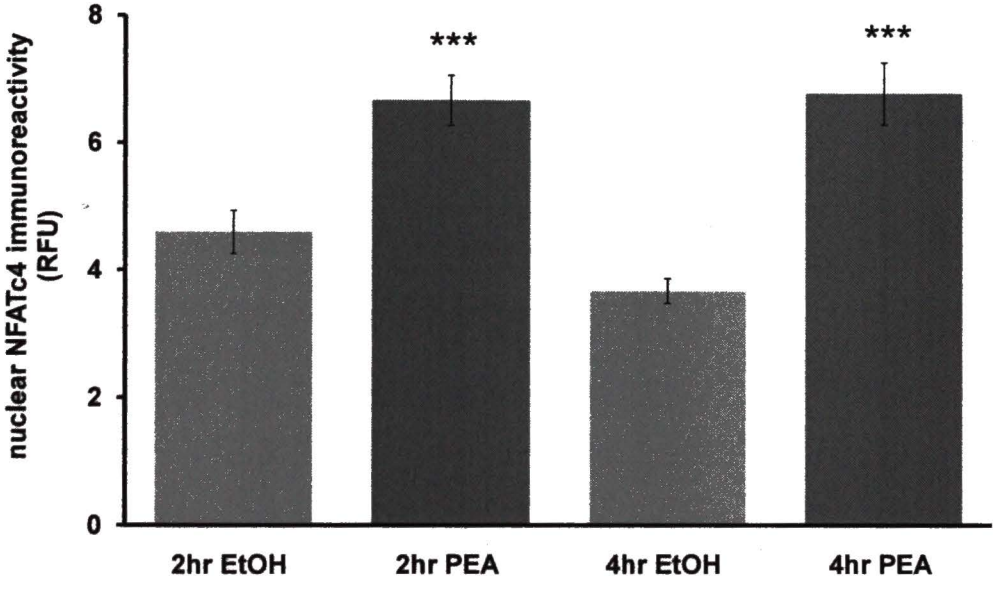
nuclear NFATc4 immunoreactivity (RFU)
8
6
4
2
0
***
***
2hr EtOH
2hr PEA
4hr EtOH
4hr PEA

Fig. 5 – Treatment of HT22 cells with the CB2 agonist, JWH-015, has no effect on NFATc4 immunreactivity. Treatment of HT22 cells with the CB2 agonist JWH-015 fails to significantly increase NFAT immunoreactivity. For this study, *n* equals 60 and 63 cells for vehicle and JWH-015 treatments, respectively. A P-value of ≤ 0.05 and ≤ 0.001 is indicated by * and ***, respectively.

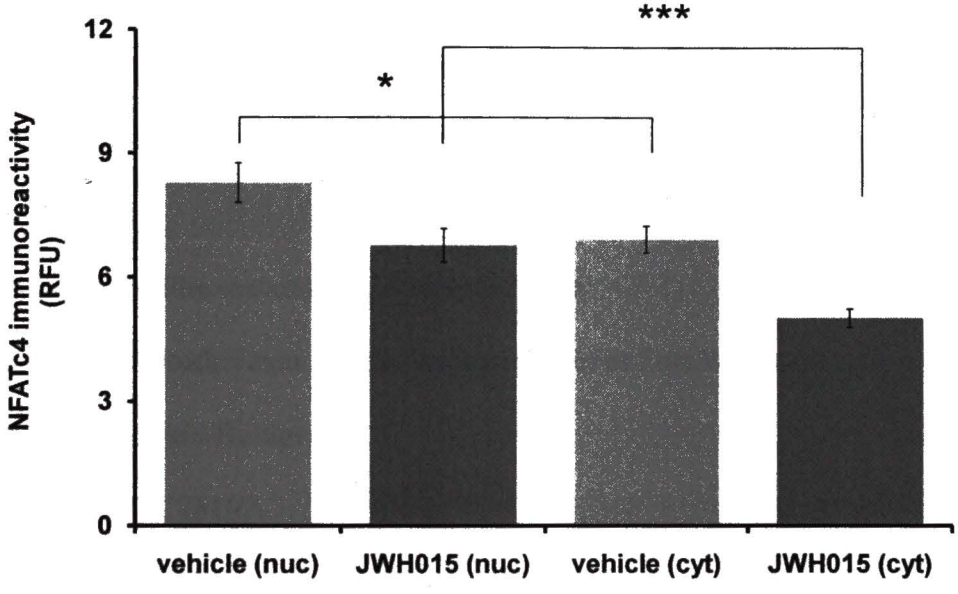
***
*
12
9
6
3
0
NFATc4 immunoreactivity (RFU)
vehicle (nuc)
JWH015 (nuc)
vehicle (cyt)
JWH015 (cyt)

CHAPTER 4.1 – DIFFERENTIAL INOSITOL 1, 4, 5-TRISPHOSPHATE RECEPTOR SIGNALING IN A NEURONAL CELL LINE

R. Scott Duncan[1, 2, #], Sung-Yong Hwang[1, 2, #], and Peter Koulen[1, 2, 3, *]

[1]Department of Pharmacology and Neuroscience, [2]Institute for Aging and Alzheimer's Disease Research, and [3]North Texas Eye Research Institute, University of North Texas Health Science Center at Fort Worth, Fort Worth, TX 76107

*Corresponding author:

Peter Koulen

Department of Pharmacology and Neuroscience

University of North Texas Health Science Center at Fort Worth

3500 Camp Bowie Boulevard

Fort Worth, TX 76107.

Tel.: (817) 735-2068 ; Fax: (817) 735-0408

E-mail: pkoulen@hsc.unt.edu

[#] These authors contributed equally to this work

Character number: 20,316

This chapter of the thesis has been published in The International Journal of Biochemistry and Cell Biology, volume 39, issue 10, pp. 1852 – 1862, 2007.

ABSTRACT

Differential intracellular distribution of the three pharmacologically and biophysically distinct types of IP_3Rs can lead to different subcellular Ca^{2+} transients each coupled to discrete intracellular functions. Here, we report the functional localization of differentially distributed IP_3 receptor types in the commonly-used hippocampal cell line HT22. The distinct subcellular localization and Ca^{2+} signaling properties of these receptors determine the potential role of specific IP_3 receptor types in cellular function. By utilizing immunoblotting, we conclude that HT22 cells express all three IP_3 receptors with types 1 and 3 being expressed predominantly in the endoplasmic reticulum and perinuclear regions and type 2 being expressed predominantly in the nuclear envelope. Optical imaging studies using the Ca^{2+}-sensitive indicator dye fluo-3 show that nuclear IP_3 responses have greater amplitude and faster kinetics than cytosolic IP_3 responses corresponding to the biophysical characteristics of the differentially distributed receptor types. These results support the hypothesis that differentially distributed IP_3R isotypes mediate distinct cellular functions through differential, organelle-specific Ca^{2+} signaling.

INTRODUCTION

Calcium (Ca^{2+}) is a critical second messenger that facilitates a variety of cellular processes including gene expression (Hardingham et al., 1997; Bading, 2000; West et al., 2001), neurotransmitter release (Atlas, 2001) and apoptosis (Paschen, 2003). Cytoplasmic Ca^{2+} is maintained at a low concentration (20 – 100nM) relative to the endoplasmic reticulum (ER) lumen and the extracellular environment (Berridge, 1997). The regulation of Ca^{2+} homeostasis is

critical for normal cellular function and survival and prolonged disruption of the cytoplasmic Ca^{2+} concentration is detrimental (Verkhratsky and Toescu, 2003). Release of Ca^{2+} from intracellular stores is mediated predominantly through inositol 1, 4, 5-trisphosphate receptors (IP_3Rs) (Streb et al., 1983; Berridge and Irvine, 1984), ryanodine receptors (RyRs) (Fill and Coronado, 1988) and polycystin-2 (Koulen et al., 2002).

The IP_3Rs are well characterized intracellular Ca^{2+} channels that are activated by their ligand, inostol-1,4,5-trisphosphate (IP_3) (Streb et al., 1983;, Berridge and Irvine, 1984; Ehrlich and Watras, 1988), and are regulated by Ca^{2+} (Iino, 1987; Iino, 1990; Bezprozvanny et al., 1991), ATP (Ehrlich and Watras, 1988; Maeda et al., 1991; Bezprozvanny and Ehrlich, 1993) and multiple interacting proteins (Bootman et al., 2002; Thrower et al., 2003; Yang et al., 2002; Ando et al., 2003). These channels are also regulated by phosphorylation from cAMP-dependent protein kinase and Akt kinase (Volpe and Alderson-Lang, 1990; Tang et al., 2003; Khan et al., 2006).

There are three types of IP_3Rs with distinct physiological, pharmacological and biophysical properties: type 1, type 2 and type 3 (Furuichi et al., 1989; Mignery et al., 1989; Mignery et al., 1990; Sudhof et al., 1991; Ross et al., 1992, Yoshikawa et al., 1992; Blondel et al., 1993; Koulen and Thrower, 2001). They exist predominantly in the endoplasmic reticulum (Maeda et al., 1991; Ross et al., 1989; Maeda et al., 1990; Koulen et al., 2005) although localization has been reported in other intracellular membranes contingent with the ER, such as the nuclear envelope (Koulen et al., 2005; Humbert et al., 1996; Leite et al., 2003). Each type of IP_3R is differentially expressed in some tissues and exhibits different properties such as affinity for IP_3 and sensitivity to Ca^{2+} and ATP. The affinity of IP_3R isotypes for IP_3 follow a potency rank of $IP_3R2 > IP_3R1 > IP_3R3$ (Miyakawa et al., 1999) and this affinity is influenced by the cytosolic Ca^{2+} concentration

(Bezprozvanny et al., 1991; Cardy et al., 1997). IP_3Rs, like RyRs, are calcium-induced calcium release channels and, as a result, optimal cytosolic Ca^{2+} concentrations potentiate IP_3-mediated Ca^{2+} release (Bezprozvanny et al., 1991; Cardy et al., 1997; Iino and Endo, 1992). High intracellular levels of Ca^{2+} bound to IP_3R1 and IP_3R3 leads to decreased affinity for IP_3 through distinct mechanisms demonstrating differential regulation between these receptors (Cardy et al., 1997). IP_3R1 exhibits a bell-shaped Ca^{2+} response curve whereas IP_3R3 does not, demonstrating differences in Ca^{2+} regulation between different IP_3 receptor isotypes (Bezprozvanny et al., 1991; Bezprozvanny and Ehrlich, 1993; Hagar et al., 1998). The sensitivity of IP_3Rs to Ca^{2+} activation follow a rank of $IP_3R1 > IP_3R2 > IP_3R3$ (Miyakawa et al., 1999).

Activation of specific IP_3R isotypes leads to distinct Ca^{2+} transients mediating diverse functions within a cell. In non-pigmented epithelial cells, for example, stimulation of IP_3 production with acetycholine results in IP_3R3-mediated Ca^{2+} waves from the apical pole and repetitive IP_3R1-mediated Ca^{2+} increases in the basal pole (Hirata et al., 1999). Activation of IP_3R1 and IP_3R3 in DT40 B-cells leads to less prominent monophasic Ca^{2+} transients whereas activation of IP_3R2 exhibits prominent prolonged Ca^{2+} oscillations (Miyakawa et al., 1999). In retinal rod bipolar cells, intracellular Ca^{2+} transients in somata and dendrites with distinct physiological profiles are mediated by differentially distributed IP_3R1 and IP_3R2 subpopulations (Koulen et al., 2005) while, in a liver cell line, Ca^{2+} transients in the nucleoplasm and the cytoplasm are controlled separately by differentially distributed IP_3R2 and IP_3R3 subpopulations (Leite et al., 2003). Differential distribution of IP_3R1 and IP_3R3 also explains differences in Ca^{2+} transients in soma versus neurites in cultured PC12 cells (Johenning et al., 2002). The functional consequence of these differentially distributed IP_3R types has not been fully established in neurons.

HT22 cells are a murine hippocampal cell line commonly used as a model for studying neuroprotection against oxidative stress (Sagara et al., 1998; Green et al., 1998). In this study, we hypothesized that HT22 cells express all three IP_3R isotypes and that they each exhibit differential distribution and Ca^{2+} signaling properties. We identified the distribution and Ca^{2+} signaling properties of all three IP_3R subtypes using immunocytochemical and optical imaging techniques. Direct stimulation of IP_3 receptors with their ligand led to nucleoplasm- and cytoplasm-specific Ca^{2+} signaling patterns. Our data suggest that a hippocampal cell line relevant for neurodegeneration research is capable of utilizing differentially distributed intracellular Ca^{2+} release channels to regulate separate Ca^{2+} dependent signaling pathways independently. This potentially represents novel targets for regulation of neuronal development and function.

MATERIALS AND METHODS

Antibodies

Antibodies against IP_3R1 was purchased from Calbiochem (San Diego, CA) and Chemicon (Temecula, CA), IP_3R2 antibodies were purchased from Calbiochem and Chemicon, and IP_3R3 antibodies were purchased from Sigma (St. Louis, MO) and BD Transduction Laboratories (San Diego, CA). For immunoblotting, horseradish peroxidase-conjugated goat anti-rabbit IgG secondary antibody (Calbiochem) was used. For immunofluorescence detection, Alexa 488-labeled goat anti-rabbit IgG and Alexa 594-labeled goat anti-mouse IgG antibodies (Invitrogen, Carlsbad, CA) were used.

Immunoblotting

Cells used for immunoblotting were grown in 150cm^2 flasks to a high confluency (80 – 100%) in the appropriate medium at 37°C in 5% CO_2. HT22 cells were cultured in Dulbecco's Modified Eagle's (DME) medium with 4.5g/mol glucose, 2mM glutamine, 1mM sodium pyruvate (Hyclone, Logan, UT) containing 10% heat-inactivated bovine growth serum (BGS) (Hyclone). AR42J cells were cultured in F-12K media with L-glutamine (Mediatech Inc., Herndon, VA) containing 10% BGS and RIN-5F cells were cultured in RPMI media with glutamine (Mediatech Inc.) containing 10% BGS to maximal confluency. Cells were collected by first rinsing with PBS for one minute followed by scraping with a rubber cell scraper in PBS. Cells were then centrifuged at low speed (500 x g) and the pellets were frozen at -80°C until later use. Cell lysates for immunoblotting were generated by solublizing HT22, AR42J and RIN-5F cell pellets in ice-cold cell lysis buffer (50mM Tris-HCl (pH 7.4), 150mM NaCl, 1mM EGTA, 1mM Na_3VO_4, 1mM NaF, 2% NP-40) with added protease inhibitor cocktail (Roche Diagnostics, Mannheim, Germany). Mouse cerebella from postnatal day 3 mice were minced with small scissors and solublized by the same method as the cell culture samples. Excess HT22 lysate volume over control samples was loaded in acrylamide gels because HT22 cells were not expected to express high amounts of any one IP3R subtype relative to controls. Samples for electrophoresis were denatured in 6X SDS-PAGE loading buffer (135mM Tris-Cl (pH 6.8), 30% glycerol, 1% SDS, 500mM DTT and 1.2mg bromophenol blue), boiled for 3 minutes, and placed on ice to cool. Samples were loaded along with either prestained or biotinylated broad range molecular weight markers (BioRad, Hercules, CA) and run in 4-15% gradient SDS polyacrylamide gels (BioRad, Hercules, CA). Proteins were transferred to PVDF membranes (Pall Life Sciences, Ann Arbor, MI) followed by incubation in milk block solution (5%

powdered milk, 1% BSA, 0.005% tween-20 in phosphate-buffered saline; pH 7.4). The membrane was then incubated in primary antibody diluted in milk block solution overnight gently shaking at 4° C. Primary antibodies for IP_3R1, IP_3R2 and IP_3R3 were from Calbiochem, Chemicon and Sigma, respectively. The membrane was then washed three times before addition of milk block solution containing horseradish peroxidase-labeled goat anti-rabbit (for IP_3R1 and IP_3R2 primary antibody) or goat anti-mouse (for IP_3R3 antibody) secondary antibody. Incubation in secondary antibody was done at room temperature gently shaking in the dark for 1 hour. After three washes in PBS, the membrane was developed with Super Signal West Dura chemiluminescent reagent (Pierce Biotechnology, Rockford, IL). Membranes were visualized using a UVP Epichemi 3 darkroom (UVP, Inc/, Upland, CA) with a mounted Hamamatsu C8484-51-03G camera (Hammamatsu, Japan) and LabWorks 4.5.0 software version 4.5.0 (UVP, Inc., Upland, CA).

Immunocytochemistry and immunofluorescence

HT22 cells used for immunocytochemistry were removed from flasks using 0.25% trypsin in HBSS (Hyclone). Cells were grown for 48 hours to a confluency of 20 – 30% on glass coverslips (22mm) coated with 0.01% poly-L-lysine (Sigma-Aldrich) using culture media and incubation conditions described above. Cells were fixed with 4% paraformaldehyde for 15 minutes and then washed three times for 5 minutes with PBS. Cells were then blocked with preincubation solution (10% normal goat serum, 1% BSA, 0.05% tween-20 in PBS) for 1 hour. Primary antibodies used to label IP_3R1 (Calbiochem), IP_3R2 (Calbiochem) and IP_3R3 (BD Tansduction laboratories) were diluted in incubation buffer (3% normal goat serum, 1% BSA, 0.05% tween-20 in PBS) and added to cells and incubated at 4°C overnight and then washed three times for 5

minutes with PBS. Fluorescent Alexa488- or Alexa594-labeled goat anti-rabbit or goat anti-mouse IgG secondary antibody (Invitrogen) was diluted in incubation solution (1:1000) and applied to cells for 1 hour at room temperature in the dark. Coverslips were then washed in PBS three times for 5 minutes with PBS and then mounted onto glass slides using ProLong anti-fade reagent with DAPI (Invitrogen) and left to cure overnight at 4°C overnight. Slides were viewed within 5 days after mounting. Samples were visualized at ambient temperature (21 - 23° C) under a fluorescence microscope (Olympus IX70, Japan) using a 20X interference contrast or fluorescence microscopy. A constant exposure time was maintained among images to facilitate the comparison among images. Images were saved in a 24-bit TIFF file format.

Optical imaging of intracellular Ca^{2+} concentrations

HT22 cells (1×10^5) were plated on poly-L-lysine-coated 15mm glass coverslips and grown for 24hr as described above. HT22 cells were incubated in 4μM of the cell-permeant fluorescent dye Fluo-3-AM (Invitrogen) at 37°C for 30 minutes in L15 media (Invitrogen). The coverslips with dye-loaded cells were placed in a perfusion chamber containing extracellular solution (137mM NaCl, 5mM KCl, 1mM Na_2HPO_4, 10mM HEPES, 22mM Glucose, and 5mM EGTA, pH 7.4) and placed on an inverted microscope (Olympus IX70, Japan) at ambient temperature. Changes in fluorescence intensity were recorded using time-lapse videomicroscopy and calculated by dividing the measured fluorescence intensity during drug application (F) by the measured average baseline fluorescence intensity before drug application (F_0) using an inverted fluorescence microscope (Olympus IX70) with Simple PCI software (C-Imaging). The cells were treated with bath-applied 1μM cell-permeant IP_3-AM (A.G. Scientific, Inc., San Diego, CA). For some experiments, cells were pretreated with 1uM XeD (Calbiochem) to block IP_3 receptors.

The slope of Ca^{2+} transients was calculated by plotting the mean fluorescence intensity within the 20 to 80 percent range of the maximum fluorescence intensity over time followed by addition of a linear trendline. The duration of Ca^{2+} transients was calculated by subtracting the average time at which the Ca^{2+} transient returned to baseline level from the time when the ligand was applied to the perfusion chamber. The $Tmax_{1/2}$ was calculated by subtracting the time at which the half maximal fluorescence intensity was reached after ligand application from the time at which the ligand was applied. The slope, duration and $Tmax_{1/2}$ were calculated using Microsoft Excel.

RESULTS

Detection of IP_3Rs in HT22 Cells by Immunoblotting

Immunoblot analysis indicates the presence of all three IP_3R isotypes (Fig. 1). A band of approximately 260 kD corresponding to IP_3R1 was detected in the lane containing the HT22 lysate (Fig. 1, top panel, C) and this band showed the same molecular weight as the IP_3R1 band from the positive control cerebellum lysate lane (Fig. 1, top panel, B) (Ross et al., 1989) and the 250 kD prestained molecular weight marker band (BioRad) (Fig. 1, top panel, A). For IP_3R2, AR42J cells were run as a positive control (Wojcikiewicz and He, 1995). As expected, a band of approximately 260 kD was observed in the HT22 lysate lane (Fig. 1, middle panel, C) which showed the same molecular weight as the IP_3R2 band in the AR42J lysate lane (Fig.1, middle panel, B). A similar result for HT22 lysate was seen for IP_3R3 (Fig.1, bottom panel, C) which corresponded with the 260 kD IP_3R3 band from the RIN-5f cell positive control lane (Fig.1, bottom panel, B) (Wojcikiewicz and He, 1995). The molecular weight marker band shown in the

middle and bottom panels is a 200 kD band from the biotinylated broad range molecular weight marker (BioRad).

Immunocytochemical Characterization of IP_3Rs in HT22 Cells

Immunocytochemistry was used to determine the expression of IP_3Rs in cultured HT22 cells. All three IP_3Rs are expressed in HT22 cells (Fig. 2) confirming our Western blot data (Fig. 1). IP_3R1 immunoreactivity is localized predominantly to the endoplasmic reticulum (ER) and is also found in the perinuclear region (Fig. 2a). IP_3R3 is localized predominantly to the endoplasmic reticulum but it exhibits less perinuclear expression than IP_3R1 (Fig. 2c). IP_3R2, on the other hand, displays a different distribution and is localized predominantly to the nuclear envelope with relatively little ER localization (Fig. 2b). Differential localization of IP_3R types suggests that there are different IP_3R signaling complexes within specific compartments within the cell. Semi-quantitative analysis was done using Simple-PCI software to examine the relative expression levels of IP_3R types in nucleus versus cytosol/ER for each antibody used (Fig. 3). There is no significant difference between nuclear and cytosolic/ER expression levels of IP_3R1 (Fig. 3). The other two isotypes, however, exhibit significant differential localization (Fig. 3). IP_3R3 is predominantly localized to the cytosol/ER compartment (Fig. 2C and Fig. 3), whereas IP_3R2 exhibits predominant nuclear expression with only a small amount of punctate expression in the cytosol/ER (Fig. 2B and Fig. 3).

Optical Imaging of IP_3-mediated intracellular Ca^{2+} transients

To measure Ca^{2+} responses of HT22 cells to IP_3, cultured cells were loaded with 4μM Fluo-3-acetoxymethyl ester (Fluo-3-AM), placed in a perfusion chamber and observed under a

fluorescence microscope during either vehicle treatment or 1μM IP_3-acetoxymethyl ester (IP_3-AM) treatment (Fig. 4). Application of IP_3-AM to cells resulted in an increase in intracellular Ca^{2+} concentration ($[Ca^{2+}]_i$) as determined by an increase in Fluo-3 fluorescence (Fig. 4, right panel, Fig. 5A, and Fig. 6). Treatment of cells with vehicle alone elicited minimal Ca^{2+} response (Fig. 4, left panel, Fig. 5B, and Fig. 6). Because the extracellular solution contained no Ca^{2+}, these responses were due to release of Ca^{2+} from intracellular stores. To further confirm that these IP_3-mediated Ca^{2+} transients were generated by IP_3 receptors, cells were pretreated with the IP_3 receptor-selective antagonist Xestospongin D (XeD) prior to IP_3AM application (Fig. 5C and Fig. 6). Pretreatment of cells with XeD prevented the IP_3-AM-mediated Ca^{2+} release suggesting that the observed Ca^{2+} transients originated from IP_3Rs (Fig. 5C and Fig. 6).

Analysis of Ca^{2+} imaging data demonstrates that the slope of the rate of Ca^{2+} release is significantly greater for IP_3AM-treated cells than for vehicle-treated cells (Fig. 7), indicating that the Ca^{2+} responses were IP_3-mediated. The slope of the nuclear Ca^{2+} response was statistically significantly greater than that of the cytosolic response (Fig. 7), suggesting that nuclear IP_3 receptors (Fig. 2) exhibit greater sensitivity to the ligand IP_3. Interestingly, the vehicle (DMSO) elicits a statistically significant difference in slope between nuclear and cytosolic responses. The duration of the cytosolic Ca^{2+} response was statistically significantly greater for IP_3AM-treated cells compared to that of vehicle-treated cells (Table 1). Interestingly, there was no statistically significant difference in the duration of nuclear Ca^{2+} response between vehicle-treated and IP_3-AM-treated cells (Table 1). There was also no statistically significant difference in duration of Ca^{2+} responses between the nuclear and cytosolic regions for each condition (Table 1). There is no statistically significant difference in $Tmax_{1/2}$ of nuclear versus cytosolic Ca^{2+} transients for each treatment condition (Table 1). There is, however, a statistically significant difference in

$Tmax_{1/2}$ of both nuclear and cytosolic Ca^{2+} transients between vehicle- and IP_3-AM-treated cells (Table 1).

DISCUSSION

The present study provided evidence for differentially distributed IP_3R isotypes in HT22 cells. IP_3R2 was found predominantly in the nuclear envelope and IP_3R1 and IP_3R3 were detected in the ER. Optical imaging of Ca^{2+} responses demonstrated that IP_3AM-mediated release of Ca^{2+} in the nucleus through IP_3R2 occurs before release of Ca^{2+} from the ER through IP_3R1 and IP_3R3. This data agrees with earlier studies demonstrating that nuclear Ca^{2+} responses are regulated differently than cytosolic responses in a HepG2 cell line (Leite et al., 2003). The nuclear IP_3 receptor isotype, IP_3R2, exhibits a higher affinity for IP_3 and, as a result, gives rise to earlier and higher Ca^{2+} transients than that seen from IP_3R3 in the cytosol. The presence of all three IP_3 receptor isotypes in HT22 cells, however, does not rule out a contribution of IP_31 and IP_3R3 to nuclear Ca^{2+} responses as well as IP_3R2 Ca^{2+} responses in the ER. In addition to the parallel activation of IP_3R subtypes, expression of IP_3 receptor heterotetramers can not be ruled out (Wojcikiewicz and He, 1995). In contrast to Miyakawa et al., 1999, one study demonstrates that IP_3R1 exhibits a slightly higher affinity for IP_3 than IP_3R2 (K_m of 1μM versus 2μM, respectively), suggesting that IP_3R1 would likely become activated by IP_3 before IP_3R2 (Wojcikiewicz and Luo, 1998). In this study, however, we show that Ca^{2+} release from the IP_3R2-enriched nucleus occurs before release from the IP_3R1-enriched ER (Fig. 5) supported by the reported higher affinity of IP_3R2 for IP_3 than for the other IP_3R types (Miyakawa et al., 1999).

It is possible in HT22 cells that IP_3 is generated near the plasma membrane upon activation of phospholipase C where it diffuses to the nuclear envelope to activate high affinity receptors. Exogenous application of cell-permeable IP_3, which was done in the present study, would be expected to activate cytosolic IP_3Rs before IP_3Rs in the nuclear envelope, provided affinities of IP_3Rs are equal among organelles. An alternative explanation for faster nuclear Ca^{2+} response by endogenously-generated IP_3 may be due to IP_3 being generated at intracellular membranes such as the ER or nuclear envelope in addition to generation at the plasma membrane. The extracellular application of cell-permeable IP_3 can be used to substitute for endogenaously-generated IP_3. Interestingly, nuclear PLCβ expression and activity has been described in different cell models (Irvine, 2003). The presence of the PLCβ in the nuclear envelope suggests that IP_3 may more readily activate nuclear IP_3 receptors. The ability to produce IP_3 near its binding site would likely decrease the time required to activate the receptor. Furthermore, IP_3 receptors have been detected in the nucleoplasm of adrenal chromaffin tissue and NIH3T3 cells using immunogold electron microscopy (Huh and Yoo, 2003).

The biological significance of IP_3 receptors in the nuclear membrane is apparent as there are Ca^{2+}-sensitive transcriptional activators and repressors that could potentially be regulated by Ca^{2+}. The activation of Ca^{2+}-sensitive kinases and phosphatases such as Ca^{2+}/calmodulin-dependent protein kinases and calcineurin B, respectively, have been shown to regulate gene transcription (Ikura et al., 2002). A transcriptional repressor that is regulated directly by Ca^{2+} is downstream response element antagonist modulator which has been shown to bind to downstream response elements in gene promoters such as the c-fos and prodynorphin genes in the absence of Ca^{2+} (Osawa et al., 2001). When Ca^{2+} is present, it leads to derepression (Osawa et al., 2001). It is possible that IP_3 receptor-mediated release of Ca^{2+} from the nucleoplasmic

reticulum into perinuclear cytoplasm, or into the nucleoplasm directly, may be a mechanism by which cells can activate transcriptional activators or repressors and regulate the expression of genes in response to Ca^{2+} signaling events.

The differential distribution of IP_3Rs can be a means for the cell to generate signal diversity and to regulate the strength of a Ca^{2+} signal in a tissue. In the retina, for example, a differential distribution of IP_3 receptors in rod bipolar cells allows for distinct Ca^{2+} signals to be generated within a particular subcellular compartment (Koulen et al., 2005). Interestingly, the strength of group I metabotropic glutamate receptor activation leads to differential activation of IP_3R isotypes residing in distinct cellular compartments (Koulen et al., 2005). For example, in cultured rod bipolar cells, application of 10μM of the group I metabotropic glutamate receptor agonist (S)-3,5-dihydroxyphenylglycine leads to IP_3R2 receptor-mediated Ca^{2+} release predominantly in dendrites whereas activation with 100μM generates Ca^{2+} transients through IP_3R1 receptors in both the soma and dendrites (Koulen et al., 2005). In differentiated PC12 cells, intracellular Ca^{2+} channel types (IP_3R and RyR types) elicit different Ca^{2+} responses in neurites than in the soma, suggesting that location of these channels plays a major role in their physiological function (Johenning et al., 2002).

The HT22 cell line was used in this study because it is well characterized and it has been a good model system for neuroprotection studies and studying the effects of oxidative stress on cell function (Sagara et al., 1998; Green et al., 1998). Little has been reported on IP3 receptor signaling and function in HT22 cells and the effects of IP3R activity on Ca^{2+} homeostasis as it relates to neurodegeneration and neuroprotection. The HT22 line is polyclonal and consists of cells of different morphological and physiological characteristics. This was originally of interest when conducting these studies because differences in IP_3R expression and Ca^{2+} responses

between individual cells could make analysis of data difficult. Immunofluorescence results demonstrate, however, that there is little variation in labeling of any one particular IP_3 receptor isotype between individual cells (Fig. 2). There was also little variation in Ca^{2+} responses when conducting optical Ca^{2+} imaging experiments (Fig. 4). The vast majority of cells exhibited similar Ca^{2+} responses with respect to amplitude and duration of response in each treatment condition. This study using the HT22 cell line lays the groundwork for future studies on IP_3 receptor-mediated Ca^{2+} signaling, especially selective Ca^{2+} release from nuclear stores in a neuronal cell line relevant for neurodegeneration and neuroprotection research.

Acknowledgements

This work was in part supported by NIH/NEI grant EY014227, NIH/NIA grants AG010485, AG022550 and T32AG20494, a Young Investigator Award from The National Alliance for Research on Schizophrenia and Depression (PK).

Abbreviations

BGS – bovine growth serum

Ca^{2+} - calcium

Fluo-3-AM – Fluo-3-acetoxymethyl ester

IP3 – inositol 1, 4, 5-trisphosphate

IP3-AM – inositol 1, 4, 5-trisphoshpate acetoxymethyl ester

IP3R – inositol 1, 4, 5-trisphosphate receptor

$Tmax_{1/2}$ – time to half-maximal

RyR – ryanodine receptor

XeD – xestospongin D

REFERENCES

Ando H., A. Mizutani, T. Matsu-ura, and K. Mikoshiba. 2003. IRBIT, a novel inositol 1,4,5-trisphosphate (IP_3) receptor-binding protein, is released from the IP_3 receptor upon IP_3 binding to the receptor. *J. Biol. Chem.* 278:10602-10612.

Atlas, D. 2001. Functional and physical coupling of voltage-sensitive calcium channels with exocytotic proteins: ramifications for the secretion mechanism. *J. Neurochem.* 77:972-985.

Bading, H. 2000. Transcription-dependent neuronal plasticity the nuclear calcium hypothesis. *Eur. J. Biochem.* 267:5280-5283.

Berridge, M.J. 1997. Elementary and global aspects of calcium signaling. *J. Exp. Biol.* 200:315-319.

Berridge M.J., and R.F. Irvine. 1984. Inositol trisphosphate, a novel second messenger in cellular signal transduction. *Nature.* 312:315-321.

Bezprozvanny I., and B.E. Ehrlich. 1993. ATP modulates the function of inositol 1,4,5-trisphosphate-gated channels at two sites. *Neuron.* 10:1175-1184.

Bezprozvanny I., J. Watras, and B.E. Ehrlich. 1991. Bell-shaped calcium-response curves of Ins(1,4,5)P_3- and calcium-gated channels from endoplasmic reticulum of cerebellum. *Nature.* 351:751-754.

Blondel O., J. Takeda, H. Janssen, S. Seino, and G.I. Bell. 1993. Sequence and functional characterization of a third inositol trisphosphate receptor isotype, IP_3R-3, expressed in pancreatic islets, kidney, gastrointestinal tract, and other tissues. *J. Biol. Chem.* 268:11356-11363.

Bootman M.D., M.J. Berridge, and H.L. Roderick. 2002. Activating calcium release through inositol 1,4,5-trisphosphate receptors without inositol 1,4,5-trisphosphate. *Proc. Natl. Acad. Sci. U.S.A.* 99:7320-7322.

Cardy T.J., D. Traynor, and C.W. Taylor. 1997. Differential regulation of types-1 and -3 inositol trisphosphate receptors by cytosolic Ca^{2+}, *Biochem. J.* 328:785-793.

Ehrlich B.E., and J. Watras. 1988. Inositol 1,4,5-trisphosphate activates a channel from smooth muscle sarcoplasmic reticulum. *Nature.* 336:583-586.

Fill, M., and R. Coronado. 1988. Ryanodine receptor channel of sarcoplasmic reticulum. *Trends Neurosci.* 11:453-457.

Furuichi T., S. Yoshikawa, A. Miyakawi, K. Wada, N. Maeda, and K. Mikoshiba. 1989. Primary structure and functional expression of the inositol 1,4,5-trisphosphate-binding protein P400. *Nature.* 342:32-38.

Green, P.S., K.E. Gridley, J.W. Simpkins. 1998. Nuclear estrogen receptor-independent neuroprotection by estratrienes: a novel interaction with glutathione. *Neuroscience.* 84:7-10.

Hagar R.E., A.D. Burgstahler, M.H. Nathanson, and B.E. Ehrlich. 1998. Type III $InsP_3$ receptor channel stays open in the presence of increased calcium. *Nature.* 396:81-84.

Hardingham G.E., S. Chawla, C.M. Johnson, and H. Bading. 1997. Distinct functions of nuclear and cytoplasmic calcium in the control of gene expression. *Nature*. 385:260-265.

Hirata K., M.H. Nathanson, A.D. Burgstahler, K. Okazaki, E. Mattei, and M.L. Sears. 1999. Relationship between inositol 1,4,5-trisphosphate receptor isotypes and subcellular Ca^{2+} signaling patterns in nonpigmented ciliary epithelia. *Invest. Ophthalmol. Vis. Sci.* 40:2046-2053.

Huh Y.H., and S.H. Yoo. 2003. Presence of the inositol 1,4,5-triphosphate receptor isoforms in the nucleoplasm. *FEBS Lett.* 555:411-418.

Humbert J.P., N. Matter, J.C. Artault, P. Koppler, and A.N. Malviya. 1996. Inositol 1,4,5-trisphosphate receptor is located to the inner nuclear membrane vindicating regulation of nuclear calcium signaling by inositol 1,4,5-trisphosphate. Discrete distribution of inositol phosphate receptors to inner and outer nuclear membranes. *J. Biol. Chem.* 271:478-485.

Iino, M. 1987. Calcium dependent inositol trisphosphate-induced calcium release in the guinea-pig taenia caeci. *Biochem. Biophys. Res. Commun.* 142:47-52.

Iino, M. 1990. Biphasic Ca^{2+} dependence of inositol 1,4,5-trisphosphate-induced Ca^{2+} release in smooth muscle cells of the guinea pig taenia caeci. *J. Gen. Physiol.* 95:1103-1122.

Iino, M., and M. Endo. 1992. Calcium-dependent immediate feedback control of inositol 1, 4, 5-trisphosphate-induced Ca^{2+} release. *Nature.* 360:76-78.

Ikura M., M. Osawa, and J.B. Ames. 2002. The role of calcium-binding proteins in the control of transcription: structure to function. *Bioessays.* 24:625-636.

Irvine, R.F. 2003. Nuclear lipid signalling. *Nat. Rev. Mol. Cell Biol.* 4:349-60.

Johenning F.W., M. Zochowski, S.J. Conway , A.B. Holmes, P. Koulen, and B.E. Ehrlich. 2002. Distinct intracellular calcium transients in neurites and somata integrate neuronal signals. *J. Neurosci.* 22:5344-5353.

Khan M.T., L. Wagner 2nd, D.I. Yule, C. Bhanumathy, and S.K. Joseph. 2006. Akt kinase phosphorylation of inositol 1,4,5-trisphosphate receptors. *J. Biol. Chem.* 281:3731-3737.

Koulen P., Y. Cai, L. Geng, Y. Maeda, S. Nishimura, R. Witzgall, B.E. Ehrlich, and S. Somlo. 2002. Polycystin-2 is an intracellular calcium release channel. *Nat. Cell Biol.* 4:191-197.

Koulen P., and E.C. Thrower. 2001. Pharmacological modulation of intracellular $Ca^{(2+)}$ channels at the single-channel level. *Mol. Neurobiol.* 24:65-86.

Koulen, P. J. Wei, C. Madry, J. Liu, and E. Nixon. 2005. Differentially distributed IP_3 receptors and Ca^{2+} signaling in rod bipolar cells. *Invest. Ophthalmol. Vis. Sci.* 46:292-298.

Leite M.F., E.C. Thrower, W. Echevarria, P. Koulen, K. Hirata, A.M. Bennett, B.E. Ehrlich, and M.H. Nathanson. 2003. Nuclear and cytosolic calcium are regulated independently. *Proc. Natl. Acad. Sci. U.S.A.* 100:2975-2980.

Maeda N., T. Kawasaki, S. Nakade, N. Yokota, T. Taguchi, M. Kasai, and K. Mikoshiba. 1991. Structural and functional characterization of inositol 1,4,5-trisphosphate receptor channel from mouse cerebellum. *J. Biol. Chem.* 266:1109-1116.

Maeda N., M. Ninobe, and K. Mikoshiba. 1990. A cerebellar Purkinje cell marker P400 protein is an inositol 1,4,5-trisphosphate ($InsP_3$) receptor protein. Purification and characterization of InsP3 receptor complex. *EMBO. J.* 9(1):61-67.

Mignery G.A., C.L. Newton, B.T. Archer 3rd, and T.C. Sudhof. 1990. Structure and expression of the rat inositol 1,4,5-trisphosphate receptor. *J. Biol. Chem.* 265:12679-12685.

Mignery G.A., T.C. Sudhof, K. Takei, P. and De Camilli. 1989. Putative receptor for inositol 1,4,5-trisphosphate similar to ryanodine receptor. *Nature.* 342:192-195.

Miyakawa T., A. Maeda, T. Yamazawa, K. Hirose, T. Kurosaki, and M. Iino. 1999. Encoding of Ca^{2+} signals by differential expression of IP_3 receptor isotypes. *EMBO. J.* 18:1303-1308.

Osawa M, K.I. Tong, C. Lilliehook, W. Wasco, J.D. Buxbaum, H.Y. Cheng, J.M. Penninger, M. Ikura, and J.B. Ames. 2001. Calcium-regulated DNA binding and oligomerization of the

neuronal calcium-sensing protein, Calsenilin/DREAM/KChIP3. *J. Biol. Chem.* 276:41005-41013.

Paschen, W. 2003. Mechanisms of neuronal cell death: diverse roles of calcium in the various subcellular compartments. *Cell Calcium.* 34:305-310.

Ross C.A., S.K. Danoff, M.J. Schell, S.H. Snyder, and A. Ullrich. 1992. Three additional inositol 1,4,5-trisphosphate receptors: molecular cloning and differential localization in brain and peripheral tissues. *Proc. Natl. Acad. Sci. U.S.A.* 89:4265-4269.

Ross C.A., J. Meldolesi, T.A. Milner, T. Satoh, S. Supattapone, and S.H. Snyder. 1989. Inositol 1,4,5-trisphosphate receptor localized to endoplasmic reticulum in cerebellar Purkinje neurons. *Nature.* 339:468-70.

Sagara Y., R. Dargusch, D. Chambers, J. Davis, D. Schubert, and P. Maher. 1998. Cellular mechanisms of resistance to chronic oxidative stress. *Free Radic. Biol. Med.* 24:1375-1389.

Streb H., R.F. Irvine, M.J. Berridge, and I. Schulz. 1983. Release of Ca^{2+} from a nonmitochondrial intracellular store in pancreatic acinar cells by inositol-1,4,5-trisphosphate. *Nature.* 306:67-69.

Sudhof T.C, C.L. Newton, B.T. Archer 3rd, Y.A. Ushkaryov, and G.A. Mignery. 1991. Structure of a novel InsP3 receptor. *EMBO. J.* 10:3199-3206.

Tang T.S., H. Tu, Z. Wang, and I. Bezprozvanny. 2003. Modulation of type 1 inositol (1,4,5)-trisphosphate receptor function by protein kinase a and protein phosphatase 1alpha. *J. Neurosci.* 23:403-415.

Thrower E.C., C.U. Choe, S.H. So, S.H. Jeon, B.E. Ehrlich, and S.H. Yoo. 2003. A functional interaction between chromogranin B and the inositol 1,4,5-trisphosphate receptor/Ca^{2+} channel. *J. Biol. Chem.* 278:49699-49706.

Verkhratsky, A., and E.C. Toescu. 2003. Endoplasmic reticulum $Ca^{(2+)}$ homeostasis and neuronal death. *J. Cell. Mol. Med.* 7:351-361.

Volpe P., and B.H. Alderson-Lang. 1990. Regulation of inositol 1,4,5-trisphosphate-induced Ca^{2+} release. II. Effect of cAMP-dependent protein kinase. *Am. J. Physiol.* 258:C1086-1091.

West A.E., W.G. Chen, M.B. Dalva, R.E. Dolmetsch, J.M. Kornhauser, A.J. Shaywitz, M.A. Takasu, X. Tao, and M.E. Greenberg. 2001. Calcium regulation of neuronal gene expression. *Proc. Natl. Acad. Sci.* U.S.A. 98:11024-11031.

Wojcikiewicz, R.J., and Y. He. 1995. Type I, II and III inositol 1,4,5-trisphosphate receptor co-immunoprecipitation as evidence for the existence of heterotetrameric receptor complexes *Biochem. Biophys. Res. Commun.* 213:334-341.

Wojcikiewicz, R.J., and S.G. Luo. 1998. Differences among type I, II, and III inositol-1,4,5-trisphosphate receptors in ligand-binding affinity influence the sensitivity of calcium stores to inositol-1,4,5-trisphosphate. *Mol. Pharmacol.* 53:656-662.

Yang J., S. McBride, D.O. Mak, N. Vardi, K. Palczewski, F. Haeseleer, and J.K. Foskett. 2002. Identification of a family of calcium sensors as protein ligands of inositol trisphosphate receptor $Ca^{(2+)}$ release channels. *Proc. Natl. Acad. Sci. U.S.A.* 99:7711-7716.

Yoshikawa S, T. Tanimura, A. Miyawaki, M. Nakamura, M. Yuzaki, T. Furuichi, and K. Mikoshiba. 1992. Molecular cloning and characterization of the inositol 1,4,5-trisphosphate receptor in Drosophila melanogaster. *J. Biol. Chem.* 267:16613-16619.

TABLES

Table 1. Ca^{2+} response kinetics of IP_3AM-treated HT22 cells.

Parameter / Experimental Condition	**Duration (sec)**		**$Tmax_{1/2}$ (sec)**	
	Nucleus	**Cytosol**	**Nucleus**	**Cytosol**
Vehicle-treated cells (n = 12)	37.78 ± 1.31	32.85 ± 2.64*	18.18 ± 0.34**	17.41 ± 0.45**
IP3-AM-treated cells (n = 16)	42.51 ± 2.65 (peaks combined)	39.75 ± 1.31* (peaks combined)	8.79 ± 0.11** (peak 1) 24.29 ± 1.05** (peak 2)	8.18 ± 0.26** (peak 1) 22.75 ± 0.76** (peak 2)

*- p = <0.05 for Student's T-test comparison of duration of cytosolic transients between vehicle-treated and IP3-AM-treated cells

** - p = <0.01 for Student's T-test comparison of Tmax1/2 of Ca2+ transients between vehicle-treated and IP3-AM-treated cells (1st peak and 2nd peak).

There is no statistically significant difference between the Tmax1/2 of Ca2+ transients between nuclear and cytosolic compartments.

No statistical significance was found for duration or Tmax1/2 using a Student's T-test when comparing nuclear versus cytosolic Ca^{2+} transients for each treatment condition and for comparing the duration of nuclear transients between vehicle-treated and IP3-AM-treated cells.

FIGURES

Fig. 1. Western blot of HT22 cell lysate to detect IP_3R isotypes. Detection of IP_3R1 receptor (top panel) in HT22 cell lysate (C), mouse cerebellar lysate (B) and 250 kD molecular weight marker (A). IP_3R2 receptor (middle panel) visible in HT22 cell lysate (C) and AR42J cell lysate (B) with 200 kD molecular weight marker (A). IP_3R3 receptor (bottom panel) visible in HT22 cell lysate (C) and RIN-5f cell lysate (B) with biotinylated broad range molecular weight marker (A). Note that the molecular weight marker band indicated for IP_3R1 (top panel) are from prestained broad range standards and they are different from molecular weight marker bands for IP_3R2 (middle panel) and IP_3R3 (bottom panel) which are from biotinylated broad range standards.

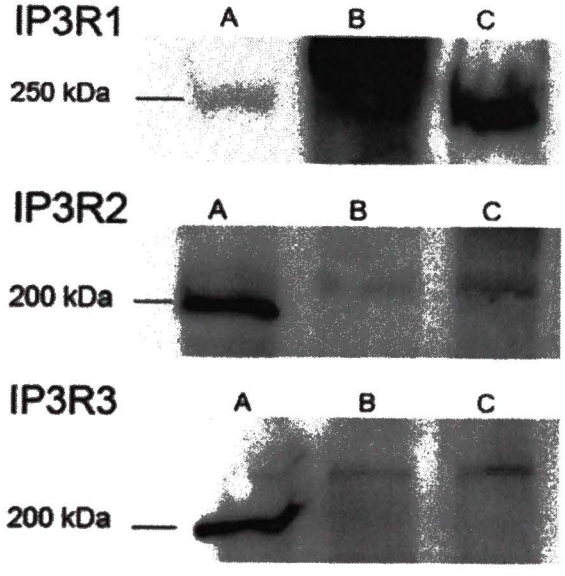
IP3R1
A
B
C
250 kDa
IP3R2
A
B
C
200 kDa
IP3R3
A
B
C
200 kDa

Fig. 2. Immunofluorescent localization of IP_3Rs in cultured HT22 cells. Cultured HT22 cells were processed for immunocytochemistry using primary antibodies against specific types of IP_3Rs. IP_3R1 (A) , IP_3R2 (B), and IP_3R3 (C) were detected in HT22 cells. Red arrows denote the nuclear region while white arrows denote the nuclear region in a representative cell. The images shown were acquired with an Olympus UApo/340 20X objective (numerical apperature of 0.75) and the scale bar in A, B and C is 25μm.

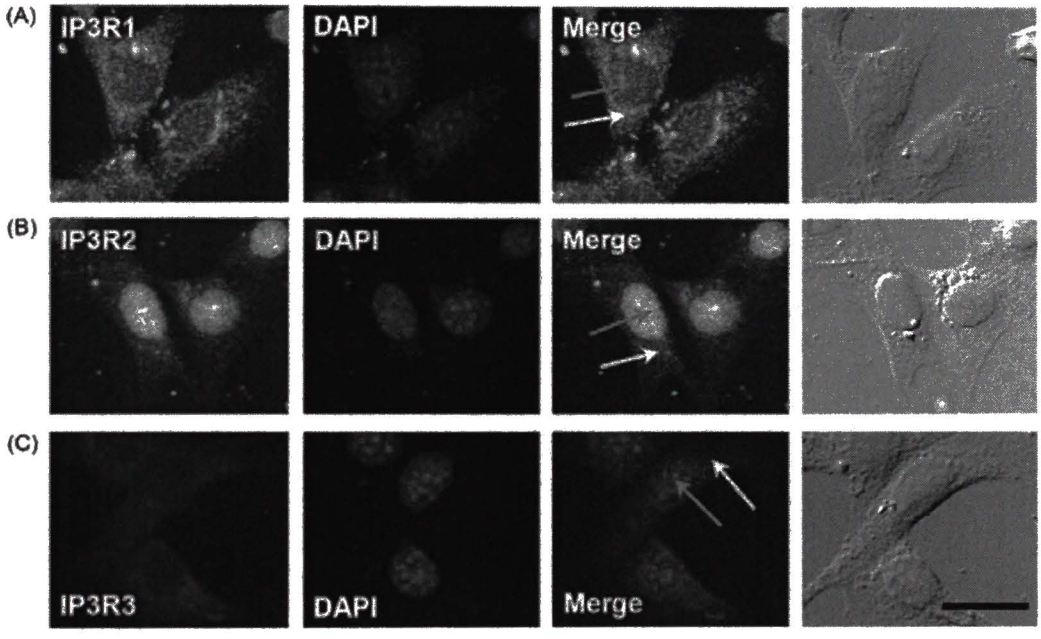
(A)
IP3R1
DAPI
Merge
(B)
IP3R2
DAPI
Merge
(C)
IP3R3
DAPI
Merge

Fig. 3. Semi-quantitative comparison between nuclear and cytosolic immunoreactivities for IP_3Rs in HT22 cells. Cells were fixed and immunocytochemistry was conducted to label IP_3R types. Cytosolic and nuclear regions of interest were defined and fluorescence intensity was measured and quantitated using Simple PCI software. Nuclear / cytosolic IP_3R immunoreactivity was calculated and compared among each IP_3R type using a two sample t-test. Statistical significance at $p = <0.01$ is indicated by double asterisks (**). For IP_3R1 and IP_3R2, N = 34. For IP_3R3, N = 31.

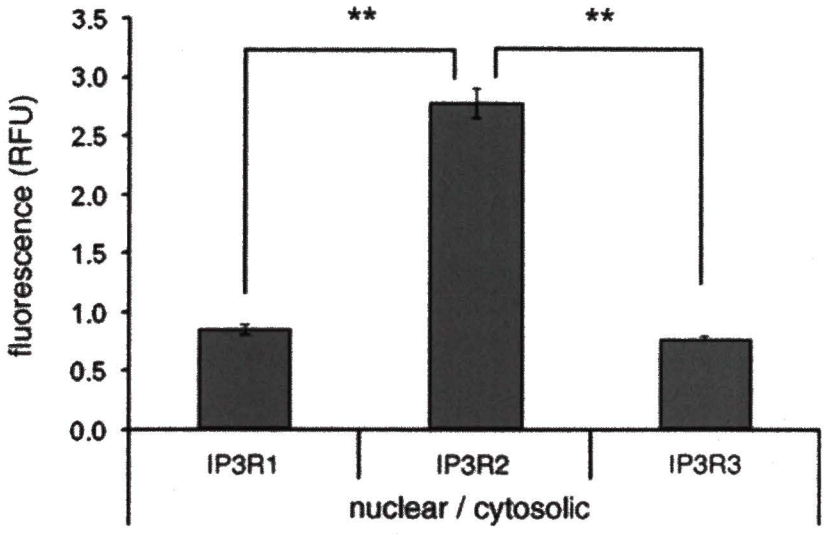
**
**
3.5
3.0
2.5
2.0
1.5
1.0
0.5
0.0
fluorescence (RFU)
IP3R1
IP3R2
IP3R3
nuclear / cytosolic

Fig. 4. Optical imaging of Ca^{2+} in IP_3-AM-stimulated HT22 cells. Cultured HT22 cells were ester-loaded with fluo-3 dye and treated with either DMSO vehicle (left panel) or cell-permeable IP_3 (right panel). Intracellular Ca^{2+} release was measured as the change in fluorescence at different time points (20s, 45s or 80s) after vehicle or IP_3-AM application. All images were obtained at 20X magnification.

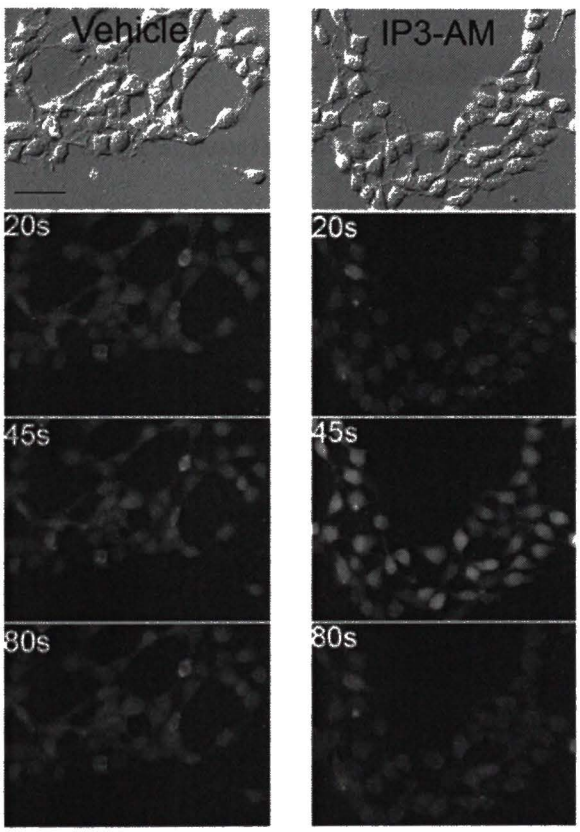
Vehicle
IP3-AM
20s
20s
45s
45s
80s
80s

Fig. 5. (A), the nuclear and cytosolic Ca^{2+} responses in HT22 cells are indicated for a representative cell. Fluorescence over the average initial baseline fluorescence (F/Fo) is represented on the y-axis. Changes in nuclear and cytosolic Ca^{2+} concentrations over time were recorded in IP_3-AM-treated (top panel) and vehicle-treated (middle panel) cells as well as IP_3-AM-treated cells in the presence of the IP_3R blocker Xestospongin D (bottom panel). IP_3-AM-treated cells demonstrate a robust Ca^{2+} transient (top panel) while vehicle treatment elicits no statistically significant Ca^{2+} response in either subcellular compartment (middle panel). Xestospongin D pretreatment (bottom panel), prevents the IP_3-AM-mediated Ca^{2+} response.

(B), The maximal amplitude of changes in fluorescence in response to IP_3-AM-treated HT22 cells were measured. Maximal fluorescence over the initial baseline fluorescence (F/Fo) is represented on the y-axis. HT22 cells were ester-loaded with fluo-3, treated with either vehicle (DMSO) or IP_3-AM. IP_3-AM was applied to cells that were pretrated with Xestospongin D to establish whether Ca^{2+} transients were mediated by IP_3 receptors. Fluorescence changes were measured using time trace intensity monitoring using Simple PCI software. Statistical significance among subcellular compartments was calculated for each treatment using a paired sample Student's t-test while comparison between different treatments was done using a two-sample Student's t-test. Statistical significance at $p = < 0.01$ is labeled with **. For DMSO vehicle and IP_3-AM + XeD, N= 12. For IP_3-AM, N = 16. (C), the slope of the Ca^{2+} transients from IP_3-AM-treated HT22 cells were calculated. The slope of the IP_3-AM-mediated, vehicle-mediated and IP_3-AM with XeD-mediated transients are shown for nuclear and cytosolic compartments. Statistical significance at $p = <0.01$ is labeled with **. For vehicle, IP_3-AM, and IP_3-AM+XeD, N = 10,16 and 12, respectively.

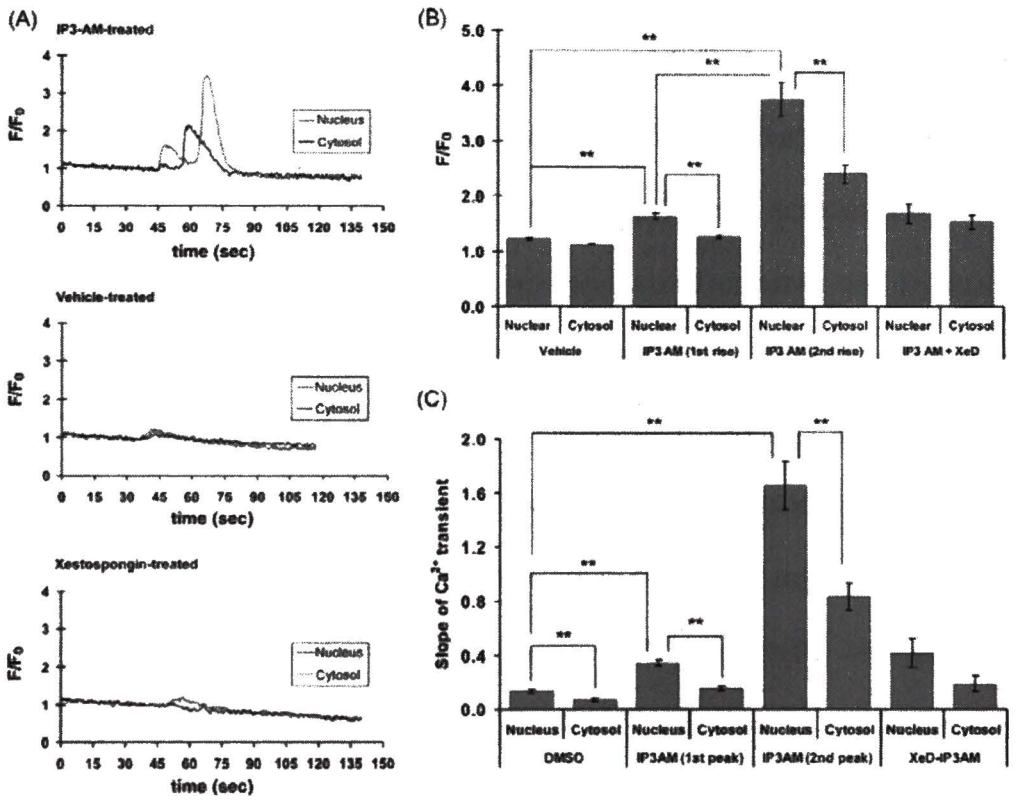
(A)
IP3-AM-treated
F/F0
Nucleus
Cytosol
time (sec)
Vehicle-treated
Xestospongin-treated
(B)
F/F0
Nuclear
Cytosol
Vehicle
IP3 AM (1st rise)
IP3 AM (2nd rise)
IP3 AM + XeD
(C)
Slope of Ca2+ transient
Nucleus
DMSO
IP3AM (1st peak)
IP3AM (2nd peak)
XeD-IP3AM

CHAPTER 4.2 - EXPRESSION OF INTRACELLULAR CALCIUM CHANNELS IN MODELS OF NEURODEGENERATION

ABSTRACT

Calcium (Ca^{2+}) is a universal signaling constituent involved in almost every cellular process (1). Intracellular Ca^{2+} channels such as inositol 1, 4, 5-trisphosphate (IP_3) receptors (IP_3Rs) and ryanodine receptors (RyRs), are critical constituents of Ca^{2+} signaling machinery in all cells (2 – 7). We previously described the differential intracellular distribution and signaling properties of IP_3R subtypes in the HT22 neuronal cell line (8). Here, I characterized the presence and distribution of IP_3Rs and RyRs in mouse primary cortical neurons and RyRs in HT22 cells. I hypothesized that HT22 cells express RyR2 and RyR3 and cultured cortical neurons express IP_3R1, IP_3R2, IP_3R3, RyR2 and RyR3. Like HT22 cells, primary cortical neurons express all three IP_3R subtypes. Unlike HT22 cells, however, IP_3R2 in cortical neurons does not exhibit a predominant nuclear localization and IP_3R3 exhibits significant nuclear localization. In addition, HT22 cells and primary cortical neurons exhibit RyR2 and RyR3 immunoreactivity. Both of these cell types represent commonly-utilized cell model systems of neurodegeneration (9 – 10). I hypothesized that IP_3R and RyR immunoreactivity is increased in response to oxidative stress. Here, I reveal that the relative immunoreactivities of IP3Rs and RyRs are increased in HT22 cells exposed to oxidative stress. Better understanding of the distribution of IP_3R and RyR subtypes and the alteration of this expression in response to oxidative stress in these model systems will allow future mechanistic analysis for the contribution the role of intracellular Ca^{2+}

channel expression and function in the progression of neurodegenerative diseases such as Alzheimer's disease.

INTRODUCTION

Calcium (Ca^{2+}) regulates a variety of biological processes within cells including neurotransmission, gene transcription and cell survival (11 - 15). Regulation of the intracellular Ca^{2+} concentration is necessary to maintain normal function and cell viability (16). Inositol 1, 4, 5-trisphosphate receptors (IP_3Rs) and Ryanodine receptors (RyRs) are the major types of channels releasing Ca^{2+} from intracellular stores (2 - 7, 17).

There are three types of IP_3Rs (types 1 – 3) each with discrete biophysical properties (3 - 7 , 18 - 21). They are expressed in the endoplasmic reticulum and the nuclear envelope and are activated to release Ca^{2+} from intracellular stores upon binding inostol-1,4,5-trisphosphate (IP_3) (6, 17, 22 - 27). Furthermore, IP3R activity is regulated by Ca^{2+} and ATP (6, 24, 28 - 31).

RyRs are activated by the same ion they conduct, Ca^{2+}, and are, thus, called Ca^{2+}-induced Ca^{2+} release (CICR) channels (2, 32). In addition, other putative ligands for RyR have been described including cyclic adenosine diphosphate-ribose (cADPR) and nicotinic acid adenine dinucleotide phosphate (NAADP) (33, 34). Release of Ca^{2+} by RyRs is also regulated in large part by the luminal and cytoplasmic Ca^{2+} concentration, ATP and multiple proteins that physically interact with them (35 - 39). Multiple kinases can phosphorylate RyRs and alter their activity (39).

Three types of RyR subtypes exist (RyR1, RyR2 and RyR3), each with distinct biophysical and physiological properties (2, 39).

Numerous studies indicate the importance of intracellular Ca^{2+} channels in neurodegenerative diseases. For example, cortical IP3R and RyR expression and function is altered in the brains of AD patients. IP3 generation and IP3 binding is reduced in brains from Alzheimer's patients (40 - 42). There is also a reduction in hippocampal RyR binding with increasing deposition of β-amyloid and AD symptoms (43).

Numerous in vitro studies demonstrate the effects of mutant presenilin proteins (PS-1 and PS-2) on RyR channel activity. For example, exposure of cultured mouse neurons with Aβ peptide results in an increase in RyR3 expression (44). In addition, exposure of cultured neurons to Aβ results in increased Ca^{2+} release from RyRs resulting in subsequent neuronal death (45). Mutant PS-1-expressing PC12 cells and mutant PS-1 knock-in mice exhibit increased RyR expression and elevated caffeine-induced Ca^{2+} release (46). Furthermore, neurons from mutant PS-1-knockin mice or PS-1/PS-2/APP triple AD transgenic mice stimulated with caffeine resulted in elevated RyR expression and increased Ca^{2+} release (47).

HT22 cells are a hippocampal cell line used often as a cell model system for neuroprotection studies (9, 10). In a previous study, we characterized the subcellular distribution and Ca^{2+} signaling properties of IP_3R subtypes in HT22 cells (8). We concluded that IP_3R2, the subtype exhibiting the highest affinity for the ligand IP_3, was expressed predominantly in the nucleus. Furthermore, we showed that IP_3-AM treatment of HT22 cells resulted in nuclear Ca^{2+} release with faster kinetics that that of cytosolic IP_3R subtypes.

The importance on intracellular Ca^{2+} channels, such as IP_3Rs and RyRs, in neurodegenerative diseases has prompted us to characterize the expression and localization of RyRs in HT22 cells and IP_3Rs and RyRs in culture primary cortical neurons. Here, I hypothesize that cultured mouse primary cortical neurons express all three IP3R subtypes and the neuron-specific RyR subtypes,

RyR2 and RyR3. In addition, I hypothesize that HT22 cells express RyR2 and RyR3. I detected all three IP_3R subtypes as well as RyR2 and RyR3 in cultured cortical neurons using immunochemical methods. In addition, I detected the expression of RyR2 and RyR3 in HT22 cells. The subcellular localization of IP3Rs in cortical neurons exhibited some discrete expression patterns.

Furthermore, I determined if exposure of cells to a sublethal peroxidative stress alters IP_3R and RyR immunoreactivities. These data suggest that cultured primary cortical neurons and HT22 cells, both relevant for the study of neurodegenerative diseases, likely utilize differentially distributed IP3R and RyR subtypes to control distinct Ca^{2+} dependent signaling pathways. Furthermore, I reveal that sublethal oxidative stress alters IP_3R and RyR immunoreactivity. These data possibly represents novel targets for the modulation of neuronal function.

MATERIALS AND METHODS

Cell Culture

HT22 cells were cultured as described elsewhere (Duncan et al., 2007). Mouse primary cortical neurons were obtained from postnatal day 2 (P2) C57B/L6 mice. After removal of the scalp and skull cap, an approximately $1mm^3$ piece of frontal cortex was removed from each hemisphere and digested in 0.25% trypsin at 37°C for 20 min. The tissue was then briefly triturated with a fire-polished glass pipet or a disposable plastic pipet tip and centrifuged at 1,000 x g for 5 minutes. After removal of the trypsin (supernatant), the resulting pellet was resuspended in complete media and triturated followed by centrifugation at 500 x g for 5 minutes. The pellet was triturated and centrifuged once more. The pellet was resuspended in

complete medium and passed through a 40μm cell strainer and the resulting cell suspension was plated onto a substrate appropriate for the given technique. Primary cortical neurons were maintained in Neurobasal A media with 2% donor horse serum (DHS), 2% B27 supplement and penicillin-streptomycin-fungizone antibiotic for 10 – 14 days depending on suitable development of neurites.

Immunocytochemistry and Immunofluorescence

HT22 cells were grown on poly-L-lysine-coated coverslips at 2,000 – 4,000 cells/coverslip (density of ~50 - 70%). Mouse primary cortical neurons were plated on oly-D-lysine/laminin-coated 12mm coverslips at a density of 1 – 2 x10^5 cells/coverslip. Immunocytochemistry was conducted as described previously (Duncan et al., 2007) using rabbit anti- IP3R1 (Calbiochem), IP3R2 (Calbiochem), RyR2 (Chemicon AB9080) and RyR3 (Chemicon AB9082. Monoclonal antibodies were used to immunolabel IP3R3 (BD Biosciences), RyR1 (University of Iowa) and RyR2 (Affinity Bioreagents). Slides were viewed on Olympus IX-70 fluorescence microscope.

Immunoblotting

Immunoblotting was conducted on HT22 cell lysates and mouse cortical tissue as described elsewhere (Duncan et al. 2007)

Statistics

An F-test was conducted in Excel between each treatment group and the untreated control group to determine which type of T-test should be used for group comparisons. The mean fluorescence intensity from each treatment group was separately compared to the mean

fluorescence intensity of the untreated control group using a two-sample T-test with either equal or unequal variances.

RESULTS

Immunofluorescent Detection of IP3R Subtypes in Cultured Mouse Primary Cortical Neurons

Immunofluorecent detection of IP3R subtypes in HT22 cells has been previously characterized using standard fluorescence microscopy (8). IP_3R1 immunoreactivity in cultured mouse primary cortical neurons exhibits a predominant ER/cytosolic localization with relatively little nuclear localization (Fig. 1). Using an additional IP_3R1-specific antibody reveals similar IP3R1 immunoreactivity (data not shown). These results suggest that IP_3R1 may be primarily involved in generating Ca^{2+} signals within the ER/cytosolic region of the cells facilitating Ca^{2+}-sensitive process there.

IP_3R2 immunoreactivity in cultured primary cortical neurons exhibits a predominant ER/cytosolic localization with moderate nuclear localization similar to that observed for IP_3R1 (Fig. 2). Using an additional IP_3R2-specific antibody reveals similar immunolabeling pattern. IP_3R2 immunolabeling in HT22 cells exhibits a predominant nuclear localization suggesting a possible involvement of this subtype in nuclear processes such as gene expression (8).

Immunolabeling of IP_3R3 with a polyclonal antibody reveals intense labeling in the ER/cytosolic compartment and moderate labeling in the nuclear region (Fig. 3). These results suggest that in cultured primary cortical neurons, but not in HT22 cells, IP_3R3 may be involved in nuclear Ca^{2+} signaling and possible regulation of gene expression. In addition, immunolabeling of IP_3R3 in cultured mouse primary cortical neurons with a widely-used

monoclonal antibody results in very weak labeling with both ER/cytosolic and nuclear localization. Since IP_3R3 immunoreactivity in HT22 cells is exclusively in the ER/cytosolic region, we would predict that it is not involved in HT22 nuclear Ca^{2+} signaling and gene expression.

Immunofluorescent Detection of RyR Subtypes in HT22 Cells and Cultured Mouse Primary Cortical Neurons

In HT22 cells, RyR2 immunoreactivity is predominant in the ER/cytocolic compartment with weaker labeling in the nuclear region (Fig. 4). The nuclear localization of RyR2 suggests a possible role in nuclear Ca^{2+} signaling regulating gene expression. Immunolabeling of mouse cortical neurons for RyR2 with a widely-used monoclonal antibody reveals weak labeling in both the ER/cytosolic and nuclear compartments (Fig. 5). Immunolabeling of mouse cortical neurons with a polyclonal antibody for RyR2 reveals strong labeling in the ER/cytosolic compartment with some (but not all) cells exhibiting strong labeling in the nucleus as well.

RyR3 immunoreactivity in HT22 cells is found in the ER and more intensely in the nuclear envelope (Fig. 6). RyR immunoreactivity is predominant in the nuclear envelope similar to that of IP_3R2, suggesting a possible involvement in gene expression. Cultured cortical neurons exhibit RyR3 immunoreactivity in both the ER/cytsolic and nuclear compartments (Fig. 7). These results suggest that RyR3, like RyR2, may be involved in nuclear Ca^{2+} signaling regulating gene expression.

Characterization of tBHP Lethality in HT22 Cells

Exposure of HT22 cells to tBHP concentrations up to 10μM have no significant effect on calcein-AM fluorescence and are thus considered to be sublethal (Fig. 8). As determined by the calcein-AM assay, the approximate LC_{50} of tBHP in HT22 cells lies within the range of 15 – 25μM (Fig. 8). Since the tBHP kill curve is very steep, the degree of tBHP toxicity varies slightly from experiment to experiment depending on the cell passage number and culture conditions such as cell density. Exposure of HT22 cells to tBHP concentrations up to 15μM exhibit no reduction in MTT absorbance (data not shown). Interestingly, concentrations of 6 – 10μM tBHP result in a significant increase in MTT absorbance but 15μM tBHP results in a decline in MTT absorbance back to baseline levels (data not shown). These data suggest different levels of mitochondrial activity at sublethal tBHP compared to mildly-lethal tBHP concentrations. Overall, we interpret these results to mean that tBHP concentrations up to 10μM do not significantly affect HT22 cell viability, but 15μM tBHP causes some reduction in viability. These studies have identified a tBHP concentration range that elicits oxidative stress but does not kill cells thereby rendering them available for study. Use of higher tBHP concentrations for shorter periods of time prevents the measurement of molecular and physiological changes that would occur in response to adaptive gene expression and protein synthesis before the onset of cell death. We feel that lower levels of oxidative insult for a longer period of time (i.e., overnight) more closely resembles the oxidative conditions occurring in neurodegenerative diseases.

Effect of Oxidative Stress on IP3R Expression in Models of Neurodegeneration

Overnight (16 – 20 hour) exposure of HT22 cells to sublethal concentrations of tBHP results in subtle but significant increases in IP_3R1 immunoreactivity in the ER/cytosolic region as determined by microfluorimetric analysis of immunolabeled cells (Fig. 9). Immunolabeling of HT22 cells with two different IP_3R1 antibodies reveals that overnight (16 – 20 hour) tBHP exposure leads to a significant increase (up to 40%) in IP_3R1 immunoreactivity compared to untreated controls (Fig. 9). This effect of tBHP, however, appears to be biphasic with tBHP concentration approaching lethality resulting in a return in IP_3R1 immunoreactivity to baseline levels.

Western blot analysis of lysates from HT22 cells exposed to sublethal tBHP concentrations results in a significant increase in IP_3R1 immunreactivity (Fig. 10). This Western blot data corroborates the immunocytochemistry (immunofluorescence) data.

In HT22 cells, exposure to low sublethal tBHP concentrations (2 – 4μM) results in a slight but significant decrease in IP_3R2 immunoreactivity (Fig. 11). Tert-BHP, however, leads to a dose-dependent increase in IP_3R2 immunoreactivity from low to higher sublethal tBHP concentrations. Unlike that observed for IP_3R1, 10μM tBHP does not cause a decline in IP_3R2 immunreactivity back to baseline levels. Overall, exposure of HT22 cells to sublethal tBHP alters the nuclear relative to cytosolic IP_3R2 immunoreactivity (Fig. 11). Exposure of HT22 cells to sublethal tBHP concentrations just below measureable toxicity (10μM) leads to a noticeable and significant increase in nuclear IP_3R2 immunoreactivity.

In another experiment, exposure of HT22 cells to sublethal tBHP results in a dose-dependent increase in both nuclear and cytosolic IP_3R2 immunoreactivity. This effect is more exaggerated for nuclear IP_3R2. Unlike that observed for IP_3R1, 10μM tBHP does not cause a decline in IP_3R2

immunreactivity back to baseline levels. Sublethal tBHP dose-dependently alters nuclear relative to cytosolic IP_3R2 immunoreactivity. Western blot analysis of lysates from HT22 cells exposed to sublethal tBHP concentrations results in a significant increase in IP_3R2 immunreactivity (Fig. 12). Western blot data corroborates the immunocytochemistry (immunofluorescence) data. This suggests that IP3R2 may be regulated differently than IP3R1 in response to oxidative stress.

Overnight (16 – 20 hour) exposure of HT22 cells to sublethal concentrations of tBHP results in significant increases in IP_3R3 immunoreactivity at low tBHP concentrations and significant decrease in IP_3R3 immunoreactivity at higher tBHP concentrations as determined by microfluorimetric analysis of immunolabeled cells (Fig. 13). The biphasic pattern of IP_3R3 immunoreactivity is similar to that observed for IP_3R1, but different than IP3R2 immunoreactivity at higher tBHP concentrations. Overall, these results suggest that IP_3R1 and IP_3R3 may be regulated in a similar manner in response to oxidative stress and in a manner different that that of IP_3R2.

Effect of Oxidative Stress on RyR Expression in Models of Neurodegeneration

Exposure of HT22 cells to sublethal tBHP results in a trend toward an increase in RyR2 immunoreactivity as tBHP concentrations approach lethality (15μM) when a widely-utilized monoclonal antibody is used (data not shown). Use of a polyclonal antibody, however, reveals a possible trend toward a decrease at 2μM and 10μM tBHP but does not change at the intermediate (6μM and 10μM) tBHP concentrations (data not shown). These results are contradictory and unclear.

Exposure of HT22 cells to tBHP concentrations approaching lethality (10 – 15μM) result in a significant increase in RyR3 immunoreactivity (Fig. 14, arrows). These results indicate that oxidative stress may alter the expression of RyRs.

DISCUSSION

Here, I report that two commonly-used cell moel systems of neurodegeneration, HT22 cells and cultured mouse primary cortical neurons, express IP_3Rs and RyRs, both of which are critical Ca^{2+} channels regulating the release of Ca^{2+} from intracellular stores. Specifically, I detected IP_3R1, IP_3R2, IP_3R3, RyR2 and RyR3 in these cell models systems using immunochemical methods. In addition, the subcellular distribution was determined using immunofluorescence. Furthermore, I measured significant changes in IP_3R and RyR immunoreactivity in response to oxidative stress lending support to the idea that intracellular Ca^{2+} channels, such as IP3Rs and RyRs, play an important role in neurodegenerative diseases.

These data provide relevant information about the IP_3R and RYR subtypes expressed in HT22 cells and cultured cortical neurons. The differential distribution of IP_3Rs and RyRs (i.e. ER/cytosolic versus nuclear) provides clues to the potential discrete function of intracellular Ca^{2+} channels as it relates to specific cellular functions. For example, IP_3R2 in HT22 cells and IP_3R2 and IP_3R3 in cultured cortical neurons are predominantly localized to the nucleus suggesting that they may play a role in the regulation of gene transcription. The apparent discrepancy between strong nuclear IP_3R2 immunoreactivity in HT22 cells and weaker nuclear IP_3R2 immunoreactivity in primary cortical neurons could be attributed to the proliferative properties of the HT22 cell line versus the terminally differentiated state of cultured neurons. Others have identified a role that IP_3Rs and RyR play in gene regulation, but little information on which

subtypes are involved in this process have been determined (12, 13, 15). Colabeling of cultured mouse primary cortical neurons with IP_3R1- and IP_3R3-specific antibodies reveals that there is no complete colocalization and only partial colocalization at best. All observed cells exhibiting a neuronal phenotype and expressing IP_3R3 also express IP_3R1. Interestingly, some neuronal cells exhibiting high levels of IP_3R1 immunoreactivity do not have appreciable IP_3R3 immunoreactivity. These results suggest that cultured cortical neurons may express IP_3R1 more exclusively compared to IP_3R3.

The alterations observed in IP_3R and RyR immunoreactivity in response to oxidative stress suggests possible alteration in their function in neurodegenerative diseases exhibiting oxidative stress. IP_3Rs and RyR have been shown to play a role in neurotransmitter release (11). Any changes in their expression may have implication in neurotransmission. The changes in IP_3R and RyR expression described in this work underscore the possible contribution they may have in neurodegeneration.

It is interesting to note that the biphasic nature of the change in IP3R1 and IP3R3 immunoreactivities in response to oxidative stress. A possible interpretation for the initial increase in immunoreactivity at low concentrations of tBHP could be that oxidative stress alters the structure or conformation of the receptor thereby increasing the affinity of the antibody for the epitope. This interpretation, however, can be ruled out due to the fact that denatured protein used in Western blots also exhibits the same initial increase. Alternatively, higher tBHP concentration likely result in some change in cellular morphology such as the adaptation of a spherical shape which results in greater cell depth and consolidation and clustering of epitope leading to subsequent increases in fluorescence.

Our interpretation is that oxidative stress activates an adaptive response leading to IP_3R gene transcription. These adaptive changes could conceivably be facilitated by the activation (or deactivation) of a kinase, phosphatase or transcription factor. Others have identified numerous kinases and transcription factors that can be activated under conditions of oxidative stress (48, 49).

The decrease in immunoreactivity near lethal tBHP concentrations could be due to possible degradation of proteins which can occur during apoptosis and necrosis (50). In addition, the decrease in immunoreactivity near lethal tBHP concentrations could be due to the initiation of an additional signaling pathway counteracting or antagonizing the pathway responsible for increasing gene expression at low levels of oxidative stress.

To our knowledge, we are the first to measure changes in IP_3R and RyR immunoreactivity elicited by oxidative stress in cultured neurons. Others have measured changes in IP_3 signaling and binding as well as IP_3R and RyR expression in brains of animals or humans (40 - 44). My data supports the data from others revealing that exposure of neurons to toxic stimuli result in an elevation of RyR3 expression (44, 46).

Immunocytochemical characterization of IP_3R and RyR expression in response to a stimulus such as oxidative stress does not establish a functional consequence such as Ca^{2+} release. As a result, optical imaging of intracellular Ca^{2+} with and without oxidant treatment should be conducted to determine if observed changes in IP_3R or RyR immunoreactivity have functional consequences.

REFERENCES

1. Berridge, M.J. 1997. Elementary and global aspects of calcium signaling. *J. Exp. Biol.* 200:315-319.
2. Fill, M., and R. Coronado. 1988. Ryanodine receptor channel of sarcoplasmic reticulum. *Trends Neurosci.* 11:453-457.
3. Furuichi T., S. Yoshikawa, A. Miyakawi, K. Wada, N. Maeda, and K. Mikoshiba. 1989. Primary structure and functional expression of the inositol 1,4,5-trisphosphate-binding protein P400. *Nature.* 342:32-38.
4. Mignery G.A., T.C. Sudhof, K. Takei, P. and De Camilli. 1989. Putative receptor for inositol 1,4,5-trisphosphate similar to ryanodine receptor. *Nature.* 342:192-195.
5. Mignery G.A., C.L. Newton, B.T. Archer 3rd, and T.C. Sudhof. 1990. Structure and expression of the rat inositol 1,4,5-trisphosphate receptor. *J. Biol. Chem.* 265:12679-12685.
6. Maeda N., T. Kawasaki, S. Nakade, N. Yokota, T. Taguchi, M. Kasai, and K. Mikoshiba. 1991. Structural and functional characterization of inositol 1,4,5-trisphosphate receptor channel from mouse cerebellum. *J. Biol. Chem.* 266:1109-1116.
7. Blondel O., J. Takeda, H. Janssen, S. Seino, and G.I. Bell. 1993. Sequence and functional characterization of a third inositol trisphosphate receptor isotype, IP_3R-3, expressed in pancreatic islets, kidney, gastrointestinal tract, and other tissues. *J. Biol. Chem.* 268:11356-11363.
8. Duncan RS, Hwang SY and Koulen P (2007) Differential inositol 1,4,5-trisphosphate receptor signaling in a neuronal cell line. Int J Biochem Cell Biol. 39(10):1852-62.

9. Green, P.S., K.E. Gridley, J.W. Simpkins. 1998. Nuclear estrogen receptor-independent neuroprotection by estratrienes: a novel interaction with glutathione. *Neuroscience.* 84:7-10.

10. Sagara Y., R. Dargusch, D. Chambers, J. Davis, D. Schubert, and P. Maher. 1998. Cellular mechanisms of resistance to chronic oxidative stress. *Free Radic. Biol. Med.* 24:1375-1389.

11. Atlas, D. 2001. Functional and physical coupling of voltage-sensitive calcium channels with exocytotic proteins: ramifications for the secretion mechanism. *J. Neurochem.* 77:972-985.

12. Bading, H. 2000. Transcription-dependent neuronal plasticity the nuclear calcium hypothesis. *Eur. J. Biochem.* 267:5280-5283.

13. Hardingham G.E., S. Chawla, C.M. Johnson, and H. Bading. 1997. Distinct functions of nuclear and cytoplasmic calcium in the control of gene expression. *Nature.* 385:260-265.

14. Paschen, W. 2003. Mechanisms of neuronal cell death: diverse roles of calcium in the various subcellular compartments. *Cell Calcium.* 34:305-310.

15. West A.E., W.G. Chen, M.B. Dalva, R.E. Dolmetsch, J.M. Kornhauser, A.J. Shaywitz, M.A. Takasu, X. Tao, and M.E. Greenberg. 2001. Calcium regulation of neuronal gene expression. *Proc. Natl. Acad. Sci.* U.S.A. 98:11024-11031.

16. Verkhratsky, A., and E.C. Toescu. 2003. Endoplasmic reticulum $Ca^{(2+)}$ homeostasis and neuronal death. *J. Cell. Mol. Med.* 7:351-361.

17. Berridge M.J., and R.F. Irvine. 1984. Inositol trisphosphate, a novel second messenger in cellular signal transduction. *Nature.* 312:315-321.

18. Ross C.A., S.K. Danoff, M.J. Schell, S.H. Snyder, and A. Ullrich. 1992. Three additional inositol 1,4,5-trisphosphate receptors: molecular cloning and differential localization in brain and peripheral tissues. *Proc. Natl. Acad. Sci. U.S.A.* 89:4265-4269.

19. Sudhof T.C, C.L. Newton, B.T. Archer 3rd, Y.A. Ushkaryov, and G.A. Mignery. 1991. Structure of a novel InsP3 receptor. *EMBO. J.* 10:3199-3206.

20. Yoshikawa S, T. Tanimura, A. Miyawaki, M. Nakamura, M. Yuzaki, T. Furuichi, and K. Mikoshiba. 1992. Molecular cloning and characterization of the inositol 1,4,5-trisphosphate receptor in Drosophila melanogaster. *J. Biol. Chem.* 267:16613-16619.

21. Koulen P., and E.C. Thrower. 2001. Pharmacological modulation of intracellular $Ca^{(2+)}$ channels at the single-channel level. *Mol. Neurobiol.* 24:65-86.

22. Streb H., R.F. Irvine, M.J. Berridge, and I. Schulz. 1983. Release of Ca^{2+} from a nonmitochondrial intracellular store in pancreatic acinar cells by inositol-1,4,5-trisphosphate. *Nature.* 306:67-69.

23. Ross C.A., J. Meldolesi, T.A. Milner, T. Satoh, S. Supattapone, and S.H. Snyder. 1989. Inositol 1,4,5-trisphosphate receptor localized to endoplasmic reticulum in cerebellar Purkinje neurons. *Nature.* 339:468-70.

24. Ehrlich B.E., and J. Watras. 1988. Inositol 1,4,5-trisphosphate activates a channel from smooth muscle sarcoplasmic reticulum. *Nature.* 336:583-586.

25. Maeda N., M. Ninobe, and K. Mikoshiba. 1990. A cerebellar Purkinje cell marker P400 protein is an inositol 1,4,5-trisphosphate ($InsP_3$) receptor protein. Purification and characterization of InsP3 receptor complex. *EMBO. J.* 9(1):61-67.

26. Koulen, P. J. Wei, C. Madry, J. Liu, and E. Nixon. 2005. Differentially distributed IP_3 receptors and Ca^{2+} signaling in rod bipolar cells. *Invest. Ophthalmol. Vis. Sci.* 46:292-298.

27. Leite M.F., E.C. Thrower, W. Echevarria, P. Koulen, K. Hirata, A.M. Bennett, B.E. Ehrlich, and M.H. Nathanson. 2003. Nuclear and cytosolic calcium are regulated independently. *Proc. Natl. Acad. Sci. U.S.A.* 100:2975-2980.

28. Iino, M. 1987. Calcium dependent inositol trisphosphate-induced calcium release in the guinea-pig taenia caeci. *Biochem. Biophys. Res. Commun.* 142:47-52.

29. Iino, M. 1990. Biphasic Ca^{2+} dependence of inositol 1,4,5-trisphosphate-induced Ca^{2+} release in smooth muscle cells of the guinea pig taenia caeci. *J. Gen. Physiol.* 95:1103-1122.

30. Bezprozvanny I., J. Watras, and B.E. Ehrlich. 1991. Bell-shaped calcium-response curves of Ins(1,4,5)P_3- and calcium-gated channels from endoplasmic reticulum of cerebellum. *Nature.* 351:751-754.

31. Bezprozvanny I., and B.E. Ehrlich. 1993. ATP modulates the function of inositol 1,4,5-trisphosphate-gated channels at two sites. *Neuron.* 10:1175-1184.

32. Iino M (1989) Calcium-induced calcium release mechanism in guinea pig taenia caeci. J Gen Physiol. 94(2):363-83.

33. Meszaros LG, Bak J and Chu A (1993) Cyclic ADP-ribose as an endogenous regulator of the non-skeletal type ryanodine receptor Ca2+ channel. Nature. 364(6432):76-9.

34. Dousa TP, Chini EN and Beers KW (1996) Adenine nucleotide diphosphates: emerging second messengers acting via intracellular Ca2+ release. Am J Physiol. 271(4 Pt 1):C1007-24.

35. Hidalgo C and Donoso P (1995) Luminal calcium regulation of calcium release from sarcoplasmic reticulum. Biosci Rep. 15(5):387-97.

36. Carroll S, Skarmeta JG, Yu X, Collins KD and Inesi G (1991) Interdependence of ryanodine binding, oligomeric receptor interactions, and Ca2+ release regulation in junctional sarcoplasmic reticulum. Arch Biochem Biophys. 290(1):239-47.

37. Hwang SY, Wei J, Westhoff JH, Duncan RS, Ozawa F, Volpe P, Inokuchi K and Koulen P (2003) Differential functional interaction of two Vesl/Homer protein isoforms with ryanodine receptor type 1: a novel mechanism for control of intracellular calcium signaling. Cell Calcium.34(2):177-84.

38. Westhoff JH, Hwang SY, Duncan RS, Ozawa F, Volpe P, Inokuchi K and Koulen P (2003) Vesl/Homer proteins regulate ryanodine receptor type 2 function and intracellular calcium signaling. Cell Calcium. 34(3):261-9.

39. Zalk R, Lehnart SE and Marks AR (2007) Modulation of the ryanodine receptor and intracellular calcium. Annu Rev Biochem. 76:367-85.

40. Stokes, CE & Hawthorne, JN (1987) Reduced phosphoinositide concentrations in anterior temporal cortex of Alzheimer-diseased brains. J Neurochem. 48(4):1018-21.

41. Ferrari-DiLeo, G & Flynn, DD (1993) Diminished muscarinic receptor-stimulated [3H]-PIP2 hydrolysis in Alzheimer's disease. Life Sci. 53(25):PL439-44.

42. Crews, F. T., Kurian, P., & Freund, G. Cholinergic and serotonergic stimulation of phosphoinositide hydrolysis is decreased in Alzheimer's disease. Life Sci. 55(25-26):1993-2002 (1994).

43. Kelliher, M., Fastbom, J., Cowburn, R. F., Bonkale, W., Ohm, T. G., Ravid, R., Sorrentino, V. & O'Neill, C. Alterations in the ryanodine receptor calcium release channel correlate

with Alzheimer's disease neurofibrillary and beta-amyloid pathologies. Neuroscience. 92(2):499-513 (1999).

44. Supnet, C., Grant, J., Kong, H., Westway, D. & Mayne, M. (2006) Abeta 1-42 increases ryanodine receptor-3 expression and function in TgCRND8 mice. J Biol Chem. Oct 18th, Epub ahead of print.

45. Ferreiro, E., Resende, R., Costa, R., Oliveira, C. R. & Pereira, C. M. An endoplasmic-reticulum-specific apoptotic pathway is involved in prion and amyloid-beta peptides neurotoxicity. Neurobiol Dis. 23(3):669-78 (2006).

46. Chan, S. L., Mayne, M., Holden, C. P., Geiger, J. D. & Mattson, M. P. (2000) Presenilin-1 mutations increase levels of ryanodine receptors and calcium release in PC12 cells and cortical neurons. J Biol Chem. 275(24):18195-200.

47. Smith, I. F., Hitt, B., Green, K. N, Oddo, S. & LaFerla, F. M. (2005) Enhanced caffeine-induced Ca2+ release in the 3xTg-AD mouse model of Alzheimer's disease. J Neurochem. 94(6):1711-8.

48. Kamata H and Hirata H (1999) Redox regulation of cellular signalling. Cell Signal. 11(1):1-14.

49. Li X and Stark GR (2002) NFkappaB-dependent signaling pathways. Exp Hematol. 30(4):285-96.

50. Solary E, Eymin B, Droin N and Huagg M (1998) Proteases, proteolysis, and apoptosis. Cell Biol Toxicol. 14(2):121-32. Review

FIGURES

Fig. 1 - Cultured Mouse Primary Cortical Neurons Express IP_3R1. IP_3R1 immunoreactivity in cultured mouse primary cortical neurons exhibits a predominant ER/cytosolic localization (arrow) with relatively little nuclear localization (scalebar is 25μm).

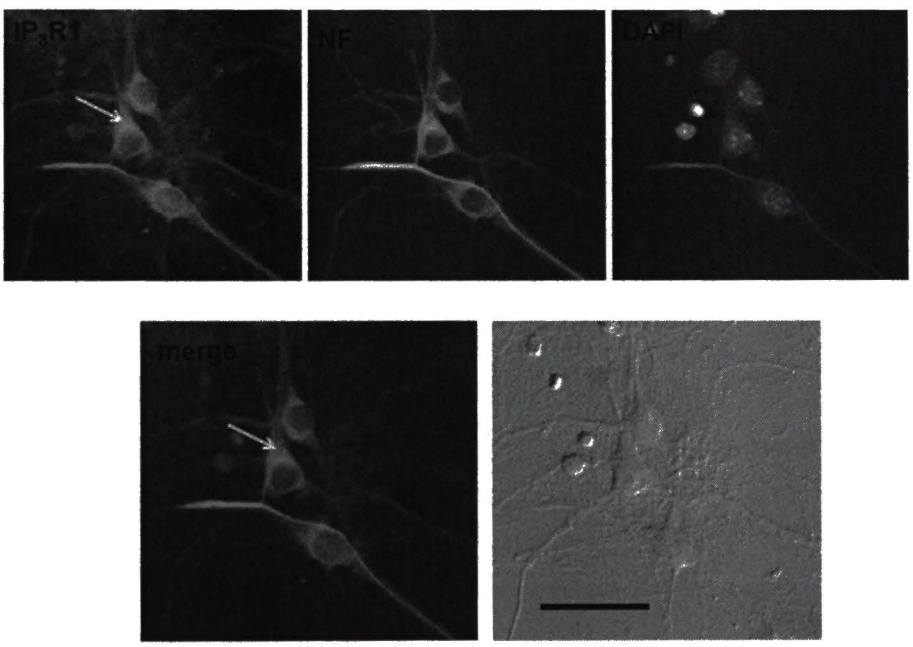
IP3R1
NF
DAPI
merge

Fig. 2 - Cultured Mouse Primary Cortical Neurons Express IP_3R2. IP_3R2 immunoreactivity in cultured primary cortical neurons exhibits a predominant ER/cytosolic localization (white arrow) with moderate nuclear localization (red arrow) similar to that observed for IP_3R1 (scalebar is 25μm).

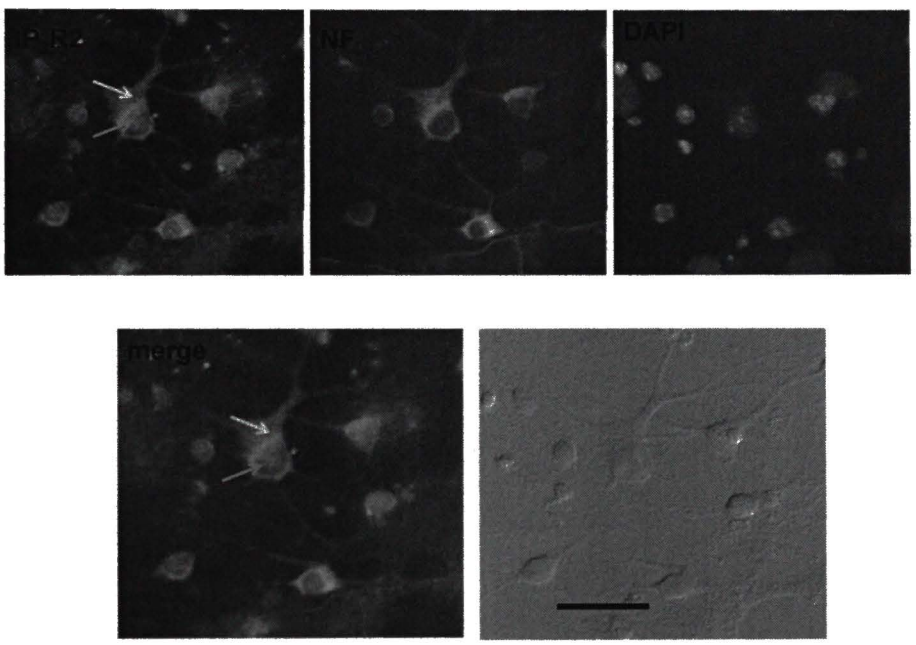
NF
DAPI
merge

Fig. 3 - Cultured Mouse Primary Cortical Neurons Express IP_3R3. Immunolabeling of IP_3R3 with a polyclonal antibody reveals strong labeling in the nuclear region (red arrow) similar to that observed in the ER/cytosolic compartment (white arrow) (scalebar is 25μm).

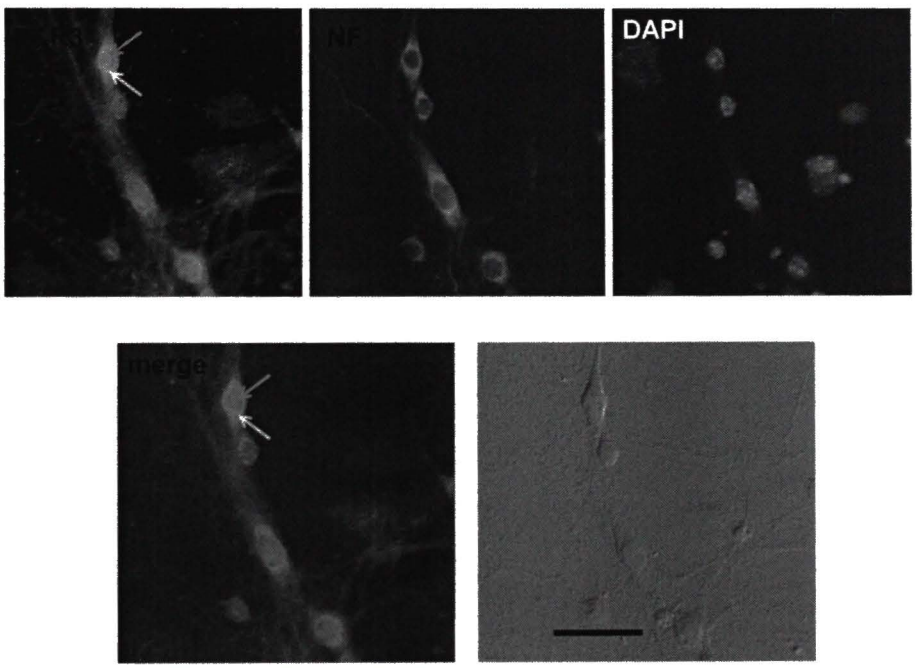
NF
DAPI
merge

Fig. 4 - HT22 Cells Express RyR2. Using polyclonal RyR2-specific antibody, RyR2 immunoreactivity is apparent in HT22 cells with labeling predominantly in the ER/cytosolic compartment and little in the nuclear region (scalebar is 25μm). Western blot analysis HT22 lysate (triplicate samples) reveals a band at greater than 500 kDa consistent with the molecular weight of RyR2 (arrow).

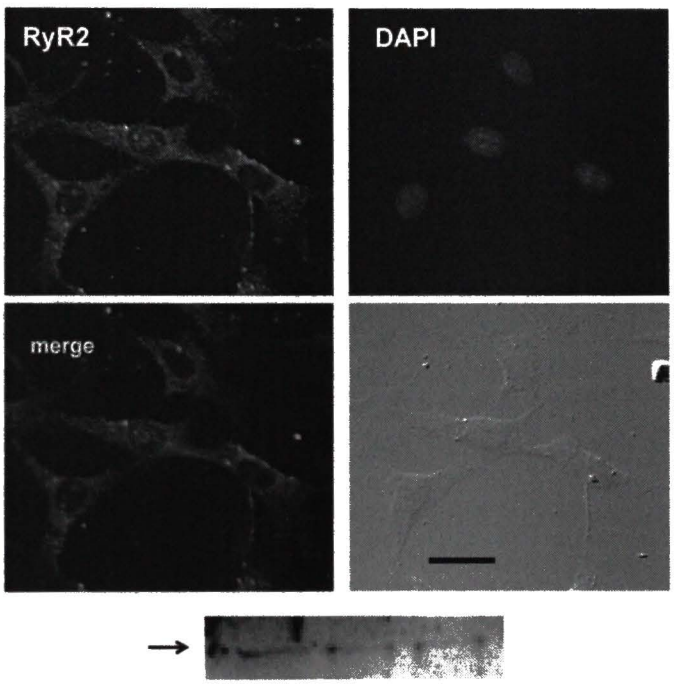
RyR2
DAPI
merge

Fig. 5 - Cultured Mouse Primary Cortical Neurons Express RyR2. Immunolabeling of mouse cortical neurons with a polyclonal antibody for RyR2 reveals strong labeling in the ER/cytosolic compartment with some cells exhibiting strong labeling in the nucleus as well (red arrow) (scalebar is 25μm).

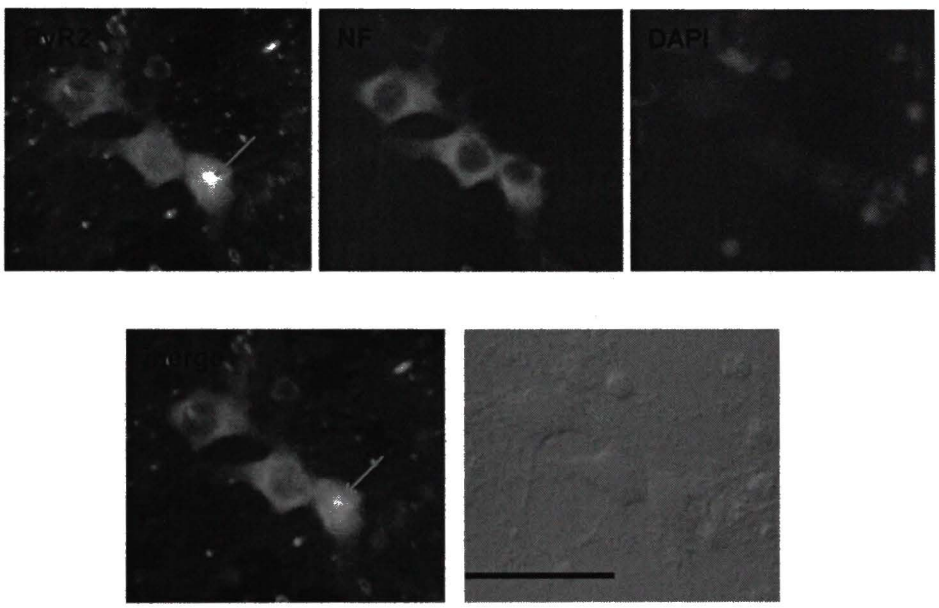
vRZ
NF
DAPI
Merge

Fig. 6 - HT22 Cells Express RyR3. RyR3 immunoreactivity in HT22 cells is strong and it exhibits ER/cytosolic as well as some nuclear localization (scalebar is 25μm). Western blot analysis HT22 lysate (triplicate samples) reveals a band at greater than 500 kDa consistent with the molecular weight of RyR3 (arrow).

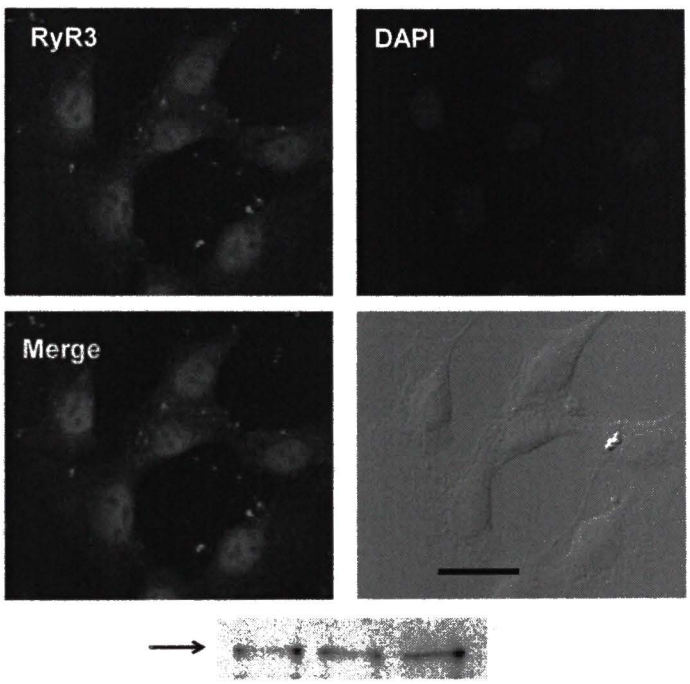
RyR3
DAPI
Merge

Fig. 7 - Cultured Mouse Primary Cortical Neurons Express RyR3. Cultured cortical neurons exhibit RyR3 immunoreactivity in both the ER/cytsolic and nuclear compartments (scalebar is 25μm).

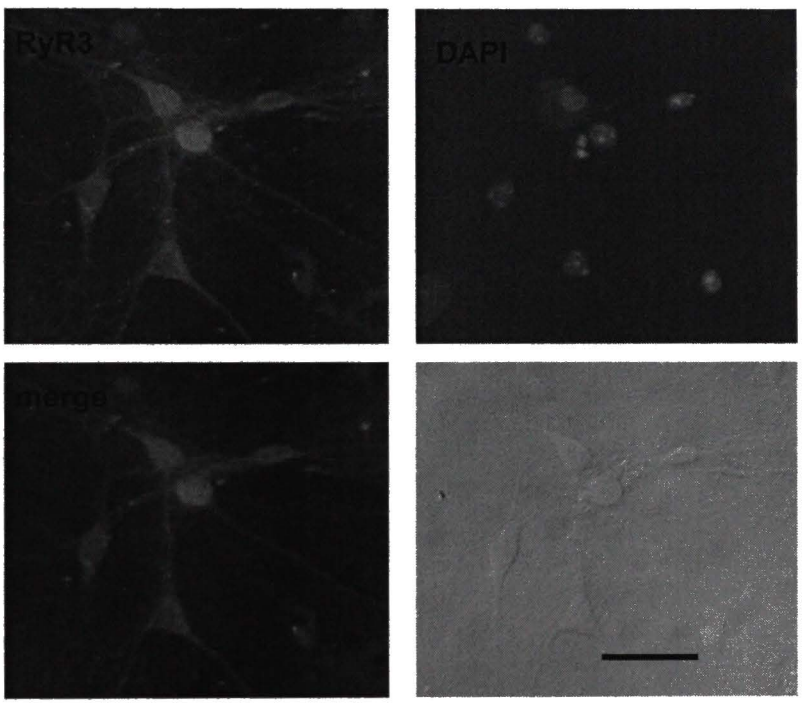
RyR3
DAPI
merge

Fig. 8 - Characterization of HT22 Viability in Response to Various tBHP Concentrations. Exposure of HT22 cells to tBHP concentrations up to 10μM has no significant effect on HT22 cell viability (% calcein-AM fluorescence compared to untreated cells) and is thus considered to be sublethal. These results suggest that the approximate LC_{50} of tBHP in HT22 cells is within the range of 15 – 25μM. For this study, *n* equals six (6) wells per condition. Comparisons between treatment groups and the control group were done using a two-sample T-test. A P-value of ≤ 0.01 and ≤ 0.001 is indicated by ** and ***, respectively.

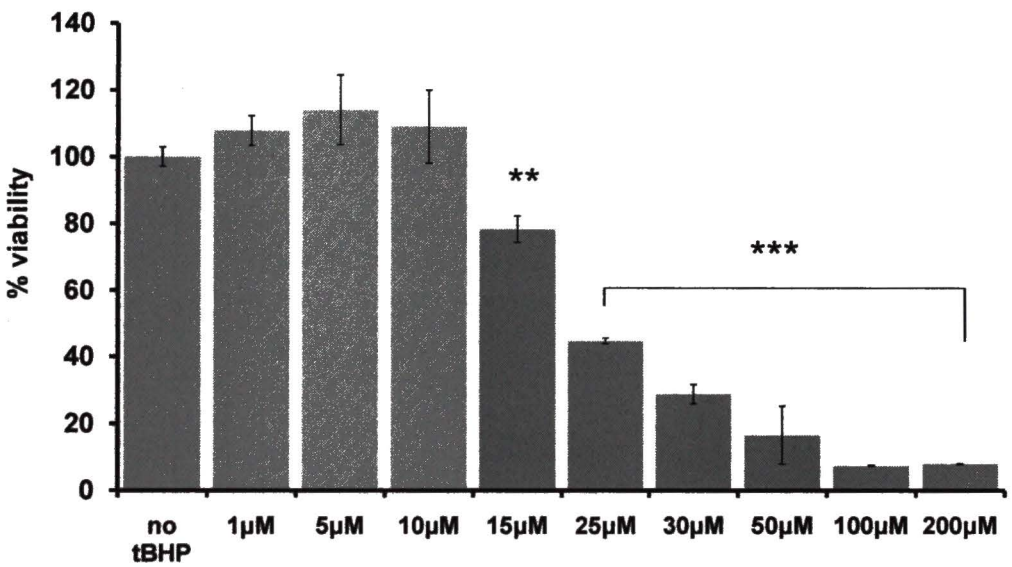
140
120
100
80
60
40
20
0
% viability
**
***
no tBHP
1μM
5μM
10μM
15μM
25μM
30μM
50μM
100μM
200μM

Fig. 9 - Exposure of HT22 Cells to Sublethal tBHP Concentrations Alters IP_3R1 Immunoreactivity. Overnight (16 – 20 hour) exposure of HT22 cells to sublethal concentrations of tBHP results in subtle but significant increases in IP_3R1 immunoreactivity as determined by microfluorimetric analysis of immunolabeled cells. The top graph and bottom graph were generated from data obtained from the use of two distinct anti-IP_3R1 antibodies. At tBHP concentrations approaching lethality (10μM), immunoreactivity for IP_3R1 in both graphs decreases back to baseline. For this study, *n* equals 45 cells and 120 cells per treatment group for the top and bottom graph, respectively. Comparisons between treatment groups and the control group were done using a two-sample T-test. A P-value of ≤ 0.05 and ≤ 0.01 is indicated by * and **, respectively.

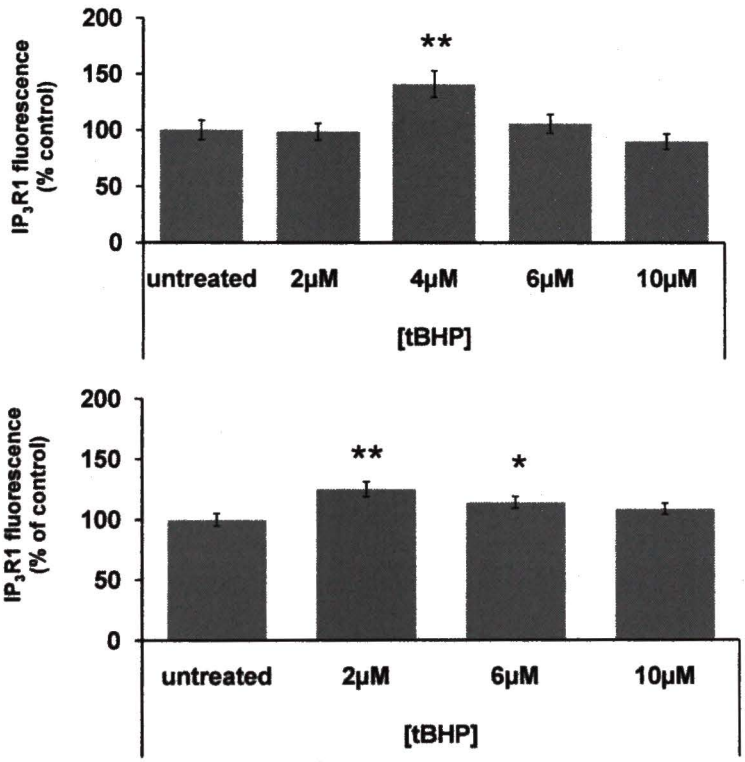
200
150
100
50
0
IP3R1 fluorescence (% control)
**
untreated
2μM
4μM
6μM
10μM
[tBHP]
200
150
100
50
0
IP3R1 fluorescence (% of control)
**
*
untreated
2μM
6μM
10μM
[tBHP]

Fig. 10. - Exposure of HT22 Cells to Sublethal tBHP Concentrations Alters IP_3R1 Immunoreactivity. (A), Western blot semiquantitative analysis of lysates from HT22 cells exposed to sublethal tBHP concentrations (2 and 10μM) results in a significant increase in IP_3R1 immunoreactivity. (B), The bottom panel shows duplicate HT22 lysate samples previously unexposed or exposed overnight to 10μM tBHP. This Western blot data corroborates the immunocytochemistry (immunofluorescence) data. For this study, *n* equals 2 experiments for the 2μM tBHP-treated while *n* equals 3 for the untreated and 10μM tBHP-treated groups. Comparisons between treatment groups and the control group were done using a two-sample T-test. A P-value of ≤ 0.05 and ≤ 0.01 is indicated by * and **, respectively.

A

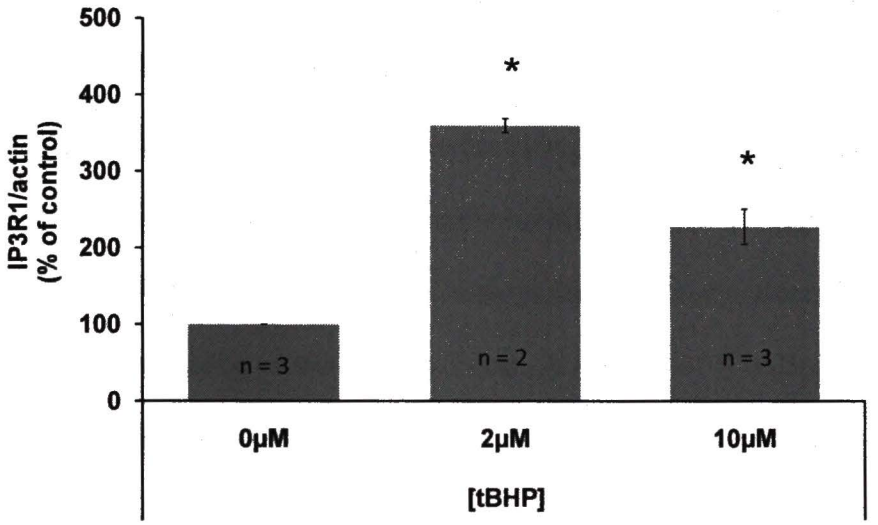
500
400
300
200
100
0
IP3R1/actin
(% of control)
*
*
n = 3
n = 2
n = 3
0μM
2μM
10μM
[tBHP]

B

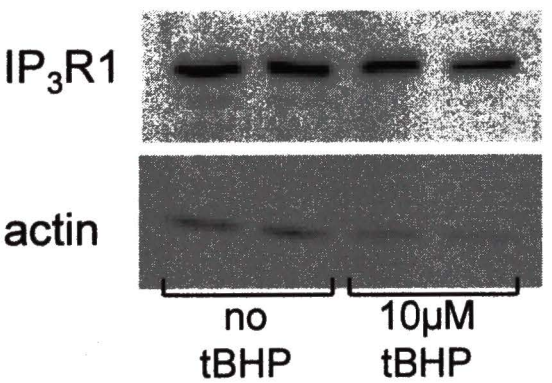
IP3R1
actin
no
tBHP
10μM
tBHP

Fig. 11 - Exposure of HT22 Cells to Sublethal tBHP Concentrations Alters IP_3R2 Immunoreactivity. (A), Cells exposed overnight to 10μM tBHP exhibit an increase in IP3R2 immunoreactivity, especially in the nuclear region (white arrows; scalebar is 25μm). (B), Exposure to low sublethal tBHP concentrations (2 – 4μM) has no effect on IP_3R2 immunoreactivity. Higher tBHP concentrations (6μM - 10μM), however, lead to a dose-dependent increase in IP_3R2 immunoreactivity. Unlike that observed for IP_3R1, 10μM tBHP does not cause a decline in IP_3R2 immunoreactivity back to baseline levels. For this study, *n* equals 35 cells per treatment group. Comparisons between treatment groups and the control group were done using a two-sample T-test. A P-value of ≤ 0.05 and ≤ 0.001 is indicated by * and ***, respectively.

A

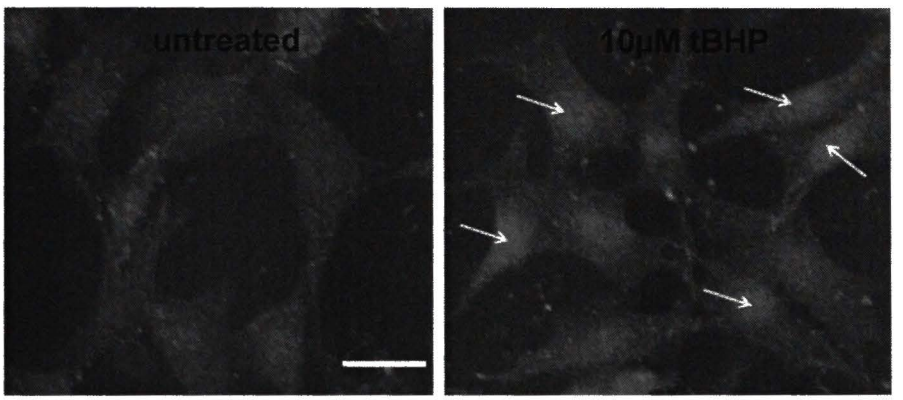
untreated
10μM tBHP

B

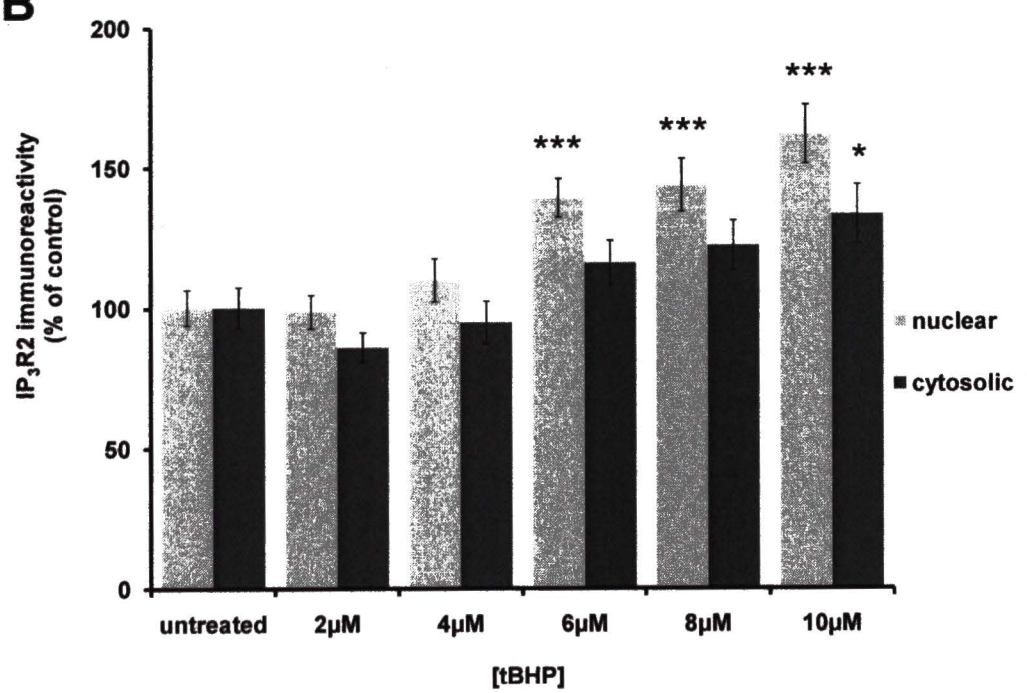
200
150
100
50
0
IP3R2 immunoreactivity
(% of control)
***
***
***
*
nuclear
cytosolic
untreated
2μM
4μM
6μM
8μM
10μM
[tBHP]

Fig. 12 - Exposure of HT22 Cells to Sublethal tBHP Concentrations Alters IP_3R2 Immunoreactivity. Semiquantitative Western blot analysis of lysates from HT22 cells exposed to low sublethal tBHP concentrations (2μM and 10μM) leads to a non-significant trend toward an increase in IP_3R2 immunoreactivity. For this study, *n* equals one (1) experiment for the 2μM tBHP-treated while *n* equals two (2) for the untreated and 10μM tBHP-treated groups. Comparisons between treatment groups and the control group were done using a two-sample T-test.

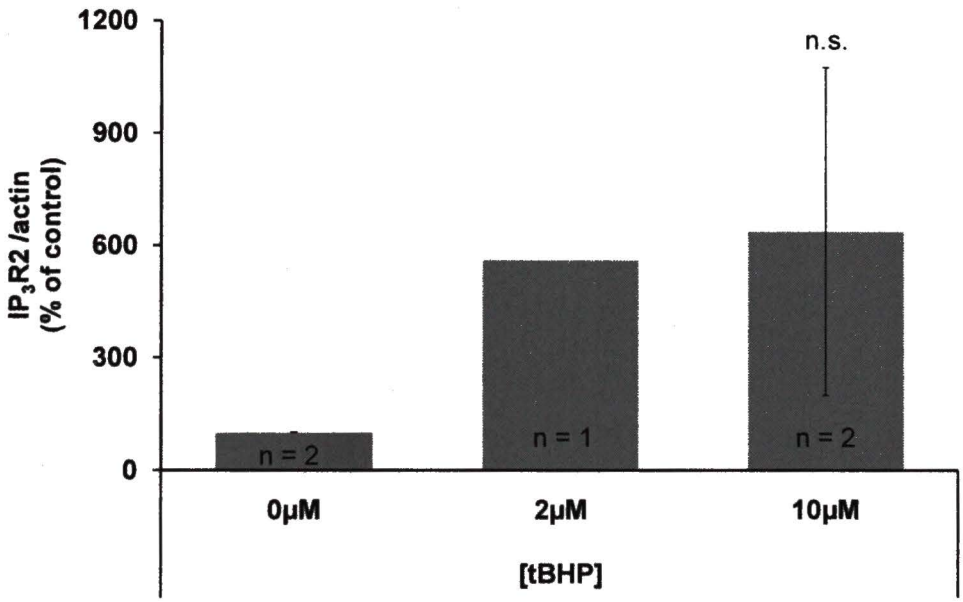
1200
900
600
300
0
IP3R2 /actin
(% of control)
n.s.
n = 2
n = 1
n = 2
0μM
2μM
10μM
[tBHP]

Fig. 13 - Exposure of HT22 Cells to Sublethal tBHP Concentrations Alters IP_3R3 Immunoreactivity. Overnight (16 – 20 hour) exposure of HT22 cells to sublethal concentrations of tBHP results in significant increases in IP_3R3 immunoreactivity as determined by microfluorimetric analysis of immunolabeled cells. The biphasic pattern of IP_3R3 immunoreactivity is similar to that observed for IP_3R1. For this study, *n* equals 93, 85, 121, 104 and 126 cells for the untreated, 2μM-, 4μM-, 6μM- and 10μM-treated groups, respectively. Comparisons between treatment groups and the control group were done using a two-sample T-test. A P-value of ≤ 0.05 and ≤ 0.01 is indicated by * and **, respectively.

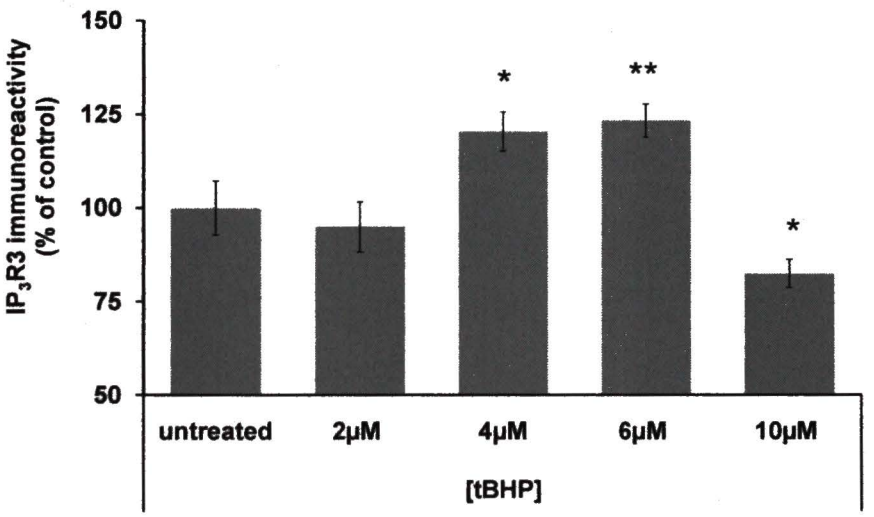
150
125
100
75
50
IP3R3 immunoreactivity
(% of control)
*
**
*
untreated
2μM
4μM
6μM
10μM
[tBHP]

Fig. 14 - Exposure of HT22 Cells to Sublethal tBHP Concentrations Alters RyR3 Immunoreactivity. (A), Exposure of HT22 cells to tBHP concentrations approaching lethality (10 – 15μM) result in a significant increase in RyR3 immunoreactivity within the ER/cytosolic region (arrows; scalebar is 25μm). (B), a graphical representation of the immunofluorescence data reveals that sublethal tBHP exposure leads to a significant increase in RyR3 immunroeactivity in HT22 cells. For this study, *n* equals 46, 69, 63, 68 and 55 cells for the untreated, 2μM-, 6μM-, 10μM- and 15μM-treated groups, respectively. Comparisons between treatment groups and the control group were done using a two-sample T-test. A P-value of ≤ 0.05 and ≤ 0.001 is indicated by * and ***, respectively.

A

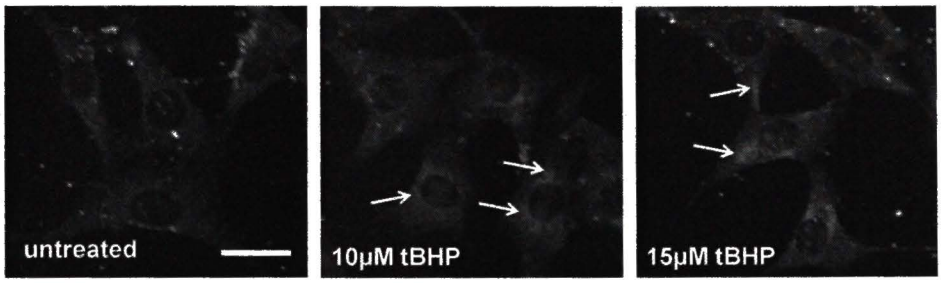
untreated
10μM tBHP
15μM tBHP

B

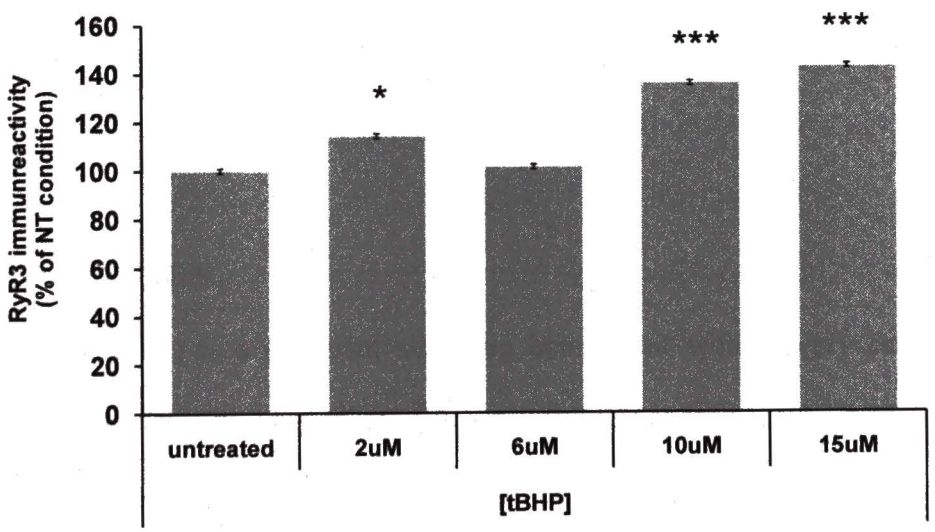
RyR3 immunreactivity
(% of NT condition)
160
140
120
100
80
60
40
20
0
*
***
***
untreated
2uM
6uM
10uM
15uM
[tBHP]

CHAPTER 5 – EFFECT OF NAE APPLICATION OF INTRACELLULAR Ca^{2+} CHANNEL ACTIVITY IN MODELS OF NEURODEGENERATION

ABSTRACT

Calcium is an important messenger involved in a variety of critical cellular functions (1). The maintenance of calcium homeostasis is vital for normal cell function and survival (2, 3). Neurodegenerative diseases such as Alzheimer's disease exhibit multiple pathological hallmarks including loss of calcium homeostasis (3). As a result, the control of calcium release from intracellular stores has recently gained attention as a potential therapeutic approach in combating neurodegenerative diseases (2 - 4). It has been shown that lipid neuroprotectants, the N-acylethanolamines (NAEs), in addition to activating cannabinoid receptors, may also alter intracellular calcium concentrations potentially leading to neuroprotection (5 – 7). I hypothesize that the NAE, palmitoylethanolamine (PEA) reduces intracellular Ca^{2+} release. My results reveal that PEA reduces intracellular Ca^{2+} release in response to chemical depolarization with KCl in the neuronal cell line HT22.

INTRODUCTION

Calcium (Ca^{2+}) is a universal signaling component within every cell in all organisms (1). Furthermore, intracellular Ca^{2+} (Ca^{2+}_i) is involved in every known physiological function within cells (1). As a result, the temporal and spatial regulation of Ca^{2+}_i concentration is critical for cellular function and cell survival (1 – 3). The major sources of Ca^{2+}_i are from the extracellular space and intracellular organelles such as the endoplasmic reticulum (ER) and mitochondria (1).

The major Ca^{2+} channels regulating release of Ca^{2+} from intracellular stores are the inositol 1, 4, 5-trisphosphate (IP_3) receptors (IP_3Rs) and ryanodine (Ry) receptors (RyRs) (8 - 11). IP_3Rs are activated by the ligand IP_3 and activation is further regulated by ATP, Ca^{2+} and multiple proteins that interact with the receptors (8, 9, 12 -18). The RyRs, on the other hand, are activated by the very same ion they conduct, Ca^{2+}, and their activation is regulated by ATP, Ca^{2+} and multiple interacting proteins (19 – 24).

The role that some Ca^{2+} channels play in neurodegenerative diseases is well understood. For example, the N-methyl-D-aspatate (NMDA) receptor (NMDAR), is the major Ca^{2+} channel causing excitotoxicity (25, 26). NMDA receptor antagonists exhibit neuroprotective effects in *in vitro* models of neurodegenerative diseases involving excitotoxicity (27).

The role that intracellular Ca^{2+} channels, IP3Rs and RyRs, play in neurodengenerative diseases is less clear. The generation of IP_3 and the expression of IP_3Rs are altered in Alzheimer's disease. Phosphatidylinositol and IP_3 generation is altered in brains of AD patients and also IP_3 binding sites are reduced in several brain regions from AD patients (28 – 33). Furthermore, there is some evidence that IP_3Rs can contribute to neuronal survival and neuronal death. Cortical neurons treated with Aβ leads to IP_3R-mediated Ca^{2+} release resulting in oxidative stress and cell death (34). Intracellular calcium release is altered in cultured cells expressing mutant presenilin (PS) proteins. For example, IP_3-mediated Ca^{2+} transients are significantly increased in mutant PS1 knock-in mice while cells from PS double knockout mice exhibit reduced luminal endoplasmic reticulum Ca^{2+} concentration in addition to increased expression of IP_3R1 (35, 36). In cell lines, PS1 and PS2 FAD mutants interact with IP3Rs and significantly increase their activity elicited IP_3 (37). Studies in neurons also show increased IP_3R-mediated Ca^{2+} release elicited by FAD PS-1 and PS-2 mutatns (37).

RyR expression and function is also altered in Alzheimer's disease. For example, there is a 40% decrease in cortical ryanodine binding and in tissue from Alzheimer's disease patients (38). There is a 20% decrease in RyR2 expression in these tissues. Furthermore, there are significant reductions in RyR binding in the hippocampus that correlate with AD symptoms and Aβ deposition (38). Exposure of cultured cortical neurons to Aβ peptide specifically increases expression of RyR3 (39). Treatment of cultured cortical neurons with Aβ treatment of cortical neurons results in RyR-mediated Ca^{2+} release and cell death (34). Mutant APP or PS-1-expressing mice and cell lines expressing mutatnt PS-1 exhibit elevated cellular RyR expression and caffeine-induced Ca^{2+} release (40). Furthermore, caffeine treatment of cells expressing mutant PS-1 results in increased vulnurability to Aβ exposure (40). Cultured neurons from mutant PS-1-expressing and triple transgenic (PS-1/PS-2/APP) mice resulted in elevated Ca^{2+} release in response to caffeine treatment due to an increase in RyR expression (41). In addition, neurons from an AD transgenic mice exhibit elevated ryanodine-mediated Ca^{2+} release specifically from the RyR3 subtype (39).

N-acylethanolamine (NAEs) have gained prominence as neuroprotectants in a wide variety of disease models including AD (42, 43). The most widely-studied NAE, arachidonylethanolamine (AEA), exhibits cytoprotective properties (44 - 46), however, it accounts for only a fraction of the NAEs generated in response to tissue injury. This suggests that other NAEs may play a prominent role in cytoprotection as well. AEA is an endogeonous ligand for the G-protein-coupled cannabinoid receptors (CB1/CB2) (47, 48).

Other predominant NAEs, including palmitoylethanolamine (PEA) do not bind cannabinoid receptors with appreciable affinity (49, 50). These non-cannabinoid NAEs have been implicated

in cytoprotection and as 'entourage' compounds (51). These entourage NAEs may enhance the activity of other ligands such as anandamide at specific protein targets (51).

Some saturated and monounsaturated non-cannabinoid NAEs have been shown to activate ERK1/2 phosphorylation pathway through a CB1-independent mechanism (52). The NAE oleoylethanolamine (OEA) reduces the formation of iron-induced malondialdehyde (MDA) in rat heart mitochondria, suggesting that it may act as an antioxidant reducing lipid peroxidation (53). Furthermore, some NAEs, including PEA, decrease the mitochondrial inner membrane permeability and may protect cells from ischemic insult (54). Interestingly, the yeast *Saccharomyces cerevisiae*, which does not express cannabinoid or vanilloid receptors, synthesizes various NAE species in response to oxidative stress (55). This result further substantiates a non-cannabinoid receptor- and a non-vailloid receptor-mediated function for some NAEs.

In rat cerebellar Purkinje neurons, AEA reduces presynaptic P-type Ca^{2+} currents by a mechanism independent of CB1 or VR1 (56). In addition to other unsaturated lipids, AEA inhibits T-type Ca^{2+} channel currents through a direct interaction depending upon both the hydroxyl group and acyl chain (57). Treatment of cultured endothelial cells with AEA elicits an increase in intracellular Ca^{2+} through a CB1-dependent mechanism (58).

Lipids can alter the activity of intracellular Ca^{2+} channels. For example, arachidonic acid inhibits IP_3R activity and leukotriene B4 activates RyRs (59). There is growing evidence that some of the N-acylethanolamine (NAE) lipids such as arachidonylethanolamine (AEA) and palmitoylethanolamine (PEA) can elicit the release of intracellular Ca^{2+}. In canine kidney cells, AEA leads to intracellular Ca^{2+} release and extracellular Ca^{2+} influx (60). In human osteosarcoma cells, the AEA transport inhibitor inhibitor and VR1 antagonist, AM404, causes

release of Ca^{2+} from intracellular stores and Ca^{2+} influx from the extracellular space (61). In cultured hippocampal neurons, the plant cannabinoid, cannabidiol (CBD), leads to Ca^{2+} release from intracellular stores and influx from the extracellular space (62). CB1 and VR1 antagonist treatment resulted in a reduction in these effects (62).

In addition, AEA also leads to Ca^{2+} release via a phospholipase C-linked CB2 receptor (63). In HEK293 cells overexpressing CB1 receptors, treatment with the CB1 agonsit, WIN55,212-2 led to an increase in intracellular Ca^{2+} (64). This response was blocked by inhibiting phospholipase, depleting intracellular stores with thapsigargin and inhibitionof IP3Rs and RyRs (64). Recently, another G-protein-coupled receptor (GPCR), GPR55, had been shown to be activated by cannabinoids including AEA (65). GPR55 couples to $G\alpha_q$ and $G\alpha_{12}$ and can lead to the release of Ca^{2+} through IP3Rs (65). In addition, GPR55 results in Rho-A-mediated Ca^{2+} transients and subsequent NFAT activation in response to lysophosphatidylinositol (LPI) treatment (66). Furthermore, the NAE oleoylethanolamide (OEA) is believed to be the endogenous ligand for GPR119, a GPCR previously classified as an orphan receptor (67).

AEA treatment of endothelial cells causes the release of Ca^{2+} from caffeine-sensitive stores, suggesting the involvement of RyRs (68). This effect was slightly, but not fully, reduced by the application of a CB1 antagonist (68). Treatment of cultured hippocampal neurons with CB1 agonists reduces NMDA-mediated Ca^{2+} released from RyRs by reducing PKA phosphorylation of RyR channels (69).

Both AEA and PEA exhibit neuroprotective properties in models of neurodegenerative diseases making the study of their cellular functions in neurons significant (44, 70). In previous studies, I determined that pretreatment of HT22 cells with PEA six (6) hours prior to tBHP exposure increased cell viability (see Chapter 3.2). In addition, PEA pretreatment of HT22 cells

and cultured cortical neurons for up to 6 hours led to an increase in ERK1/2 phosphorylation, Akt phosphorylation and nuclear translocation, and NFκB and NFATc4 nuclear translocation, all of which are consistent with activation of a neuroprotective response (Chapters 3.3 and 3.4). Activation of these signaling proteins, in addition to the time frame of these observed events, led me to hypothesize that PEA treatment may lead to an alteration in release of Ca^{2+} from intracellular stores. I determined that exposure of HT22 cells to PEA for six (6) hours or more led to a significant reduction in depolarization-induced Ca^{2+} release in the nuclear region. Unexpectedly, overnight exposure of HT22 cells to PEA led to a significant increase, not a decrease, in IP_3R2, RyR and RyR3 immunoreactivity. These result suggests that PEA may induce an activity-dependent change in IP_3R and RyR expression. Together, these data suggest that, after several hours, PEA can reduce the activity of Ca^{2+}-induced Ca^{2+} release channels in the nucleus despite increasing intracellular Ca^{2+} channel immunoreactivities.

MATERIALS AND METHODS

Cell Culture

HT22 cells were cultured as described elsewhere (71). Mouse primary cortical cultures were maintained in Neurobasal A medium (Invitrogen) containing 2mM Glutamax (Invitrogen), 2% horse serum, 2% B-27 supplement (Invitrogen) and penicillin-streptomycin-fungizone antibiotic (Mediatech). Mouse cortical tissue was obtained from postnatal day two (2) C57B/L6 mice. Mouse pups were anaesthetized on ice followed by decapitation. After removal of the scalp and skull cap, small pieces of cortical tissue approximately 1 - 1.5 mm^3 in size were removed from the frontal cortex of both hemispheres and placed in 0.25% trypsin. Tissue was incubated in trypsin at 37°C for 20 minutes. Two volumes of complete Neurobasal A medium was then added

to the tissue followed by gentle trituration using a fire-polished glass pipet. The tissue was then centrifuged at 500 x g for 5 minutes. The resulting pellet was resuspended in complete Neurobasal A medium, triturated again and centrifuged at 200 x g. The resulting cell pellet was resuspended, triturated and cells were passed through a 40μm cell strainer. The cell suspension was then quantitated with a hemocytometer. The cell concentration was adjusted to approximately 1 X 10^6 cells/ml. The cortical cells were plated on either poly-L-lysine- or poly-D-lysine/laminin-coated coverslips. A one-half volume media exchange was conducted on the third or fourth day after plating. Cultures used for optical imaging of intracellular Ca^{2+} were used between 7 and 17 days *in vitro* after microscopic inspection revealed adequate neurite outgrowth.

Immunocytochemistry and Immunofluorescence

HT22 cells were plated on 12mm poly-L-lysine-coated coverslips and grown overnight (16 – 20 hours). Cultured primary cortical neurons were maintained on 12mm coverslips in complete Neurobasal medium for 7 – 14 days until treatments and immunocytochemistry. Cells were exposed to NAE (100μM LEA or PEA) or EtOH vehicle for overnight. After overnight NAE exposure, cells were fixed with 4% paraformaldehyde and immunocytochemistry was conducted as described elsewhere using antisera recognizing IP3R1 (Calbiochem), IP3R2 (Calbiochem), RyR2 (Chemicon) and RyR3 (Chemicon) (71). After mounting, slides were viewed within a week using an Olympus-IX70 fluorescence microscope. Fluorescence intensity was measured using Simple PCI v 6.0 by highlighting three (3) background regions of interest (ROIs) followed by a nuclear then cytosolic ROI for each cell. Nuclear and cytosolic greylevel values were separated and graphed in Microsoft Excel.

N-Acylethanolamine treatments and optical imaging of intracellular Ca^{2+}

HT22 cells were plated onto poly-L-lysine-coated 25mm glass coverslips and grown overnight in DMEM containing 5% bovine growth serum and penicillin/streptomycin. Cultured primary cortical neurons were maintained on poly-D-lysine/laminin-coated 12mm coverslips in complete Neurobasal medium for 7 – 14 days until treatments and subsequent optical imaging. N-acylethanolamines (NAEs) were dissolved in 100% EtOH and stock solutions were stored at 4°C until use. HT22 cells were treated with NAEs within a concentration range of 1 - 100μM diluted in complete medium for varying amounts of time. After the desired treatment time, cells were incubated in fresh complete DMEM medium containing 4μM of the cell-permeant fluorescent dye Fluo-3-AM (Invitrogen) at 37°C for 30 minutes. The coverslips with dye-loaded cells were rinsed with HBSS buffer, placed in a perfusion chamber containing either HBSS without Ca^{2+} and Mg^{2+} (Invitrogen) or extracellular solution (137mM NaCl, 5mM KCl, 1mM Na_2HPO_4, 10mM HEPES, 22mM Glucose, and 5mM EGTA, pH 7.4) and placed on an inverted microscope (Olympus IX70, Japan) at ambient temperature. Alternatively, HBSS or ECS solution containing 2mM $CaCl_2$ was used in experiments requiring extracellular Ca^{2+}. Optical imaging of intracellular Ca2+ was done using an Olympus-IX70 inverted objective fluorescence microscope with Simple PCI software (C-Imaging). Time lapse videomicroscopy was conducted as described elsewhere (71). In brief, fluorescence intensity was measured using Simple PCI software during and after the application of the stimulus (F) and was divided by the measured average baseline fluorescence intensity before application of the stimulus (F_0) in Microsoft Excel. Cells were stimulated with bath-applied 1 - 10μM cell-permeant IP_3-AM (A.G. Scientific, Inc., San Diego, CA), 10mM caffeine or 100mM KCl. After F/F_0 was calculated in Microscoft Excel, data was exported to GraphPad Prism software (version 5.0, LaJolla, CA) and row

averages (an average F/F_0 value at each time point) was calculated for the cell population in each recording. The average of the row averages was graphed for each treatment to visualize and compare the responses between treatment conditions.

Statistics

An F-test was conducted in Excel between each treatment group and the untreated control group to determine which type of T-test should be used for group comparisons. The mean fluorescence intensity from each treatment group was separately compared to the mean fluorescence intensity of the untreated control group using a two-sample T-test with either equal or unequal variances. A P-value of less than or equal to 0.05 was considered significant.

RESULTS

Effect of NAE exposure on IP3R and RyR immunoreactivity in HT22 cells

Overnight exposure of HT22 cells to PEA had no consistent and no overall significant effect on IP_3R1 immunoreactivity (Fig. 1). Furthermore, we can find no evidence that overnight PEA alters IP_3R3 immunoreactivity in HT22 cells (data not shown). In HT22 cells, IP_3R2 immunoreactivity is predominant in the nuclear region and exists at lower levels in the ER/cytosolic region of the cell. Overnight exposure to PEA resulted in a significant increase in both nuclear and cytosolic IP_3R2 immunoreactivity (Fig. 2). In some cases, overnight PEA exposure significantly increases the nuclear over cytosolic (nuc/cyt) IP_3R2 immunoreactivity ratio (Fig. 2). No apparent change in cell area or measured change in nuclear area was observed after PEA treatment (data not shown). These results suggest that PEA may alter nuclear IP_3R2 Ca^{2+} responses relative to ER/cytosolic IP_3R2 Ca^{2+} responses in HT22 cells. Overnight exposure

of HT22 cells to LEA, however, had no effect on IP_3R2 immunoreactivity. Overnight exposure of HT22 cells to 100μM PEA led to a significant increase in both RyR2 and RyR3 immunoreactivity (Fig. 3 and Fig. 4, respectively). These data suggest a possible transcriptional or protein trafficking effect of PEA on intracellular Ca^{2+} channel expression.

Effect of short-term NAE exposure on intracellular Ca^{2+} channel activity

Acute treatment of HT22 cells with PEA had no effect on fluo-3 fluorescence (Fig. 5), suggesting that PEA does not activate Ca^{2+} channels. A short-term pretreatment (1 – 2 hours) of HT22 cells with PEA had no consistent significant effect on IP_3-AM- caffeine- and KCl-stimulated Ca^{2+} responses. Specifically, stimulation of HT22 cells with bath-applied IP_3-AM in the absence of extracellular Ca^{2+} leads to a low percentage of responding cells. As a result, analysis of peak amplitude, slope and $Tmax_{1/2}$ were not practicable. Interestingly, in the presence of extracellular Ca^{2+} (Ca^{2+}_o), IP_3-AM-mediated Ca^{2+} responses were much higher in amplitude and were much more variable with respect to the number of responding cells, the onset time of the response, the slope of the response, time to half maximal response ($T_{max1/2}$) when compared to responses in Ca^{2+}-free media.

Exposure of HT22 cells to PEA 1–2 hour prior to stimulation with caffeine results in Ca^{2+} responses that vary greatly in response time after stimulation making comparison of average peak amplitudes over the entire recording unfeasible (Fig. 6). As a result, only the peak amplitude of the responsive portion of the recordings was analyzed and compared (Fig 6). This analysis revealed that there were no significant differences between vehicle- and PEA-treated cells (Fig. 6).

PEA pretreatment decreases depolarization-induced Ca^{2+} release in HT22 cells

Treatment of HT22 cells with PEA for 6 hours prior to KCl stimulation resulted in a significant decrease in peak fluo-3-AM fluorescence in the nuclear region of HT22 cells (Fig. 7). This suggests that at this time point, PEA exerts an inhibitory effect on depolarization-induced nuclear calcium release. A prolonged (14 hour) PEA pretreatment had no significant effect on IP_3-AM-mediated Ca^{2+} responses in HT22 cells possibly due to high variability between recordings (Fig. 8), but prolonged PEA pretreatment reduced caffeine-mediated responses (Fig. 9). Likewise, a prolonged PEA pretreatment led to a dramatic and significant reduction in depolarization-induced Ca^{2+} release, especially in the nuclear region of HT22 cells (Fig. 8). LEA pretreatment resulted in less pronounced decreases in depolarization-induced Ca^{2+} responses compared to that for PEA-pretreated cells. Since chemically-induced depolarization with KCl activates voltage-gated cation channels, thus leading to elevated cytoplasmic Ca^{2+} concentrations, the prominent nuclear responses observed here are likely due to Ca^{2+}-induced Ca^{2+} release channels such as RyRs. Thus, we suggest that PEA reduces RyR activity.

DISCUSSION

Here I have determined that an overnight exposure of HT22 cells to PEA increases IP_3R2, RyR and RyR3 immunoreactivity. In addition, I determined that PEA treatment of HT22 cells for 6 – 14 hours reduces depolarization-induced Ca^{2+} release in the nuclear region of HT22 cells. As a result, I conclude that PEA may reduce Ca^{2+} toxicity associated with neurodegenerative diseases. The upregulation of IP_3R2, RyR2 and RyR3 expression in response to PEA may be due to a compensatory response to this inhibition.

Short-term exposure (1 – 2 hour) of HT22 cells to PEA had questionable effects on IP_3-AM- and caffeine-mediated Ca^{2+} responses. For example, IP3AM- and caffeine-mediated responses

were highly variable and heterologous amking a straightforward analysis of peak amplitude and slopes difficult. In an attempt to detect differences in amplitude, slope, $Tmax_{1/2}$ and area under the curve (AUC) as a direct measure of total Ca^{2+} release between the highly variable responses obtained in the presence of $Ca^{2+}{}_0$, responses exhibiting similar morphological characteristics were compared. For example, responses from a treatment condition exhibiting a 'sawtooth'-shaped profile on line graphs were compared between treatment groups. Overall, analysis of Ca^{2+} transients categorized according to response type reveals no significant differences between PEA-treated cells and vehicle controls (data not shown).

HT22 cells pretreated with PEA for 2 hours followed by stimulated with caffeine resulted in no definitive change in fluo-3 fluorescence. This result was determined by analyzing the peak amplitude of only the responsive portion of the recordings. Alternatively, responses with similar amplitudes were selected for the comparison of the slope or AUC of the responses. In addition, responses exhibiting similar AUC were selected for the comparison of the amplitude or slope of the responses. The comparison of vehicle- and PEA-pretreated cells exhibiting similar AUC values reveals that PEA-pretreated cells exhibit a non-significant trend toward an increase in peak amplitude of IP3-AM responses. Comparison of vehicle- and PEA-pretreated cells exhibiting similar peak amplitude values, however, reveals that PEA-pretreated cells exhibit a slight but significant decrease in the AUC.

Similar analysis was conducted on caffeine-stimulated cells. The comparison of vehicle- and PEA-pretreated cells exhibiting similar small AUC values (AUC < 50), but not large AUC (AUC > 50) values, reveals that PEA-pretreated cells exhibit a significant decrease in peak amplitude of caffeine responses. Furthermore, comparison of vehicle- and PEA-pretreated cells exhibiting similar peak amplitude values reveals that PEA-pretreated cells exhibit a slight but significant

increase in the AUC for small amplitude responses (F/F_0 of 0.5 to 1.5) and a significant decrease in the AUC for large amplitude responses (F/F_0 of > 2.50).

The mechanism by which AEA and PEA elicit neuroprotection has focused almost entirely on their activation of CB_1 and CB_2 receptors, respectively. The consensus is that AEA is an endogenous ligand for CB_1 receptors, although other endogenous high affinity ligands also exist. PEA, however, is not likely to be the endogenous agonist for CB_2 since its affinity for the receptor is quite low compared to other endogenous ligands (49). Recently, an orphan G-protein coupled receptor (GPCRs), GRP55, has been shown to exhibit a high affinity for PEA compared to CB_2 (72). Similarly, the orphan GPCR, GRP119, has been shown to bind oleoylethanolamine (OEA) and, to a lesser extent, PEA with high affinity (67). Since GPR119 activation results in an increase in cellular cAMP, many of its effects are likely mediated by protein kinase A (PKA).

These recent data suggest that some orphan GPCRs may be the target for NAEs of unknown function. Since PEA treatment of HT22 cells did not itself elicit a Ca^{2+} response, we have provided evidence against any G_q-coupled GPCR that can be activated by PEA in HT2cells.

The increase in the number of responding cells, amplitude of responses and slope of responses in the presence of ($Ca^{2+}{}_o$) compare to that of responses in Ca^{2+}-free media may be due to the contribution of store-operated Ca^{2+} channels (SOCs). Store filling is highly affected by the presence or absence of ($Ca^{2+}{}_o$) (73). In the absence of ($Ca^{2+}{}_o$), SOCs can maintain and possibly increase the Ca^{2+} storing capacity of the ER. It is interesting to note that in the absence of $Ca^{2+}{}_o$, baseline fluo-3 AM fluorescence levels are greatly reduced compare to the baseline fluorescence levels in the presence of $Ca^{2+}{}_o$. This suggests that the reduced or weak responses observed in the absence of $Ca^{2+}{}_o$ may in part be due to a reduction in ER store filling or maintenance of normal ER store capacity.

Data from the present work suggest that, after several hours of expsore to cells, the non-cannabinoid NAE, PEA, can reduce nuclear depolarization-induced Ca^{2+} release. Since chemically-induced depolarization with KCl activates voltage-gated cation channels and thus leads to elevated cytoplasmic Ca^{2+} concentrations, the prominent nuclear responses are likely due to Ca^{2+}-induced Ca^{2+} release channels such as RyRs. Thus, I suggest that PEA reduces RyR activity.

REFERENCES

1. Berridge, M.J. 1997. Elementary and global aspects of calcium signaling. *J. Exp. Biol.* 200:315-319.
2. LaFerla FM (2002) Calcium dyshomeostasis and intracellular signalling in Alzheimer's disease. Nat Rev Neurosci. 3(11):862-72. Verkhratsky, A., and E.C. Toescu. 2003. Endoplasmic reticulum $Ca^{(2+)}$ homeostasis and neuronal death. *J. Cell. Mol. Med.* 7:351-361.
3. Paschen, W. 2003. Mechanisms of neuronal cell death: diverse roles of calcium in the various subcellular compartments. *Cell Calcium.* 34:305-310.
4. Brookes PS, Yoon Y, Robotham JL, Anders MW and Sheu SS (2004) Calcium, ATP, and ROS: a mitochondrial love-hate triangle. Am J Physiol Cell Physiol. 287(4):C817-33.
5. Mombouli JV, Schaeffer G, Holzmann S, Kostner GM and Graier WF (1999) Anandamide-induced mobilization of cytosolic Ca2+ in endothelial cells. Br J Pharmacol. 126(7):1593-600.

15. Bezprozvanny I., and B.E. Ehrlich. 1993. ATP modulates the function of inositol 1,4,5-trisphosphate-gated channels at two sites. *Neuron.* 10:1175-1184.

16. Cardy T.J., D. Traynor, and C.W. Taylor. 1997. Differential regulation of types-1 and -3 inositol trisphosphate receptors by cytosolic Ca^{2+}, *Biochem. J.* 328:785-793.

17. Hagar R.E., A.D. Burgstahler, M.H. Nathanson, and B.E. Ehrlich. 1998. Type III $InsP_3$ receptor channel stays open in the presence of increased calcium. *Nature.* 396:81-84.

18. Tang T.S., H. Tu, Z. Wang, and I. Bezprozvanny. 2003. Modulation of type 1 inositol (1,4,5)-trisphosphate receptor function by protein kinase a and protein phosphatase 1alpha. *J. Neurosci.* 23:403-415.

19. Iino M (1989) Calcium-induced calcium release mechanism in guinea pig taenia caeci. J Gen Physiol. 94(2):363-83.

20. Hidalgo C and Donoso P (1995) Luminal calcium regulation of calcium release from sarcoplasmic reticulum. Biosci Rep. 15(5):387-97.

21. Carroll S, Skarmeta JG, Yu X, Collins KD and Inesi G (1991) Interdependence of ryanodine binding, oligomeric receptor interactions, and Ca2+ release regulation in junctional sarcoplasmic reticulum. Arch Biochem Biophys. 290(1):239-47.

22. Hwang SY, Wei J, Westhoff JH, Duncan RS, Ozawa F, Volpe P, Inokuchi K and Koulen P (2003) Differential functional interaction of two Vesl/Homer protein isoforms with ryanodine receptor type 1: a novel mechanism for control of intracellular calcium signaling. Cell Calcium.34(2):177-84.

23. Westhoff JH, Hwang SY, Duncan RS, Ozawa F, Volpe P, Inokuchi K and Koulen P (2003) Vesl/Homer proteins regulate ryanodine receptor type 2 function and intracellular calcium signaling. Cell Calcium. 34(3):261-9.

6. Oz M, Alptekin A, Tchugunova Y and Dinc M (2005) Effects of saturated long-chain N-acylethanolamines on voltage-dependent Ca2+ fluxes in rabbit T-tubule membranes. Arch Biochem Biophys. 434(2):344-51.

7. Yeh JH, Cheng HH, Huang CJ, Chung HM, Chiu HF, et al. (2006) Effect of anandamide on cytosolic Ca(2+) levels and proliferation in canine renal tubular cells. Basic Clin Pharmacol Toxicol. 98(4):416-22.

8. Berridge M.J., and R.F. Irvine. 1984. Inositol trisphosphate, a novel second messenger in cellular signal transduction. *Nature.* 312:315-321.

9. Ehrlich B.E., and J. Watras. 1988. Inositol 1,4,5-trisphosphate activates a channel from smooth muscle sarcoplasmic reticulum. *Nature.* 336:583-586.

10. Mignery G.A., T.C. Sudhof, K. Takei, P. and De Camilli. 1989. Putative receptor for inositol 1,4,5-trisphosphate similar to ryanodine receptor. *Nature.* 342:192-195.

11. Fill, M., and R. Coronado. 1988. Ryanodine receptor channel of sarcoplasmic reticulum. *Trends Neurosci.* 11:453-457.

12. Maeda N., T. Kawasaki, S. Nakade, N. Yokota, T. Taguchi, M. Kasai, and K. Mikoshiba. 1991. Structural and functional characterization of inositol 1,4,5-trisphosphate receptor channel from mouse cerebellum. *J. Biol. Chem.* 266:1109-1116.

13. Volpe P., and B.H. Alderson-Lang. 1990. Regulation of inositol 1,4,5-trisphosphate-induced Ca^{2+} release. II. Effect of cAMP-dependent protein kinase. *Am. J. Physiol.* 258:C1086-1091.

14. Bezprozvanny I., J. Watras, and B.E. Ehrlich. 1991. Bell-shaped calcium-response curves of Ins(1,4,5)P_3- and calcium-gated channels from endoplasmic reticulum of cerebellum. *Nature.* 351:751-754.

15. Bezprozvanny I., and B.E. Ehrlich. 1993. ATP modulates the function of inositol 1,4,5-trisphosphate-gated channels at two sites. *Neuron.* 10:1175-1184.

16. Cardy T.J., D. Traynor, and C.W. Taylor. 1997. Differential regulation of types-1 and -3 inositol trisphosphate receptors by cytosolic Ca^{2+}, *Biochem. J.* 328:785-793.

17. Hagar R.E., A.D. Burgstahler, M.H. Nathanson, and B.E. Ehrlich. 1998. Type III $InsP_3$ receptor channel stays open in the presence of increased calcium. *Nature.* 396:81-84.

18. Tang T.S., H. Tu, Z. Wang, and I. Bezprozvanny. 2003. Modulation of type 1 inositol (1,4,5)-trisphosphate receptor function by protein kinase a and protein phosphatase 1alpha. *J. Neurosci.* 23:403-415.

19. Iino M (1989) Calcium-induced calcium release mechanism in guinea pig taenia caeci. J Gen Physiol. 94(2):363-83.

20. Hidalgo C and Donoso P (1995) Luminal calcium regulation of calcium release from sarcoplasmic reticulum. Biosci Rep. 15(5):387-97.

21. Carroll S, Skarmeta JG, Yu X, Collins KD and Inesi G (1991) Interdependence of ryanodine binding, oligomeric receptor interactions, and Ca2+ release regulation in junctional sarcoplasmic reticulum. Arch Biochem Biophys. 290(1):239-47.

22. Hwang SY, Wei J, Westhoff JH, Duncan RS, Ozawa F, Volpe P, Inokuchi K and Koulen P (2003) Differential functional interaction of two Vesl/Homer protein isoforms with ryanodine receptor type 1: a novel mechanism for control of intracellular calcium signaling. Cell Calcium.34(2):177-84.

23. Westhoff JH, Hwang SY, Duncan RS, Ozawa F, Volpe P, Inokuchi K and Koulen P (2003) Vesl/Homer proteins regulate ryanodine receptor type 2 function and intracellular calcium signaling. Cell Calcium. 34(3):261-9.

24. Zalk R, Lehnart SE and Marks AR (2007) Modulation of the ryanodine receptor and intracellular calcium. Annu Rev Biochem. 76:367-85.

25. Frandsen A, Drejer J and Schousboe A (1989) Direct evidence that excitotoxicity in cultured neurons is mediated via N-methyl-D-aspartate (NMDA) as well as non-NMDA receptors. J Neurochem. 53(1):297-9

26. Peterson C, Neal JH and Cotman CW (1989) Development of N-methyl-D-aspartate excitotoxicity in cultured hippocampal neurons. Brain Res Dev Brain Res. 48(2):187-95

27. Weller M, Finiels-Marlier F and Paul SM (1993) NMDA receptor-mediated glutamate toxicity of cultured cerebellar, cortical and mesencephalic neurons: neuroprotective properties of amantadine and memantine. Brain Res. 613(1):143-8.

28. Stokes, C. E. & Hawthorne, J. N. Reduced phosphoinositide concentrations in anterior temporal cortex of Alzheimer-diseased brains. J Neurochem. 48(4):1018-21 (1987).

29. Ferrari-DiLeo, G. & Flynn, D. D. Diminished muscarinic receptor-stimulated [3H]-PIP2 hydrolysis in Alzheimer's disease. Life Sci. 53(25):PL439-44 (1993).

30. Crews, F. T., Kurian, P., & Freund, G. Cholinergic and serotonergic stimulation of phosphoinositide hydrolysis is decreased in Alzheimer's disease. Life Sci. 55(25-26):1993-2002 (1994).

31. Young, L. T., Kish, S. J., Li, P. P. & Warsh, J. J. Decreased brain [3H]inositol 1,4,5-trisphosphate binding in Alzheimer's disease. Neurosci Lett. 94(1-2):198-202 (1988).

32. Garlind, A., Cowburn, R. F., Forsell, C., Ravid, R., Winblad, B. & Fowler, C. J. Diminished [3H]inositol(1,4,5)P3 but not [3H]inositol(1,3,4,5)P4 binding in Alzheimer's disease brain. Brain Res. 681(1-2):160-6 (1995).

33. Kurumatani, T., Fastbom, J., Bonkale, W. L., Bogdanovic, N., Winblad, B., Ohm, T. G. & Cowburn, R. F. Loss of inositol 1,4,5-trisphosphate receptor sites and decreased PKC levels correlate with staging of Alzheimer's disease neurofibrillary pathology. Brain Res. 796(1-2):209-21 (1998).

34. Ferreiro, E., Resende, R., Costa, R., Oliveira, C. R. & Pereira, C. M. An endoplasmic-reticulum-specific apoptotic pathway is involved in prion and amyloid-beta peptides neurotoxicity. Neurobiol Dis. 23(3):669-78 (2006).

35. Stutzmann, G. E., Caccamo, A., LaFerla, F. M. & Parker, I. Dysregulated IP3 signaling in cortical neurons of knock-in mice expressing an Alzheimer's-linked mutation in presenilin1 results in exaggerated Ca2+ signals and altered membrane excitability. J Neurosci. 24(2):508-13 (2004).

36. Kasri, N. N., Kocks, S. L., Verbert, L., Hebert, S. S., Callewaert, G., Parys, J. B., Missiaen, L. & De Smedt, H. Up-regulation of inositol 1,4,5-trisphosphate receptor type 1 is responsible for a decreased endoplasmic-reticulum Ca2+ content in presenilin double knock-out cells. Cell Calcium 40(1):41-51 (2006).

37. Cheung KH, Shineman D, Muller M, Cardenas C, Mei L, Yang J, Tomita T, Iwatsubo T, Lee VM and Foskett JK (2008) Mechanism of Ca2+ disruption in Alzheimer's disease by presenilin regulation of InsP3 receptor channel gating. Neuron. 58(6):871-83.

38. Kelliher, M., Fastbom, J., Cowburn, R. F., Bonkale, W., Ohm, T. G., Ravid, R., Sorrentino, V. & O'Neill, C. Alterations in the ryanodine receptor calcium release channel correlate with Alzheimer's disease neurofibrillary and beta-amyloid pathologies. Neuroscience. 92(2):499-513 (1999).

39. Supnet, C., Grant, J., Kong, H., Westway, D. & Mayne, M. Abeta 1-42 increases ryanodine receptor-3 expression and function in TgCRND8 mice. J Biol Chem. Oct 18th, Epub ahead of print (2006).

40. Chan, S. L., Mayne, M., Holden, C. P., Geiger, J. D. & Mattson, M. P. Presenilin-1 mutations increase levels of ryanodine receptors and calcium release in PC12 cells and cortical neurons. J Biol Chem. 275(24):18195-200 (2000).

41. Smith, I. F., Hitt, B., Green, K. N, Oddo, S. & LaFerla, F. M. Enhanced caffeine-induced Ca2+ release in the 3xTg-AD mouse model of Alzheimer's disease. J Neurochem. 94(6):1711-8 (2005).

42. Benito C, Nunez E, Tolon RM, Carrier EJ, Rabano A, Hillard CJ and Romero J (2003) Cannabinoid CB2 receptors and fatty acid amide hydrolase are selectively overexpressed in neuritic plaque-associated glia in Alzheimer's disease brains. J Neurosci. 23(35):11136-41.

43. Ramirez BG, Blazquez C, Gomez del Pulgar T, Guzman M and de Ceballos ML (2005) Prevention of Alzheimer's disease pathology by cannabinoids: neuroprotection mediated by blockade of microglial activation.J Neurosci. 25(8):1904-13.

44. Marsicano G, Goodenough S, Monory K, Hermann H, Eder M, Cannich A, Azad SC, Cascio MG, Gutierrez SO, van der Stelt M, Lopez-Rodriguez ML, Casanova E, Schutz G, Zieglgansberger W, Di Marzo V, Behl C and Lutz B (2003) CB1 cannabinoid receptors and on-demand defense against excitotoxicity. Science. 302(5642):84-8.

45. Kim SH, Won SJ, Mao XO, Jin K and Greenberg DA (2005) Involvement of protein kinase A in cannabinoid receptor-mediated protection from oxidative neuronal injury. J Pharmacol Exp Ther. 2005 Apr;313(1):88-94.

46. Shouman B, Fontaine RH, Baud O, Schwendimann L, Keller M, Spedding M, Lelievre V and Gressens P (2006) Endocannabinoids potently protect the newborn brain against AMPA-kainate receptor-mediated excitotoxic damage. Br J Pharmacol. 148(4):442-51.

47. Devane WA, Hanus L, Breuer A, Pertwee RG, Stevenson LA, Griffin G, Gibson D, Mandelbaum A, Etinger A and Mechoulam R (1992) Isolation and structure of a brain constituent that binds to the cannabinoid receptor. Science. 258(5090):1946-1949.

48. Vogel Z, Barg J, Levy R, Saya D, Heldman E and Mechoulam R (1993) Anandamide, a brain endogenous compound, interacts specifically with cannabinoid receptors and inhibits adenylate cyclase. J Neurochem. 61(1):352-355.

49. Lambert DM and Di Marzo V (1999) The palmitoylethanolamide and oleamide enigmas : are these two fatty acid amides cannabimimetic? Curr. Med. Chem. 6 (8):757-773.

50. Sugiura T, Kondo S, Kishimoto S, Miyashita T, Nakane S, Kodaka T, Suhara Y, Takayama H and Waku L (2000) Evidence that 2-arachidonoylglycerol but not N-palmitoylethanolamine or anandamide is the physiological ligand for the cannabinoid CB2 receptor. Comparison of the agonistic activities of various cannabinoid receptor ligands in HL-60 cells. J Biol Chem. 275(1):605-12.

51. Smart D, Jonsson KO, Vandervoorde S, Lambert DM and Fowler CJ (2002) 'Entourage' effects of N-acyl ethanolamines at human vanilloid receptors. Comparison of effects upon anandamide-induced vanilloid receptor activation and upon anandamide metabolism. Br J Pharmoacol. 136(3):452-8

52. Berdyshev EV, Schmid PC, Krebsbach RJ, Hillard CJ, Hunag C, Chen N, Dong Z and Schmid HH (2001) Cannabinoid-receptor-independent cell signalling by N-acylethanolamines.Biochem J. 360(Pt 1):67-75.

53. Parinandi NL and Schmid HH (1988) Effects of long-chain N-acylethanolamines on lipid peroxidation in cardiac mitochondria. FEBS Lett. 237(1-2):49-52.

54. Epps DE, Palmer JW, Schmid HH and Pfeiffer DR (1982) Inhibition of permeability-dependent Ca2+ release from mitochondria by N-acylethanolamines, a class of lipids synthesized in ischemic heart tissue.J Biol Chem. 257(3):1383-1391.

55. Merkel O, Schmid PC, Paltauf F and Schmid HH (2005) Presence and potential signaling function of N-acylethanolamines and their phospholipid precursors in the yeast Saccharomyces cerevisiae. Biochim Biophys Acta. 1734(3):215-9.

56. Fisyunov A, Tsintsadze V, Min R, Burnashev N and Lozovaya N (2006) Cannabinoids modulate the P-type high-voltage-activated calcium currents in purkinje neurons. J Neurophysiol. 96(3):1267-77. Epub 2006 May 31.

57. Chemin J, Monteil A, Perez-Reyes E, Nargeot J and Lory P (2001) Direct inhibition of T-type calcium channels by the endogenous cannabinoid anandamide. EMBO J. 20(24):7033-40.

58. Fimiani C, Mattocks D, Cavani F, Salzet M, Deutsch D, Pryor S, Bilfinger TV and Stefano GB (1999) Morphine and anandamide stimulate intracellular calcium transients in human arterial endothelial cells: coupling to nitric oxide release. Cell Signal. 1999 Mar;11(3):189-93.

59. Striggow F and Ehrlich BE (1997) Regulation of intracellular calcium release channel function by arachidonic acid and leukotriene B4.Biochem Biophys Res Commun. 237(2):413-8.

60. Yeh JH, Cheng HH, Hunag CJ, Chung HM, Ghiu HF, Yang YL, Yeh MY, Chen WC, Kao CH, Chou CT and Jan CR (2006) Effect of anandamide on cytosolic Ca(2+) levels and proliferation in canine renal tubular cells. Basic Clin Pharmacol Toxicol. 98(4):416-22.

61. Chang HT, Huang CC, Cheng HHm Wang JL, Lin KL, Hsu PT, Tsai JY, Liao WC, Lu YC, Huang JK and Jan CR (2008) Mechanisms of AM404-induced [Ca(2+)](i) rise and death in human osteosarcoma cells. Toxicol Lett. 179(1):53-8.

62. Drysdale AJ, Ryan D, Pertwee RG and Platt B (2006) Cannabidiol-induced intracellular Ca2+ elevations in hippocampal cells. Neuropharmacology. 50(5):621-31.

63. Zoratti C, Kipmen-Korgun D, Osibow K, Malli R and Graier WF (2003) Anandamide initiates Ca(2+) signaling via CB2 receptor linked to phospholipase C in calf pulmonary endothelial cells. Br J Pharmacol. 140(8):1351-62.

64. Lauckner JE, Hille B and Mackie K (2005) The cannabinoid agonist WIN55,212-2 increases intracellular calcium via CB1 receptor coupling to Gq/11 G proteins. Proc Natl Acad Sci U S A. 102(52):19144-9.

65. Lauckner JE, Jensen JB, Chen HY, Lu HC, Hille B and Mackie K (2008) GPR55 is a cannabinoid receptor that increases intracellular calcium and inhibits M current. Proc Natl Acad Sci U S A. 105(7):2699-704.

66. Henstridge CM, Balenga NA, Ford LA, Ross RA, Waldhoer M and Irving AJ (2008) The GPR55 ligand L-{alpha}-lysophosphatidylinositol promotes RhoA-dependent Ca2+ signaling and NFAT activation. FASEB J. 2008 Aug 29.

67. Overton HA, Babbs AJ, Doel SM, Fyfe MC, Gardner LS, Griffin G, Jackson HC, Procter MJ, Rasamison CM, Tang-Christensen M, Widdowson PS, Williams GM and Reynet C

(2006) Deorphanization of a G protein-coupled receptor for oleoylethanolamide and its use in the discovery of small-molecule hypophagic agents. Cell Metab. 3(3):167-75.

68. Mombouli JV, Schaeffer G, Holzmann S, Kostner GM and Graier WF (1999) Anandamide-induced mobilization of cytosolic Ca2+ in endothelial cells. Br J Pharmacol. 126(7):1593-600.

69. Zhuang SY, Bridges D, Grigorenko E, McCloud S, Boon A, Hampson RE and Deadwyler SA (2005) Cannabinoids produce neuroprotection by reducing intracellular calcium release from ryanodine-sensitive stores. Neuropharmacology. 48(8):1086-96.

70. Skaper SD, Buriani A, Dal Toso R, Petrelli L, Romanello S, Facci L and Leon A (1996) The ALIAmide palmitoylethanolamide and cannabinoids, but not anandamide, are protective in a delayed postglutamate paradigm of excitotoxic death in cerebellar granule neurons. Proc Natl Acad Sci U S A. 93(9):3984-9.

71. Duncan RS, Hwang SY and Koulen P (2007) Differential inositol 1,4,5-trisphosphate receptor signaling in a neuronal cell line. Int J Biochem Cell Biol. 39(10):1852-62.

72. Ryberg E, Larsson N, Sjogren S, Hjorth S, Hermansson NO, Leonova J, Elebring T, Nilsson K, Drmota T and Greasley PJ (2007) The orphan receptor GPR55 is a novel cannabinoid receptor. Br J Pharmacol. 152(7):1092-101.

73. Parekh AB and Putney JW Jr. (2005) Store-operated calcium channels. Physiol Rev. 85(2):757-810.

Fig. 1 – Overnight treatment of HT22 cells with PEA has no effect on IP_3R1 immunoreactivity. For this study, *n* equals 55 and 60 cells for the EtOH vehicle and PEA treatment conditions, respectively.

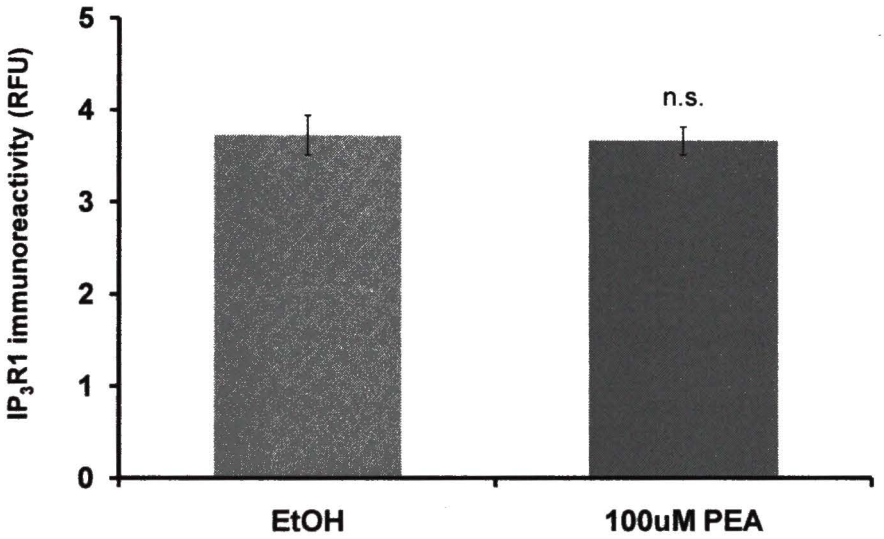
5
4
3
2
1
0
IP3R1 immunoreactivity (RFU)
n.s.
EtOH
100uM PEA

Fig. 2 – Overnight treatment of HT22 cells with PEA increases IP_3R2 immunoreactivity. Both nuclear and cytosolic IP3R2 immunoreactivity in increased in HT22 cells (top graph) and, in addition, the nuclear / cytoslic IP_3R2 ratio is increased (bottom graph). For this study, *n* equals 132 and 149 cells for the EtOH vehicle and PEA treatment conditions, respectively. A P-value of ≤ 0.05 and ≤ 0.001 is indicated by * and ***, respectively.

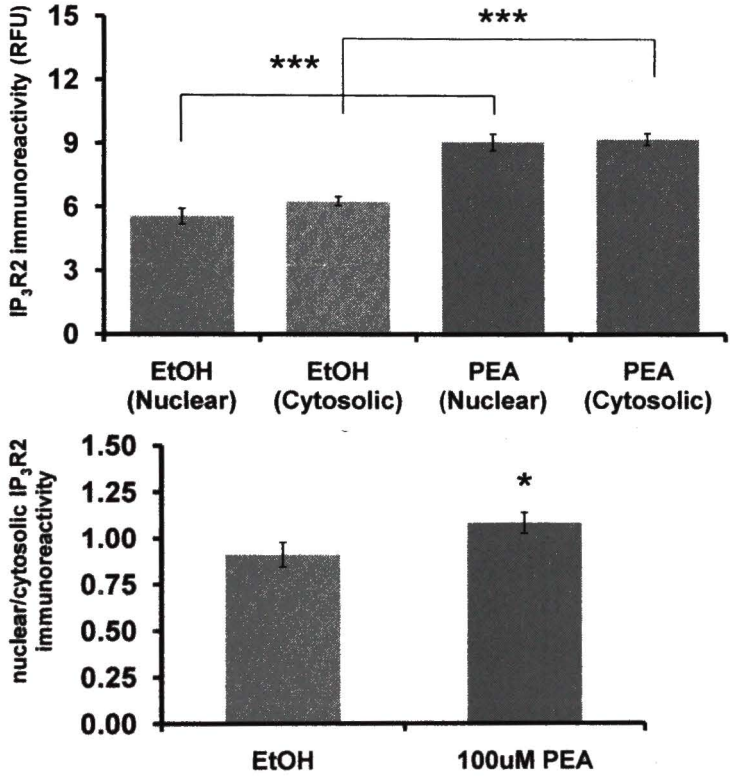
IP3R2 immunoreactivity (RFU)
15
12
9
6
3
0
***
***
EtOH (Nuclear)
EtOH (Cytosolic)
PEA (Nuclear)
PEA (Cytosolic)
nuclear/cytosolic IP3R2 immunoreactivity
1.50
1.25
1.00
0.75
0.50
0.25
0.00
*
EtOH
100uM PEA

Fig. 3 – Overnight treatment of HT22 cells with PEA increases cytosolic RyR2 immunoreactivity. For this study, *n* equals 79 and 96 cells for the EtOH vehicle and PEA treatment conditions, respectively. A P-value of ≤ 0.001 is indicated by ***.

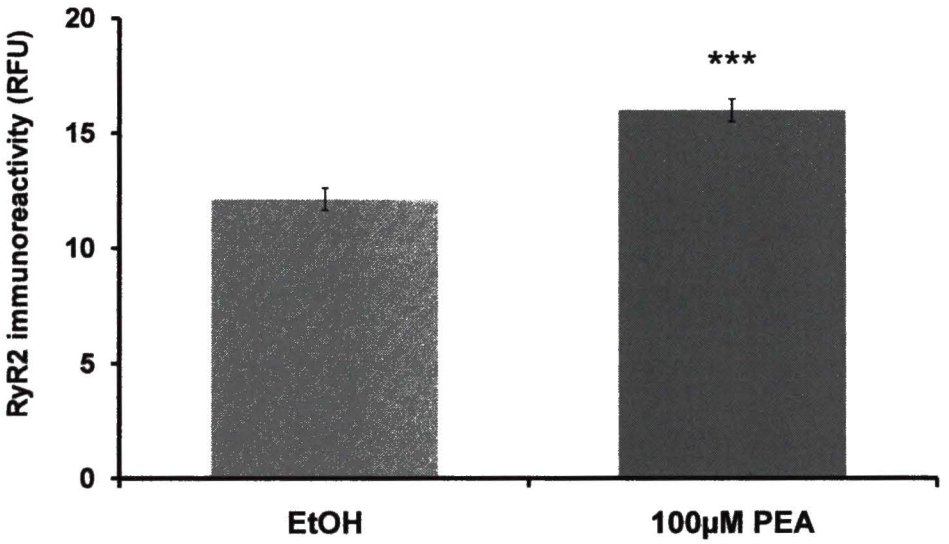
RyR2 immunoreactivity (RFU)
20
15
10
5
0
***
EtOH
100μM PEA

Fig. 4 – Overnight treatment of HT22 cells with PEA increases cytosolic RyR3 immunoreactivity. For this study, *n* equals 98 and 83 cells for the EtOH vehicle and PEA treatment conditions, respectively. A P-value of ≤ 0.01 is indicated by **.

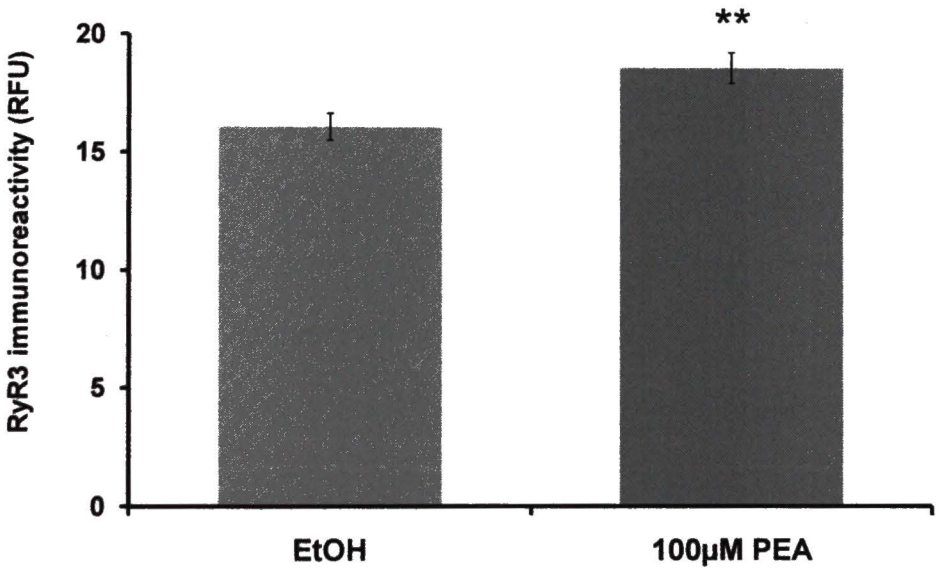
**
20
15
10
5
0
RyR3 immunoreactivity (RFU)
EtOH
100µM PEA

Fig. 5 – Application of PEA to HT22 cells elicits no Ca^{2+} response. For this study, *n* equals two microscope fields (two coverslips), one with 30 cells and the other with 34 cells being analyzed.

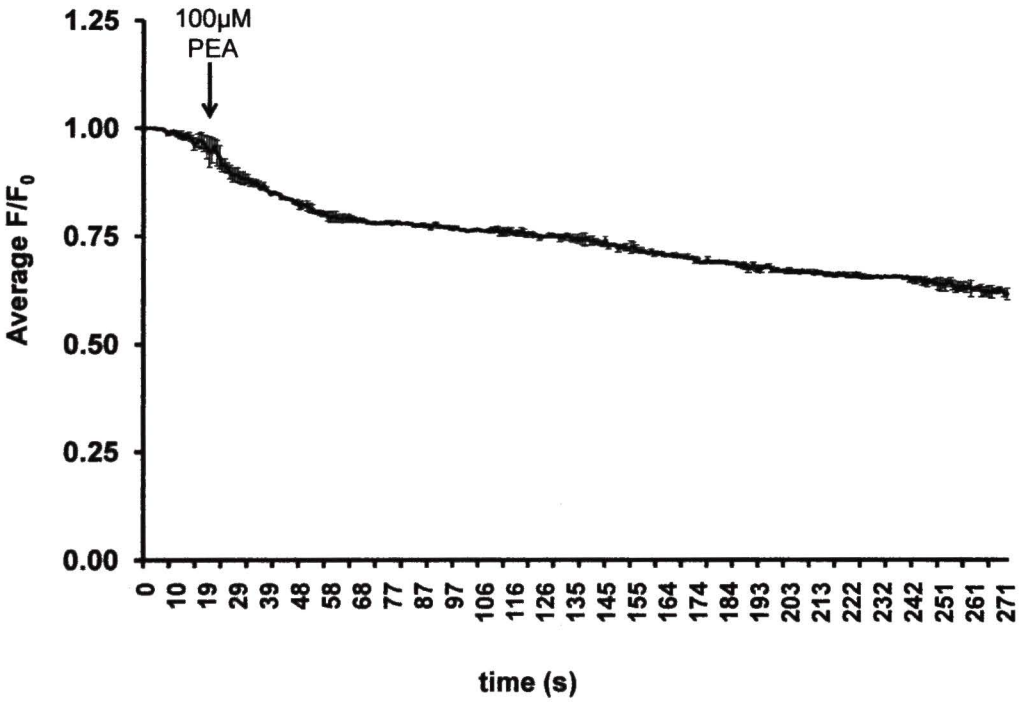
100μM
PEA
1.25
1.00
0.75
0.50
0.25
0.00
Average F/F0
0
10
19
29
39
48
58
68
77
87
97
106
116
126
135
145
155
164
174
184
193
203
213
222
232
242
251
261
271
time (s)

Fig. 6 – A short-term (1 – 2 hour) PEA pretreatment has no significant effect on caffeine-mediated Ca^{2+} responses in HT22 cells. The x-axis of the graph starts at the addition of caffeine (red arrow). For this study, *n* equals four microscope fields per treatment group, one with 153 cells (EtOH vehicle treatment group) and the other with 163 cells (PEA treatment group) being analyzed.

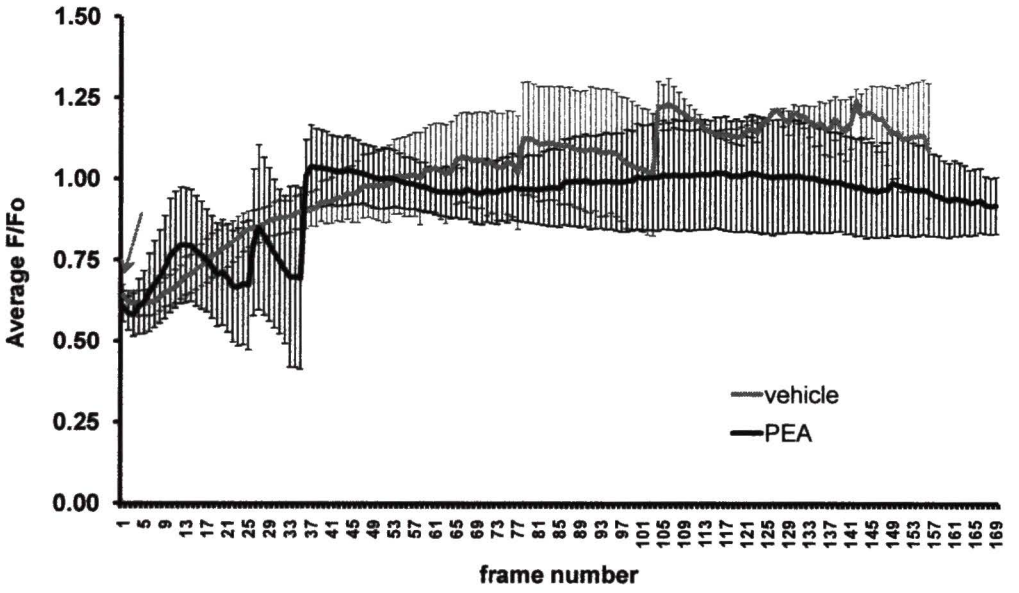
1.50
1.25
1.00
0.75
0.50
0.25
0.00
Average F/Fo
vehicle
PEA
1 5 9 13 17 21 25 29 33 37 41 45 49 53 57 61 65 69 73 77 81 85 89 93 97 101 105 109 113 117 121 125 129 133 137 141 145 149 153 157 161 165 169
frame number

Fig. 7 – A 6 hour PEA pretreatment decreases depolarization-mediated (KCl-mediated) Ca^{2+} release in HT22 cells. For this study, *n* equals three coverslips per treatment group. For EtOH vehicle-treated condition, a total of 90 cells were analyzed. For EtOH vehicle-treated condition, a total of 74 cells were analyzed. A two-sample t-test was conducted to compare the PEA-treated groups to the EtOH vehicle-treated group. P-values ranging from ≤ 0.05 to ≤ 0.001 are indicated by */***.

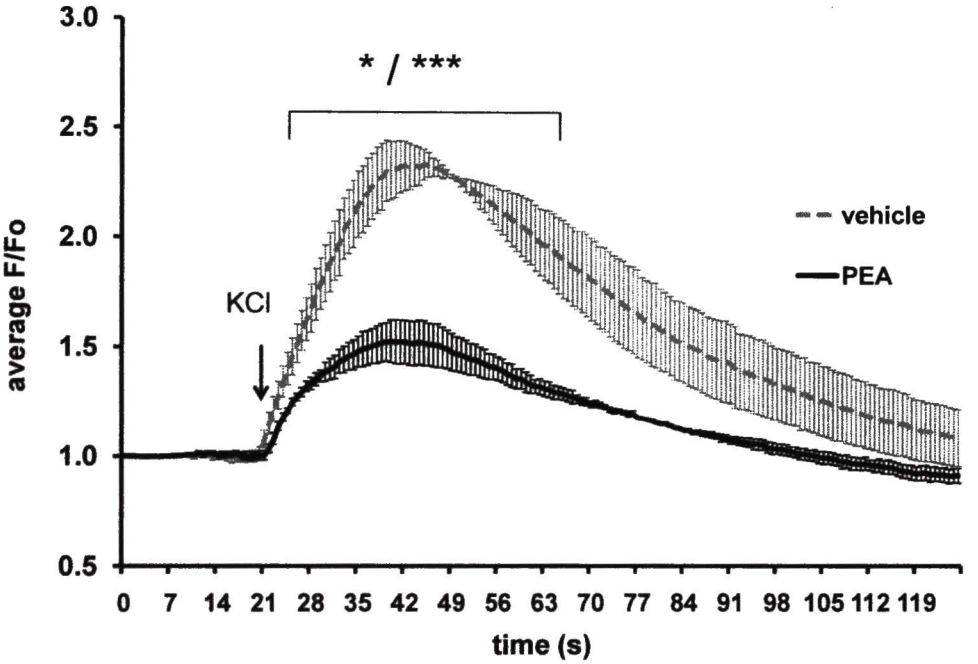
3.0
2.5
2.0
1.5
1.0
0.5
average F/Fo
* / ***
KCl
vehicle
PEA
0 7 14 21 28 35 42 49 56 63 70 77 84 91 98 105 112 119
time (s)

Fig. 8 – A prolonged (14 hour) PEA pretreatment has no significant effect on IP3-AM-mediated Ca^{2+} responses in HT22 cells. For this study, *n* equals one coverslip for the EtOH vehicle and LEA treatment group and two coverslips for the PEA treatment group. For EtOH vehicle- and LEA-treated conditions, a total of 32 and 28 cells were analyzed, respectively. For the PEA-treated condition, a total of 53 cells were analyzed.

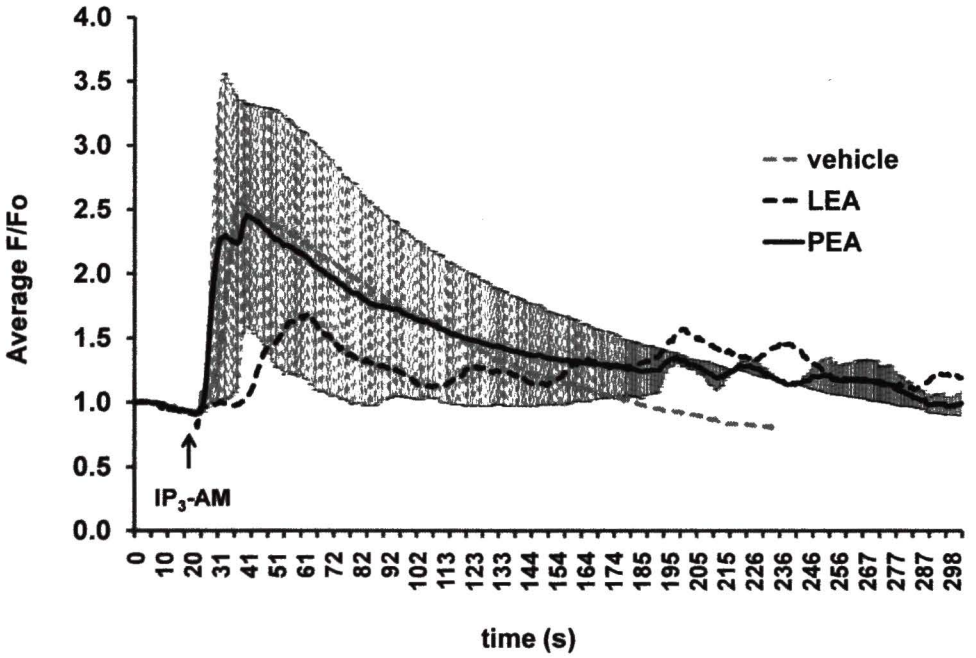
4.0
3.5
3.0
2.5
2.0
1.5
1.0
0.5
0.0
Average F/Fo
vehicle
LEA
PEA
IP3-AM
0
10
20
31
41
51
61
72
82
92
102
113
123
133
144
154
164
174
185
195
205
215
226
236
246
256
267
277
287
298
time (s)

Fig. 9 - A prolonged (14 hour) LEA and PEA pretreatment decreases caffeine-mediated Ca^{2+} responses in HT22 cells. For this study, *n* equals one coverslip for each treatment group. A total of 25, 25 and 16 cells were analyzed for vehicle, LEA and PEA, respectively.

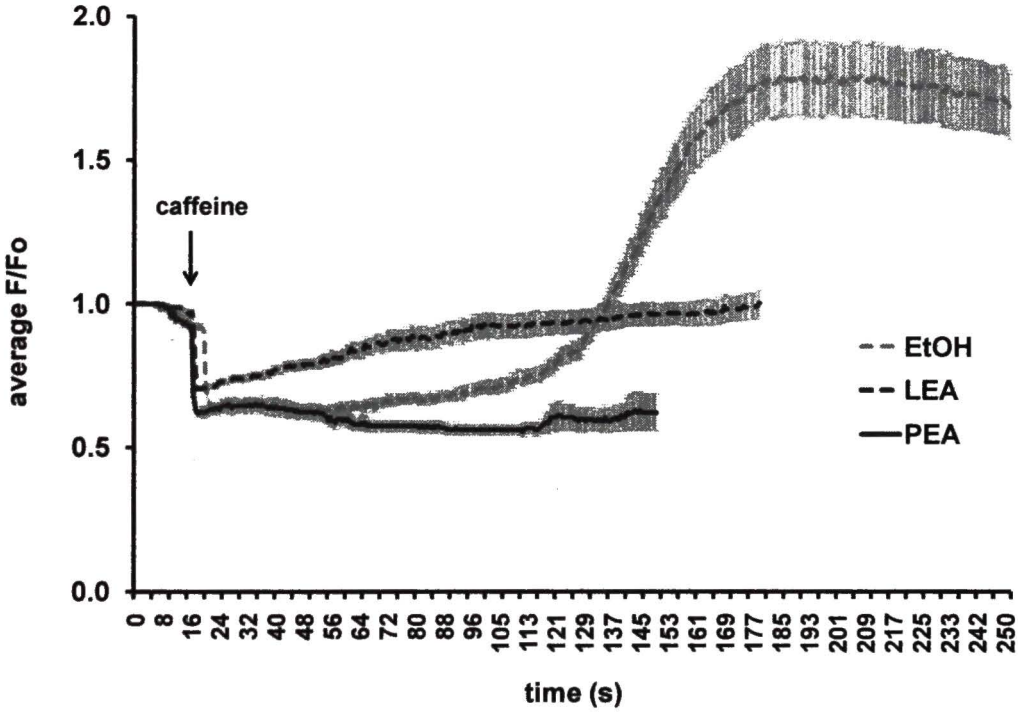
2.0
1.5
1.0
0.5
0.0
average F/Fo
caffeine
EtOH
LEA
PEA
0
8
16
24
32
40
48
56
64
72
80
88
96
105
113
121
129
137
145
153
161
169
177
185
193
201
209
217
225
233
242
250
time (s)

Fig. 10 - A prolonged (14 hour) LEA and PEA pretreatment decreases depolarization-induced (KCl-induced) Ca^{2+} responses in HT22 cells. For this study, *n* equals one coverslip for the LEA treatment group and two coverslips for the EtOH vehicle and PEA treatment groups. For EtOH vehicle- and PEA-treated conditions, a total of 82 and 58 cells were analyzed, respectively. For the LEA-treated condition, a total of 30 cells were analyzed.

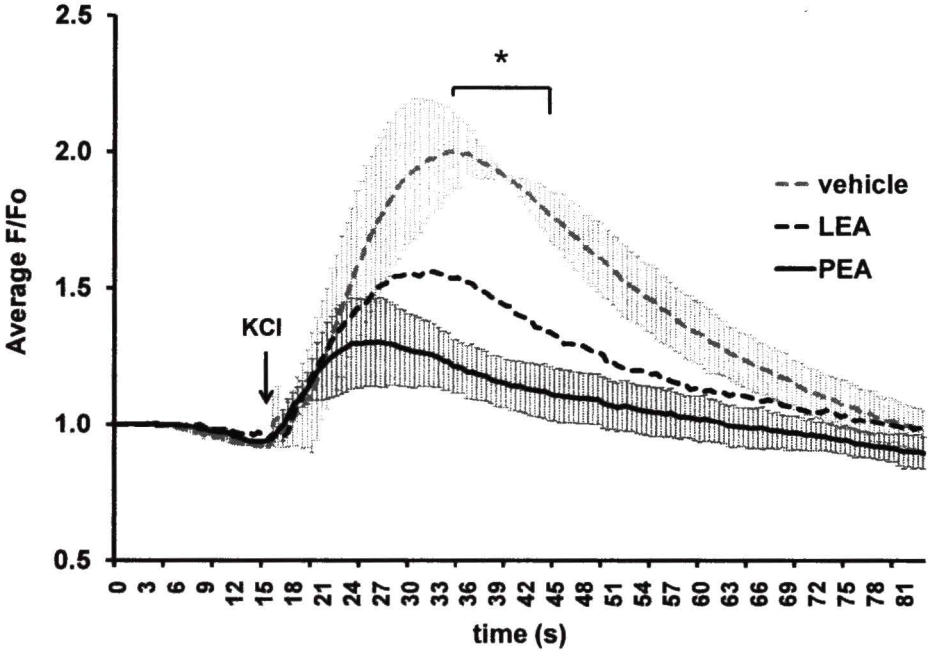
2.5
2.0
1.5
1.0
0.5
Average F/Fo
*
KCl
vehicle
LEA
PEA
0
3
6
9
12
15
18
21
24
27
30
33
36
39
42
45
48
51
54
57
60
63
66
69
72
75
78
81
time (s)

CHAPTER 6 - OVERALL DISCUSSION

Here, I report that two commonly-used cell model systems of neurodegeneration, HT22 cells and cultured mouse primary cortical neurons, express the NAE signaling proteins CB1, CB2, VR1, FAAH, NAAA and NAPE-PLD (Fig.1). This data suggests that CB2 is expressed in HT22 cells and primary cortical neurons and, therefore, should be considered a receptor in the CNS. In addition, I measured changes in NAAA immunoreactivity in response to oxidative stress further supporting the important role that the NAE signaling system plays in neurodegenerative diseases (Fig. 1).

This data provides relevant information about both cannabinoid and non-cannabinoid proteins in two cell model systems of neurodegeneration. Characterization of the relevant proteins involved in NAE signaling will determine what pharmacological interventions, if any, must be included in experimental studies seeking to elucidate the function of non-cannabinoid NAEs and to rule out the so-called entourage effects of some NAEs.

Since a wide variety of NAEs are produced in response to toxic stimuli and the well-characterized NAE AEA exhibits neuroprotective properties, the NAE species that do not activate cannabinoid and vanilloid receptors also likely play a role in the neuroprotective process, albeit through a different mechanism of action (1, 2). My data underscores the need to include cannabinoid and vanilloid receptor antagonists when determining any potential non-cannabinoid/non-vanilloid effects of NAEs or similar compounds in these cell culture model systems. Furthermore, a pharmacological approach will determine if the mechanism of action for NAEs, such as PEA or OEA, act through the proposed AEA-enhancing entourage effect. It is not clear that this observed entourage effect is physiologically-relevant.

In addition, I provided evidence that PEA exhibits antiproliferative effects in the hippocampal cell line HT22 (Fig. 2). These results indicate that caution must be taken when assessing any potential neuroprotective effects elicited by PEA. Since PEA reduces cellular proliferation, cells pretreated with it may be more vulnerable to oxidative stress or other insults. As a result, any neuroprotective effect elicited by PEA may be underestimated. It also stands to reason that a measureable protective effect by PEA may be masked by antiproliferation.

My findings also suggest that PEA may be an attractive compound to study for diseases where cellular proliferation plays a role in overall pathology, such as cancer. My results also provide preliminary evidence that PEA treatment of HT22 cells results in a decrease in markers of mitochondrial activity.

I also determined that PEA (at 100μM) protects HT22 cells from peroxidative stress but only if cells are pretreated with PEA for 5 – 6 hours prior to tBHP exposure (Fig. 2). Shorter PEA pretreatment times led to a trend toward protection in some cases. Interestingly, PEA pretreatment of HT22 cells for several hours did not protect cells from tBHP insult. This study identifies PEA as a neuroprotectant that is endogenous to cells. In addition, present study indicates that PEA pretreatment (10μM and 50μM) for 5 hours prior to exposure to a brief anoxic insult led to a slight but significant decrease in CH_2DCFDA fluorescence (approximately 9.3% decrease) (data not published). This suggests that PEA may decrease cellular oxidative stress in cells.

Short pretreatment of cells with PEA offers no protection. I interpret this as a possible requirement for cells to accumulate exogenously-applied PEA before protective effects can be observed. Alternatively, PEA treatment may initiate protective signaling pathways within the cells that require a minimum amount of time to exert their effects thereby rendering the cell more

resistant to oxidative stress. Treatment of cells with PEA for several hours does not protect cells. It is possible that this prolonged PEA treatment results in reduced proliferative capacity of cells thus rendering them more sensitive to oxidative stress. The present study identified antiproliferative effects of PEA which supports this hypothesis. Alternatively, exposure of cells to prolonged PEA may result in significant degradation into palmitic acid at a time when the initial stages of oxidative stress begin. It is possible that this renders the cells sensitive to oxidative stress. It is also possible that prolonged exposure to PEA may lead to a downregulation in target proteins involved in the neuroprotective effect thus rendering cells sensitive to oxidative stress.

From these studies with PEA, it is apparent that PEAs ability to protect HT22 cells from oxidative stress increases as the severity of the tBHP insult increases. For example, when HT22 cells are pretreated with 100μM PEA for 6 hours followed by overnight exposure to low (sublethal) tBHP concentrations (0 - 10μM tBHP), calcein-AM fluorescence and MTT was reduced compared to vehicle controls. When PEA-pretreated HT22 cells are exposed to high (lethal) tBHP concentrations (20 - 40μM tBHP) there is an increase in calcein-AM fluorescence compared to the vehicle controls. PEA had no effect on decreased MTT reduction resulting from toxic tBHP concentrations. Furthermore, pretreatment of cells with 10μM PEA did not have the same effect as 100μM concentrations. This kill curve experimental approach revealed that PEA is antiproliferative to HT22 cells under normal and sublethal conditions, but protective under conditions of toxicity.

Furthermore, I established that PEA treatment, and to lesser extent LEA treatment, can facilitate the nuclear translocation of Akt and pAkt in a neuronal cell line and in cultured cortical neurons (Fig. 2). Furthermore, I determined that PEA and LEA can lead to a rapid and transient

increase in nuclear and cytosolic pERK1/2, but not ERK1/2 (Fig. 2). In addition, I determined that PEA exposure leads to a significant reduction in nuclear and cytoslic phopsho-p38 immunoreactivity in HT22 cells. PEA pretreatment for five (5) to six (6) hours protects HT22 cells from oxidative stress and, together, these data suggest that PEA and LEA activate kinases known to be involved in neuroprotective signaling, thus providing a possible mechanism by which NAEs neuroprotect.

Numerous studies have revealed that the cannabinoid NAE, AEA, is neuroprotective through activation of CB1 (1, 2). Since the saturated NAEs, PEA and LEA, do not bind CB1 and they exhibit poor affinity for CB2, we hypothesized that these NAEs exhibit neuroprotective properties by a mechanism independent of CB2. To rule out CB2-mediated effects in PEA neuroprotective signaling, I measured the effect of CB2 agonists on Akt/pAkt and ERK/pERK immunoreactivity. The CB2 agonist, JWH-015 had no effect on nuclear Akt or pAkt immunoreactivity in HT22 cells. The CB2 agonist AM1241, however, increased nuclear Akt immunoreactivity, but it had no effect on pAkt immunoreactivity. Together, these data suggest that PEAs effect on Akt and pAkt were not mediated through CB2 activation. Further evidence for this comes from the observation that treatment of cells with the CB2 antagonist, AM630, mimics instead of inhbits the effects of PEA on cytosolic Akt immunoreactivity and nuclear and cytosolic pAkt immunoreactivity in HT2 cells.

There are several reports of AEA activating MAPK pathways through activation of CB1 (3 - 5). Here, we determined that the non-cannabinoid PEA can increase nuclear pERK1/2 translocation and this effect can not be mimicked by the CB2 agonist JWH-015. Also, the p38 MAPK pathway is altered by PEA. PEA treatment of HT22 cells leads to a rapid reduction in nuclear and cytosolic phospo-p38 immunoreactivity.

Overall, these data suggests that PEA activates the neuroprotective Akt and ERK1/2 MAPK signaling pathways by a CB2-independent mechanism. These effects are within the timeframe required to cause neurorptection in HT22 cells. Interestingly, PEA-mediated elevation of pERK1/2 immunoreactivity occurs much earlier that measured elevation of Akt and pAkt nuclear translocation. This suggests that the ERK1/2 MAPK pathway is activated before the Akt signaling pathway.

Previous studies indicate that activation of Akt can result in phosphorylation of inositol 1, 4, 5-trisphosphate receptors (IP3Rs) and lead to enhanced Ca^{2+} release (6, 7). Interestingly, intracellular Ca^{2+} can activate a wide variety of signaling pathways including those mediated by Ras, which include the PI3-K/Akt and MAPK pathways (8). These data, in part, are consistent with a possible effect of PEA on Ca^{2+} signaling in neurons.

I established that PEA treatment can facilitate the nuclear translocation of NFκB (RelA/p65) and NFATc4 in a neuronal cell line and in cultured cortical neurons (Fig. 2). I previously determined that PEA pretreatment for five (5) to six (6) hours protects HT22 cells from oxidative stress. Together, these data suggest that PEA can activate transcription factors known to be involved in neuroprotective signaling, thus providing a possible mechanism by which NAEs neuroprotect.

Numerous studies have revealed that the cannabinoid NAE, AEA, is neuroprotective through activation of CB1 (3 - 5). Since the saturated NAEs, PEA and LEA, do not bind CB1 and they exhibit poor affinity for CB2, we hypothesized that these NAEs exhibit neuroprotective properties by a mechanism independent of CB2. To rule out any potential role of CB2 activation on the alteration of NFκB and NFATc4 immunoreactivity, we measured the effect of a CB2 agonist on nuclear NFATc4 immunoreactivity. The CB2 agonist, JWH-015 had no effect on

nuclear NFATc4 immunoreactivity in HT22 cells, suggesting that PEAs effect on NFATc4 were not mediated through CB2 activation. This result is similar to our observation that CB2 agonists do not mimic the effects of PEA on Akt/pAkt and ERK/pERK immunreactivities in HT22 cells.

Overall, our data suggests that PEA activates NFκB and NFATc4 signaling pathways by a CB2-independent mechanism. These effects are within the timeframe required to cause PEA-mediated neuroroptection in HT22 cells. Activation of CB1 leads to the regulation of Akt and calcineurin activity in the amygdala (9). This suggests that cannabinoids may activate down stream componenets of Akt and calcineurin such as NFκB and NFAT, respectively. In the present study, I determined that PEA can induce Akt and pAkt nuclear translocation. This result is consistent with the hypothesis that PEA-mediated effects on Akt may be, in turn, be involved in NFκB nuclear tranlocation.

Previous studies indicate that activation of Akt can result in phosphorylation of inositol 1, 4, 5-trisphosphate receptors (IP3Rs) and lead to enhanced Ca^{2+} release (6, 7). Interestingly, intracellular Ca^{2+} can activate calcineurin and, subsequently NFAT (10, 11). These data, in part, are consistent with a possible effect of PEA on Ca^{2+} signaling in neurons as evidenced by NFAT nuclear translocation.

I also provided evidence for differentially distributed IP_3R isotypes in HT22 cells (Fig. 3). IP_3R2 was the predominant subtype in the nuclear envelope and IP_3R1 and IP_3R3 were predominant in the ER (Fig. 3). Optical imaging of intracellular Ca^{2+} concentrations revealed that IP_3AM-mediated release of nuclear Ca^{2+} through IP_3R2 occurs prior to release of Ca^{2+} from the ER through IP_3R1 and IP_3R3. This data corroborates previous studies in a HepG2 cell line demonstrating that nuclear Ca^{2+} responses are regulated differently than cytosolic responses (12). The IP_3R2 subtype in the nuclear region exhibits a higher affinity for IP_3 and, as a result, gives

rise to earlier and higher Ca^{2+} transients than that seen from IP_3R3 in the cytosol. In this study, we reveal that Ca^{2+} release from the IP_3R2-enriched nucleus occurs prior to Ca^{2+} release from the IP_3R1-enriched ER supported by the reported higher affinity of IP_3R2 for IP_3 than for the other IP_3R types (13).

Because there are Ca^{2+}-sensitive transcriptional regulators regulated by Ca^{2+}, the presence of IP_3 receptors in the nuclear membrane is of biological significance. Calcium-sensitive kinases and phosphatases such as Ca^{2+}/calmodulin-dependent protein kinases and calcineurin B, respectively can regulate gene transcription (14). In addition, a Ca^{2+}-regulated transcriptional repressor, downstream response element antagonist modulator, can bind to promoter response elements in the c-fos and prodynorphin genes (15). IP_3 receptor-mediated release of Ca^{2+} from the nucleoplasmic reticulum could be a mechanism by which cells can regulate the expression of genes. The differential distribution of IP_3Rs within cells may be a means to generate a diversity of signals in a tissue.

The HT22 cell line was utilized in this study because it is a good model system for studying the effect of oxidative stress on cell function (16, 17). Little knowledge exists on the role of IP3 receptor signaling and function in HT22 cells as it relates to Ca^{2+} homeostasis and neurodegeneration. The present studies utilizing HT22 cells lay the groundwork for future studies on IP_3 receptor-mediated Ca^{2+} signaling relevant to neurodegeneration and neuroprotection.

I also report that two commonly-used cell model systems of neurodegeneration, HT22 cells and cultured mouse primary cortical neurons, express IP_3Rs and RyRs, both of which are critical Ca^{2+} channels regulating the release of Ca^{2+} from intracellular stores (Fig. 3). Specifically, I detected RyR2 and RyR3 in HT22 cells and IP_3R1, IP_3R2, IP_3R3, RyR2 and RyR3 in primary

cortical neurons using immunochemical methods. In addition, the subcellular distribution was determined using immunofluorescence. Furthermore, I measured significant changes in IP_3R and RyR immunoreactivity in response to oxidative stress lending support to the idea that intracellular Ca^{2+} channels, such as IP3Rs and RyRs, play an important role in neurodegenerative diseases (Fig. 3).

My data provide relevant information about the IP_3R and RYR subtypes expressed in HT22 cells and cultured cortical neurons. The differential distribution of IP_3Rs and RyRs (i.e. ER/cytosolic versus nuclear) provides clues to the potential discrete function of intracellular Ca^{2+} channels as it relates to specific cellular functions. Others have identified a role that IP_3Rs and RyR play in gene regulation, but little information on which subtypes are involved in this process have been determined (14, 18, 19).

The alterations observed in IP_3R and RyR immunoreactivity in response to oxidative stress suggests possible alteration in their function in neurodegenerative diseases exhibiting oxidative stress. IP_3Rs and RyR have been shown to play a role in neurotransmitter release (20 - 23). Any changes in their expression may have implication in neurotransmission. The changes in IP_3R and RyR expression described in this work underscore the possible contribution they may have in neurodegeneration.

My interpretation is that oxidative stress activates an adaptive response leading to IP_3R gene transcription. These adaptive changes could conceivably be facilitated by the activation (or deactivation) of a kinase, phospahtase or transcription factor. Work from others has identified numerous kinases and transcription factors that can be activated under conditions of oxidative stress (24 - 27).

To my knowledge, this study is the first to measure changes in IP_3R and RyR immunoreactivity elicited by oxidative stress in cultured neurons. Immunocytochemical characterization of IP_3R and RyR expression in response to a stimulus such as oxidative stress does not establish a functional consequence such as Ca^{2+} release. As a result, optical imaging of intracellular Ca^{2+} with and without oxidant treatment should be conducted to determine if observed changes in IP_3R or RyR immunoreactivity have functional consequences.

I also determined that an overnight exposure of HT22 cells to PEA increases IP_3R2, RyR and RyR3 immunoreactivity (Fig. 3). In addition, I determined that PEA treatment of HT22 cells for 6 – 14 hours reduces depolarization-induced Ca^{2+} release in the nuclear region of HT2 cells (Fig. 3). Short-term exposure (1 – 2 hour) of HT22 cells to PEA had questionable effects on IP_3-AM- and caffeine-mediated Ca^{2+} responses. As a result, I conclude that PEA may reduce Ca^{2+} toxicity associated with neurodegenerative diseases. The upregulation of IP_3R2, RyR2 and RyR3 expression in response to PEA may be due to a compensatory response to this inhibition.

The mechanism by which AEA and PEA elicit neuroprotection has focused almost entirely on their activation of CB_1 and CB_2 receptors, respectively. The consensus is that AEA is an endogenous ligand for CB_1 receptors, although other endogenous high affinity ligands also exist. PEA, however, is not likely to be the endogenous agonist for CB_2 since its affinity for the receptor is quite low compared to other endogenous ligands (28). Recently, an orphan G-protein coupled receptor (GPCRs), GRP55, has been shown to exhibit a high affinity for PEA compared to CB_2 (29). Activation of GRP55 couples to $G_{\alpha 13}$ which likely affects cytoskeleton dynamics and cellular morphology and motility (30). Similarly, the orphan GPCR, GRP119, has been shown to bind oleoylethanolamine (OEA) and, to a lesser extent, PEA with high affinity (31).

Since GPR119 activation results in an increase in cellular cAMP, many of its effects are likely mediated by protein kinase A (PKA).

These recent data suggest that some orphan GPCRs may be the target for NAEs of unknown function. Since PEA treatment of HT22 cells did not itself elicit a Ca^{2+} response, we have provided evidence against any G_q-coupled GPCR that can be activated by PEA in HT2cells.

The increase in the number of responding cells, amplitude of responses and slope of responses in the presence of ($Ca^{2+}{}_o$) compare to that of responses in Ca^{2+}-free media may be due to the contribution of store-operated Ca^{2+} channels (SOCs). Store filling is highly affected by the presence or absence of ($Ca^{2+}{}_o$) (32). In the absence of ($Ca^{2+}{}_o$), SOCs can maintain and possibly increase the Ca^{2+} storing capacity of the ER. It is interesting to note that in the absence of $Ca^{2+}{}_o$, baseline fluo-3 AM fluorescence levels are greatly reduced compare to the baseline fluorescence levels in the presence of $Ca^{2+}{}_o$. This suggests that the reduced or weak responses observed in the absence of $Ca^{2+}{}_o$ may in part be due to a reduction in ER store filling or maintenance of normal ER store capacity.

Data from this work suggest that, after several hours of exposure to cells, the non-cannabinoid NAE, PEA, can reduce nuclear depolarization-induced Ca^{2+} release. Since KCl depolarization activates voltage-gated cation channels and thus leads to elevated cytoplasmic Ca^{2+} concentrations, the prominent nuclear responses are likely due to Ca^{2+}-induced Ca^{2+} release channels such as RyRs. Thus, we suggest that PEA reduces RyR activity.

REFERENCES

42. Milton NG (2002) Anandamide and noladin ether prevent neurotoxicity of the human amyloid-beta peptide. Neurosci Lett. 332(2):127-30.
43. Shouman B, Fontaine RH, Baud O, Schwendimann L, Keller M, Spedding M, Lelievre V and Gressens P (2006) Endocannabinoids potently protect the newborn brain against AMPA-kainate receptor-mediated excitotoxic damage. Br J Pharmacol. 148(4):442-51.
44. Bouaboula M, Poinot-Chazel C, Bourrie B, Canat X, Calandra B, Rinaldi-Carmona M, Le Fur G and Casellas P (1995) Activation of mitogen-activated protein kinases by stimulation of the central cannabinoid receptor CB1. Biochem J. 1995 Dec 1;312 (Pt 2):637-41.
45. Wartmann M, Campbell D, Subramaninan A, Burstein SH and Davis RJ (1995) The MAP kinase signal transduction pathway is activated by the endogenous cannabinoid anandamide. FEBS Lett. 359(2-3):133-6.
46. Bouaboula M, Poinot-Chazel C, Marchand J, Canat X, Bourrie B, Rinaldi-Carmona M, Calandra B, Le Fur G and Casellas P (1996) Signaling pathway associated with stimulation of CB2 peripheral cannabinoid receptor. Involvement of both mitogen-activated protein kinase and induction of Krox-24 expression. Eur J Biochem.237(3):704-711.
47. Koulen P, Madry C, Duncan RS, Hwang JY, Nixon E, McClung N, Gregg EV and Singh M (2008) Progesterone potentiates IP(3)-mediated calcium signaling through Akt/PKB. Cell Physiol Biochem. 21(1-3):161-72.
48. Hwang JY, Duncan RS, Madry C, Singh M and Koulen P, Effects of progesterone on calcium signaling in hippocampal neurons, Cell Calcium, in press.

49. Rosen LB, Ginty DD, Weber MJ and Greenberg ME (1994) Membrane depolarization and calcium influx stimulate MEK and MAP kinase via activation of Ras. Neuron. 12(6):1207-21

50. Cannich A, Wotiak CT, Kamprath K, Hermann H, Lutz B and Marsicano G (2004) CB1 cannabinoid receptors modulate kinase and phosphatase activity during extinction of conditioned fear in mice. Learn Mem. 11(5):625-32.

51. Graef IA, Mermelstein PG, Stankunas K, Neilson JR, Deisseroth, Tsien RW and Crabtree GR (1999) L-type calcium channels and GSK-3 regulate the activity of NF-ATc4 in hippocampal neurons. Nature. 401(6754):703-8.

52. Valdes JA, Gaggero E, Hidalgo J, Leal N, Jaimovich E and Carrasco MA (2008) NFAT activation by membrane potential follows a calcium pathway distinct from other activity-related transcription factors in skeletal muscle cells. Am J Physiol Cell Physiol. 294(3):C715-25.

53. Leite M.F., E.C. Thrower, W. Echevarria, P. Koulen, K. Hirata, A.M. Bennett, B.E. Ehrlich, and M.H. Nathanson. 2003. Nuclear and cytosolic calcium are regulated independently. *Proc. Natl. Acad. Sci. U.S.A.* 100:2975-2980.

54. Miyakawa T., A. Maeda, T. Yamazawa, K. Hirose, T. Kurosaki, and M. Iino. 1999. Encoding of Ca^{2+} signals by differential expression of IP_3 receptor isotypes. *EMBO. J.* 18:1303-1308.

55. Ikura M., M. Osawa, and J.B. Ames. 2002. The role of calcium-binding proteins in the control of transcription: structure to function. *Bioessays.* 24:625-636.

56. Osawa M, K.I. Tong, C. Lilliehook, W. Wasco, J.D. Buxbaum, H.Y. Cheng, J.M. Penninger, M. Ikura, and J.B. Ames. 2001. Calcium-regulated DNA binding and oligomerization of the

neuronal calcium-sensing protein, Calsenilin/DREAM/KChIP3. *J. Biol. Chem.* 276:41005-41013.

57. Green, P.S., K.E. Gridley, J.W. Simpkins. 1998. Nuclear estrogen receptor-independent neuroprotection by estratrienes: a novel interaction with glutathione. *Neuroscience.* 84:7-10.
58. Sagara Y., R. Dargusch, D. Chambers, J. Davis, D. Schubert, and P. Maher. 1998. Cellular mechanisms of resistance to chronic oxidative stress. *Free Radic. Biol. Med.* 24:1375-1389.
59. Bading, H. 2000. Transcription-dependent neuronal plasticity the nuclear calcium hypothesis. *Eur. J. Biochem.* 267:5280-5283.
60. West A.E., W.G. Chen, M.B. Dalva, R.E. Dolmetsch, J.M. Kornhauser, A.J. Shaywitz, M.A. Takasu, X. Tao, and M.E. Greenberg. 2001. Calcium regulation of neuronal gene expression. *Proc. Natl. Acad. Sci.* U.S.A. 98:11024-11031.
61. Herrero I, Miras-Portugal MT and Sanchez-Prieto J (1992) Positive feedback of glutamate exocytosis by metabotropic presynaptic receptor stimulation. Nature. 360(6400):163-6.
62. Mori F, Okada M, Tomiyama M, Kaneko S and Wakabayashi K (2005) Effects of ryanodine receptor activation on neurotransmitter release and neuronal cell death following kainic acid-induced status epilepticus. Epilepsy Res. 65(1-2):59-70.
63. Amano T, Aoki S, Setsuie R, Sakurai M, Wada K and Noda M (2006) Identification of a novel regulatory mechanism for norepinephrine transporter activity by the IP3 receptor. Eur J Pharmacol. 536(1-2):62-8.
64. Zissimopoulos S, West DJ, Williams AJ and Lai FA (2006) Ryanodine receptor interaction with the SNARE-associated protein snapin. J Cell Sci. 2006 Jun 1;119(Pt 11):2386-97.
65. Guerrini L, Blassi F and Denis-Donini S (1995) Synaptic activation of NF-kappa B by glutamate in cerebellar granule neurons in vitro. Proc Natl Acad Sci U S A. 92(20):9077-81.

66. Pahl HL (1999) Activators and target genes of Rel/NF-kappaB transcription factors. Oncogene. 18(49):6853-66.

67. Zhang L and Jope RS (1999) Oxidative stress differentially modulates phosphorylation of ERK, p38 and CREB induced by NGF or EGF in PC12 cells. Neurobiol Aging. 20(3):271-8.

68. Luo Y and DeFranco DB (2006) Opposing roles for ERK1/2 in neuronal oxidative toxicity: distinct mechanisms of ERK1/2 action at early versus late phases of oxidative stress. J Biol Chem. 281(24):16436-42.

69. Lambert DM and Di Marzo V (1999) The palmitoylethanolamide and oleamide enigmas : are these two fatty acid amides cannabimimetic? Curr. Med. Chem. 6 (8):757-773.

70. Ryberg E, Larsson N, Sjogren S, Hjorth S, Hermansson NO, Leonova J, Elebring T, Nilsson K, Drmota T and Greasley PJ (2007) The orphan receptor GPR55 is a novel cannabinoid receptor. Br J Pharmacol. 152(7):1092-101.

71. Henstridge CM, Balenga NA, Ford LA, Ross RA, Waldhoer M and Irving AJ (2008) The GPR55 ligand L-{alpha}-lysophosphatidylinositol promotes RhoA-dependent Ca2+ signaling and NFAT activation. FASEB J. 2008 Aug 29.

72. Overton HA, Babbs AJ, Doel SM, Fyfe MC, Gardner LS, Griffin G, Jackson HC, Procter MJ, Rasamison CM, Tang-Christensen M, Widdowson PS, Williams GM and Reynet C (2006) Deorphanization of a G protein-coupled receptor for oleoylethanolamide and its use in the discovery of small-molecule hypophagic agents. Cell Metab. 3(3):167-75.

73. Parekh AB and Putney JW Jr. (2005) Store-operated calcium channels. Physiol Rev. 85(2):757-810.

Fig. 1. Characterization of the expression of proteins involved in NAE signaling. Using immunochemical methods, the presence of receptors (CB1, CB2 and VR1) and metabolic enzymes (NAPE-PLD, FAAH and NAAA) involved in NAE signaling were identified in HT22 cells and cultured cortical neurons. Exposure of HT22 cells to oxidative stress resulted in an increase in immunoreactivity of the metabolic enzymes involved in NAE signaling (red text and arrows). The PEA enzymatic breakdown products, palmitic acid and ethanolamine are indicated by PA and EtNH+, respectively.

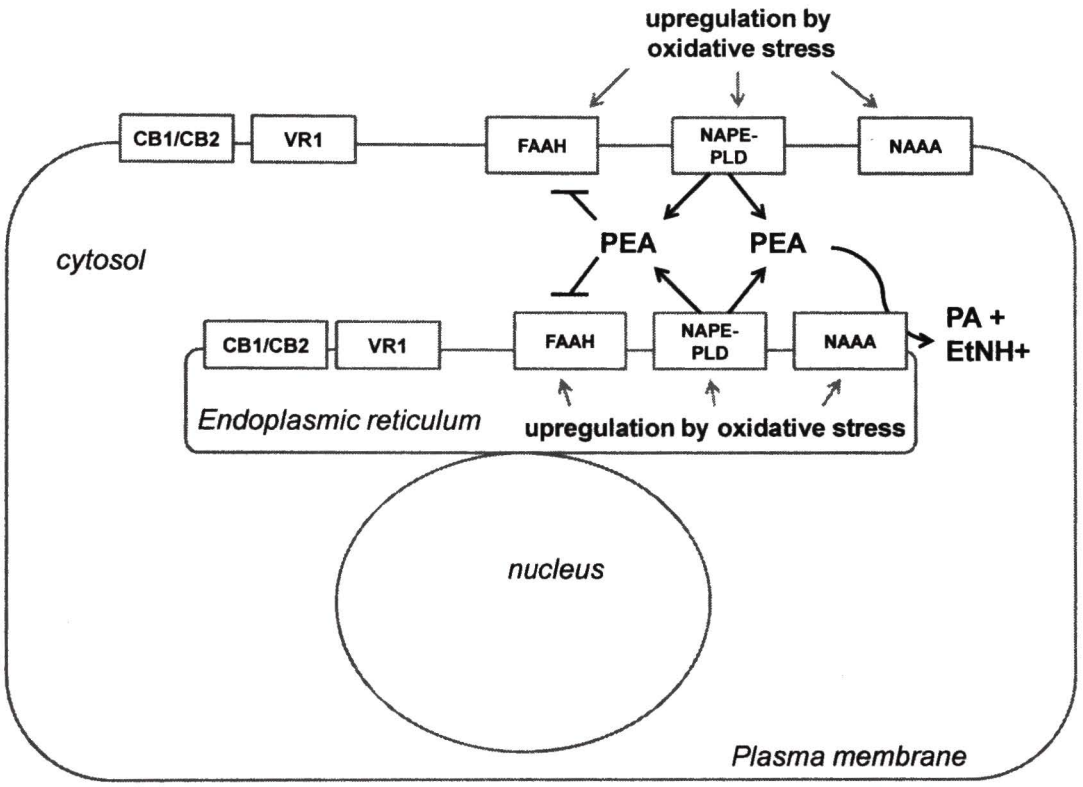
upregulation by
oxidative stress
CB1/CB2
VR1
FAAH
NAPE-
PLD
NAAA
cytosol
PEA
PEA
CB1/CB2
VR1
FAAH
NAPE-
PLD
NAAA
PA +
EtNH+
Endoplasmic reticulum
upregulation by oxidative stress
nucleus
Plasma membrane

Fig. 2. A working model for the neuroprotective mechanism of action of PEA. Treatment of HT22 cells with PEA reduces cellular proliferation by a mechanism independent of CB2 and possibly involving mitochondria (Chapter 3.1). Furthermore, PEA treatment of HT22 cells protects against oxidative stress (Chapter 3.2) by a mechanism possibly involving Akt and ERK1/2 kinases (Chapter 3.3) and NFκB and NFATc4 (Chapter 3.4).

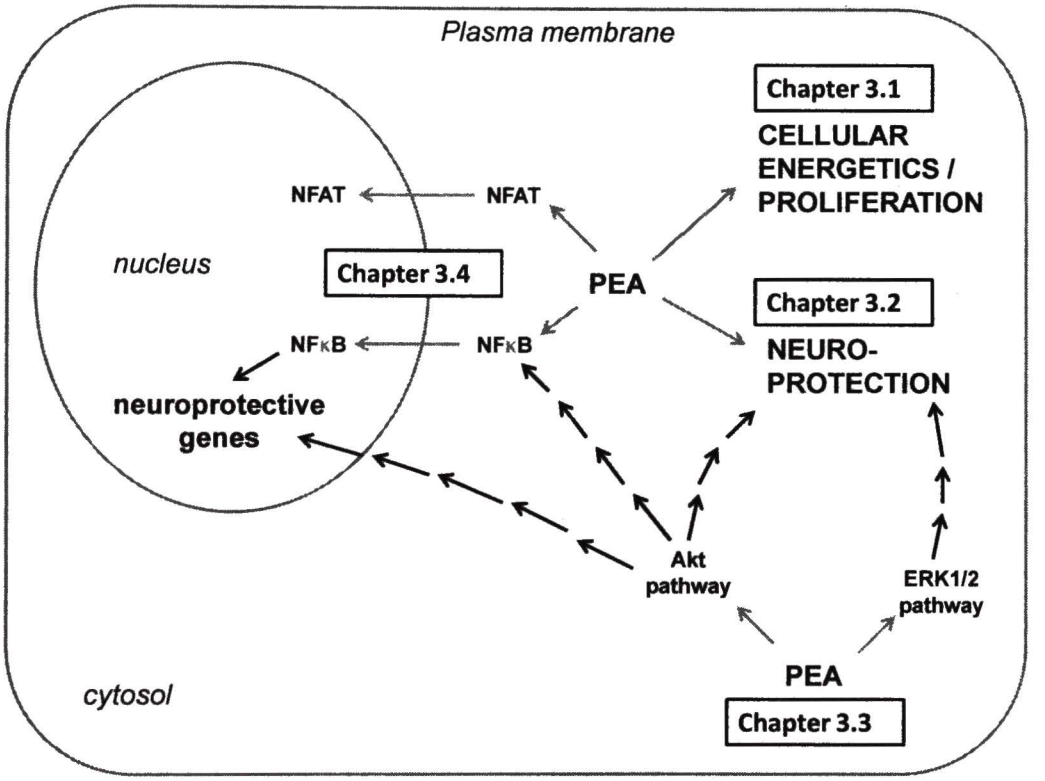
Plasma membrane
Chapter 3.1
CELLULAR ENERGETICS / PROLIFERATION
NFAT
NFAT
nucleus
Chapter 3.4
PEA
Chapter 3.2
NFκB
NFκB
NEURO-PROTECTION
neuroprotective genes
Akt pathway
ERK1/2 pathway
PEA
cytosol
Chapter 3.3

Fig. 3. A working model for the mechanism of action of PEA in intracellular Ca^{2+} homeostasis. Using immunochemical methods, the presence of IP_3Rs (IP_3R1 – IP_3R3) and RyRs (RyR2 and RyR3) in HT22 cells and cultured cortical neurons. Exposure of HT22 cells to oxidative stress resulted in an increase in immunoreactivity of the all IP_3R subtypes and RyR2 and RyR3 (red text and arrows). Treatment of HT22 cells to PEA leads to an increase in IP_3R2 and RyR3 immunoreactivity and a reduction in caffeine- and chemical depolarization-induced Ca^{2+} release (Chapter 5).

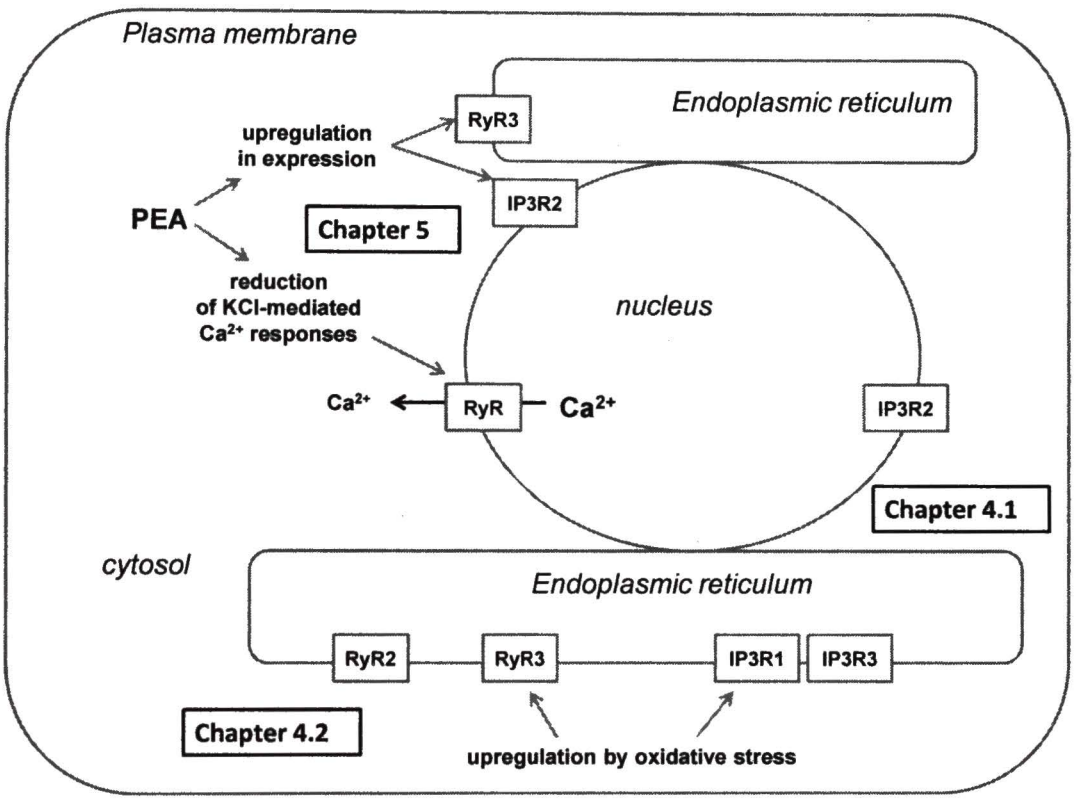
Plasma membrane
Endoplasmic reticulum
RyR3
upregulation
in expression
IP3R2
PEA
Chapter 5
reduction
of KCl-mediated
Ca2+ responses
nucleus
Ca2+
RyR
Ca2+
IP3R2
Chapter 4.1
cytosol
Endoplasmic reticulum
RyR2
RyR3
IP3R1
IP3R3
Chapter 4.2
upregulation by oxidative stress